Spring 2019

Modular Synthesis and Hydroalkylation of Vicinally Functionalized Ketopiperazines: A solution to the Piperazine Problem

Antonio Moreno
Central Washington University, morenoant@cwu.edu

MODULAR SYNTHESIS AND HYDROALKYLATION OF VICINALLY FUNCTIONALIZED KETOPIPERAZINES: A SOLUTION TO THE PIPERAZINE PROBLEM

A Thesis

Presented to

The Graduate Faculty

Central Washington University

In Partial Fulfillment

of the Requirements for the Degree

Master of Science

Chemistry

---

by

Antonio Moreno

June 2019

CENTRAL WASHINGTON UNIVERSITY

Graduate Studies

We hereby approve the thesis of

Antonio Moreno

Candidate for the degree of Master of Science

APPROVED FOR THE GRADUATE FACULTY

_____ _____
Dr. Timothy Beng, Committee Chair

_____ _____
Dr. JoAnn Peters, Committee Member

_____ _____
Dr. Levente Fabry-Asztalos, Committee Member

_____ _____
Dr. Gil Belofsky, Committee Member

_____ _____
Dean of Graduate Studies

ABSTRACT

MODULAR SYNTHESIS AND HYDROALKYLATION OF VICINALLY FUNCTIONALIZED KETOPIPERAZINES: A SOLUTION TO THE PIPERAZINE PROBLEM

by

Antonio Moreno

June 2019

The stereocontrolled synthesis of functionalized piperazines is of great interest to pharmaceutical companies owing to their multiple biological activities such as antidepressant, antiparasitic, anticancer and antiretroviral. Current methods towards functionalized piperazines include intramolecular cyclization of appropriately tethered on acyclic precursors as well as α-C–H functionalization of intact piperazine rings. Although effective for the most part, these methods suffer from drawbacks such as the use of expensive catalysts, potentially toxic reagents, limited scope and functional group compatibility. Seeking to side-step some of the aforementioned limitations, we herein describe a step-economical-, cost-effective-, transition metal-free-, and mild approach to highly functionalized piperazines, including [3.3.1]-bicyclic piperazines. The success of a novel enolate hydroalkylation methodology hinges on a cascade reaction triggered by the addition of allyl magnesium bromide to a vicinally functionalized piperazinonate. Furthermore, we have successfully synthesized fluorinated ketopiperazine, in hopes of potentially modulating biological properties such as pharmacokinetic and physicochemical properties. The [3.3.1] azabicyclic piperazinols and fluorine-containing 2-oxopiperazines are subsequently engaged in structure-activity-relationship (SAR) studies on neglected tropical diseases (NTDs), including leishmaniasis.

ACKNOWLEDGEMENTS

I would like to thank all the faculty and staff that have helped me grow as a scholar and person throughout my six years at Central Washington University. Specifically, the Chemistry Department who have provided me with knowledge and opportunities to grow as a chemist. I have had the pleasure of taking classes, been in lab or TAed with almost all the professors who have enhanced my passion for chemistry.

I would also like to thank Dr. Beng who has been an incredible mentor in the last two years. He always demonstrated patience, spread his wisdom, promoted leadership skills and is an overall great role model in both a research setting and beyond. He is a great contributor for my enjoyment of organic chemistry. I also want to thank my committee members Dr. Peters, Dr. Fabry and Dr. Belofsky. Dr. Peters was my organic chemistry professor for two quarters and I had the pleasure of doing undergraduate research with her. She made organic chemistry so enjoyable which began my interest in it.

I would like to thank the Science Talent Expansion Program (Toni Snowden and Lucinda Carnell) and Chemistry Department for graduate assistantships and moral support (Lisa Stowe). I am grateful for the funding from the School of Graduate Studies and Research for a Summer Fellowship and to go to the National American Chemical Society Meeting. I also want to thank Cindy White and Emil Babik for instrumentation help throughout the last two years.

Lastly, I want to thank my research group members especially Omar Farrah and Cecilia Gordner. I would also like to thank my friends (Olivia Camacho, Pati Flores, Veronica Hernandez and Susana Camacho), sisters (Cecilia Moreno and Rosa Moreno) and parents (Narcizo Moreno and Huri Leon) for their continuous support in my two year journey as a graduate student.

TABLE OF CONTENTS

TABLE OF CONTENTS (CONTINUED)

Chapter Page

TABLE OF CONTENTS (CONTINUED)

Chapter Page

TABLE OF CONTENTS (CONTINUED)

Chapter Page

LIST OF FIGURES

Figure Page

LIST OF FIGURES (CONTINUED)

Figure Page

LIST OF SCHEMES

Scheme Page

LIST OF TABLES

Table Page

CHAPTER 1: INTRODUCTION

1.1 Relevance of N-Heterocycles

Heterocyclic compounds are carbon-based molecules that contain at least one different atom within the ring. A renowned class of heterocycles are nitrogen-containing heterocycles commonly referred to as *N*-heterocycles or azaheterocycles. There is a great range of diversity of *N*-heterocycles that can be easily accessed. For example, the ring size of azaheterocycles can vary from the minimum of 3 atoms to macrocyclic structures with >11 atoms. Other properties include molecular geometry, rigidity, and aromaticity. However, all these subtle differences do not hinder the ability for possible bioactivity and presence in Food and Drug Administration (FDA)-approved pharmaceuticals. Ring structures in general are important building blocks in pharmaceuticals. A survey of the most common rings found in pharmaceuticals revealed that 33 of the top 50 are nitrogen containing heterocycles.[1] There are distinguishable features between these azaheterocycles, including aromaticity, bicyclic structures, and inclusion of multiple heteroatoms. It is important to note that 5- and 6-membered azaheterocycles dominate in this context.

As of 2014, 59% of small-molecule FDA-approved drugs contain an azaheterocycle.[2] Aside from small-molecule/synthetic drugs, azaheterocycles are found in bioactive compounds isolated from plants, fungi, and animals. Drug classification of azaheterocycles is greatly diverse. Some sub-classes include antihistamines, anesthetics, antidepressants, and antibiotics. Additionally, many have shown promising activity in antiparkinson, anticancer, and antiretroviral treatments. The abundance of *N*-heterocycles and their potent bioactivity has intrigued both medicinal and synthetic chemists. Particularly, a main interest and challenge for synthetic organic chemists are approaches towards highly functionalized saturated *N*-heterocyclic scaffolds.

As seen in **Figure 1-1**, one of these azaheterocycles is the piperazine motif which is currently the third most common azaheterocycle found in FDA-approved pharmaceuticals.[2] Aside from its prevalence in drugs, piperazines are also found in plastics, fragrances, ligands, pesticides and brake fluid. Additionally, amine blends containing piperazine and methyldiethanolamine (MDEA) are used for the sweetening of crude oil through the removal of carbon dioxide and hydrogen sulfide.[3,4] Piperazine rings are known for increasing binding affinity, hydrophilicity, and solubility as well as for their hydrogen bonding abilities.[5] In this research, we seek to explore synthetic application towards functionalized piperazines and post-diversification of the scaffold.

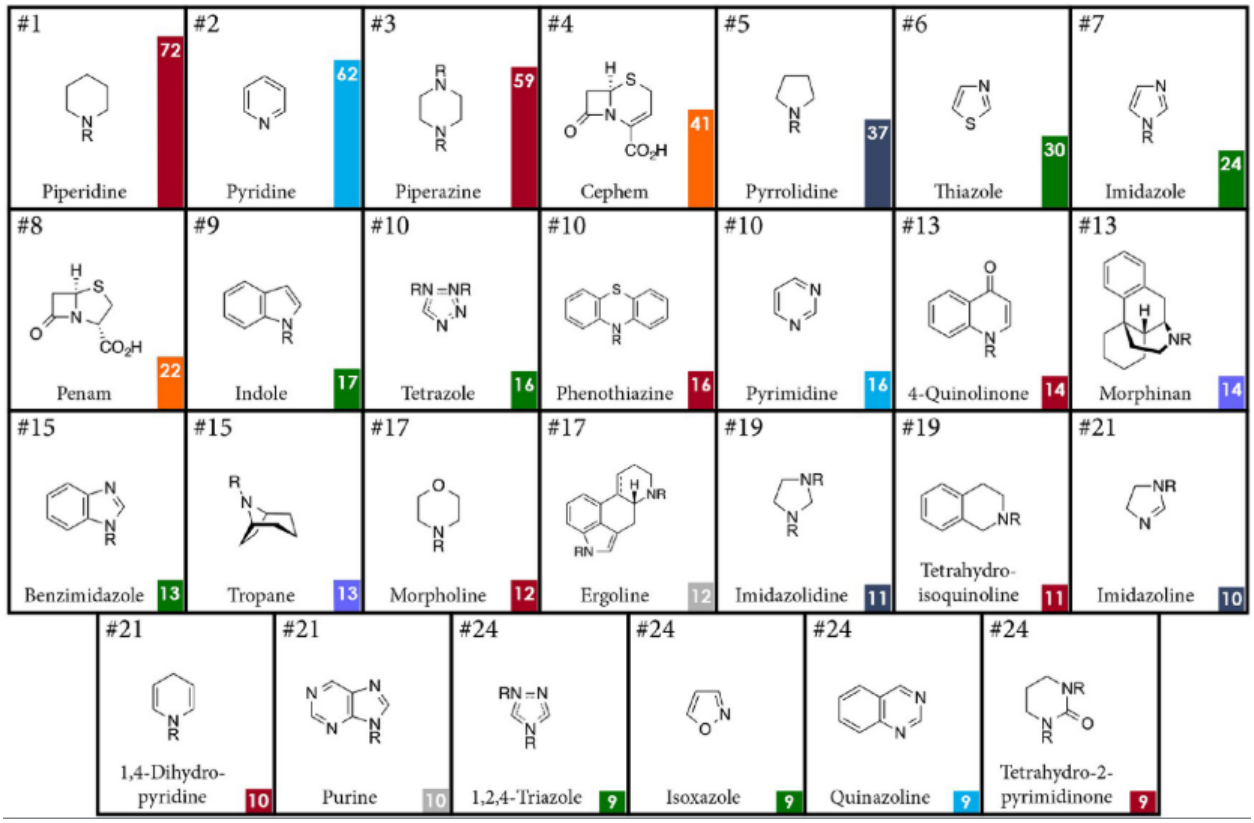

Figure 1-1 Top 24 azaheterocyclic motifs found in FDA approved pharmaceuticals

1.1.1 Relevance of Piperazines

As stated in the preceding section, the piperazine scaffold is the third most abundant *N*-heterocycle in FDA-approved drugs. Although the third position is impressive, this placement may be attributed to the synthetic challenges that the piperazine entity poses in contrast to the two azaheterocycles before it. As more efficient syntheses are developed, there is a possibility that the piperazine motif will rank higher. This idea is supported by the status of the piperazine ring as a privileged scaffold owing to its multiple biological activities. Examples of piperazines in pharmaceuticals are illustrated in **Figure 1-2**.

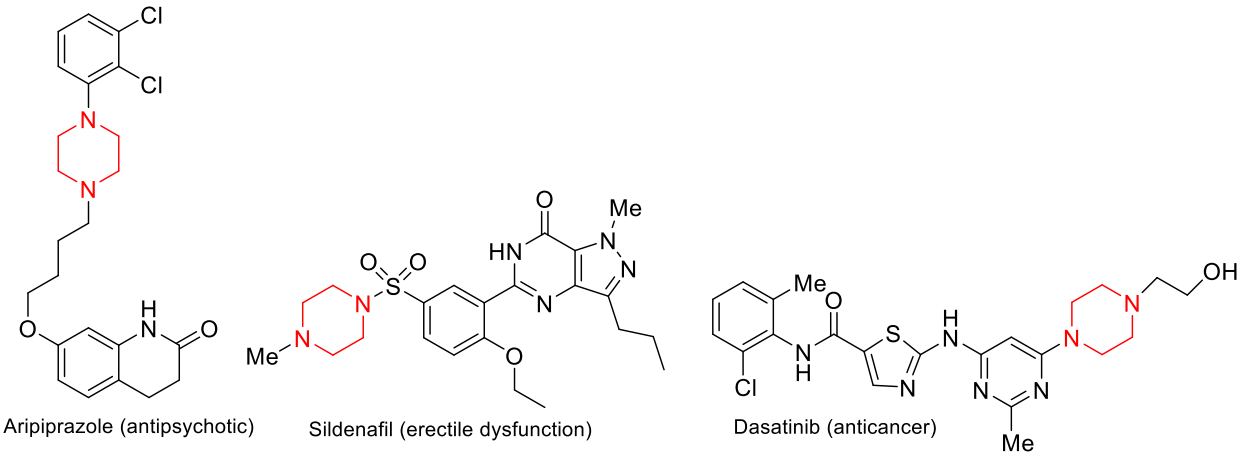

Figure 1-2 Examples of piperazine containing FDA approved drugs

Aripiprazole (Abilify®) is an atypical third generation antipsychotic (TGA) that is currently used for the treatment of schizophrenia, bipolar I disorder and irritability associated with both Tourette's syndrome and autism spectrum disorder.[6] Likewise, it is used as an accompanying drug in the treatment of major depression disorder (MDD).[7] Aripiprazole is a unique antipsychotic since it acts as a partial agonist of the D2 dopamine auto-receptor. This TGA distinguishable traits are its low extra pyramidal side effects and low weight gain, which are common in first generation antipsychotics (FGA) and second generation antipsychotic (SGA), respectively. The approval of aripiprazole motivated antipsychotic drug discovery to lean

towards an agonist-based form rather than antagonist-based form. Aripiprazole has a piperazine scaffold with two substituents on the nitrogen atoms. On one nitrogen atom, there is an aryl group and on the other nitrogen is a tethered δ-lactam motif. Sildenafil (Viagra®) acts as a phosphodiesterase type 5 (PDE5) inhibitor to treat erectile dysfunction.[8] It blocks degradation of cyclic guanosine monophosphate (cGMP) by PDE5 to allow vasodilation and increase blood flow. Apart from its medical use, sildenafil is a great example of drug discovery through clinical observations. It was initially developed to treat angina but was found to have no clinical effect on blood flow of this desired location.[9] An interesting side effect was the increase of erectile function. It was ultimately concluded that corporal erectile tissue was abundant in PDE5. Sildenafil only has substituents on the nitrogen with one being a methyl group and the other a sulfonyl group. Dasatinib (Sprycel®) is a highly effective anticancer pharmaceutical that is used to treat chronic myelogenous leukemia and Philadelphia-positive acute lymphoblastic leukemia (Ph+ ALL).[10] Dasatinib is classified as a second-generation BCR-ABL tyrosine kinase inhibitor and has the distinction of being a dual SRC/ABL kinase inhibitor.[11] This is highly valuable as activation of SRC can cause brain, breast, colon, lung, and pancreatic cancer. It has demonstrated greater potency than nilotinib, another second generation BCR-ABL kinase inhibitor, by 16-fold.[12] There are three azaheterocycles present in the structure, which are a piperazine, thiazole and pyrimidine. Congruent with aripiprazole and sildenafil, the piperazine topology in dasatinib only has substituents on the nitrogen atoms.

1.1.2 Relevance of Ketopiperazines

Piperazine derivatives are sought after not only for their potential biological activity but also intermediates for synthetic applications.[13] One of such derivatives is the ketopiperazine, which is resident in synthetic and natural FDA-approved pharmaceuticals. Although, not as

predominant as the reduced piperazine scaffold, nature's bias toward this motif demonstrates potential. Examples of ketopiperazines in FDA-approved pharmaceuticals can be seen in **Figure 1-3**.

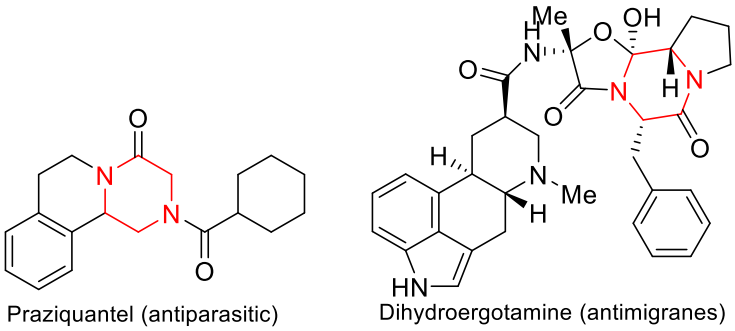

Figure 1-3 Examples of monoketopiperazines found in FDA-approved drugs

Praziquantel (Biltricide®) is a popular drug used to treat schistosomiasis caused by Schistosoma mansoni (*S. mansoni*) or Schistosoma haematobium (*S. haematobium*).[14] These two fresh water-born parasites lead to intestinal or urogenital schistosomiasis, respectively. There are currently around 207 million people affected by it globally of which around 85% live in sub-Saharan Africa region. This parasitic disease is considered a neglected tropical disease (NTD). One of the main hurdles of praziquantel has been to verify its safety and efficiency in children. Recent studies have proven its efficiency against schistosomiasis in both schoolchildren in Ethiopia[15] and pre-school aged children in Kenya.[16] Praziquantel is composed of a tricyclic azaheterocylic motif. The piperazine ring itself is tetrasubstituted and has a stereocenter which introduces a challenge for synthetic approaches. Although sold as a racemic mixture, studies indicate that the *R*-enantiomer is more biologically active than the *S*-enantiomer.[17]

Dihydroergotamine (Migranal®) is a semi-synthetic pharmaceutical used in the treatment of acute migraines. It is a derivative of ergotamine which is isolated from a fungi of the genus Claviceps. Dihydroergotamine acts as an agonist to various serotonin (5-HT) receptors including

-1B, -1D and -1F receptor and adrenergic and dopamine receptors.[18] In contrast to ergotamine, dihydroergotamine users exhibit less side effects such as nausea, vomiting and undesired vasoconstriction. The piperazine ring on dihydroergotamine is highly substituted with all the carbon atoms having at least one substituent on it which reiterates the importance of finding synthetic pathways to highly carbo-functionalized piperazines.

1.2 Frequently Encountered Challenges in Synthetic Organic Chemistry

The abundance of azaheterocycles in FDA-approved pharmaceuticals had led to exploration of step-economical, cost-saving and high-yielding synthetic strategies for their construction and post-diversification. In general, three challenges are associated with the efficient construction of azaheterocycles, namely, chemoselectivity, regioselectivity and stereoselectivity.

1.2.1 Importance and Overcoming: Chemoselectivity

Chemoselectivity is the preferential reaction of a chemical reagent with one of two or more different functional groups. Chemoselectivity allows bond construction with increased synthetic efficiency since it obviates the need for functional group protection and oxidation adjustment. There have been reagents developed for chemoselective reactions such as the Schwartz's reagent which is a zirconium based species. **Figure 1-4** illustrates the allylation of an amide, which was chemoselectivity implemented using the Schwartz reagent.[19] This was done in presence of other highly reactive functional groups such as an ester (**3a**) and a nitro group (**3b**) at moderate yields.

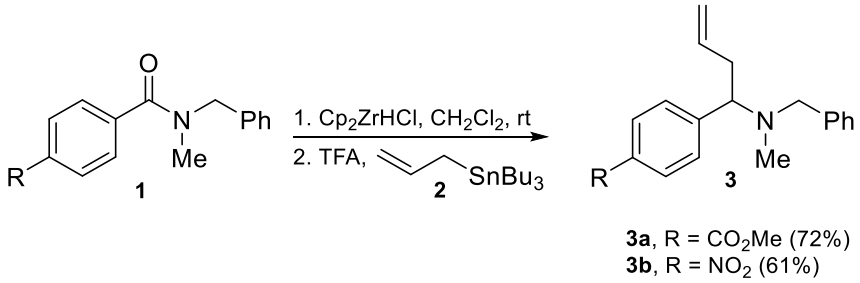

Figure 1-4 Chemoselective allylation of amide **1**

1.2.2 Regioselective Functionalization

Regioselectivity refers to the site-selective addition of an unsymmetrical reagent to an unsymmetrical substrate. A prevalent form of regioselectivity is that of *C(sp^3)-C(sp3)* bond formation on unsymmetrical alkenes. **Figure 1-5** illustrates Hou's work on hydroaminoalkylation of *N*-methylpiperidine with styrene derivatives and alkyl olefins.[20] In both cases, the reaction conditions were identical, featuring a scandium transition metal. Aryl and silyl alkenes resulted solely in linear product **6** while alkyl alkenes resulted in branched products such as **7**.

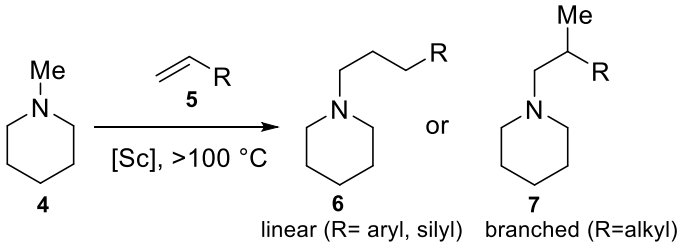

Figure 1-5 Substrate controlled regioselective hydroaminoalkylation of alkenes

1.2.3. Stereoselectivity and its Relevance in the Pharmaceutical Industry

Stereoselectivity refers to the spatial-selective functionalization of molecules with same molecular formula and connectivity. Steroselectivity is a vital concept that synthetic organist chemists take into account when designing an efficient retrosynthesis for core structures that are seen in pharmaceuticals. Of the trinity, stereoselectivity poses arguably the greatest challenge in

drug design. Currently, the FDA requires pharmaceuticals to be at least 95:5 enantio- or diastereopure. The importance of steroselectivity can be seen in a variety of pharmaceuticals including ketamine[21], thalidomide[22], albuterol[23] and dobutamine[24] (**Figure 1-6**).

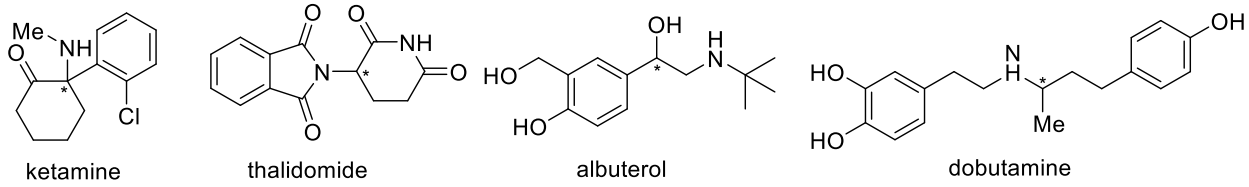

Figure 1-6 Examples of stereocenter containing FDA approved pharmaceuticals

Recently, the FDA-approved esketamine, the (*S*) enantiomer of ketamine, as an intranasal treatment for major depressive disorder (MDD).[25] Ketamine itself, is used as an analgesic, anesthetic, and antidepressant. The mode of action of ketamine is as an antagonist of the *N*-methyl-*D*-aspartate (NMDA) receptor. Esketamine has up to an eight-fold higher affinity for NMDA receptors than arketamine.[26] There have been studies performed on both animals and humans that showed that arketamine shows higher and longer-lasting antidepressant effectiveness in animal models.[27] Yet, esketamine displayed more analgesic and anesthetic activity in human trials.[28] The interest in esketamine stems from less psychotomimetic and dissociative effects seen for it than from the racemic mixture and arketamine. Relative to the racemic mixture and arketamine, esketamine reduces drowsiness, lethargy, impairment of cognitive capacity, concentration capacity and primary memory loss.[29] Exploration of stereoselective reactions is crucial since many of these compounds have significant pharmaceutical values.

The concept of stereoselective functionalization has been explored by many organic chemists and has led to the discovery of reactions that give high yields of a single stereoisomer. There has been success on the formation of *C(sp3)-C(sp3)* bonds that are both regio- and stereoselective through hydroalkylation. As seen in **Figure 1-7**, Goldfogel obtained products

such as **10**, which bear vicinal stereocenters in highly diastereoselective form from an oxazolone **8** and a 1-substituted-1,3-diene **9**.[30]

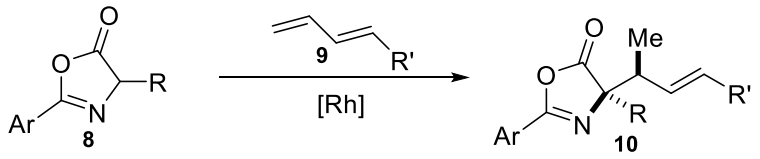

Figure 1-7 Diastereoselective branched hydroalkylation of dienes onto oxazolones

1.3 Diversity-Oriented Synthesis

Diversity-Oriented-Synthesis (DOS) in organic chemistry has become a popular method to follow. The DOS method allows for an investigation of pharmaceutical value for structurally similar compounds. Three elements of diversity in the DOS method are the building blocks, stereochemistry, and molecular skeleton that can be generated. In many cases the building blocks/ starting material are highly affordable and can be synthetically transformed into small complex molecules. The other main type of synthetic approach is Target-Oriented-Synthesis (TOS), which is used for total synthesis of compounds such as natural products. Although useful for the synthesis of compounds with known biological activity, the time commitment can be discouraging.

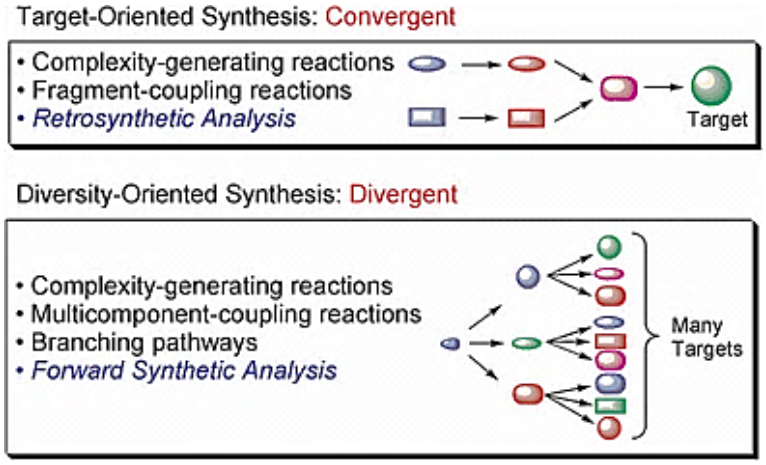

Figure 1-8 Comparison between TOS and DOS methods

One of the merits of DOS is the ability to produce a vast library of small molecules from a common precursor in a timely manner (**Figure 1-8**). Additionally, a variety of prevalent and highly coveted scaffolds found in pharmaceuticals can be used as the backbone and be easily manipulated. Small molecules are very important in the pharmaceutical field and are an intriguing research area. Another virtue of DOS is the sequential engagement of the produced compounds to structure activity relationship (SAR) studies. Unfortunately, the DOS approach can be thought of as a blind approach with the possibility of none of the produced compounds showing bioactivity. The DOS method takes advantage of the numerous examples of subtle changes within a molecule that have altered the bioactivity of the compound.

1.3.1 Structure Activity Relationship (SAR) studies

As seen in **Figure 1-9**, the three piperazine-containing drugs are HIV integrase strand transfer inhibitors (INSTI) that contain a tricyclic piperazine motif. In this tricyclic motif there is a difference in the ring's size between the three drugs. Aside from the ring size difference, bictegravir has an extra fluorine atom. Prime characteristics contributing to the success of these drugs are their high intracellular half-life, absence of a booster drug, lack of negative interactions between other anti-retroviral drugs and tolerance towards resistance from HIV-1 strains.[31] Booster drugs are known to increase the desired effect of other drugs. In HIV treatment, booster drugs include ritonavir (Norvir®) and cobicistat (Tybost®). Success of these similar structured INSTIs can be attributed to the addition of the fluoro-substituted benzyl group that can bind with hydrophobic pockets near the active site and the presence of three chelating oxygen atoms that can coordinate to Mg^{2+} ions.[32]

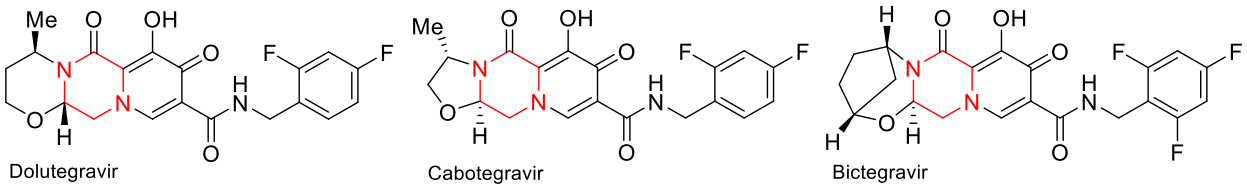

Figure 1-9 Example of structurally and bioactive similar HIV integrase strand transfer inhibitors

Dolutegravir (Tivicay®) was FDA approved in 2013 and is administered as Triumeq® (Abacavir/dolutegravir/lamivudine) or Juluca® (dolutegravir/rilpivirine).[33] It has proven effective in the treatment for HIV/AIDS in pediatric patients[34], transmittance prevention from infected mother to child[35] and individuals whose current treatment was inadequate.[36] Moreover, it is used as a once-daily dosing option for first time treatment patients. The main structural difference of dolutegravir is the six-membered *O*-heterocycle fused to the piperazine ring.

Bictegravir (Biktarvy®) is used in the treatment of HIV-1 infected in adults as a first treatment option or replacement for a virological suppressed treatment.[37] Biktarvy was FDA approved in 2018 and is administered once-daily in combination with emtricitabine and tenofovir alafenamide. Furthermore, it shows superior antiviral activity against HIV-1 isolates with advanced INSTI resistance when compared to dolutegravir. The ring structure on this drug is unique since it is bridged [3.2.1]octane containing two heteroatoms.

Cabotegravir is currently in phase 3 for FDA approval and can take on two different forms: a long-acting nanosuspension and tablets.[38] The main difference being the administration time and route which are monthly or quarterly subcutaneous or intramuscular for the nanosuspesnion or daily for oral tablets. It has similar characteristics as dolutegravir yet it has a longer half-life. The longer half-life can be attributed to the rigid 5-membered ring it possesses in contrast to the 6-membered ring on dolutegravir.[38] Moreover, cabotegravir has the potential to be utilized as both a treatment and prevention option.[39]

A common study performed on the three drugs was to assess antiviral activity in a short-term monotherapy of 10 days.[40–42] Change of HIV-1 RNA present after 11 days was recorded at a scale of $\log_{10}$ copies/mL. Dolutegravir doses were 2, 10 and 50 mg which resulted in a decrease of HIV-1 RNA of 1.51, 2.03 and 2.46, respectively. Bictegravir results were 1.45, 2.08, 2.06 and 2.43 decrease of RNA for 5, 25, 50 and 100mg, respectively. Cabotegravir quantities were 5 and 30 mg which resulted in the RNA decrease of 2.2 to 2.3, respectively. The results indicate that Dolutegravir works the best at 50 mg when compared to bictegravir and cabotegravir. Surprisingly, the only non-FDA approved drug demonstrated similar depletion of HIV-1 RNA at both small and large quantities. Additionally, all three drugs were well tolerated with no safety issues.

1.4 Current approaches towards functionalized piperazines

There is a notable trend within synthetically derived FDA-approved piperazine containing drugs, which is the lack of functionalization on the carbon atoms. Currently, around 80% of FDA-approved piperazines contain substituents only on the nitrogen atoms.[43] This adversity has been reduced by introducing functionality on diamine or amino acid derived acyclic precursors and α-C–H functionalization on intact piperazines.

1.4.1 Tin (Sn) Amine Protocol (SnAP) and Silicone Amine Protocol (SLAP) reagents

A well-established method for formation of substituted piperazines was developed by Bode using Tin (Sn) Amine Protocol (SnAP) reagents (**Figure 1-10**).[44] A combination of SnAP reagents (**11**) and aldehydes (**12**) are used to construct multiple azaheterocycles, including thiomorpholines, morpholines, and piperazines. The ability to use electron-poor, electron-rich, hetero-aromatic, and aliphatic aldehydes along with possible addition of methyl groups on the SnAP reagent has attributed to the outstanding contribution this protocol has made in constructing *N*-heterocycles including piperazines. An intermediate imine is formed between the SnAP reagent and aldehyde. At this stage, there is an addition of $Cu^{(II)}$ which helps form a stable radical that can undergo *6-endo* cyclization with the intermediate imine to form the functionalized piperazines. Recently, a synthesis yielding higher carbon functionality was reported using cyclic ketones (**14**) and SnAP reagent, which resulted in a ketimine intermediate and ultimately a spirocyclic compound containing a piperazine (**15**).[45] Unfortunately, the use of a toxic tin reagent has been a major downfall in the protocol. **Figure 1-10** illustrates how this issue has been mitigated by the introduction of Silicon Amine Protocol (SLAP) reagents (**16**) by the same group.[46] Both of these processes are highly modular, yet lack enantioselectivity.

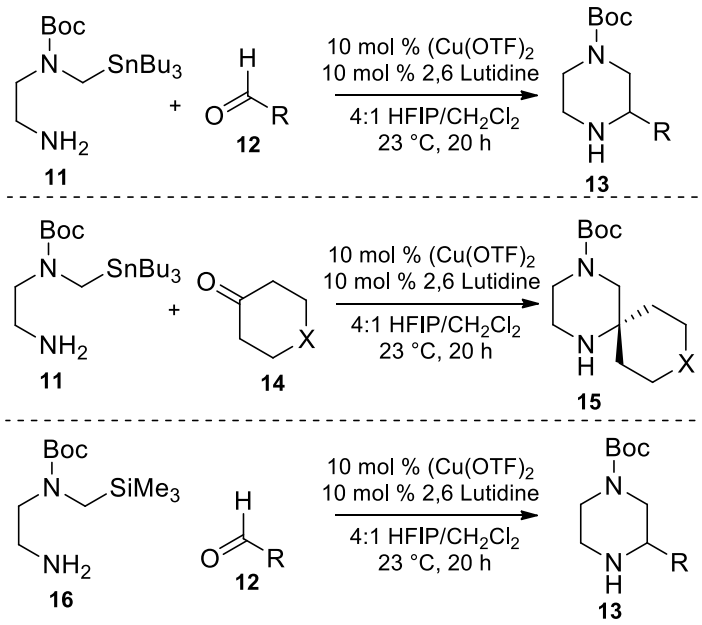

Figure 1-10 Bode's work with SnAP (top and middle) and SLAP reagents (bottom) on piperazines ring

1.4.2 Annulation reaction via phenylvinyl sulfonium salts

Cycloadditions are a common way to form six-membered rings and this does not exclude *N*-heterocycles. Aggarwal's group demonstrated a [4 + 2] annulation reaction between β-amino amines and diphenylvinylsulfonium triflate to construct the piperazine motif. In the initial protocol there are two major setbacks (i) the preparation and scalability of the vinylsulfonium salt due to its sensitive and oily nature and (ii) inability for substituents to be placed on both sides of the ring. To overcome the first obstacle, conditions for *in-situ* generation of the vinylsulfonium triflate were investigated and optimized. This was done by using a bromoethyl sulfonium salt (**18**) and treating it with sodium hydride.[47] The second setback was addressed by using α-phenylvinylsulfonium salts (**20**), yet only phenyl groups were appended and yields and diastereoselectivity were fairly low (**Figure 1-11**).[48]

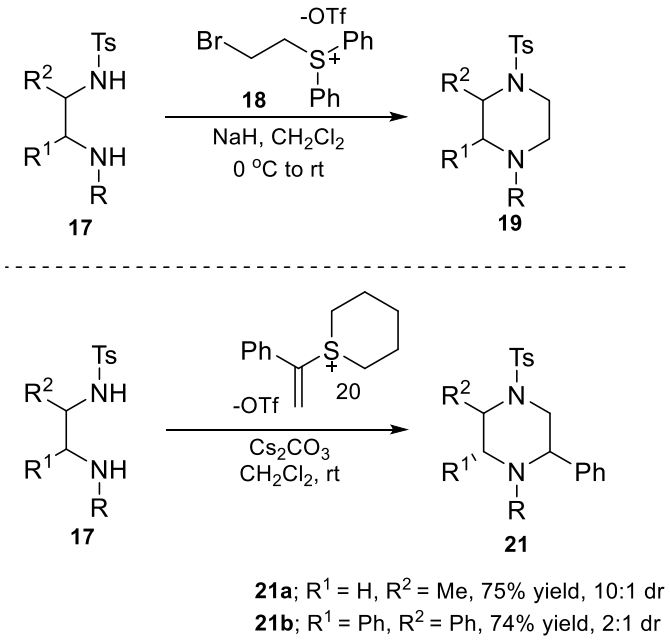

Figure 1-11 Two approaches towards functionalized piperazines via *in-situ* generated phenylvinylsulfonium salts (top) and pre-generated α-phenylvinylsulfonium salts (bottom)

1.4.3 Transition Metal Catalyzed Approaches

Transition-metal based catalysis has also been employed to form highly substituted piperazines. This can be seen in the works of Wolfe and Nelson that used palladium catalyst [49] and gold catalyst[50], respectively (**Figure 1-12**). The merits behind these works is the asymmetric products that are achieved. Notably, Wolfe's work is highly modular and stereoselective with the final product (**28**) having four substituents around the ring. This reaction uses a Pd-catalyst for carboamination across an alkene. This forms two new vicinal bonds, an intramolecular C(sp^3)-N(sp^2) bond and intermolecular C(sp^3)-C(sp^3) bond to produce the piperazine. Additionally, Wolfe's group demonstrated a vast selection of functionalization on the nitrogen atoms unlike other groups who required a Boc group or had no substituent.

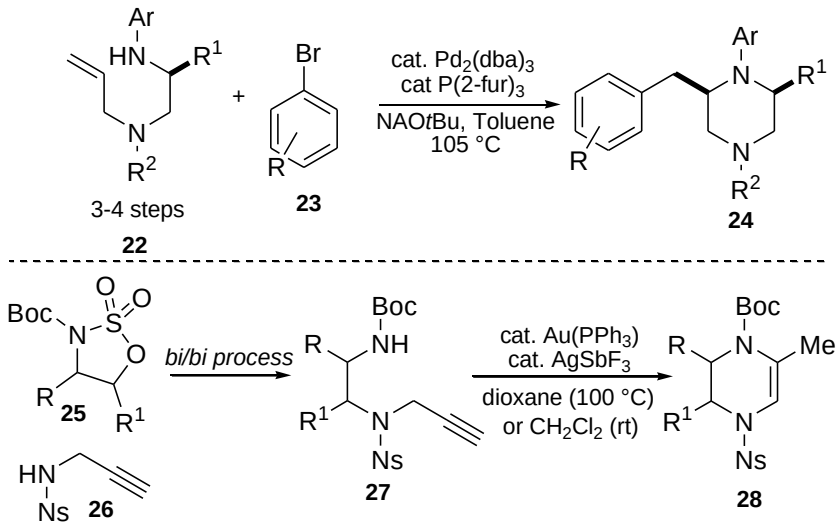

Figure 1-12 Two transition metal-based strategies towards functionalized piperazines

1.4.4 Formation of monoketopiperazines

The interest for highly substituted piperazines is continuous which has lead groups to investigate piperazine derivatives such as vicinal ketopiperazines. This has led to multiple methods for the construction of this motif such as those employed by Dömling[51], Viso[52], Denoyelle[53], Procopiou[54], Powell[55] and Kokotos[56]. Although useful, many of these tactics have major setbacks including lack of stereocontrol, lack of modularity, costly catalysts and/or excessive steps. It is important to mention that Viso's synthesis, although step heavy, allows for isolation of various ketopiperazine derivatives along the way, all of which are potential pharmaceuticals.[52] The acyclic precursors are highly accessible and can be treated with chloroacetyl chloride to generate *N*-sulfinyl ketopiperazines (**29**). Elimination of the sulfur moiety renders an imino ketopiperazine (**30**) which was used to add various alkyl tethers by nucleophilic additions. There is a slight drawback of the reaction since it requires a protecting group that is kept throughout. The Viso group demonstrated cyclization to a piperazine without the protecting group on a single substrate, yet the yield was compromised.

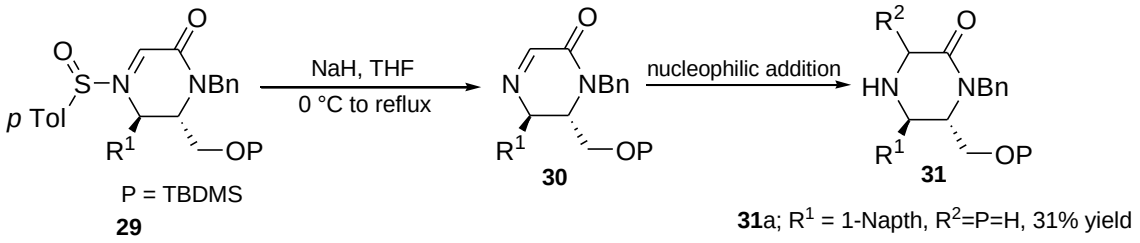

Figure 1-13 Preparation of functionalized monoketopiperazines

1.4.5 Piperazine formation through a cascade reaction

In organic chemistry, the pursuit for cascade reactions is significant since it lowers the number of steps and can increase the overall yield. This strategy has been employed by the Carreira group through ring expansion of spirocycles (**34**) derived from 3-oxetanone (**33**) to form *N*-heterocycles including morpholines, thiomorpholines and piperazines (**Figure 1-14**).[57] A combination of two known forms of reactivity (i) ring strain and (ii) Lewis basicity of ethers were used as their starting point to explore cascade reaction conditions. A cyano nucleophile was appended onto the piperazine via trimethylsilyl cyanide (TMSCN) which allows for post-diversification of the piperazine.

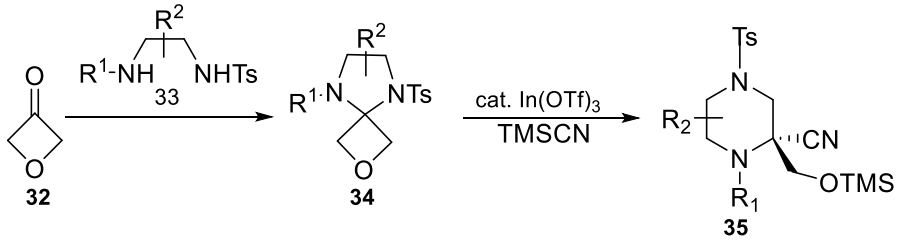

Figure 1-14 Ring expansion protocol for functionalized piperazines

1.5 Peripheral functionalization of intact piperazine rings

Formation of highly functionalized piperazines from acyclic precursors is well established yet there lies an interest in peripheral functionalization on the piperazine ring itself. There are currently three main methods of α-C–H functionalization on piperazines: transition-metal-catalysis, lithiation trapping and photoredox catalysis.

1.5.1 Hydroaminoalkylation promoted by transition metal catalyst

As previously mentioned transition metal (TM)-catalysts are known to produce highly substituted piperazines from acyclic precursor. Fortunately, TM-catalyzed functionalization falls at both ends of the spectrum and can also be used for α-C–H functionalization on intact piperazines. As seen in **Figure 1-15**, through the use of a transition metal-catalyst such as tantalum, C(sp^3)-C(sp^3) bonds have successfully been formed using simple alkenes, styrenes and cycloalkenes via hydroaminoalkylation.[58] This method has resulted in diastereoselective α-C–H functionalization on piperazines yet it has two main shortcomings: (i) costly TM-catalysts and (ii) the use of high temperatures for product formation.

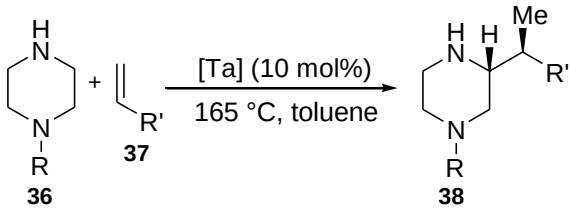

Figure 1-15 Synthesis of carbo-substituted piperazines by tantalum catalyzed hydroaminoalkylation

1.5.2 Enhanced method for lithiation-trapping on piperazines

Direct α-lithiation and electrophile trapping for α-functionalization of *N*-Boc azaheterocycles involves more concrete and atom-economic procedures making it a prevalent used method. Originally, McDermott established the possibility of lithiation-trapping chemistry on piperazines.[59] Unfortunately, yields and enantioselectivity were low. O'Brein proposed that the setbacks in McDermott's work included (i) the electrophile and (ii) the second *N*-substituent. Development of an enantioselective lithiation-trapping protocol was rightfully anticipated after addressing the limitations.[60,61] Presence of a sterically hindered *N*-alkyl group such as *N*-*tert*-butyl or *N*-α-methylbenzyl increased the yield with *N*-α-methylbenzyl being preferred due to it

being readily removable. As suspected by O'Brien, the electrophile chosen was crucial for an increase of yield (**Figure 1-16**).

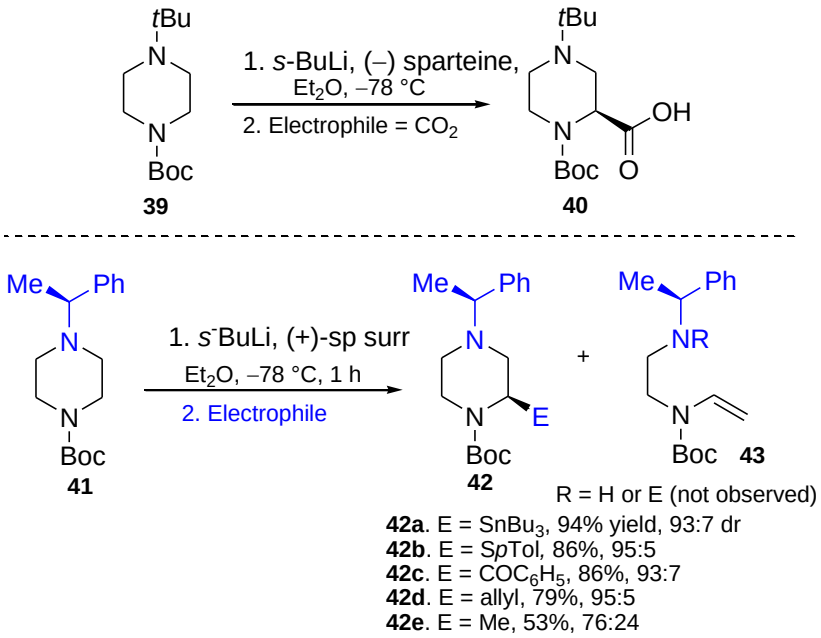

Figure 1-16 McDermott (top) and O'Brien (bottom) approach towards lithiation-trapping on piperazines

1.5.3 Functionalization of piperazine by photoredox activation

Lately, direct photoredox C–H activation of the α-position of amines, piperidines, morpholines and *N*-Boc piperazines has been an implemented for functionalization.[62] Excitation of an iridium III complex, such as $Ir(ppy)_3$ by a photon from a 26-W light source generates an excited $*Ir^{III}(ppy)_3$ complex which is a reductant. A single electron transfer (SET) with an arene (**45**) produces an arene radical anion species and $IrI^{V}(ppy)_3$, the latter of which is an oxidant. Likewise, the newly formed complex can undergo a SET with an azaheterocycle (**44**) to generate a radical cation leading to the radical-radical coupling and formation of product. Unfortunately, photoredox catalysis for direct α-C–H functionalization of piperazines has not been highly explored and is currently limited on the number of examples (**Figure 1-17**).

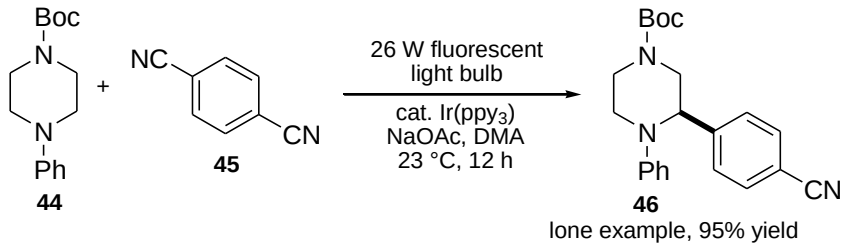

Figure 1-17 Functionalization of intact piperazine ring by photoredox chemistry

1.5.4 Enolate functionalization of piperazines

Although these three previously mentioned strategies appear to be the most popular other methods are being introduced for α-C–H functionalization. Enolate functionalization has recently been used as a method to obtain substituted piperazines. In 2012, enolate functionalization on piperazines was demonstrated as an intermediate towards homopiperazines.[63] Cossy's work focuses on the formation of piperidines and azepanes with a sole example on the piperazine (**Figure 1-18**). Although the enantioselectivity is high on piperidines and azepanes, it was unreported for the piperazine example. This of course should not lead others from this type of carbon functionalization. **Figure 1-18** also demonstrates Stoltz approach towards enantioselective decarboxylation allylic alkylation to produce highly substituted piperazines using enolate functionalization. There were two main setbacks as yields were low and hardships were faced in post-diversification of the *N*-substituents.[64] However, both of these setbacks were addressed mainly by replacing the previous benzyl group with a Boc group. In this instance, the electron-withdrawing nature of the Boc group reduces the nucleophilicity of the nitrogen, allowing for formation of different piperazinones via enolate functionalization of the dicarbonyl precursor.[65]

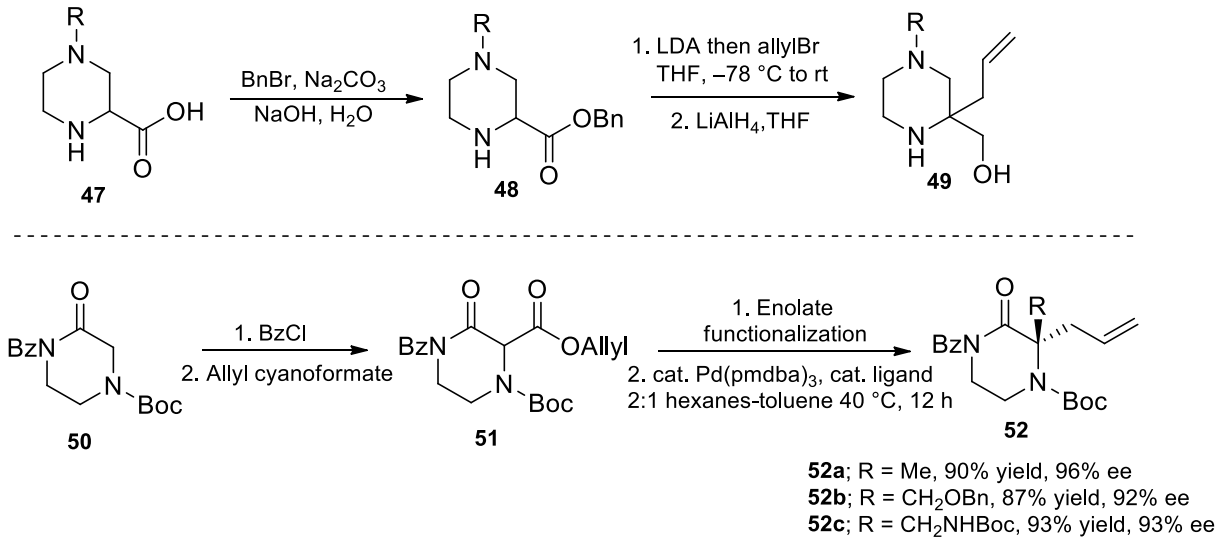

Figure 1-18 Enolate alkylation as a precursor for ring expansion (top) and for enantioselective synthesis of gem-substituted piperazines (bottom)

1.6 Significance of fluorine chemistry

In the previously mentioned syntheses, it was demonstrated that a fluorine atom can be incorporated onto the piperazine containing compound. **Figure 1-19** illustrates an array of piperazine and fluorine containing compounds including those from Bode's SnAP (**13a**) and SLAP protocols (**13b**), Wolfe (**53**), Nelson (**54**), Viso (**55**), and Stoltz (**56**) works. Integration of fluorine atoms in possible drug candidates has become a popular practice owing to its electronegativity, size, stability of C-F bond vs a C-H bond and lipophilicity compared to hydrogen.[66] A fluorine atom is known to increase the bioavailability of drug sand drug candidates by three different modes: improving metabolic stability, increasing binding affinity and altering physicochemical properties.[67]

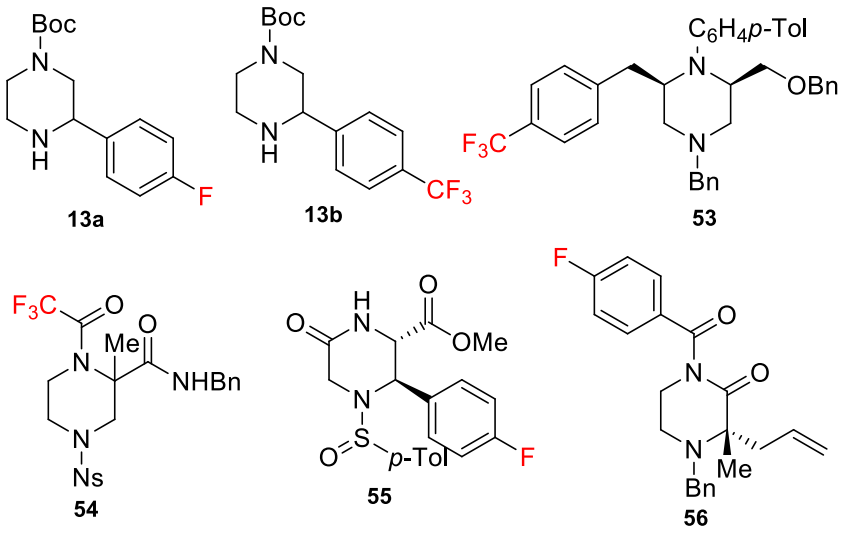

Figure 1-19 Representation of fluorine containing piperazines from previous examples

Metabolic stability is a challenge that is continuously faced in the drug discovery realm which can be confronted by the addition of fluorine at the site of metabolic attack. Fluorine atoms stabilize the site of substitution, as well as adjacent and distal sites by inductive/resonance or conformational/electrostatic effects. Specifically, this can inhibit oxidative metabolism since a C–F bond is more resistant to metabolism than a C–H bond. A fluorine atom can take part in hydrogen bonding which increases binding affinity and stabilizes the compound at the drug-receptor site. Many physiochemical properties are effected by a fluorine such as the pKa, dipole moment, chemical reactivity, stability, cLogP, ADME properties and solubility of the compound. The inductive effect attributed to F atoms can lower the pKa of the compound including heterocycles which become less basic with β-, γ- and δ- fluorine substituents. This can help in overcoming the lack of diffusion of drugs such as in the brain blood barrier. Fluorine atoms also allow drugs to be more suitable for oral administration which is preferred by both physicians and patients.

1.6.1 Relevance of fluorine containing piperazine scaffolds

As seen in **Figure 1-20**, there are currently a number of examples of fluorine present in compounds containing a piperazine ring.

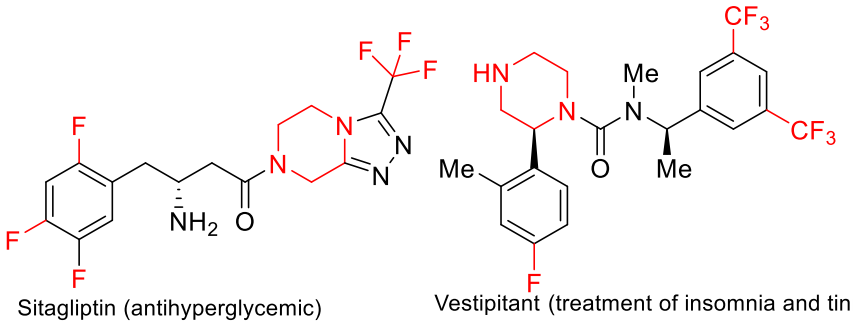

Figure 1-20 Examples of fluorine and piperazine containing bioactive compounds

Sitagliptin (Januvia®) is a competitive inhibitor of dipeptidyl peptidase 4 (DPP-4) and is used to treat type 2 diabetes. Inhibition of DPP-4 increases activity of glucagon-like peptide-1 (GLP-1) and glucose-dependent insulinotropic polypeptide (GIP) which are involved in stabilizing and maintaining the proper amount of insulin and glucagon.[68] There are minimal side effects contributed with sitagliptin such as cardiovascular trouble[69] and weight gain[70] that can be seen in other similar drugs. Sitagliptin contains a trifluoromethyl containing triazole-fused piperazine along with a trifluorinated aryl ring.

Vestipitant is a neurokinin-1(NK-1) receptor antagonist which binds substance P with potential for the treatment of insomnia and tinnitus. Substance P is a neurotransmitter and a neuromodulator. The effectiveness of vestipitant has been demonstrated on primary insomnia which improved sleep continuity by reducing wake after sleep onset (WASO), increasing total sleep time (TST) and increasing rapid eye movement (REM) sleep.[71] These type of receptors are also located in the inner ear giving confidence for its potential treatment of tinnitus.[72] There are three fluorinated positions including two trifluoromethyl groups and one monofluoro atom. Unlike other piperazine rings, one nitrogen atom does not have a substitutient.

1.6.2 Synthetic applications focused on fluorinated piperazines

As previously stated, multiple groups have incorporated fluorine atoms yet the focus was not precisely on this modification. Bode adapted the SnAP protocol to an azido SnAP protocol to facilitated condensation between regular SnAP reagent and acyclic ketones (**Figure 1-21**).[45] Intermediate ketimines are formed by Staudinger and aza-Wittig reactions. Unfortunately, the three examples resulted in low yields (43% highest). Likewise, **Figure 1-21** also demonstrates Sánchez-Roselló reported fluorination of piperazines through the Ruppert-Prakash reagent trifluoromethyltrimethylsilane ($TMSCF_3$).[73] Nucleophilic addition of the Ruppert−Prakash reagent has been a popular method in organic synthesis to add a trifluoromethyl group. Ellman's *N*-(*tert*-butanesulfinyl)imine (**60**) was the key intermediate for addition of the trifluoromethyl group. The resulting diastereoselective $–CF_3$ bearing piperazines are unique and unexplored, unfortunately the described synthesis is step-costly. The main issue being that the synthesis of the enantioselective diamine is step-uneconomical.

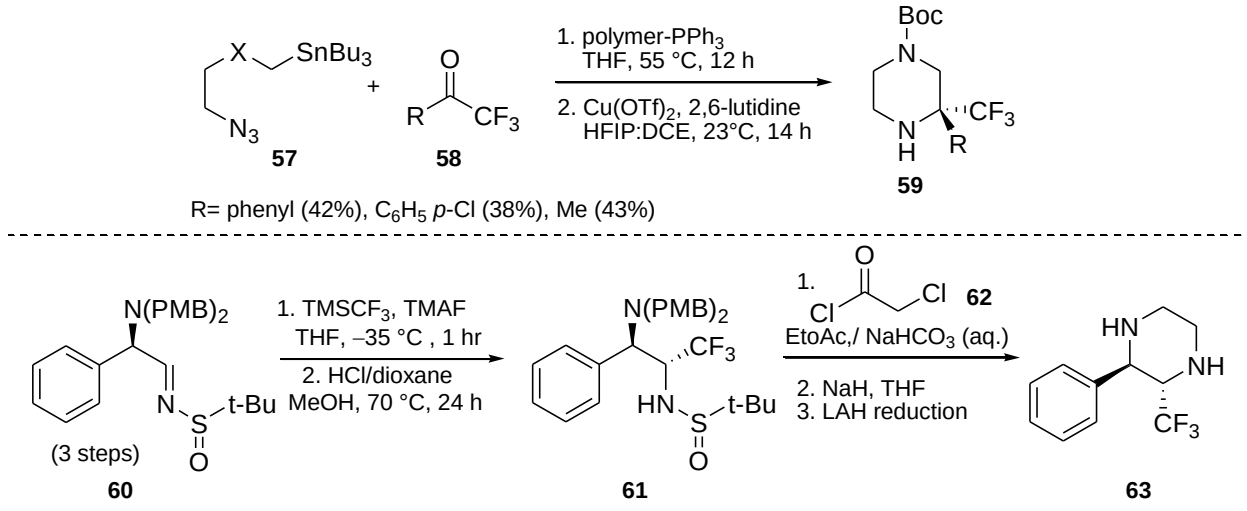

Figure 1-21 Preparation of fluorine containing piperazines

1.7 Statement of Purpose: The specific aims of this thesis are as follows:

- Develop a modular and stereoselective protocol for the construction and post-diversification of vicinally functionalized and fluorinated piperazines.
- Investigate the scope and mechanism of intramolecular hydroalkylation of novel piperazinonates.

CHAPTER 2: MODULAR ACCESS TO VICINALLY FUNCTIONALIZED AND FLUORINATED PIPERAZINE DERIVATIVES USING A READILY AFFORDABLE CYCLIC ANHYDRIDE

2.1 Introduction

The prevalence of the piperazine ring in natural products and FDA-approved pharmaceuticals has granted it the status of a privileged scaffold. This title is aggrandized by the variety of biological activities it exhibits, including antidepressant, antipsychotics, antibacterial, and antiretroviral properties (**Figure 2-1**).

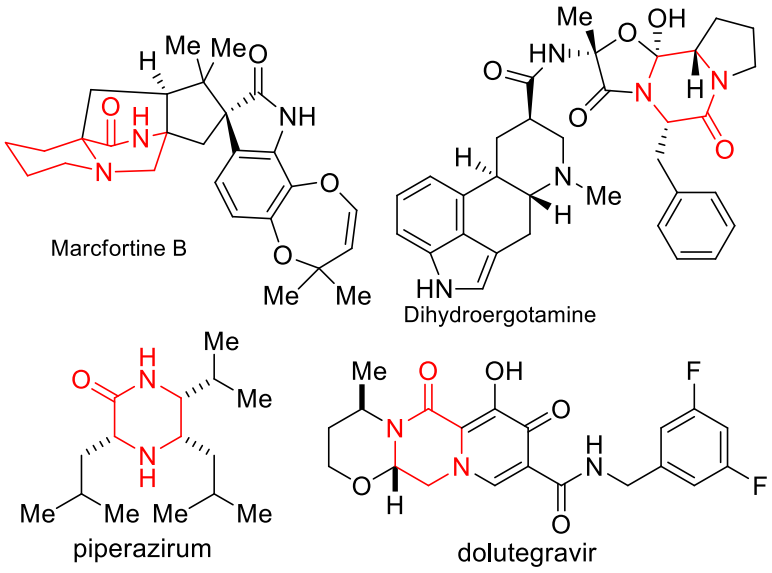

Figure 2-1 Examples of bioactive (keto)piperazines

The addition of a fluorine atom on organic compounds has become a common tactic to alter physicochemical properties and potentially enhance bioavailability.[66,67,74] Specifically, fluorine atoms substitute hydrogen atoms in multiple ways including single hydrogen, methyl group and displacement of multiple hydrogens around a phenyl ring. This is explained by the relative small size of a fluorine atom (1.47 Å) and its high electronegativity.[74] Therefore, merging these two components can be beneficial to the synthetic and medical communities.

As previously stated, methods for carbo-functionalization on piperazines are relatively scarce. Nevertheless, their prevalence in natural products and FDA-approved pharmaceuticals continues to attract the attention of many organic chemists. Some notable strategies include Bode's SnAP[44,45] and SLAP[46] methodology, Agarwaal's [4 + 2] cycloaddition using phenylvinylsulfonium salts[47,48,75], transition-metal catalysis[49,50,58], enolate functionalization as employed by Stoltz[64,65], etc. Although successful, the necessity of costly catalysts, potential health hazards, step-uneconomical, limited modularity and lack of post diversification opportunities has maintained an interest for improved synthetic pathways to the piperazine scaffold.

The Castagnoli-Cushman reaction (CCR) has been identified as a viable way to construct vicinally functionalized azaheterocycles in a modular and step-economical fashion. Advantages of the CCR is the use of feedstock chemicals such as aldehydes, amines and anhydrides, the highly diastereoselective and modular nature, which bodes well for structure-activity relationship (SAR) studies. Initial studies on the CCR were done through reactive cyclic anhydrides such as homophthalic anhydride[76] (**Figure 2-2A**) and succinic anhydride.[77] The scope of the CCR anhydride has also recently been expanded to functionalized sulfone- and cyano-substituted pyrrolidines[78,79], piperidines[80], morpholines and thiomorpholines[81] and benzannulated azepanes.[82]

Our group has contributed to the success of the CCR by reacting commercially available cyclic anhydrides such as glutaric anhydride and digylcolic anhydride with 1,3-azadienes to generate highly functionalized allylic piperidines[83] and morpholines,[84] respectively. The method included subjecting the lactamoyl ester precursor to a Vilsmeier-Haack reaction to append two functional handles; a chloride and a formyl group. The chloride handle was subsequently

employed as a functional handle for cross-coupling to arrive at 2,3,5,6 dihydropiperidines via transition-metal catalyzed cross-couplings.[83] This highly modular approach allowed for efficient alkynylations, alkenylations and arylations of tetrahydropyridines. Additionally, we have also been able to access functionalized bicyclic morpholines.[84] This was achieved by subjecting the lactamoyl esters to a Grignard addition to form a tertiary alcohol. The resulting lactam-bearing alkenol was engaged in a copper-catalyzed intramolecular dehydrogenative alkoxylation.

In recent years, Krasavin and co-workers have revealed that tosyl-substituted *N*-heterocyclic anhydrides such as **4** (prepared in at least three steps from commercially available diacids) participate in the CCR with aryl aldimines of type **5**, leading to adducts such as **6** (**Figure 2-2B**).[81] Gleaning from these prior reports, and in the wake of our recent success with CCR methodology,[85,86] we sought to evaluate the performance of novel and easy-to-prepare *N*-heterocyclic anhydride **7** in annulation protocols featuring several reactive partners, including lactim ethers, imidoyl chlorides, aryl aldimines such as **5**, and 1,3-azadienes of type **9** (**Figure. 2-2C/D**). We reasoned that successful implementation of the planned strategy would likely expand the chemical space for the discovery of new fluorinated piperazine pharmacophores. Detailed efforts toward the implementation of our plans are herein disclosed.

2.2 Results and Discussion

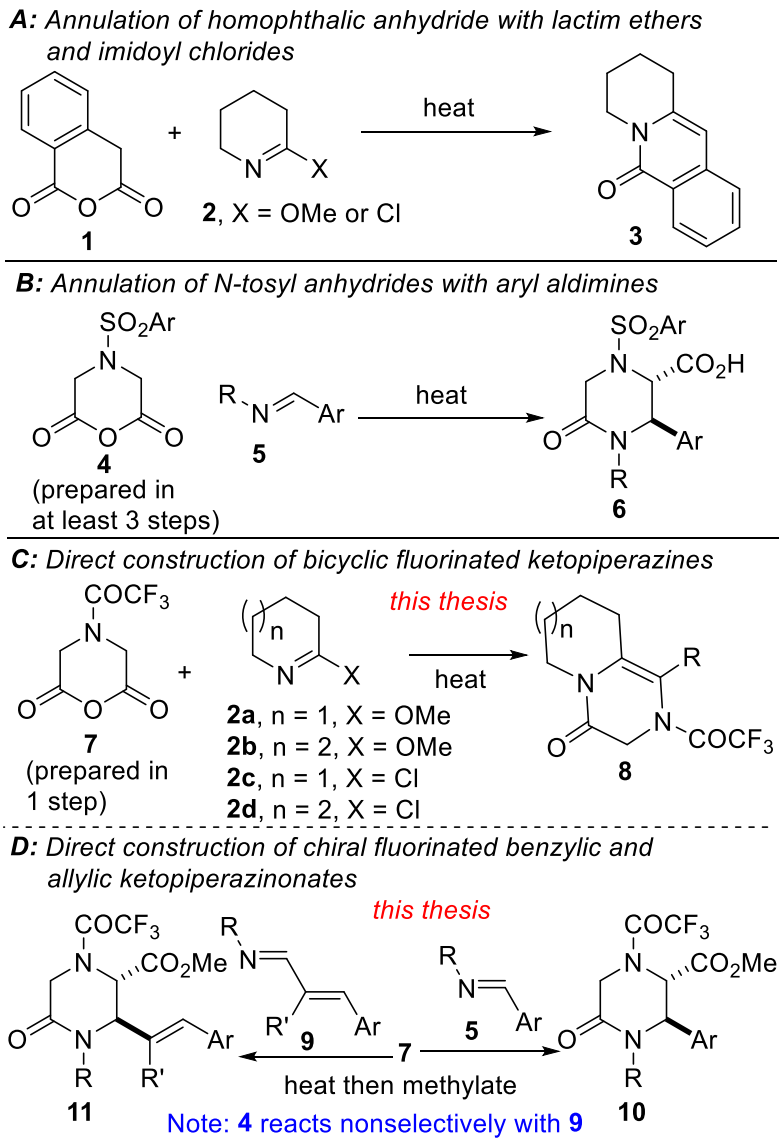

Figure 2-2. Previous studies on the CCR and our proposed plan for accessing fluorinated and vicinally functionalized (bicyclic) ketopiperazines

We initiated studies on the construction and post-diversification of vicinally functionalized fluorinated ketopiperazines using commercially available lactim ether **2a** as the model annulation partner for **7** (prepared in one step from commercially available iminodiacetic acid, see **Scheme 2-1**). Encouragingly, when an equimolar mixture of **2a** and **7**, in benzene, was

heated to 90 °C, a clean chemoselective annulation reaction occurred and CCR product **8a** was obtained in 49% yield along with unreacted starting materials (**Table 2-1**, entry 1). Reaction optimization was carried out and it was established that toluene out-performs other reaction media (*e.g.*, benzene, xylenes, chlorobenzene, 2-MeTHF, DMF and 1,4-dioxane). Much like homophthalic anhydride **1**, the strong electron-withdrawing prowess of the trifluoroacetyl group presumably enhances the *α-CH acidity* of **7** and renders it a competent substrate for the annulation. Of note, [6,6]-bicycles of type **8a** constitute the core of several pharmaceuticals, including the most recent antiretroviral approved for the treatment of HIV-1 infection (*i.e.*, dolutegravir, see **Figure 2-1**).

Table 1 Optimization of the annulation of lactim ether **2a** with anhydride **7**

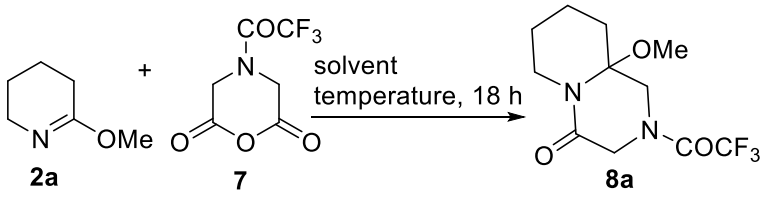

2a **7** **8a**

Entry	solvent	temp (°C)	% Yield of **8a**
1	benzene	90	49
2	xylenes	140	57
3	chlorobenzene	120	70
4	2-MeTHF	100	<5
5	toluene	110	88
6	DMF	110	0
7	1,4-dioxane	110	12
8	toluene	100	69[a]
9	toluene	120	81[b]
10	toluene	150	52[c]

(a) after 36 h, (b) after 16 h (c) after 6 h

As further illustrated in **Scheme 2-1**, **7** reacts satisfactorily with homologous lactim ether **2b** to furnish [7,6]-bicycle **8b**. The ability to retain the methoxy group is noteworthy given that cyclic *N*,*O*-aminals of type **8a/b** are suitable synthons for further diversification whereby the methoxy group serves as a functional handle.[87–90]

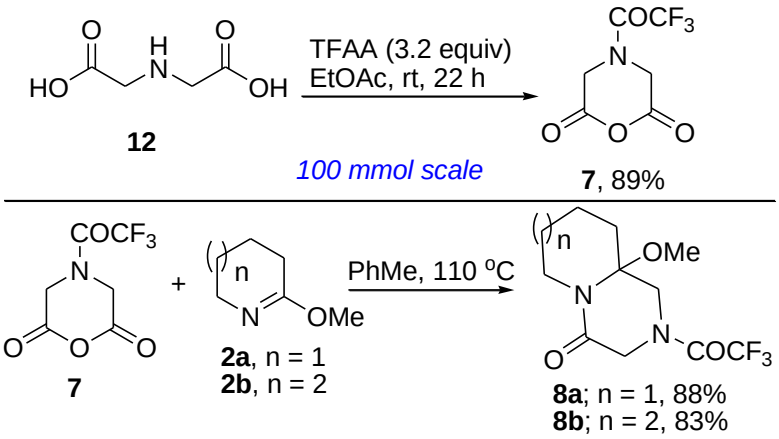

Scheme 2-1. Synthesis and annulation of anhydride **7** with lactim ethers

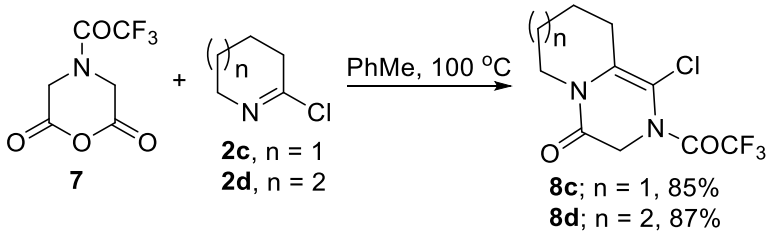

Scheme 2-2. Annulation of **7** with imidoyl chlorides

Imidoyl chlorides such as **2c/d** react competently with **7** (**Scheme 2-2**). However, in this scenario, a cascade process ensues whereby decarboxylation and elimination are accompanied by concomitant chlorination of the inherently nucleophilic C3 position of the bicyclic enaminone (see **8c/d**). The mechanistic nuances of this cascade process are still being fleshed out.

Recognizing the merits of the Castagnoli-Cushman reaction[77] *(e.g.*, the use of feedstock chemicals such as amines, aldehydes and cyclic anhydrides to readily access nonplanar sp^3-enriched core structures bearing vicinal stereocenters), the performance of fluorinated anhydride **7** in annulation protocols featuring aryl aldimines was evaluated. In the event, we found that **7** undergoes a stereoselective and efficient cycloaddition with aryl aldimines of type **5** followed by methyl esterification to furnish vicinally functionalized ketopiperazines such as **10** (**Scheme 2-3**). In all cases, the *trans* adducts were obtained as the predominant diastereomer (as judged by

coupling constant analyses). The relative configuration is also consistent with Krasavin's complementary findings on *N*-tosyl anhydride **4**.[81] Imines harboring *N*-benzyl- or *N*-alkyl substituents outperform their *N*-aryl counterparts (see **10b** *vs* **10c**). The reaction tolerates mainly electron-rich aryl aldimines, including ones bearing benzyloxy (see **10j/m**) and allyloxy groups (see **10k**). As exemplified through the synthesis of thiophene-bearing 2-oxopiperazine **10p**, heteroaryl aldimines react satisfactorily with **7**. The successful annulation of **7** with **5** is noteworthy given that the *N*-Boc congener is an incompetent reactive partner.[81]

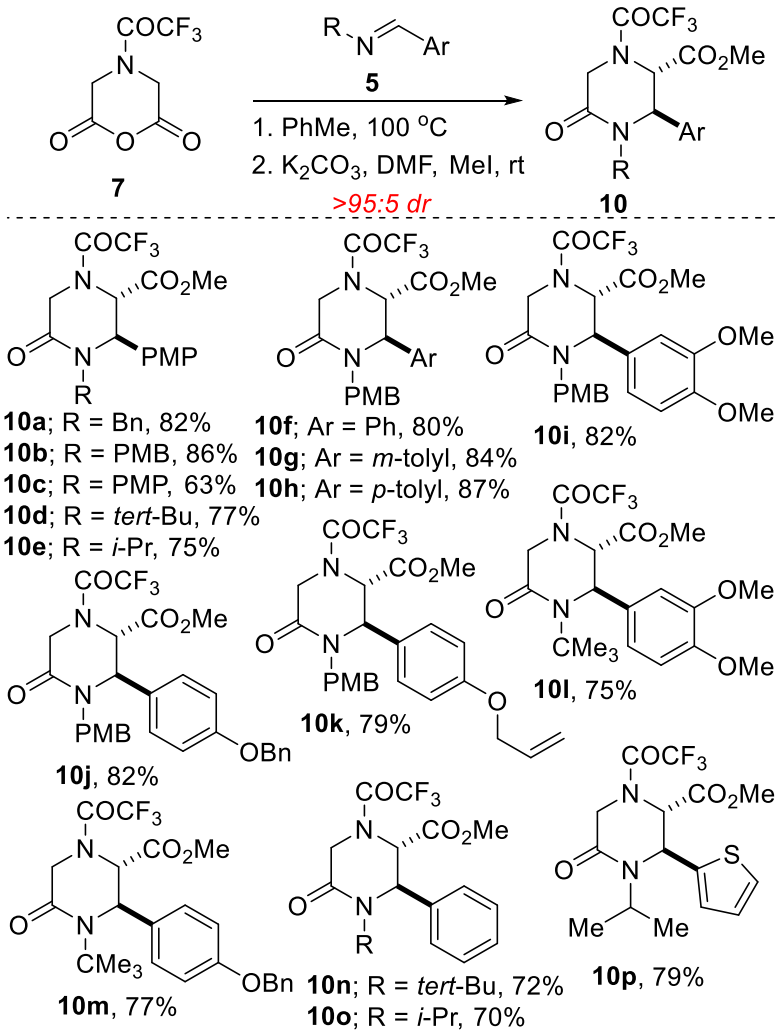

Scheme 2-3. Annulation of **7** with diversely *N*-substituted aryl aldimines

Following successful construction of a small library of vicinally functionalized fluorinated benzylic 2-oxopiperazines, we next sought to prepare their allylic congeners. The installation of an alkenyl motif on the skeleton of a piperazinic acid could pave the way for harnessing reactivity modes such as halolactonization,[91] dehydrogenative alkoxylation,[84] and dehydrative coupling.[86] Towards this end, the amenability of 1,3-azadienes of type **9** to a CCR with **7** was explored. We were cognizant of the notoriously promiscuous reactivity of **9** with cyclic anhydrides bearing relatively acidic *α-CH protons.* For example, homophthalic anhydride reacts with **9** to afford a plethora of products, including Tamura-like, Castagnoli-like, and Perkin-type products.[92] Meanwhile, **9** reacts efficiently with glutaric anhydride and diglycolic anhydride to furnish exclusively the CCR products.[85] In the event, **7** reacted chemoselectively with several differentially substituted 1,3-azadienes to afford the vicinally functionalized allylic ketopiperazines depicted in **Scheme 2-4**. Strikingly, unlike **7**, tosyl-bearing anhydride **4** reacts non chemoselectively with **9** and furnishes a complex mixture. This result further highlights that minor structural modifications of the anhydride component can lead to profound changes in chemoselectivity when 1,3-azadienes are employed.

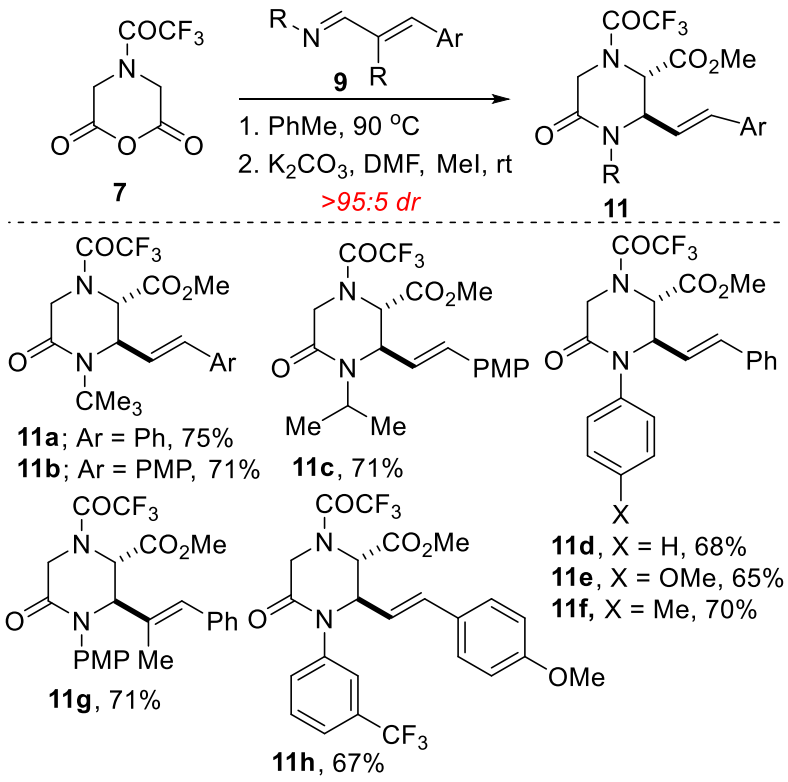

Scheme 2-4. Annulation of 1,3-azadienes with *N*-trifluoroacetyl anhydride **7**

A potentially beneficial aspect of this methodology is the scalable nature of the reactions given that products such as **8a**, **8d**, **10m**, **11a**, and **11c** have been prepared in gram scale, without any compromise in efficiency. This has set the stage for post-diversification studies. For example, fully substituted dihydro-1,4-diazines are affordable when piperazinonates such as **11c** are subjected to a lactam-selective Vilsmeier-Haack reaction (**Scheme 2-5**, see **12**). This outcome illustrates an example of scaffold hopping through the construction of a diazinic topology from a piperazine, which is resident in various alkaloids that exhibit a wide array of biological activities, including antitumor and antiparkinsonian properties (*e.g.*, saframycin).[93] One of the inherent limitations of CCR methodology is the futility of imines derived from enolizable aldehydes such as hydrocinnamaldehyde given that their enamine tautomers readily undergo acylation reactions with the anhydride component.[81] Using the current approach, this

limitation can be side-stepped through catalytic hydrogenation of the alkenyl motif resident in allylic lactamoyl ester **11a** (see **13**). Sodium borohydride-assisted chemoselective reduction of the ester group present in **10m** and concomitant removal of the trifluoroacetyl group affords β-aminoalcohol **14** in good yield. We have found that removal of the trifluoroacetyl group under very mild conditions is achievable when a mixture of **10b** in dichloromethane is stirred at room temperature in the presence of pyrrolidine (see **15**).

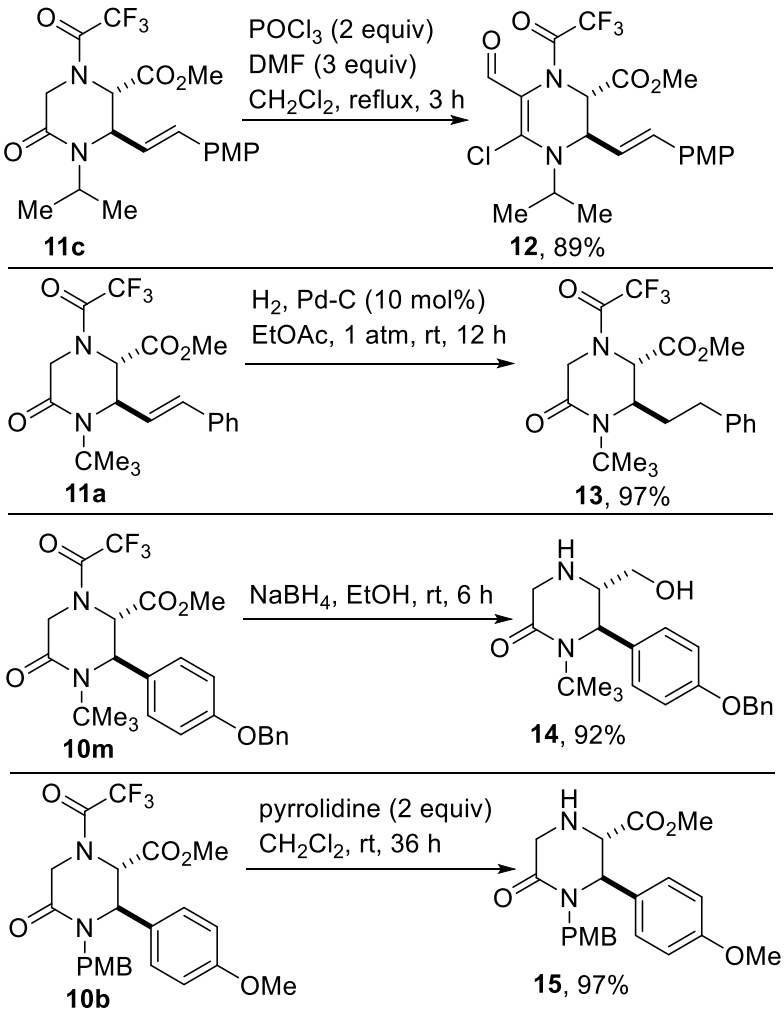

Scheme 2-5. Elaboration of functionalized fluorinated ketopiperazines

2.3 Conclusion: In summary, a small library of vicinally functionalized fluorinated bicyclic, benzylic, and allylic ketopiperazines has been constructed by engaging a readily affordable cyclic *N*-trifluoroacetylated anhydride in annulative protocols with lactim ethers, imidoyl chlorides, aryl aldimines, and 1,3-azadienes. The direct employment of cheap commodity chemicals such as amines, aldehydes and *N*-heterocyclic anhydrides in this multicomponent, chemoselective, and diastereoselective annulation protocol bodes well for future applications in medicinal chemistry. Post-diversification of the cycloadducts to piperazinyl methanols as well as highly functionalized dihydro-1,4-diazines has been accomplished. Leishmanicidal evaluation of these functionalized ketopiperazines is underway and the results will be disclosed in due course.

2.4 Methods: General Procedure

All experiments involving air and moisture sensitive reagents were carried out under an inert atmosphere of nitrogen and using freshly distilled solvents. Column chromatography was performed on silica gel (230-400 mesh). Thin-layer chromatography (TLC) was performed using Silicycle SiliaplateTM glass backed plates (250 μm thickness, 60 Å porosity, F-254 indicator) and visualized using UV (254 nm) or $KMnO_4$ stain. Unless otherwise indicated, ^{1}H, ^{13}C, and DEPT-135 NMR, COSY 45, HMQC, and NOESY spectra were acquired using DMSO-d_6, CD_3OD or $CDCl_3$ as solvent at room temperature. Chemical shifts are quoted in parts per million (ppm). HRMS-EI^+ data were obtained using either electronspray ionization (ESI) or electron impact (EI) techniques.

2.4.1 General Procedure A: Synthesis of Trifluoroacetyl cyclic anhydride

To a stirring suspension of iminodiacetic acid (1 mmol) in dry ethyl acetate (15 mL) trifluoroacetic anhydride (TFAA) (3 equiv) was added. The reaction mixture was stirred for 3

days at room temperature. The mixture was washed with petroleum ether, then concentrated under reduced pressure to afford the trifluoroacetyl bearing cyclic anhydride.

2.4.2 General Procedure C/D: Synthesis of N-Benzyl cyclic anhydride

A mixture of iminodiacetic acid (1 mmol) in acetyl chloride (3 mL) was heated at reflux for 48 h. The mixture was cooled to room temperature, concentrated under reduced pressure and washed twice with a 50:50 solution of petroleum ether and hexanes in the reaction vial.[94]

2.4.3 General Procedure C: Reaction of imine component with anhydride

A 5 mL screw-cap vial was flame-dried, evacuated and flushed with nitrogen. A solution of the 1,3-azadiene (1.0 mL, 0.10 M in freshly distilled toluene) was added to the vial at room temperature followed by anhydride **1d/e** (1 equiv). The contents were placed in a pre-heated oil bath thermostatted 100 ^{o}C. After complete consumption of the 1,3-azadiene (as judged by TLC and NMR), the mixture/suspension was cooled to room temperature and washed several times with petroleum ether, then concentrated under reduced pressure to afford the crude cycloadducts.

2.4.4 General Procedure D: Methyl esterification of cycloadducts

To a stirring suspension of the acid (1 mmol), dissolved in DMF (5 mL), and K_2CO_3 (3 equiv) methyl iodide (2 equiv) was added under nitrogen atmosphere. The reaction mixture was stirred for about 12 h (TLC monitoring). After complete conversion, it was diluted with water and extracted with EtOAc (2×20 mL). The combined organic extracts were washed with brine, dried over $MgSO_4$ and concentrated *in vacuo* to give the desired ester, which was purified by flash chromatography on silica.

2.4.5 Genreral Procedure E: Vilsmeier-Haack reaction

To a cooled solution of DMF (6 mmol, 6 equiv) in CH_2Cl_2 (5 mL) at 0 ^{o}C, phosphorus oxychloride (3 mmol, 3 equiv) was added dropwise. The resulting pale yellow mixture was

refluxed for 1 hour. A solution of the lactamoyl ester (1 mmol, 1 equiv) in CH_2Cl_2 (5 mL) was added slowly. The mixture was then cooled to room temperature and stirred for the indicated time period (TLC and GC-MS monitoring was used to follow the extent of the reaction). Upon completion, the mixture was poured into a large flask containing crushed ice. After stirring at rt for 60 min, the layers were separated. The mixture was extracted with CH_2Cl_2 twice and washed with brine. The combined organic layers were dried over $MgSO_4$ for 5 min. The mixture was filtered and concentrated under reduced pressure to give the desired product as an oil.

2.5 Peak Assignments

Reaction with lactim ethers

2.5.1 *Peak Assignment for 8a*

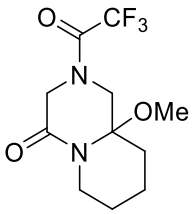

8a, 88%

Prepared from **2a** (113.3 mg, 1.0 mmol) and anhydride **7** (211.1 mg, 1.0 equiv) using General Procedure C. T = 110 ^{o}C, time = 22 h. Purification: Flash chromatography on silica eluting with hexane/EtOAc (75:25). Yield = 247 mg, 88%. ^{1}H NMR (400 MHz, Chloroform-*d, rotamers*) δ 4.67 (d, *J* = 1.6 Hz, 1H), 4.56 (s, 1H), 4.08 – 4.03 (m, 2H), 3.63 – 3.49 (m, 5H), 2.45 – 2.36 (m, 2H), 1.73 – 1.63 (m, 4H). ^{13}C NMR (101 MHz, $CDCl_3$) δ 173.69, 173.54, 171.00, 170.41, 168.26, 168.20, 157.86, 157.66, 157.50, 157.30, 156.93, 120.45, 117.59, 114.73, 111.87, 55.36, 55.32, 55.12, 52.77, 52.53, 49.61, 49.57, 49.47, 44.70, 44.62, 34.50, 34.45, 22.21, 22.18, 20.09, 19.98.

2.5.2 Peak Assignment for 8b

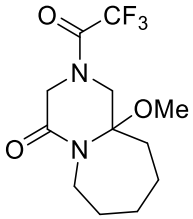

8b, 83%

Prepared from **2b** (127.5 mg, 1.0 mmol) and anhydride **7** (211.1 mg, 1.0 equiv) using General Procedure C. T = 110 ^{o}C, time = 22 h. Purification: Flash chromatography on silica eluting with hexane/EtOAc (75:25). Yield = 244 mg, 83%. ^{1}H NMR (400 MHz, Acetonitrile-d_3, rotamers) δ 4.66 (s, 2H), 4.13 – 3.99 (m, 2H), 3.77 (q, *J* = 5.5 Hz, 2H), 3.62 (s, 3H), 2.58 (m, 2H), 1.70 – 1.64 (m, 6H). ^{13}C NMR (101 MHz, $CDCl_3$) δ 178.17, 178.04, 170.48, 169.95, 168.28, 117.64, 117.60, 114.74, 55.02, 52.85, 52.62, 49.71, 43.84, 43.81, 39.34, 29.80, 29.21, 29.13, 28.46, 23.67, 23.64.

2.5.3 Peak Assignment for 8c

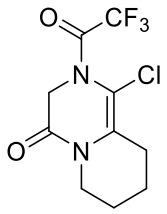

8c, 85%

Prepared from **2c** (117.6 mg, 1.0 mmol) and anhydride **7** (211.1 mg, 1.0 equiv) using General Procedure C. T = 100 °C, time = 18 h. Purification: Flash chromatography on silica eluting with hexane/EtOAc (75:25). Yield = 240 mg, 85%. ^{1}H NMR (400 MHz, Chloroform-*d*, *rotamers*) δ 4.65 (d, *J* = 1.6 Hz, 1H), 4.50 (s, 1H), 3.57 (dq, *J* = 10.2, 3.5 Hz, 2H), 2.41 (dq, *J* = 7.2, 3.0 Hz, 2H), 1.68-1.60 (m, 4H). ^{13}C NMR (101 MHz, $CDCl_3$) δ 174.03, 174.01, 171.28, 171.13, 170.54, 170.07, 169.95, 157.83, 157.47, 157.33, 157.11, 120.50, 117.64, 114.78, 111.92, 55.70, 55.67, 55.52, 44.68, 44.60, 34.37, 34.34, 22.10, 22.08, 19.97, 19.87.

2.5.4 Peak Assignment for 8d

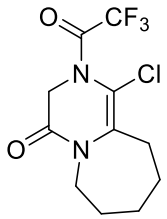

8d, 87%

Prepared from **2d** (131.7 mg, 1.0 mmol) and anhydride **7** (211.1 mg, 1.0 equiv) using General Procedure C. T = 100 °C, time = 18 h. Purification: Flash chromatography on silica eluting with hexane/EtOAc (75:25). Yield = 258 mg, 87%. ^{1}H NMR (400 MHz, Chloroform-*d*, *rotamers*) δ 4.60 (d, *J* = 1.8 Hz, 1H), 4.47 (s, 1H), 3.78 – 3.68 (m, 2H), 2.55 (dt, *J* = 10.9, 5.5 Hz, 2H), 1.60 – 1.51 (m, 6H). ^{13}C NMR (101 MHz, $CDCl_3$) δ 178.14, 178.01, 170.56, 170.04, 157.74, 157.37, 120.59, 119.66, 117.72, 114.86, 112.00, 55.67, 55.60, 55.57, 43.76, 43.74, 39.31, 29.18, 29.08, 28.43, 23.65, 23.62.

*2.5.5 Peak Assignment for **10a***

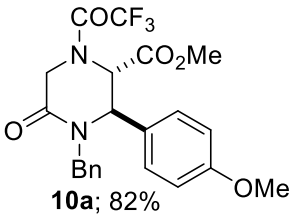

10a; 82%

Prepared from the imine (225 mg, 1.0 mmol) and anhydride **7** (211.1 mg, 1.0 equiv) using General Procedure C/D. Purification: Flash chromatography on silica eluting with hexane/EtOAc (50:50). Yield = 369 mg, 82%, 95:5 dr. ^{1}H NMR (400 MHz, Chloroform-*d*, *rotamers*) δ 7.25 – 7.03 (m, 3H), 7.02 (ddd, *J* = 6.8, 4.6, 2.0 Hz, 2H), 6.97 – 6.87 (m, 2H), 6.81 – 6.71 (m, 2H), 5.44 (dd, *J* = 14.5, 11.7 Hz, 1H), 4.77 (dd, *J* = 10.3, 2.1 Hz, 1H), 4.54 – 4.39 (m, 2H), 4.20 – 4.09 (m, 1H), 3.64 (s, 3H), 3.35 – 3.19 (m, 4H). ^{13}C NMR (101 MHz, $CDCl_3$, rotamers) δ 167.17, 167.12, 163.80, 162.95, 160.26, 160.20, 157.31, 157.10, 156.72, 156.55, 156.35, 156.18, 155.98, 155.82, 155.45, 135.61, 135.49, 128.95, 128.89, 128.70, 128.56, 128.41, 128.25, 127.52, 127.37, 127.26, 127.15, 120.17, 119.86, 117.51, 117.31, 117.00, 115.23, 114.96, 114.92, 114.66, 114.60, 114.45, 114.13, 111.59, 111.27, 61.10, 61.07, 61.04, 59.16, 58.37, 58.17, 55.44, 55.41, 53.23, 53.02, 52.86, 52.64, 48.89, 48.20, 46.67, 46.08.

*2.5.6 Peak Assignment for **10b***

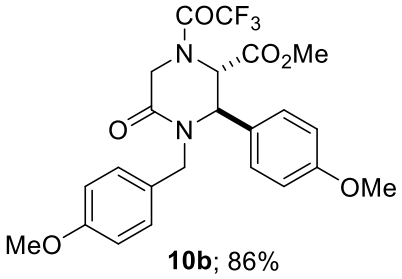

10b; 86%

Prepared in 1 mmol scale using General Procedure C/D. Purification: Flash chromatography on silica eluting with hexane/EtOAc (25:75). Yield = 413 mg, 86%, 95:5 dr. ^{1}H NMR (400 MHz, Chloroform-*d, mixture of rotamers*) δ 6.90 – 6.83 (m, 4H), 6.78 – 6.61 (m, 4H), 5.33 (dd, *J* = 14.4, 11.2 Hz, 1H), 4.76 (dd, *J* = 9.2, 2.1 Hz, 1H), 4.52 – 4.34 (m, 2H), 4.14 – 4.06 (m, 1H), 3.70 – 3.51 (m, 6H), 3.27 (s, 3H), 3.18 (dd, *J* = 14.4, 5.1 Hz, 1H). ^{13}C NMR (101 MHz, $CDCl_3$, mixture of rotamers) δ 168.15, 168.05, 167.19, 167.13, 163.67, 162.80, 160.21, 160.14, 159.60, 156.66, 156.29, 156.13, 155.77, 130.28, 130.23, 127.58, 127.53, 127.40, 127.25, 127.19, 127.14, 117.30,

116.99, 114.90, 114.86, 114.17, 114.13, 61.07, 61.04, 58.90, 58.19, 58.09, 55.38, 55.35, 55.33, 53.23, 53.02, 52.80, 52.57, 48.90, 47.60, 47.34, 46.72, 46.68, 46.05.

2.5.7 Peak Assignment for 10c

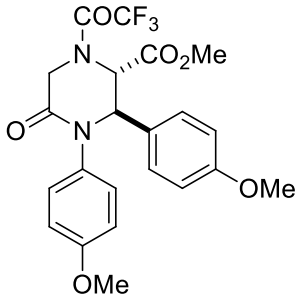

10c; 63%

Prepared in 1 mmol scale using General Procedure C/D. Purification: Flash chromatography on silica eluting with hexane/EtOAc (25:75). Yield = 294 mg, 63%, 95:5 dr. ^{1}H NMR (400 MHz, Chloroform-*d, rotamers*) δ 7.02 (dd, *J* = 8.7, 3.6 Hz, 6H), 6.93 – 6.83 (m, 2H), 6.81 – 6.71 (m, 2H), 6.75 – 6.61 (m, 2H), 5.31 (dd, *J* = 10.8, 2.3 Hz, 1H), 4.56 (dd, *J* = 18.6, 10.5 Hz, 1H), 4.43 (d, *J* = 17.9 Hz, 1H), 3.73 – 3.60 (m, 10H). ^{13}C NMR (101 MHz, $CDCl_3$, rotamers) δ 167.87, 167.75, 163.75, 162.90, 160.12, 160.06, 159.05, 159.02, 156.69, 156.31, 155.91, 133.21, 133.13, 128.16, 127.85, 127.49, 127.46, 127.30, 127.20, 121.65, 117.35, 114.85, 114.78, 114.77, 114.75, 114.49, 114.21, 114.19, 114.13, 67.17, 64.83, 63.97, 61.80, 61.77, 58.81, 55.54, 55.50, 55.42, 55.39, 54.00, 53.78, 47.16, 47.12, 46.57.

2.5.8 Peak Assignment for 10d

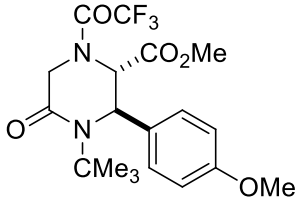

10d; 77%

Prepared in 1 mmol scale using General Procedure C/D. Purification: Flash chromatography on silica eluting with hexane/EtOAc (75:25). Yield = 320 mg, 77%, 95:5 dr. ^{1}H NMR (400 MHz, Chloroform-*d, rotamers*) δ 7.08 (dd, *J* = 8.6, 4.8 Hz, 2H), 6.86 (dd, *J* = 8.5, 4.4 Hz, 2H), 5.48 (dd, *J* = 9.0, 2.9 Hz, 1H), 5.24 + 4.76 (d, *J* = 2.8 Hz, 1H), 4.32 – 4.11 (m, 2H), 3.89 – 3.68 (m, 6H),

1.36 (s, 9H). ^{13}C NMR (101 MHz, $CDCl_3$, rotamers) δ 167.96, 167.75, 164.21, 163.28, 159.75, 159.68, 155.94, 155.65, 155.28, 132.00, 129.61, 129.23, 129.01, 128.66, 126.86, 126.80, 117.22, 114.71, 114.63, 114.36, 62.73, 62.70, 60.08, 59.56, 59.37, 58.53, 57.59, 55.32, 55.30, 53.64, 53.43, 48.03, 47.99, 47.75, 28.72, 27.99.

2.5.9 Peak Assignment for 10e

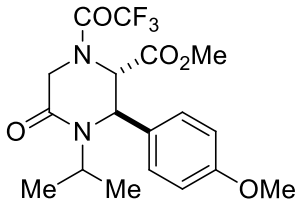

10e; 75%

Prepared in 1 mmol scale using General Procedure C/D. Purification: Flash chromatography on silica eluting with hexane/EtOAc (60:40). Yield = 302 mg, 75%, 95:5 dr. ^{1}H NMR (400 MHz, Chloroform-*d, rotamers*) 7.06 (dd, *J* = 8.5, 5.5 Hz, 2H), 6.98 – 6.79 (m, 2H), 5.27 – 5.21 (m, 1H), 5.13 (dd, *J* = 12.8, 2.5 Hz, 1H), 4.82 – 4.64 (m, 1H), 4.43 (d, *J* = 12.3 Hz, 1H), 3.82 – 3.69 (m, 6H), 1.08 (t, *J* = 6.7 Hz, 3H), 0.83 (d, *J* = 6.9 Hz, 3H). ^{13}C NMR (101 MHz, $CDCl_3$, rotamers) δ 167.62, 167.46, 163.38, 162.47, 159.78, 159.73, 156.53, 156.16, 155.58, 131.98, 130.90, 129.75, 129.59, 129.42, 128.41, 128.18, 128.13, 126.84, 126.78, 117.22, 116.96, 114.58, 114.51, 114.36, 114.33, 114.25, 114.15, 114.09, 113.39, 58.07, 56.46, 55.68, 55.59, 55.30, 55.27, 53.60, 53.38, 47.04, 47.00, 46.96, 46.69, 46.60, 46.18, 19.75, 19.70, 19.59, 19.57.

2.5.10 Peak Assignment for 10f

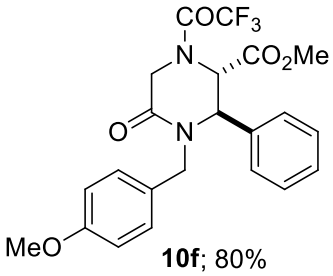

10f; 80%

Prepared in 1 mmol scale using General Procedure C/D. Purification: Flash chromatography on silica eluting with hexane/EtOAc (50:50). Yield = 360 mg, 80%, 95:5 dr. ^{1}H NMR (400 MHz, Chloroform-*d, rotamers*) δ 7.22 – 7.19 (m, 3H), 7.17 – 6.95 (m, 2H), 7.06 – 6.87 (m, 2H), 6.71 (d,

J = 8.3 Hz, 2H), 5.37 (dd, *J* = 14.4, 10.4 Hz, 1H), 4.83 (dd, *J* = 10.4, 2.0 Hz, 1H), 4.55 – 446 (m, 2H), 4.12 (d, *J* = 11.3 Hz, 2H), 3.51 (s, 3H), 3.31 (s, 3H), 3.21 (dd, *J* = 14.5, 4.9 Hz, 1H). ^{13}C NMR (101 MHz, $CDCl_3$, rotamers) δ 168.15, 168.09, 167.13, 167.08, 163.83, 162.97, 159.64, 157.69, 157.32, 156.70, 156.33, 156.12, 155.75, 135.81, 135.47, 130.33, 130.28, 129.63, 129.56, 129.37, 129.32, 129.24, 129.16, 128.92, 127.43, 127.31, 125.97, 125.90, 117.27, 114.65, 114.41, 114.31, 114.26, 114.22, 114.18, 114.15, 114.12, 114.10, 114.05, 113.87, 113.81, 60.99, 60.96, 59.40, 58.60, 58.10, 55.39, 55.36, 55.27, 53.34, 53.13, 52.87, 52.65, 49.18, 49.14, 48.91, 47.79, 47.51, 46.77, 46.73, 46.10.

*2.5.11 Peak Assignment for **10g***

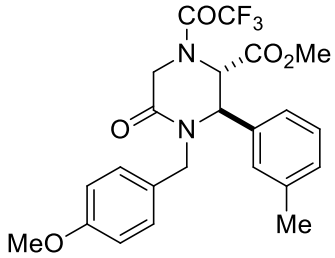

10g; 84%

Prepared in 1 mmol scale using General Procedure C/D. Purification: Flash chromatography on silica eluting with hexane/EtOAc (50:50). Yield = 390 mg, 84%, 95:5 dr. ^{1}H NMR (400 MHz, Chloroform-*d, rotamers*) δ 7.16 – 7.06 (s, 1H), 6.98 – 6.85 (m, 3H), 6.73 – 6.55 (m, 4H), 5.36 (t, *J* = 14.7 Hz, 1H), 5.12 – 5.04 (m, 1H), 4.78 (dd, *J* = 5.3, 2.1 Hz, 1H), 4.52 – 4.29 (m, 2H), 3.54 (m, 3H), 3.28 (s, 3H), 3.20 (d, *J* = 14.4 Hz, 1H), 2.17 (s, 3H). ^{13}C NMR (101 MHz, $CDCl_3$, rotamers) δ 167.20, 167.12, 163.85, 162.92, 162.61, 159.61, 156.62, 156.24, 139.53, 139.44, 135.77, 135.39, 130.30, 130.24, 130.19, 130.03, 130.00, 129.84, 129.48, 129.38, 127.53, 127.39, 126.50, 122.97, 117.31, 116.98, 114.45, 114.19, 113.92, 113.74, 61.04, 61.00, 59.37, 58.58, 58.12, 55.38, 55.32, 55.26, 53.29, 53.08, 47.74, 47.53, 46.76, 46.72, 46.11, 21.50, 21.46.

*2.5.12 Peak Assignment for **10h***

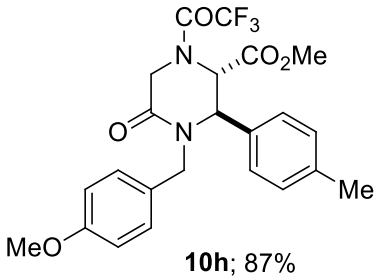

10h; 87%

Prepared in 1 mmol scale using General Procedure C/D. Purification: Flash chromatography on silica eluting with hexane/EtOAc (50:50). Yield = 404 mg, 87%, 95:5 dr. ^{1}H NMR (400 MHz, Chloroform-*d, rotamers*) δ 6.98 – 6.77 (m, 6H), 6.73 – 6.57 (m, 2H), 5.36 (dd, *J* = 14.4, 11.9 Hz, 1H), 5.12 – 5.06 (m, 1H), 4.78 (dd, *J* = 8.8, 2.1 Hz, 1H), 4.55 – 4.41 (m, 1H), 4.44 – 4.32 (m, 1H), 3.50 (s, 3H), 3.28 (s, 3H), 3.18 (dd, *J* = 14.5, 4.0 Hz, 1H), 2.17 (s, 3H). ^{13}C NMR (101 MHz, $CDCl_3$, rotamers) δ 167.22, 167.14, 163.80, 162.91, 162.60, 159.60, 156.68, 156.30, 156.12, 155.75, 139.24, 139.14, 132.74, 132.35, 130.29, 130.26, 130.24, 130.21, 130.16, 127.51, 127.38, 125.87, 125.79, 117.29, 116.98, 114.19, 61.03, 61.00, 59.16, 58.36, 58.15, 55.38, 55.32, 53.27, 53.06, 47.66, 47.42, 46.74, 46.70, 46.11, 21.14.

2.5.13 Peak Assignment for 10i

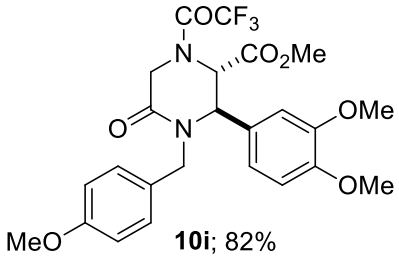

10i; 82%

Prepared in 1 mmol scale using General Procedure C/D. Purification: Flash chromatography on silica eluting with hexane/EtOAc (50:50). Yield = 418 mg, 82%, 95:5 dr. ^{1}H NMR (400 MHz, Chloroform-*d, rotamers*) δ 6.89 (ddq, *J* = 8.1, 5.8, 2.8 Hz, 2H), 6.66 (dd, *J* = 8.4, 5.2 Hz, 3H), 6.49 (td, *J* = 8.0, 2.3 Hz, 1H), 6.40 (dd, *J* = 4.8, 2.2 Hz, 1H), 5.29 (t, *J* = 14.1 Hz, 1H), 5.07 (d, *J* = 2.1 Hz, 1H), 4.72 (dd, *J* = 7.8, 2.1 Hz, 1H), 4.41 (dd, *J* = 18.3, 3.6 Hz, 2H), 3.71 – 3.59 (m, 6H), 3.58 (s, 3H), 3.27 (s, 3H), 3.20 (dd, *J* = 14.5, 2.4 Hz, 1H). ^{13}C NMR (101 MHz, $CDCl_3$) δ 167.13, 167.08, 163.69, 162.76, 159.59, 156.59, 156.21, 156.03, 155.66, 149.90, 149.85, 149.70, 149.65, 130.27, 130.20, 128.08, 127.59, 127.47, 127.34, 118.28, 118.23, 117.28, 116.99, 114.14, 111.65,

111.57, 108.88, 108.80, 61.00, 60.97, 59.16, 58.38, 58.06, 56.09, 55.97, 55.95, 55.32, 53.25, 53.05, 47.70, 47.50, 46.65, 46.60, 45.98.

*2.5.14 Peak Assignment for **10j***

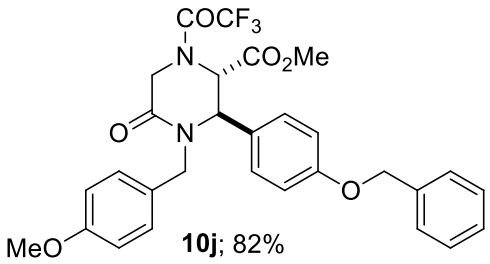

10j; 82%

Prepared in 1 mmol scale using General Procedure C/D. Purification: Flash chromatography on silica eluting with hexane/EtOAc (25:75). Yield = 456 mg, 82%, 95:5 dr. ^{1}H NMR (400 MHz, Chloroform-*d, rotamers*) δ 7.36 – 7.22 (m, 6H), 6.96 – 6.79 (m, 5H), 6.68 (d, 2H), 5.38 (dd, *J* = 14.4, 10.2 Hz, 1H), 5.02 – 4.88 (m, 2H), 4.91 – 4.77 (m, 1H), 4.59 – 4.39 (m, 2H), 3.52 (s, 3H), 3.31 (s, 3H), 3.22 (dd, *J* = 14.4, 6.1 Hz, 1H). ^{13}C NMR (101 MHz, $CDCl_3$) δ 167.23, 167.17, 163.74, 162.88, 159.65, 159.44, 159.40, 156.75, 156.38, 155.83, 136.63, 136.59, 132.10, 130.34, 130.29, 128.83, 128.79, 128.76, 128.71, 128.43, 128.26, 127.92, 127.67, 127.63, 127.61, 127.59, 127.55, 127.52, 127.43, 127.33, 127.23, 115.92, 115.83, 115.27, 114.32, 114.28, 114.24, 114.19, 114.17, 114.14, 70.25, 70.23, 58.97, 58.25, 58.17, 55.41, 53.32, 53.10, 47.69, 47.42, 46.13.

2.5.15 Peak Assignment for 10k

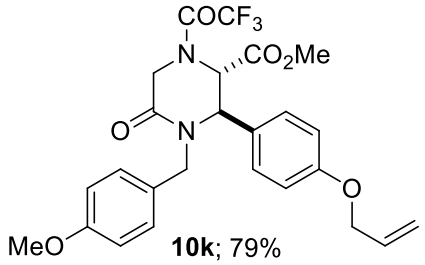

10k; 79%

Prepared in 1 mmol scale using General Procedure C/D. Purification: Flash chromatography on silica eluting with hexane/EtOAc (25:75). Yield = 400 mg, 79%, 95:5 dr. ^{1}H NMR (400 MHz, Chloroform-*d, rotamers*) δ 6.89 – 6.80 (m, 4H), 6.72 – 6.61 (m, 4H), 5.86 (ddt, *J* = 17.3, 10.5, 5.2 Hz, 1H), 5.33 – 5.04 (m, 4H), 4.77 (dd, *J* = 9.8, 2.1 Hz, 1H), 4.53 – 4.42 (m, 4H), 3.61 (s, 3H), 3.28 (s, 3H), 3.20 (dd, *J* = 14.4, 5.8 Hz, 1H). ^{13}C NMR (101 MHz, $CDCl_3$) δ 167.18, 167.13, 163.70, 162.84, 159.61, 159.23, 159.17, 156.69, 156.31, 156.15, 155.78, 132.93, 132.88, 130.30,

130.25, 127.73, 127.52, 127.39, 127.37, 127.24, 127.14, 118.01, 117.98, 115.71, 115.64, 115.08, 114.83, 114.45, 114.28, 114.23, 114.19, 114.12, 114.09, 114.07, 68.94, 61.08, 61.05, 58.93, 58.19, 58.12, 55.36, 55.30, 53.27, 53.05, 47.65, 47.38, 46.74, 46.69, 46.06.

2.5.16 Peak Assignment for 10l

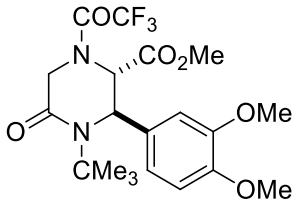

10l; 75%

Prepared in 1 mmol scale using General Procedure C/D. Purification: Flash chromatography on silica eluting with hexane/EtOAc (50:50). Yield = 335 mg, 75%, 95:5 dr. ^{1}H NMR (400 MHz, Chloroform-*d, rotamers*) δ 6.66 (dd, *J* = 8.3, 3.1 Hz, 1H), 6.55 (ddd, *J* = 8.1, 5.6, 2.2 Hz, 1H), 6.47 (t, *J* = 2.6 Hz, 1H), 5.31 (dd, *J* = 8.3, 2.8 Hz, 1H), 4.19 (s, 1H), 4.17 – 4.06 (m, 2H), 3.69 – 3.63 (m, 9H), 1.21 (s, 9H). ^{13}C NMR (101 MHz, $CDCl_3$, rotamers) δ 168.04, 167.79, 164.28, 163.32, 156.31, 155.94, 155.58, 155.22, 149.67, 149.59, 149.24, 149.18, 130.12, 129.60, 118.15, 118.01, 111.52, 111.44, 108.49, 108.45, 62.68, 62.65, 60.01, 59.64, 59.42, 58.76, 57.85, 56.04, 55.95, 55.93, 53.70, 53.48, 52.82, 52.60, 48.86, 47.77, 28.00, 27.90.

*2.5.17 Peak Assignment for **10m***

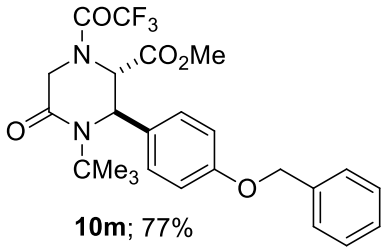

10m; 77%

Prepared in 5 mmol scale using General Procedure C/D. Purification: Flash chromatography on silica eluting with hexane/EtOAc (50:50). Yield = 1.895 g, 77%, 95:5 dr. ^{1}H NMR (400 MHz, Chloroform-*d, rotamers*) δ 7.30 – 7.21 (m, 5H), 7.02 – 6.92 (m, 2H), 6.87 – 6.78 (m, 2H), 5.36 (d, *J* = 9.6 Hz, 1H), 4.88 (d, *J* = 4.0 Hz, 2H), 4.26 – 4.10 (m, 3H), 3.70 (s, 3H), 1.25 (s, 9H). ^{13}C NMR (101 MHz, $CDCl_3$) δ 168.03, 167.82, 164.27, 163.35, 159.04, 158.99, 156.40, 156.03, 136.60, 136.57, 129.97, 128.71, 128.23, 128.22, 127.67, 127.65, 126.95, 126.89, 117.52, 117.28, 117.08,

115.69, 115.59, 114.66, 114.42, 114.21, 70.24, 70.22, 62.79, 62.76, 60.14, 59.63, 59.45, 58.60, 57.67, 53.71, 53.50, 52.86, 52.64, 48.91, 47.82, 28.06, 27.96.

2.5.18 Peak Assignment for 10n

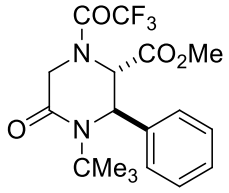

10n; 72%

Prepared in 1 mmol scale using General Procedure C/D. Purification: Flash chromatography on silica eluting with hexane/EtOAc (75:25). Yield = 278 mg, 72%, 95:5 dr. ^{1}H NMR (400 MHz, Chloroform-*d, rotamers*) δ 7.36 – 7.23 (m, 5H), 5.53 (dd, *J* = 8.8, 2.8 Hz, 1H), 5.30 (d, *J* = 2.8 Hz, 0.5H), 4.82 (d, *J* = 2.8 Hz, 0.5H), 4.32 – 4.01 (m, 2H), 3.81 (s, 3H), 1.36 (s, 9H). ^{13}C NMR (101 MHz, $CDCl_3$) δ 167.89, 167.69, 164.26, 163.36, 156.26, 155.89, 155.60, 155.24, 137.83, 137.53, 129.39, 129.30, 129.02, 128.86, 128.79, 128.71, 128.66, 125.62, 125.58, 117.19, 116.98, 114.33, 62.64, 62.61, 60.00, 59.64, 59.46, 59.00, 58.08, 53.70, 53.48, 48.09, 48.05, 47.79, 28.00, 27.90.

2.5.19 Peak Assignment for 10o

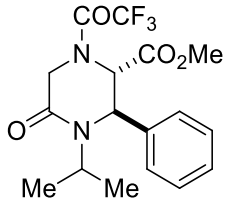

10o; 70%

Prepared in 1 mmol scale using General Procedure C/D. Purification: Flash chromatography on silica eluting with hexane/EtOAc (75:25). Yield = 260 mg, 70%, 95:5 dr. ^{1}H NMR (400 MHz, Chloroform-*d, rotamers*) δ 7.31 – 7.09 (m, 5H), 5.20 (dd, *J* = 13.8, 2.4 Hz, 1H), 4.78 (td, *J* = 14.3, 12.4, 6.9 Hz, 1H), 4.46 (d, *J* = 11.2 Hz, 2H), 4.23 (t, *J* = 18.5 Hz, 1H), 3.63 (s, 3H), 1.07 (d, *J* = 6.9 Hz, 3H), 0.85 (d, *J* = 6.9 Hz, 3H). ^{13}C NMR (101 MHz, $CDCl_3$) δ 167.6, 167.4, 163.5, 162.6, 155.9, 137.9, 137.7, 129.3, 129.2, 128.9, 128.8, 128.6, 128.3, 125.8, 125.6, 125.6, 119.7, 117.2, 116.9, 114.3, 114.1, 62.1, 62.0, 59.3, 56.9, 56.1, 53.7, 53.5, 47.1, 47.1, 47.0, 46.7, 46.6, 46.1, 19.8, 19.7, 19.6.

2.5.20 Peak Assignment for 10p

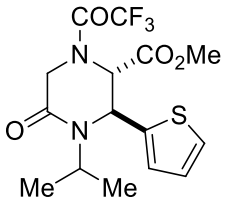

10p; 79%

Prepared in 1 mmol scale using General Procedure C/D. Purification: Flash chromatography on silica eluting with hexane/EtOAc (50:50). Yield = 299 mg, 79%, 95:5 dr. ^{1}H NMR (400 MHz, Chloroform-*d, rotamers*) δ 7.11 (td, *J* = 4.6, 1.8 Hz, 1H), 6.80 (qd, *J* = 4.9, 4.2, 2.8 Hz, 2H), 5.29 (dd, *J* = 17.0, 2.5 Hz, 1H), 4.54 (dp, *J* = 28.8, 6.9 Hz, 1H), 4.41 – 4.25 (m, 2H), 4.15 – 4.05 (m, 1H), 3.66 (d, *J* = 5.7 Hz, 3H), 3.59 (d, *J* = 10.5 Hz, 2H), 0.97 (dd, *J* = 9.0, 6.8 Hz, 3H), 0.82 (dd, *J* = 7.0, 3.3 Hz, 3H). ^{13}C NMR (101 MHz, $CDCl_3$, rotamers) δ 168.13, 168.06, 167.28, 167.08, 162.95, 162.01, 162.00, 157.66, 157.29, 156.91, 156.54, 156.12, 155.75, 141.92, 141.54, 127.44, 127.29, 126.27, 126.24, 125.80, 125.68, 120.13, 119.94, 117.48, 117.27, 117.07, 114.63, 114.41, 114.21, 111.55, 111.35, 62.23, 62.20, 59.33, 53.77, 53.57, 53.29, 52.85, 52.66, 52.63, 46.96, 46.92, 46.72, 46.64, 19.76, 19.69, 19.59, 19.56.

2.5.21 Peak Assignment for 11a

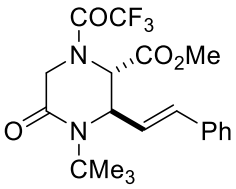

11a, 75%

Prepared from 1,3-azadiene **9a** (936.5 mg, 5.0 mmol) and anhydride **7** (1.056 g, 1.0 equiv) using General Procedure C/D. T = 100 °C, time = 8 h. Purification: Flash chromatography on silica eluting with hexane/EtOAc (50:50). Yield = 1.463 g, 75%, 95:5 dr. ^{1}H NMR (400 MHz, Chloroform-*d, mixture of rotamers*) δ 7.35 – 7.23 (m, 5H), 6.65 – 6.53 (m, 1H), 6.10 (ddd, *J* = 15.9, 5.2, 2.8 Hz, 1H), 5.25 (d, *J* = 2.7 Hz, 1H), 5.15 – 5.05 (m, 1H), 4.35 (q, *J* = 17.0 Hz, 1H), 4.18 (d, *J* = 7.2 Hz, 1H), 3.71 (s, 3H), 1.46 (s, 9H). ^{13}C NMR (101 MHz, $CDCl_3$, rotamers) δ 165.05, 164.83, 161.03, 160.21, 153.42, 152.37, 132.07, 131.04, 130.53, 125.87, 125.83, 125.71, 123.68, 122.65, 114.31, 111.45, 56.02, 55.89, 55.39, 53.79, 52.89, 50.58, 50.39, 44.97, 44.93, 25.08, 24.99.

2.5.22 Peak Assignment for 11b

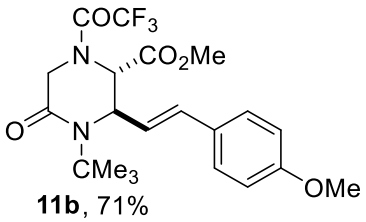

11b, 71%

Prepared from 1,3-azadiene **9b** (217.3 mg, 1.0 mmol) and anhydride **7** (211.1 mg, 1.0 equiv) using General Procedures B. T = 100 °C, time = 8 h. Purification: Flash chromatography on silica eluting with hexane/EtOAc (50:50). Yield = 331.5 mg, 71%, 95:5 dr. ^{1}H NMR (400 MHz, Chloroform-*d, mixture of rotamers*) δ 7.25 (d, *J* = 6.5 Hz, 2H), 6.90 (d, *J* = 8.5 Hz, 2H), 6.52 (t, *J* = 15.0 Hz, 1H), 5.93 (dt, *J* = 15.9, 6.0 Hz, 1H), 5.22 (d, *J* = 2.8 Hz, 1H), 5.15 – 5.02 (m, 1H), 4.82 (d, *J* = 2.8 Hz, 1H), 4.39 (d, *J* = 17.0 Hz, 1H), 4.34 – 4.25 (m, 2H), 4.19 (s, 1H), 3.91 – 3.72 (m, 6H), 1.52 (s, 9H). ^{13}C NMR (101 MHz, $CDCl_3$, rotamers) δ 168.21, 167.99, 164.11, 163.30, 160.20, 160.11, 152.81, 133.55, 133.00, 130.43, 128.05, 128.02, 123.18, 122.69, 114.32, 114.29, 60.98, 60.95, 59.04, 58.92, 58.60, 56.93, 56.00, 55.52, 55.41, 53.64, 53.45, 48.84, 48.02, 47.98, 47.84, 28.15, 28.06.

2.5.23 Peak Assignment for 11c

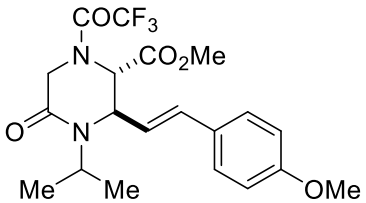

11c, 71%

Prepared from 1,3-azadiene **9c** (1016..5 mg, 5.0 mmol) and anhydride **7** (1055.5 mg, 1.0 equiv) using General Procedure C/D. T = 100 °C, time = 8 h. Purification: Flash chromatography on silica eluting with hexane/EtOAc (50:50). Yield = 1.52 g, 71%, 95:5 dr. ^{1}H NMR (400 MHz, Chloroform-*d, rotamers*) δ 7.33 – 7.22 (m, 2H), 6.94 – 6.80 (m, 2H), 6.53 (td, *J* = 15.8, 1.3 Hz, 1H), 5.96 (ddd, *J* = 15.8, 5.9, 1.4 Hz, 1H), 4.83 – 4.68 (m, 2H), 4.43 – 4.20 (m, 2H), 3.92 – 3.73 (m, 9H), 1.15 (dd, *J* = 6.8 Hz, 6H). ^{13}C NMR (101 MHz, $CDCl_3$) δ 167.86, 167.70, 163.26, 162.50, 160.20, 160.11, 157.12, 156.74, 133.59, 133.09, 128.04, 128.02, 123.15, 122.80, 114.31, 114.27, 60.45, 60.42, 57.82, 55.39, 55.38, 55.08, 54.22, 53.61, 53.40, 47.00, 46.95, 46.72, 46.50, 46.12, 19.98, 19.89, 19.81, 19.79.

*2.5.24 Peak Assignment for**11d***

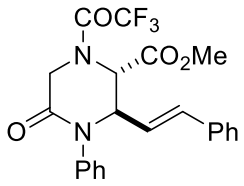

11d, 68%

Prepared from 1,3-azadiene **9d** (207.3 mg, 1.0 mmol) and anhydride **7** (211.1 mg, 1.0 equiv) using General Procedure C/D. T = 100 ºC, time = 18 h. Purification: Flash chromatography on silica eluting with hexane/EtOAc (25:75). Yield = 294 mg, 68%, 95:5 dr. ^{1}H NMR (400 MHz, Chloroform-*d, mixture of rotamers*) δ 7.64 – 7.19 (m, 10H), 6.63 (dd, *J* = 15.8, 6.6 Hz, 1H), 6.18 (td, *J* = 17.2, 16.3, 6.2 Hz, 1H), 5.14 – 4.97 (m, 1H), 4.72 – 4.53 (m, 1H), 4.44 – 4.26 (m, 2H), 3.70 (s, 3H). ^{13}C NMR (101 MHz, $CDCl_3$) δ 167.80, 167.67, 163.27, 162.51, 157.19, 156.82, 146.14, 142.83, 140.24, 140.15, 137.95, 137.76, 135.18, 134.58, 129.65, 129.08, 129.06, 129.01, 128.98, 128.95, 128.91, 128.21, 128.13, 128.09, 126.90, 126.88, 126.20, 126.18, 123.48, 123.14, 120.04, 119.96, 63.27, 62.45, 57.08, 53.97, 53.77, 47.11, 47.07, 46.70.

2.5.25 Peak Assignment for 11e

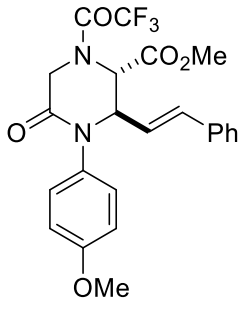

11e, 65%

Prepared from 1,3-azadiene **9e** (237.3 mg, 1.0 mmol) and anhydride **7** (211.1 mg, 1.0 equiv) using General Procedure C/D. T = 100 ºC, time = 18 h. Purification: Flash chromatography on silica eluting with hexane/EtOAc (50:50). Yield = 300 mg, 65%, 95:5 dr. ^{1}H NMR (400 MHz, Chloroform-*d, mixture of rotamers*) δ 7.40 – 7.21 (m, 5H), 7.19 (d, *J* = 8.6 Hz, 2H), 6.79 (d, *J* = 8.6 Hz, 2H), 6.61 (dd, *J* = 15.8, 7.3 Hz, 1H), 6.15 (ddd, *J* = 18.1, 15.7, 6.5 Hz, 1H), 5.48 (d, *J* = 2.3 Hz, 1H), 5.08 – 4.94 (m, 1H), 4.71 – 4.53 (m, 1H), 4.48 – 4.26 (m, 1H), 3.79 (s, 3H), 3.68 (s, 3H). ^{13}C NMR (101 MHz, $CDCl_3$) δ 167.84, 167.70, 163.35, 162.60, 159.08, 159.05, 146.31, 142.74, 135.26, 134.65, 129.10, 129.05, 128.95, 128.93, 128.90, 128.17, 127.59, 127.58, 126.89,

126.87, 123.38, 123.03, 121.58, 114.85, 114.83, 114.16, 63.54, 62.70, 59.90, 59.87, 56.96, 55.55, 53.99, 53.79, 47.06, 47.01.

*2.5.26 Peak Assignment for **11f***

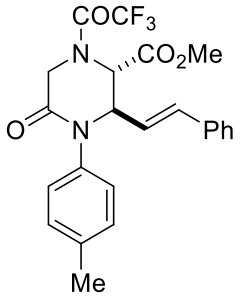

11f, 70%

Prepared from 1,3-azadiene **9f** (221.3 mg, 1.0 mmol) and anhydride **7** (211.1 mg, 1.0 equiv) using General Procedure C/D. T = 100 °C, time = 18 h. Purification: Flash chromatography on silica eluting with hexane/EtOAc (50:50). Yield = 312 mg, 70%, 95:5 dr. ^{1}H NMR (400 MHz, Chloroform-*d*, *mixture of rotamers*) δ 7.43 – 7.21 (m, 9H), 6.65 (ddd, *J* = 15.8, 4.0, 1.2 Hz, 1H), 6.22 (ddd, *J* = 18.9, 15.8, 6.4 Hz, 1H), 5.08 (ddq, *J* = 19.2, 4.1, 2.1 Hz, 1H), 4.73 – 4.59 (m, 1H), 4.45 – 4.20 (m, 1H), 3.87 (s, 3H), 3.81 – 3.65 (m, 1H), 2.33 (s, 3H). ^{13}C NMR (101 MHz, $CDCl_3$) δ 167.86, 167.71, 163.30, 162.55, 157.23, 156.85, 138.16, 135.16, 135.06, 134.56, 130.28, 130.26, 129.04, 128.98, 128.96, 128.91, 126.91, 126.89, 126.04, 123.55, 123.20, 117.45, 117.10, 114.60, 63.35, 62.52, 57.06, 53.97, 53.76, 47.11, 47.07, 46.72, 21.68, 21.17.

2.5.27 Peak Assignment for 11g

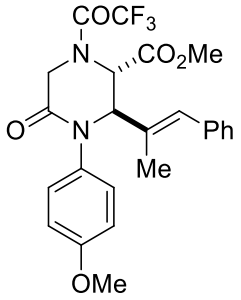

11g, 71%

Prepared from 1,3-azadiene **9g** (251 mg, 1.0 mmol) and anhydride **7** (211.1 mg, 1.0 equiv) using General Procedure C/D. Purification: Flash chromatography on silica eluting with hexane/EtOAc (25:75). Yield = 338.1 mg, 71%, 95:5 dr. ^{1}H NMR (400 MHz, Chloroform-*d*, *rotamers*) δ 7.29 – 7.05 (m, 7H), 6.87 – 6.72 (m, 2H), 6.46 (s, 1H), 4.74 (dt, *J* = 15.5, 1.7 Hz, 1H), 4.55 – 4.36 (m,

2H), 4.22 – 4.12 (m, 1H), 3.74 – 3.60 (m, 6H), 1.77 (s, 3H). ^{13}C NMR (101 MHz, $CDCl_3$) δ 168.26, 168.15, 168.08, 168.06, 163.86, 163.05, 159.02, 159.01, 157.69, 157.32, 156.94, 156.56, 135.99, 133.39, 132.49, 129.60, 128.99, 128.89, 128.83, 128.52, 128.48, 127.69, 127.54, 127.36, 127.29, 120.37, 117.51, 117.47, 114.79, 114.77, 114.68, 114.65, 114.61, 114.54, 68.17, 67.32, 58.17, 58.14, 55.54, 55.04, 54.03, 53.79, 52.86, 52.64, 49.21, 49.17, 49.14, 49.10, 48.90, 47.01, 46.97, 46.55, 16.34.

2.5.28 Peak Assignment for 11h

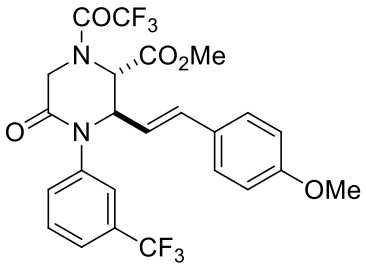

11h, 67%

Prepared from 1,3-azadiene **9h** (305.3 mg, 1.0 mmol) and anhydride **7** (211.1 mg, 1.0 equiv) using General Procedure C/D. Purification: Flash chromatography on silica eluting with hexane/EtOAc (75:25). Yield = 355.2 mg, 67%, 95:5 dr. ^{1}H NMR (400 MHz, Chloroform-*d*, *rotamers*) δ 7.38 – 7.24 (m, 4H), 7.21 – 7.16 (d, *J* = 8.7, 2H), 6.73 (d, *J* = 8.7, 2H), 6.41 (dd, *J* = 15.8, 9.8 Hz, 1H), 5.87 (td, *J* = 16.3, 6.3 Hz, 1H), 4.98 – 4.77 (m, 1H), 4.54 – 4.40 (m, 2H), 3.76 (s, 3H), 3.74 – 3.58 (m, 4H). ^{13}C NMR (101 MHz, $CDCl_3$) δ 167.72, 167.61, 163.35, 162.61, 160.51, 160.41, 157.22, 156.84, 156.45, 156.08, 140.76, 140.68, 135.07, 134.46, 130.23, 129.80, 128.29, 128.27, 127.42, 127.33, 124.88, 124.84, 124.80, 123.18, 123.14, 123.10, 123.06, 120.49, 120.15, 114.41, 114.37, 63.35, 62.54, 60.07, 60.04, 57.17, 55.45, 55.44, 55.40, 54.05, 53.84, 47.10, 47.06, 46.66.

2.5.29 Peak Assignment for 12

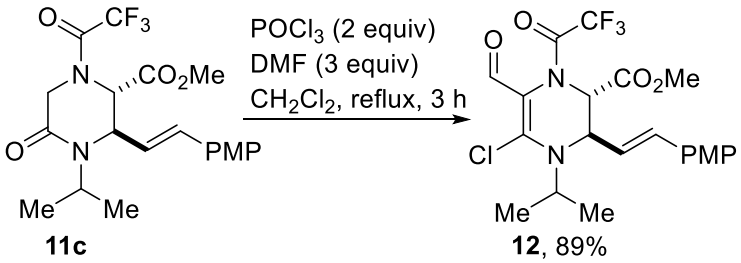

11c **12**, 89%

Prepared from **7c2** (214.2 mg, 0.50 mmol) using General Procedure C. Purification: Flash chromatography on silica (pretreated with 1% Et_3N) eluting with hexane/EtOAc (80:20). Yield = 211.3 mg, 89%, 95:5 dr. ^{1}H NMR (400 MHz, Chloroform-*d, rotamers*) δ 9.81 (s, 1H), 7.30 (d, 2H), 6.85 (d, 2H), 6.35 (d, *J* = 15.4 Hz, 1H), 5.97 & 5.84 (dd, *J* = 15.8, 6.6 Hz, 1H), 4.95 & 4.87 (ddd, *J* = 7.0, 2.9, 1.1 Hz, 2H), 4.84 – 4.70 (m, 1H), 3.82 (dd, *J* = 2.9, 1.1 Hz, 1H), 3.80 – 3.66 (m, 6H), 1.31 – 1.17 (m, 6H). ^{13}C NMR (101 MHz, $CDCl_3$) δ 185.31, 184.83, 169.39, 167.84, 159.86, 159.78, 142.36, 141.85, 133.20, 132.05, 128.29, 128.09, 128.07, 124.11, 120.18, 114.11, 114.00, 104.86, 102.27, 56.93, 56.50, 55.34, 53.19, 53.07, 52.76, 52.59, 47.99, 44.58, 22.26, 21.29, 20.63, 19.51.

2.5.30 Peak Assignment for 13

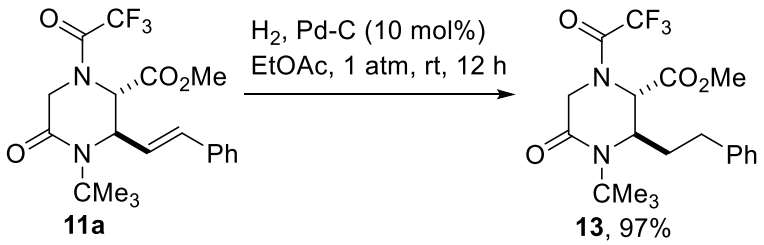

Prepared from **11a** (206.2 mg, 0.50 mmol) using General Procedure D. Yield = 201.3 mg, 97%, 95:5 dr. ^{1}H NMR (400 MHz, Chloroform-*d, rotamers*) δ 7.22 – 6.95 (m, 5H), 5.18 + 4.74 (dd, *J* = 2.9, 1.4 Hz, 1H), 4.18 – 4.02 (m, 3H), 3.63 (s, 3H), 2.58 (ddt, *J* = 18.7, 8.8, 4.0 Hz, 1H), 2.47 – 2.32 (m, 1H), 1.88 – 1.62 (m, 2H), 1.19 (s, 9H). ^{13}C NMR (101 MHz, $CDCl_3$) δ 169.09, 168.64, 163.46, 162.48, 162.47, 157.14, 156.76, 156.31, 155.94, 139.45, 139.26, 129.00, 128.95, 128.35, 128.33, 126.92, 126.82, 120.35, 117.50, 117.45, 114.64, 114.59, 58.77, 58.61, 57.68, 57.65, 55.28, 54.42, 53.59, 53.47, 53.38, 47.64, 47.48, 47.44, 36.11, 35.75, 32.29, 32.03, 28.35, 28.22.

2.5.31 Peak Assignment for 14

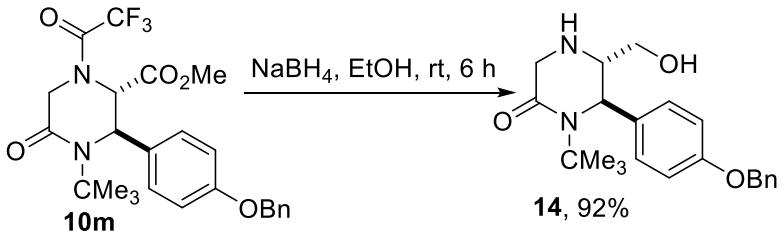

To a 10 mL round-bottomed flask equipped with a magnetic stir bar under a N2 atmosphere, in a 0 °C ice/water bath, was added ester **10m** (197 mg, 0.40 mmol) and ethanol (5 mL). $NaBH_4$ (122

mg, 3.2 mmol, 8 equiv) was then added portion-wise. The reaction mixture was allowed to warm to room temperature overnight (judged complete by GC-MS analysis). After this time, the reaction mixture was cooled to 0 °C and diluted with Et_2O (10 mL), then quenched by slow addition of a solution of 2 N NaOH(aq) (2 mL). The organic layer was washed successively with sat NH_4Cl and brine, then dried over anhydrous Na2SO4. It was filtered and concentrated *in vacuo* to yield the alcohol as a pale yellow oil. Yield = 136 mg, 92%. ^{1}H NMR (400 MHz, Chloroform-*d*) δ 7.33 – 7.15 (m, 5H), 7.03 – 6.94 (m, 2H), 6.94 – 6.81 (m, 2H), 4.92 (s, 2H), 4.60 (d, *J* = 2.1 Hz, 1H), 3.71 – 3.46 (m, 3H), 3.36 (s, 2H), 2.83 – 2.71 (m, 1H), 1.26 (q, *J* = 16.4 Hz, 1H), 1.23 (s, 9H). ^{13}C NMR (101 MHz, $CDCl_3$) δ 169.12, 158.41, 136.81, 134.68, 128.76, 128.22, 127.63, 127.34, 115.38, 70.25, 60.89, 60.09, 58.91, 58.07, 46.95, 28.33.

2.5.32 Peak Assignment for 15

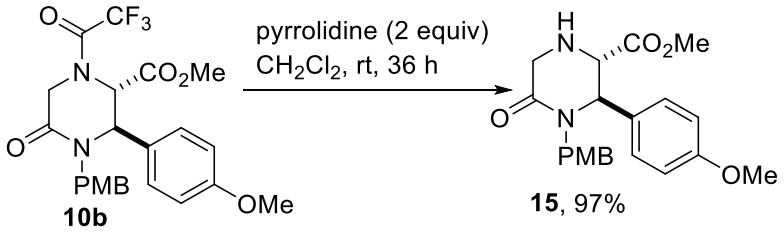

To a 10 mL round-bottomed flask equipped with a magnetic stir bar under a N2 atmosphere, at room temperature, was added ester **10b** (240 mg, 0.50 mmol) dissolved in DCM (5 mL) by means of a syringe. Pyrrolidine (71.1 mg, 1.0 mmol, 2 equiv) was then added. The reaction mixture was allowed to stir at room temperature until complete conversion (as judged by GC-MS and TLC analyses). The mixture was concentrated *in vacuo* to yield the amino ester as a pale yellow oil. Yield = 186 mg, 97%.

CHAPTER 3: EXPLORING THE SCOPE AND MECHANISM OF INTRAMOLECULAR HYDROALKYLATION OF *IN-SITU* GENERATED *BIS*-HOMOALLYLIC PIPERAZINOLS

3.1 Introduction

The 2-oxopiperazine motif constitutes the core of many alkaloid natural products and pharmaceuticals that span over thirty therapeutic areas, including antidepressants, antipsychotics, anxiolytics, and analgesics.[1] Additionally, this privileged scaffold, which ranks among the top three *N*-heterocycles in the U.S. FDA-approved-pharmaceuticals,[2] offers an excellent platform for systematic scaffolding, given that it may be transformed to other functionalized variants such as its saturated piperazine counterpart. Within this peptidomimetic research-suitable platform, is a subset of molecules that possess a bicyclic structure formally named 3,9-diazabicyclo[3.3.1] nonane (highlighted in **Figure 3-1**). For example, Ecteinascidin 743 (also known as, Ect-743, Trabectedin or Yondelis) is a natural product isolated from the *Ecteinascidia turbinate*, the sea squirt, which demonstrates potent anticancer activity.[95] Since 2004, Ect-743 is considered an orphan drug in the USA for the treatment of soft-tissue sarcoma and ovarian cancer.[96] Additionally Saframycin A, has potent antiproliferative activity against various tumor cell lines. This compound was isolated from *Streptomyces lavendulae* located in soil, making it a microbial based natural product.

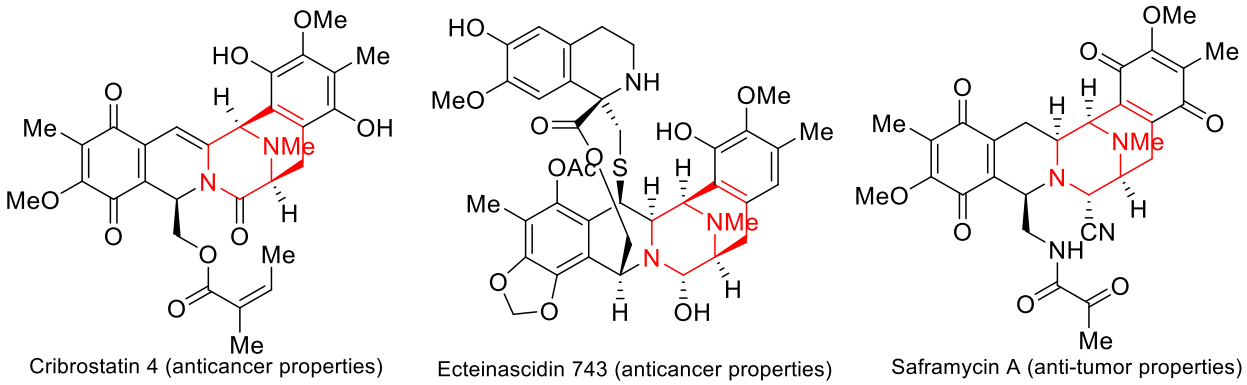

Figure 3.1 Examples of bioactive [3.3.1]-azabicyclic piperazines

The prevalence of small molecules as promising drug candidates and common occurrence of the [3.3.1] azabicyclic motif in natural products motivate synthetic chemists to find conditions for their synthesis and post-modification. This is an example of fragment-based drug discovery (FBDD). A major setback of FBDD protocols is its bias towards sp^2-enriched compounds by incorporation of aromatic rings.[97] To side-step this problem, the diversity-oriented synthesis (DOS) strategy, which aims to populate new chemical space with drug-like compounds that contain a high degree of molecular diversity, has emerged as an essential tool in chemical biology and drug discovery.[98] DOS is known for generating diverse molecules with both skeletal rearrangement and high stereoselectivity. Necessity for chiral, sp^3-enriched structures stems from nature's disposition towards these types of compounds and the 3D conformational characteristics seen in clinically evaluated compounds.[97,99,100] Fittingly, [3.3.1] azabicycles are highly sp^3 enriched.

The construction of [3.3.1] azabicycles has been demonstrated in the past by cyclization of tethers located on the piperazine ring. One of the most known methods is through iminium ions which have been long utilized for carbon−carbon and carbon−heteroatom bond formation. This tactic is employed in both Pictet-Spengler and Mannich reactions. For example, the Hiemstra group synthesized [3.3.1] azabicycles through α-amidoalkylation of *N*-acyliminium ion and π-nucleophiles including aromatic, heteroaromatic, and unsaturated α-H-amino acids groups.[101] The electrophilic properties of *N*-acyl iminium ions are due to the electron-withdrawing nature of the acyl group on nitrogen which makes the iminium carbon more electron-deficient. Furthermore, a promising renin inhibitor, named MK-8141, containing the bicyclic structure of interest lacked ability for further testing due to limited amounts of product available. Recently, scalable diastereoselective intramolecular Dieckmann cyclization of a

diester piperazine precursor was employed to forge the [3.3.1] azabicyclic motif resident in MK-8141.[102]

Our attention was brought to this caged scaffold after the opportuned construction of a [3.3.1] azabicycle containing a piperazine. In the past, we have reported Grignard addition onto our methylated CCR adducts as a form of post-diversification to generate tertiary alcohols.[84] Remarkably, this motif was observed after addition of allyl magnesium bromide onto a CCR derived piperazinonate. It is worth noting that the product contains five stereocenters, three of which are contiguous and two of which are vicinal. An investigation of the chemoselectivity, regioselectivity, and stereoselectivity of *in situ*-generated *bis*-homoallylic piperazinol by addition of allyl magnesium bromide onto CCR derived lactamoyl esters has been undertaken leading to an optimized protocol and increased modularity. Additionally, it was crucial to probe the mechanism to fully understand this intriguing transformation.

3.2 Results and Discussion

3.2.1 Synthesis of [3.3.1] azabicycles piperazines

Metallation reactions of enolizable carbonyl-containing compounds with Grignard reagents are known to be extremely problematic due to poor chemoselectivity. The most common competing processes are nucleophilic addition, reduction and aldol condensation of the carbonyl substrate. A potentially beneficial approach is to take advantage of the high electrophilicity of a Mg^{2+} cation and its propensity to form a multicoordinate complex. If preformation of a Mg(II) complex with an inherently less reactive carboxylic acid derivative such as a lactam is achievable, the acidity of the lactam would be enhanced, thus, allowing for enolization by a mild base. Three commonly employed simple basic systems are $Mg(OR)_2$,

Mg(OR)X and MgX_2/Et_3N. *To the best of our knowledge, Grignard reagents have proven to be incompetent bases for enolization of lactams.*

We commenced studies on the construction of highly functionalized [3.3.1] azabicyclic piperazines using model substrate **1g** in tetrahydrofuran (THF) with an addition of excess allyl magnesium bromide. As seen in **Table 3-1**, the reaction commenced at –78 °C and was brought up to room temperature. At the time of testing conditions, we wanted to develop a protocol that would result in high yields of the desired product while diminishing the possibility of decomposition. In the first attempts, there was no cyclization prompting us to extend the reaction time. At a time of 19 hours we were able to see cyclization. Unfortunately, nucleophilic attack on the lactam was observed (see **Scheme 3-2, 4a**).

Table 3-1 Optimization of the cyclization of *bis*-homoallylic alcohols

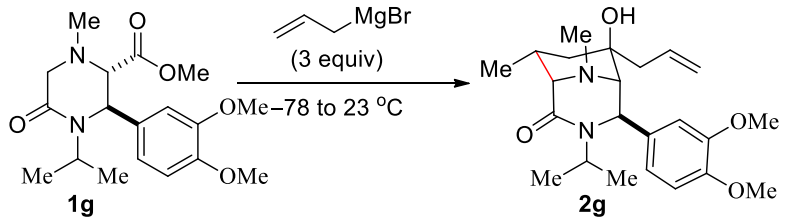

Entry	Solvent	Reaction time (cold, rt)	Outcome*
1	THF	5 hours (30m, 4h 30m)	No Cyclization
2	THF	6 hours (10m, 5h 50m)	No Cycliation
3	THF	19 hours (2h, 17h)	Cyclization

*monitored by GC/MS

Although nucleophilic attack was seen, we wanted to ensure that cyclization occurred therefore, we continued using these conditions. There was no observed nucleophilic attack on sequential reactions which signifies that nucleophilic attack may be substrate dependent. Furthermore, a second time optimization and solvent screening was conducted. In this instance, we wanted to ensure nucleophilic attack would not occur; therefore, substrate **1l** replaced **1g.** We were able to decrease reaction time by four hours and not compromise the conservation of

the tertiary alcohol to a [3.3.1] azabicycle. Additionally, the solvent THF demonstrated to be the best for the protocol when compared to Me-THF and THF/TMEDA.

Table 3-2 Optimization of time and solvent effect for cyclization of *bis*-homoallylic alcohols

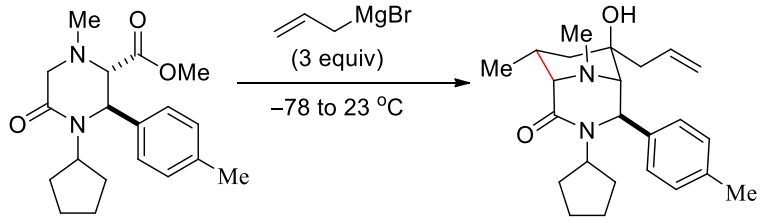

1l **2l**

Entry	Solvent	Reaction time (cold, rt)	Outcome*
1	THF	19 hours (2h, 17h)	Cyclization
2	THF	15 hours (30m, 14h 30m)	Cyclization
3	Me-THF	15 hours (30m, 14h 30m)	No Cyclization
4	THF/TMEDA	15 hours (30m, 14h, 30m)	No Cyclization

*monitored by GC/MS

Following optimization studies, we explored the scope of this cascade process. In this event, we find that various electron-rich and electron-neutral aryl-bearing piperazinonates are well-tolerated (**Scheme 3-1**, see **2a–g**). Piperazinonates bearing other *N*-alkyl substituents also react prudently with allylmagnesium bromide to afford the bicyclic architectures (see **2h–n)**. As a testament to the generality of the transformation, we have found that allylic piperazinonates undergo cascade annulation in similar efficiency to their benzylic congeners, albeit slowly (see **2o/p)**.

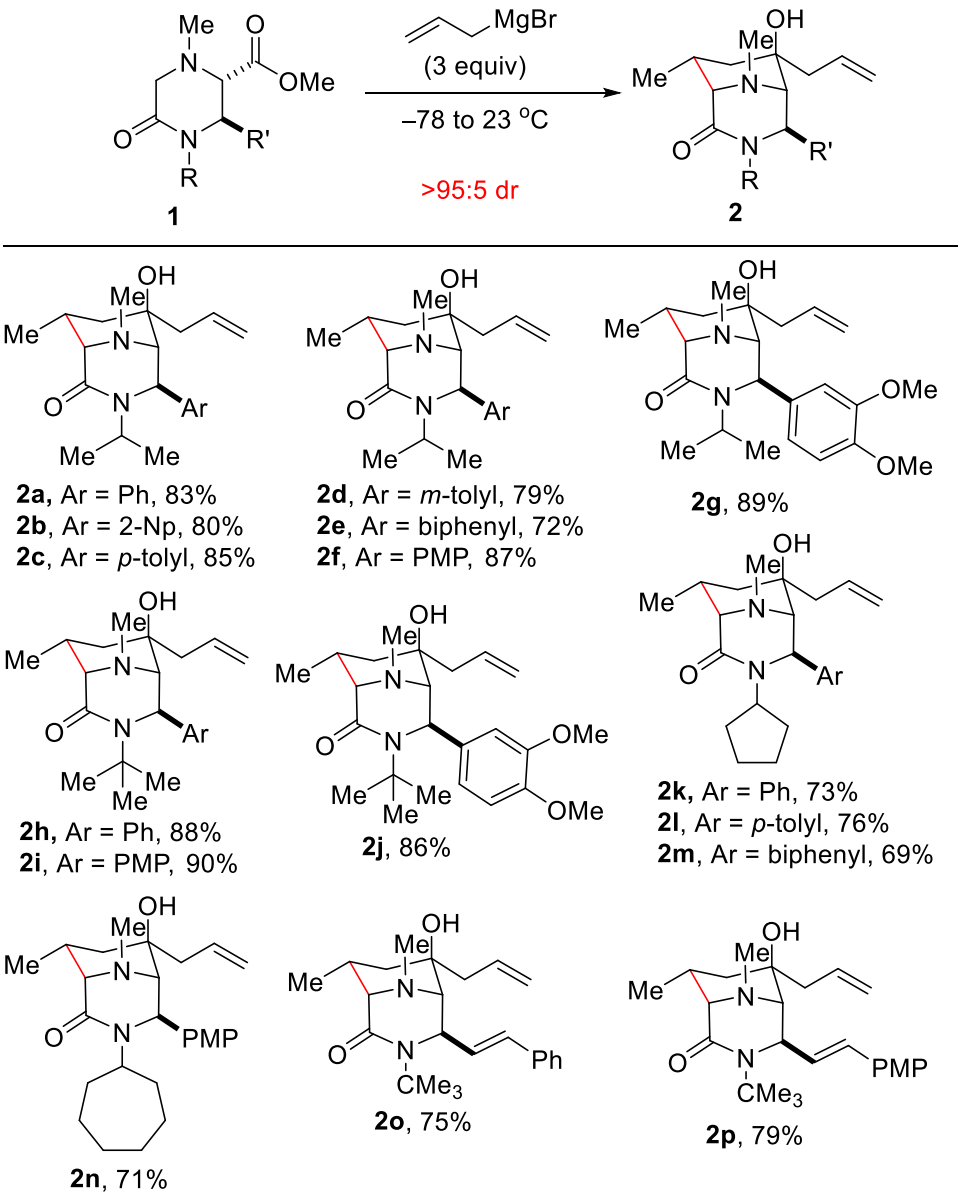

Scheme 3-1: Hydroalkylation of lactamoyl esters to produce [3.3.1] azabicyles

Scheme 3-2 shows that not all substrates engaged in cyclization such as **3a-c**, which formed the *bis*-homoallylic tertiary alcohol. We have demonstrated that *N*-alkyl substituted allylic piperazinonates are capable of cyclization (see **2o/p)**. Although speculative, the inability of **3d** to undergo cyclization suggests that *N*-aryl substituted piperazinonates are not competent substrates for this domino annulation. As stated previously, metallation reactions of enolizable carbonyl-containing compounds with Grignard reagents are quite problematic given that

nucleophilic addition is often a competing process. As an unfortunate case in point and an illustration of the importance of controlling the duration of the reaction, we find that bicycle **2g** is susceptible to nucleophilic attack after prolonged exposure to afford surprisingly isolable tertiary lactamol **4a**. These results clearly indicate that these conformationally constrained piperazinonates undergo enolization at rates that are much faster than nucleophilic addition.

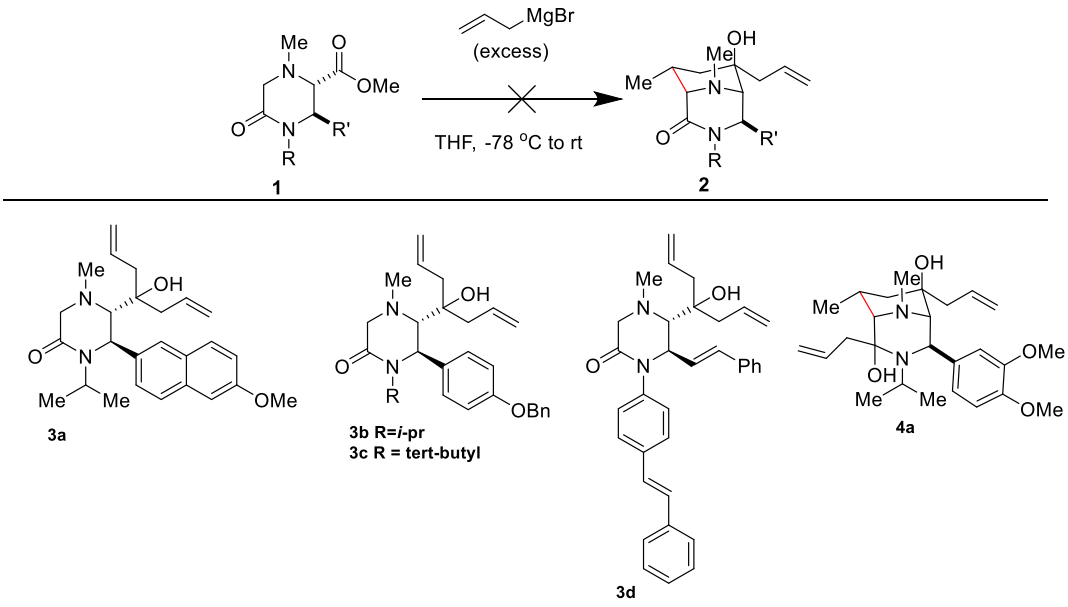

Scheme 3-2: Substrates that did not undergo cyclization or had nucleophilic attack on lactam

In an attempt to render the transformation sequential, we subjected *bis*-homoallylic alcohol **3e** to a few reaction conditions (**Scheme 3-3**). However, no cyclization was observed with the mass balance being accounted for by recovered starting material or decomposition products.

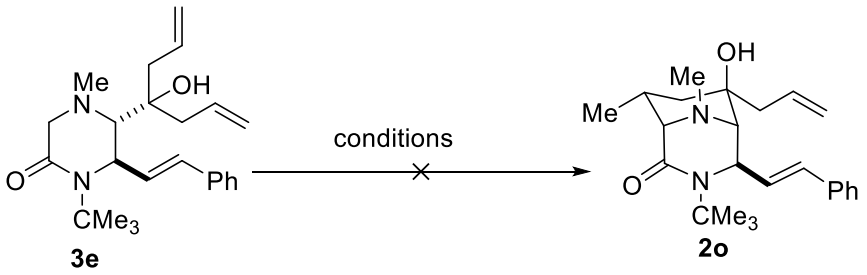

conditions A: *tert*-BuOK (30 mol%)
NMP or DMSO, rt, 3 h (decomposition)

conditions B: $Cu(OTf)_2$ (5 mol%)
dioxane, 90 °C, 16 h (no reaction)

conditions C: KBr (1 equiv), K_3PO_4 (1.2 equiv)
18-Crown-6 (1.2 equiv), DMF, 100 °C (no reaction)

conditions D: $Zn(TMP)_2$ (2 equiv), $ZnBr_2$ (3 equiv)
THF, 80 °C, 16 h (decomposition)

Scheme 3-3: Attempts to induce cyclization of piperazinol **3e**

We know that enolization of the *bis*-homoallylic piperazinol is possible since we are able to intermolecularly trap the corresponding lithium enolate of **3e** with methyl iodide (**Scheme 3-4**). This result indicates that the transient lithium enolate is incapable of engaging the pendant alkenes in a formal hydroalkylation.

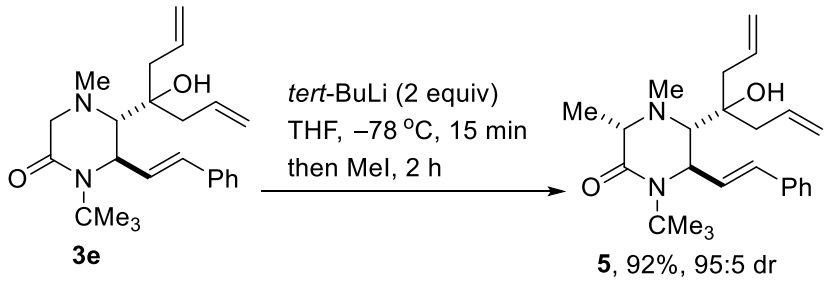

Scheme 3-4: Intermolecular enolate trapping of piperazinol **3e**

In another mechanistically intuitive outcome, these studies have revealed that the use of alkenyl Grignard reagents such as vinyl magnesium bromide affords only the *bis*-allylic tertiary piperazinols without cyclization or nucleophilic addition to the lactam (**Scheme 3-5**).

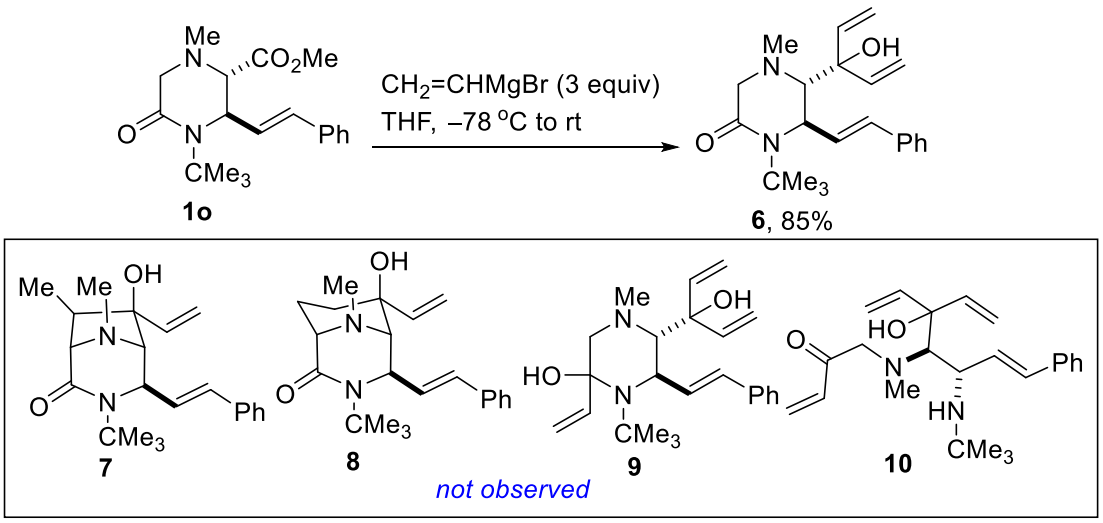

Scheme 3-5: Chemoselective addition of vinylmagnesium bromide to piperazinonate **1o**

3.2.2 Mechanistic Studies

We postulate that these [3.3.1] azabicycles are formed through a cascade reaction involving the chemoselective addition of allyl magnesium bromide to the piperazinonate followed by intramolecular cyclization. In order to fully understand the nuances of the transformation, we sought to investigate the potential role of the basic nitrogen (*i.e.*, the methyl-bearing nitrogen). Specifically, we questioned whether the cyclization proceeds via a hydroaminoalkylation or hydroalkylation pathway (**Figure 3-4 and Figure 3-5**).

Hydroaminoalkylation

Figure 3-2 depicts some literature precedence on hydroaminoalkylation of simple olefins or styrenes with *N*-heterocycles.[103] Hydroaminoalkylation refers to the addition of a carbon adjacent to a nitrogen and a hydrogen across a double bond. In this scheme there are two main limitations; (i) a covalently attached directing group such as pyridine is needed on the nitrogen

for hydroaminoalkylation to occur and (ii) the diasteroselectivity of the process is low to modest with the highest being a dr. of 80:20. Nako and co-workers were able to overcome one of the barriers of Chatani's hydroaminoalkylation by using a scandium TM-catalyst.[20] This method of hydroaminoalkylation eliminated the prior need of a directing group and it is reagent-controlled.

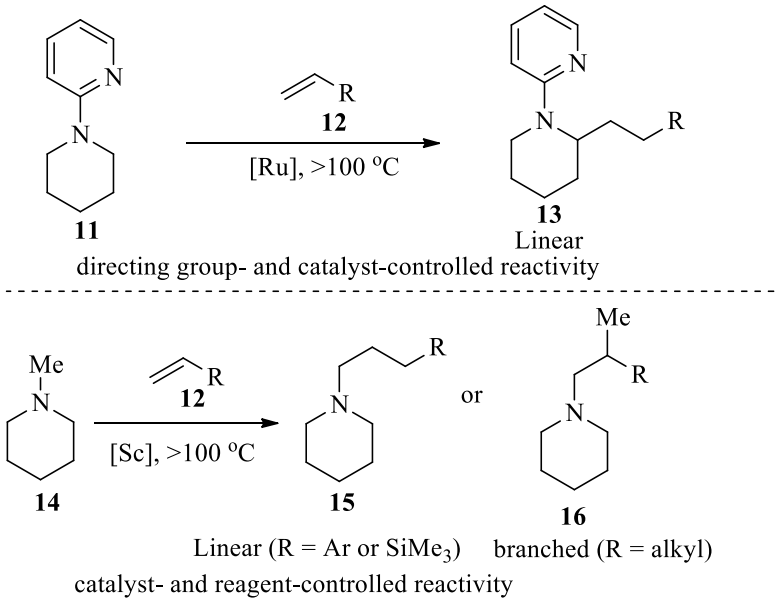

Figure 3-2 Previous hydroaminoalkylation of tertiary amines

Figure 3-3 displays possible products that could result from hydroaminoalkylation of our piperazinonates. There are four possible carbon atoms that can be engaged in a hydroaminoalkylation reactions due to them being adjacent to a nitrogen atom. In these examples, formation of 5- and 6-membered rings are possible as well as engagement of both allyl tethers. The formation of 5- or 6- membered rings is explained by the possibility of linear or branch addition of the allyl tether. However, in our case, a single highly caged bridged bicycle is formed. The newly formed 6-membered ring was derived from engagement of a single allyl tether in an exclusive regioselective branched manner to the carbon adjacent to the carbonyl.

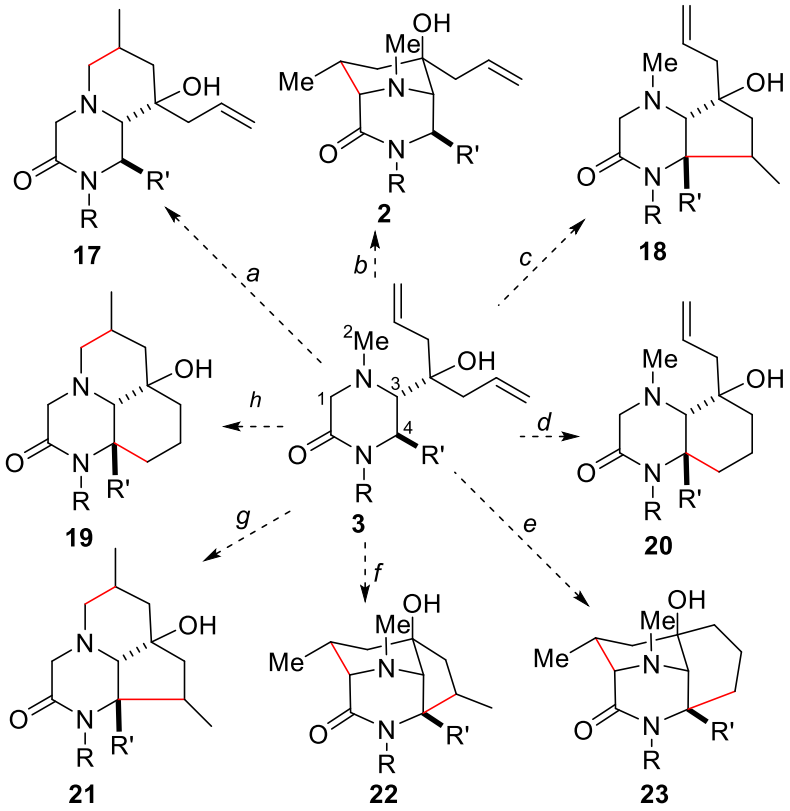

Figure 3-3 Examples of possible products through hydroaminoalkylation

In the event of a hydroaminoalkylation, we surmise that formation of the *bis*-homoallylic alcohol is accompanied by azametallacyclization to form a highly strained metalaziridine intermediate as depicted in **Figure 3-4**. Subsequent 1,2-olefin insertion delivers the branched ring-expanded azametallocyclic intermediate, which undergoes reductive elimination to produce the [3.3.1] azabicycles.[20] Such a mechanism necessitates that the methyl-bearing nitrogen play a critical role during the course of the reaction. Furthermore, a transition metal is often employed to induce the formation of the metallaaziridine intermediate. However, control experiments have revealed that piperidinonates and morpholinates also undergo cascade annulation under similar reaction conditions. This work will be revealed in a timely manner. This outcome negates the notion that the second nitrogen is necessary for cyclization to occur. These findings and the

absence of a transition metal during the course of our reaction strongly point to another pathway not involving hydroaminoalkylation.

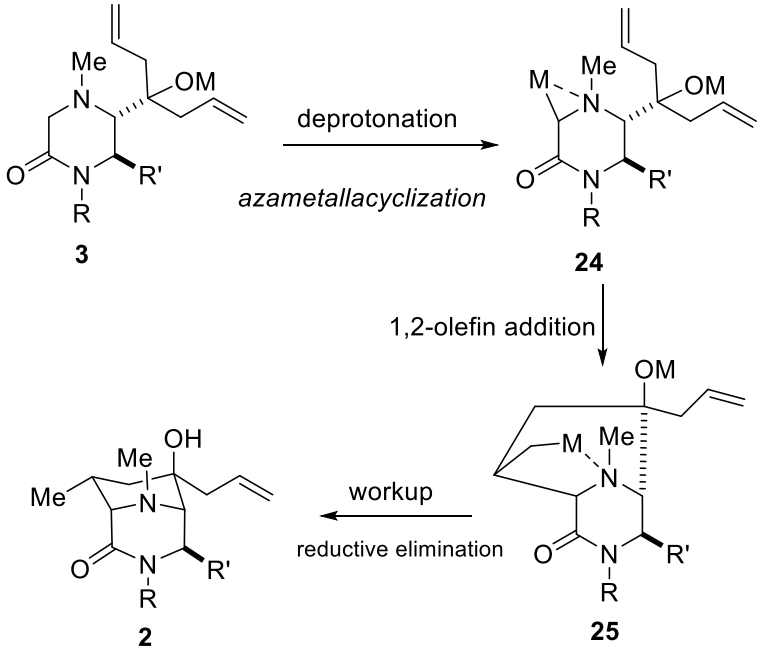

Figure 3-4 Possible mechanism of hydroaminoalkylation of *in situ*-generated piperazinols

Enolate Hydroalkylation of Alkenes

Enolate hydroalkylation is based on the presence of an enolizable carbonyl compound followed by reaction of the transient enolate with the alkene. Hydroalkylation of aryl-conjugated olefins with potassium enolates derived from *N*-methyl-2-pyrrolidinone and *N*-methyl-2-piperidone have been reported.[104] Gleaning from this precedence, we postulate that hydroalkylation of piperazinonates starts by the chemoselective addition of allylmagnesium bromide to the ester motif to afford the corresponding *bis*-homoallylic alkoxide (**Figure 3-5**). At the same time, the lactam motif is instead enolized leading to intermediate **26**.

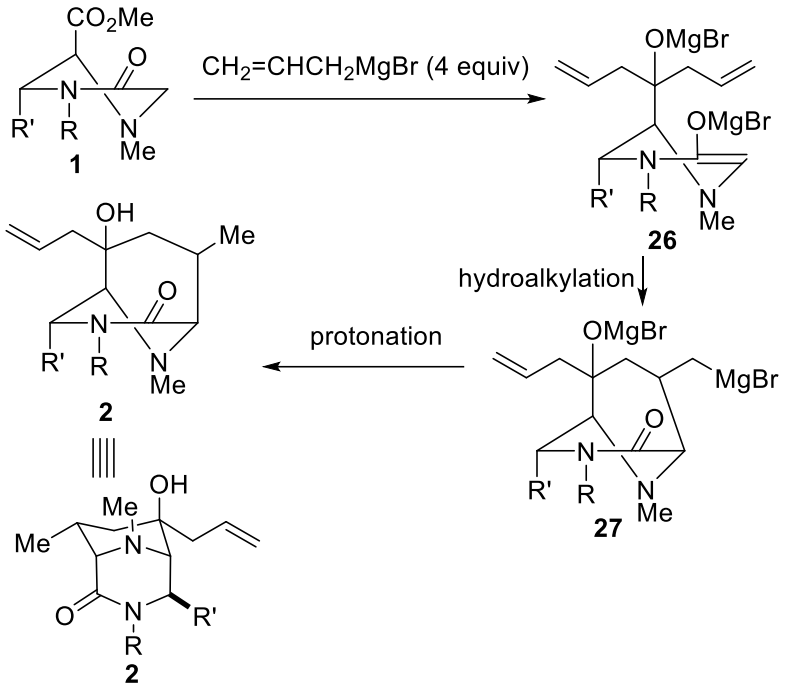

Figure 3-5 Possible mechanism of hydroalkylation

In this scenario, the Grignard reagent might be serving as both a nucleophile and a base. *To the best of our knowledge, Grignard reagents have proven to be incompetent bases for enolization of lactams.* A potentially beneficial approach is to take advantage of the high electrophilicity of an Mg^{2+} cation and its propensity to form a multicoordinate complex. If preformation of a Mg(II) complex with an inherently less reactive carboxylic acid derivative such as a lactam is achievable, the acidity of the lactam would be enhanced, thus, allowing for enolization by a mild base. Three commonly employed simple basic systems are $Mg(OR)_2$, Mg(OR)X and MgX_2/Et_3N.[105] (**Figure 3-6**). A close inspection of *bis*-homoallylic intermediate **26** reveals the presence of a magnesium alkoxide species.

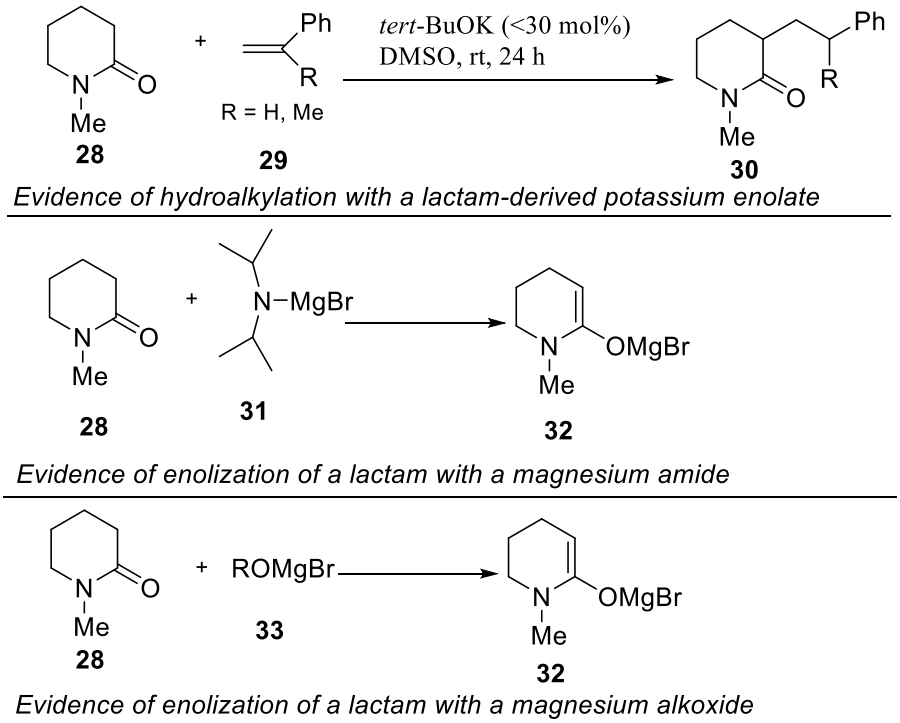

Figure 3-6 Evidence of enolate hydroalkylation of alkenes and formation of a magnesium enolate from a lactam

At this point, we propose that the all-important magnesium enolate is formed by intramolecular enolization using the transiently generated magnesium alkoxide. An updated mechanism is shown in **Figure 3-7.**

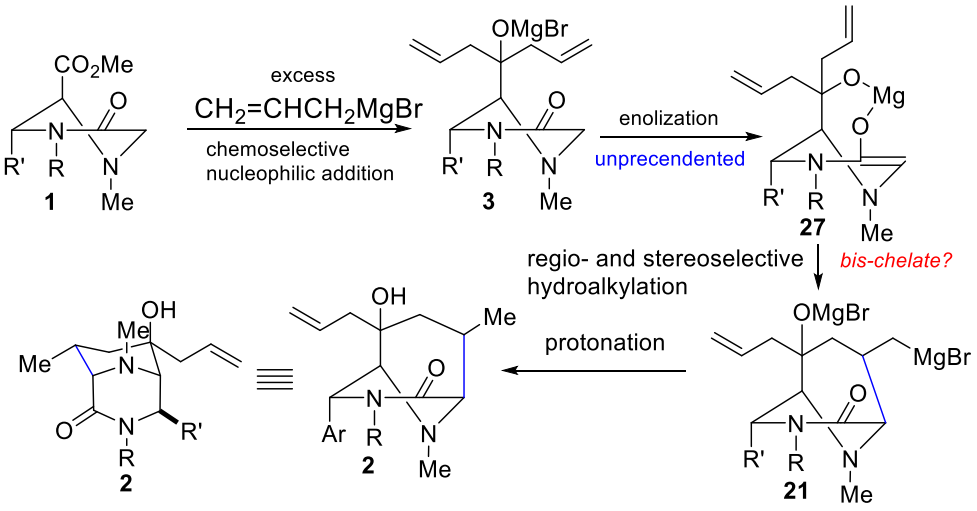

Figure 3-7 Updated mechanism of Hydroalkylation

3.3 Conclusions: In summary, the scope and mechanism of a stereoselective-, branched-regioselective-, and operationally simple approach to highly functionalized piperazines containing [3.3.1]-azabicycles has been explored. The modularity of the starting material was expanded leading to a diverse set of [3.3.1]-azabicycles. Mechanistic studies point to an intramolecular hydroalkylation process, predicated on the enolization of a relatively unreactive lactam unit by an *in situ* generated magnesium alkoxide. The [3.3.1] azabicyclic piperazinols are currently undergoing structure-activity-relationship (SAR) studies on neglected tropical diseases (NTDs), including leishmaniasis.

3.4 General Procedures

All experiments involving air and moisture sensitive reagents were carried out under an inert atmosphere of nitrogen and using freshly distilled solvents. Column chromatography was performed on silica gel (230-400 mesh). Thin-layer chromatography (TLC) was performed using Silicycle SiliaplateTM glass backed plates (250 µm thickness, 60 Å porosity, F-254 indicator) and visualized using UV (254 nm) or $KMnO_4$ stain. Unless otherwise indicated, ^{1}H, ^{13}C, DEPT-135 NMR, COSY 45, and NOESY spectra were acquired using $CDCl_3$ as solvent at room temperature. Chemical shifts are quoted in parts per million (ppm). HRMS-EI^+ data were obtained using either electronspray ionization (ESI) or electron impact (EI) techniques.

3.4.1 General Procedure A: Reaction of aryl imines with N-methyl morpholine 2,6-dione

A 5 mL screw-cap vial was flame-dried, evacuated and flushed with nitrogen. A solution of the imine (1.0 mL, 0.10 M in freshly distilled toluene) was added to the vial at room temperature followed by anhydride (1 equiv). The contents were placed in a pre-heated oil bath thermostatted 100 ^{o}C. After complete consumption of the imine (as judged by TLC and NMR),

the mixture/suspension was cooled to room temperature and washed several times with petroleum ether, then concentrated under reduced pressure to afford the crude cycloadducts.

3.4.2 General Procedure B: Methyl esterification of cycloadducts

To a stirring suspension of the acid (1 mmol), dissolved in DMF (5 mL), and K_2CO_3 (3 equiv) methyl iodide (2 equiv) was added under nitrogen atmosphere. The reaction mixture was stirred for about 12 h (TLC monitoring). After complete conversion, it was diluted with water and extracted with EtOAc (2×20 mL). The combined organic extracts were washed with brine, dried over $MgSO_4$ and concentrated *in vacuo* to give the desired ester, which was purified by flash chromatography on silica.

3.4.3 General Procedure C: Grignard Addition on methylated cycloadducts

To the crude lactamoyl ester (1.0 mmol) dissolved in freshly distilled THF (5 mL), was slowly added allyl magnesium bromide (2.0 mL, 1.0 M solution in THF, 3 equiv) under nitrogen at –78 °C. The reaction was kept at –78 °C for 30 minutes and slowly brought up to room temperature. The reaction remained in room temperature for 14 -15 hours. The mixture was quenched with sat. aq NH_4Cl and diluted with EtOAc. The layers were separated and the aqueous layer was extracted twice with EtOAc. The combined organic layers were dried over $MgSO_4$ for 20 min, filtered, and concentrated under reduced pressure to give the desired product. Purification: Flash chromatography on silica eluting with Hexane/EtOAc (75:25, 50:50 and 0:100).

3.4.4 General Procedure D: Lithium enolate- electrophile trapping

To a tertiary alcohol (1.0 mmol) dissolved in freshly distilled THF (5 mL), was slowly added *tert*-butyl lithium (2.0 mL, 1.0 M solution in THF, 3 equiv) under nitrogen at –78 °C. The reaction was kept at –78 °C for 30 minutes. The electrophile was added after the 30 minutes. The

mixture was quenched with sat. aq NH_4Cl at –78 °C and diluted with EtOAc. The layers were separated and the aqueous layer was extracted twice with EtOAc. The combined organic layers were dried over $MgSO_4$ for 20 min, filtered, and concentrated under reduced pressure to give the desired product. Purification (if needed): Flash chromatography on silica eluting with Hexane/EtOAc (75:25, 50:50 and 0:100).

3.4 Peak Assignments

3.4.1 Peak Assignment for 2a

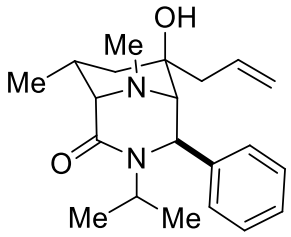

2a, 83%

Prepared in 1 mmol scale using General Procedure D. Purification: Flash chromatography on silica eluting with hexane/EtOAc (50:50). Yield = 285 mg, 83%, 95:5 dr. ^{1}H NMR (400 MHz, Chloroform-*d, rotamers*) δ 7.32 – 7.23 (m, 5H), 6.01 (tt, *J* = 17.0, 7.4 Hz, 1H), 5.27 – 5.18 (m, 2H), 4.35 (s, 1H), 3.78 (s, 1H), 3.39 (h, *J* = 6.7 Hz, 1H), 3.11 (d, *J* = 4.6 Hz, 1H), 2.75 (s, 1H), 2.54– 2.41 (m, 4H), 2.30 (dt, *J* = 13.4, 6.4 Hz, 1H), 1.67 (dd, *J* = 14.2, 4.3 Hz, 1H), 1.42 (d, *J* = 6.8 Hz, 3H), 1.30 – 1.15 (m, 4H), 1.00 (d, *J* = 6.9 Hz, 3H). ^{13}C NMR (101 MHz, $CDCl_3$) δ 169.35, 142.97, 132.96, 128.55, 127.41, 127.32, 118.85, 72.32, 68.70, 65.52, 60.42, 52.62, 44.31, 43.46, 38.61, 29.65, 21.29, 19.37, 18.20.

3.4.2 Peak Assignment for 2b

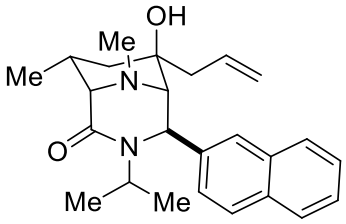

2b, 80%

Prepared in 1 mmol scale using General Procedure D. Purification: Flash chromatography on silica eluting with hexane/EtOAc (25:75). Yield = 314 mg, 80%, 95:5 dr.

3.4.3 Peak Assignment for 2c

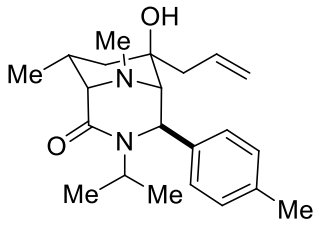

2c, 85%

Prepared in 1 mmol scale using General Procedure D. Purification: Flash chromatography on silica eluting with hexane/EtOAc (50:50). Yield = 303 mg, 85%, 95:5 dr. ^{1}H NMR (400 MHz, Chloroform-*d-rotamers*) δ 7.30 – 7.23 (m, 2H), 7.16 (d, *J* = 7.5 Hz, 2H), 6.04 (ddt, *J* = 17.3, 10.3, 7.0 Hz, 1H), 5.31 – 5.21 (m, 2H), 4.36 (s, 1H), 3.84 (s, 1H), 3.40 (hept, *J* = 6.7 Hz, 1H), 3.13 (d, *J* = 4.7 Hz, 1H), 2.78 (q, *J* = 1.3 Hz, 1H), 2.59 (s, 3H), 2.58 – 2.44 (m, 2H), 2.36 – 2.26 (m, 4H), 1.74 – 1.65 (m, 1H), 1.47 (d, *J* = 6.8 Hz, 3H), 1.33 – 1.16 (m, 4H), 1.04 (d, *J* = 7.0 Hz, 3H). ^{13}C NMR (101 MHz, $CDCl_3$) δ 169.36, 139.94, 137.11, 132.99, 129.25, 127.25, 118.77, 72.25, 68.89, 65.58, 60.30, 52.74, 44.43, 43.28, 38.50, 30.05, 21.31, 21.08, 19.32, 18.19.

3.4.4 Peak Assignment for 2d

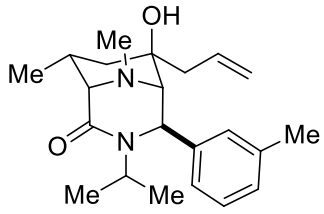

2d, 79%

Prepared in 1 mmol scale using General Procedure D. Purification: Flash chromatography on silica eluting with hexane/EtOAc (50:50). Yield = 281 mg, 79%, 95:5 dr. ^{1}H NMR (400 MHz, Chloroform-*d, rotamers*) δ 7.37 (s, 1H), 7.24 – 7.18 (dd, J = 6.6, 1.6 Hz, 2H), 7.11 – 7.04 (m, 1H), 6.05 (ddt, J = 17.2, 10.2, 7.0 Hz, 1H), 5.33 – 5.20 (m, 2H), 4.35 (s, 1H), 3.88 – 3.84 (m, 1H), 3.39 (hept, J = 6.7 Hz, 1H), 3.16 – 3.10 (m, 1H), 2.84 – 2.74 (m, 1H), 2.59– 2.45 (m, 5H), 2.43 – 2.26 (m, 5H), 1.74 – 1.65 (m, 1H), 1.48 (d, J = 6.7 Hz, 3H), 1.34 – 1.11 (m, 4H), 1.04 (d, J = 7.0 Hz, 3H). ^{13}C NMR (101 MHz, $CDCl_3$) δ 169.43, 142.90, 138.25, 133.05, 128.43, 128.12, 124.35, 118.73, 72.27, 68.78, 65.56, 60.52, 52.90, 44.42, 43.26, 38.50, 30.11, 21.53, 21.32, 19.31, 18.19.

3.4.5 Peak Assignment for 2e

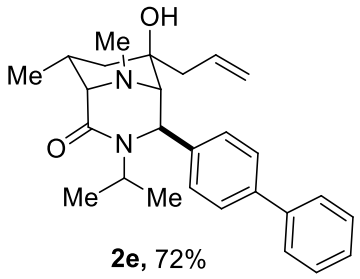

2e, 72%

Prepared in 1 mmol scale using General Procedure D. Purification: Flash chromatography on silica eluting with hexane/EtOAc (25:75). Yield = 301 mg, 72%, 95:5 dr. ^{1}H NMR (400 MHz, Chloroform-*d, rotamers*) δ 7.68 – 7.56 (m, 4H), 7.47 (dq, J = 7.8, 4.7, 2.8 Hz, 4H), 7.41 – 7.31 (m, 1H), 6.08 (ddt, J = 17.2, 10.2, 7.0 Hz, 1H), 5.35 – 5.25 (m, 2H), 4.44 (s, 1H), 3.79 (s, 1H), 3.49 (dt, J = 13.5, 6.7 Hz, 1H), 3.18 (d, J = 4.6 Hz, 1H), 2.84 (s, 1H), 2.66 – 2.36 (m, 6H), 1.72 (dd, J = 13.9, 4.2 Hz, 1H), 1.50 (d, J = 6.7 Hz, 3H), 1.37 – 1.21 (m, 4H), 1.06 (d, J = 7.0 Hz, 3H). ^{13}C NMR (101 MHz, $CDCl_3$) δ 169.34, 142.04, 140.37, 140.27, 133.00, 128.91, 127.79, 127.54, 127.22, 127.04, 118.90, 72.37, 68.76, 65.58, 60.24, 52.71, 44.38, 43.50, 38.70, 29.70, 21.36, 19.44, 18.21.

3.4.6 Peak Assignment for 2f

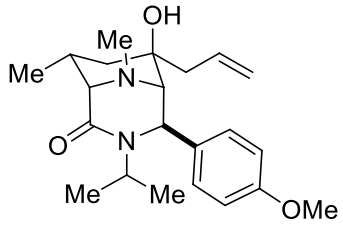

2f, 87%

Prepared in 1 mmol scale using General Procedure D. Purification: Flash chromatography on silica eluting with hexane/EtOAc (25:75). Yield = 324 mg, 87%, 95:5 dr. ^{1}H NMR (400 MHz, Chloroform-*d, rotamers*) δ 7.34 – 7.25 (m, 2H), 6.92 – 6.81 (m, 2H), 6.10 – 5.96 (m, 1H), 5.33 – 5.25 (m, 2H), 4.34 (s, 1H), 3.82 (s, 3H), 3.45 (m, J = 6.9 Hz, 1H), 3.15 (d, J = 4.7 Hz, 1H), 2.76 (s, 1H), 2.60 – 2.40 (m, 5H), 2.40 – 2.28 (m, 1H), 1.73 – 1.03 (m, 13H). ^{13}C NMR (101 MHz, $CDCl_3$) δ 169.32, 158.78, 134.80, 132.94, 128.48, 118.85, 113.86, 72.30, 68.82, 65.53, 59.89, 55.35, 52.51, 44.39, 43.37, 38.64, 29.77, 21.24, 19.41, 18.17.

3.4.7 Peak Assignment for 2g

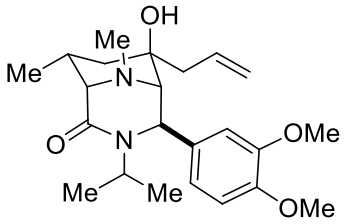

2g, 89%

Prepared in 1 mmol scale using General Procedure D. Purification: Flash chromatography on silica eluting with hexane/EtOAc (25:75). Yield = 358 mg, 89%, 95:5 dr. ^{1}H NMR (400 MHz, Chloroform-*d, rotamers*) δ 6.95 – 6.86 (m, 2H), 6.84 (d, *J* = 8.3 Hz, 1H), 6.06 (ddt, *J* = 17.1, 10.2, 7.0 Hz, 1H), 5.34 – 5.22 (m, 2H), 4.32 (s, 1H), 3.89 – 3.79 (m, *J* = 11.1 Hz, 6H), 3.42 (hept, *J* = 6.8 Hz, 1H), 3.14 (d, *J* = 4.7 Hz, 1H), 2.80 (d, *J* = 1.6 Hz, 1H), 2.62– 2.44 (m, 5H), 2.40 – 2.28 (m, 1H), 1.73 – 1.59 (m, 1H), 1.49 (d, *J* = 6.7 Hz, 3H), 1.35 – 1.17 (m, 5H), 1.04 (d, *J* = 7.0 Hz, 3H). ^{13}C NMR (101 MHz, $CDCl_3$) δ 169.34, 148.90, 148.17, 135.36, 133.16, 119.61, 118.66, 110.88, 110.42, 72.26, 68.67, 65.54, 60.16, 55.97, 52.78, 44.50, 43.23, 38.79, 29.96, 21.46, 19.35, 18.18.

3.4.8 Peak Assignment for 2h

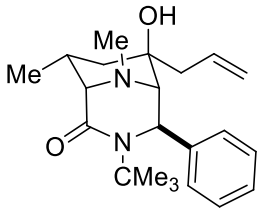

2h, 88%

Prepared in 1 mmol scale using General Procedure D. Purification: Flash chromatography on silica eluting with hexane/EtOAc (50:50). Yield = 313 mg, 88%, 95:5 dr. ^{1}H NMR (400 MHz, Chloroform-*d, rotamers*) δ 7.34 – 7.17(d, *J* = 7.7 m, 5H), 6.18 – 6.02 (m, 1H), 5.35 – 5.24 (m, 2H), 4.75 (br. s, 1H), 3.42 (s, 1H), 3.13 (d, *J* = 4.3 Hz, 1H), 2.71 (s, 1H), 2.49 – 2.29 (m, *J* = 14.2, 6.9 Hz, 6H), 1.66 (dd, *J* = 14.0, 4.4 Hz, 1H), 1.56 – 1.43 (m, 1H), 1.37 (s, 9H), 0.98 (d, *J* = 6.9 Hz, 3H). ^{13}C NMR (101 MHz, $CDCl_3$) δ 169.54, 144.67, 133.18,, 128.01, 127.46, 127.10, 118.72, 72.56, 71.71, 69.17, 67.06, 60.45, 59.33, 58.29, 56.91, 47.59, 44.42, 44.05, 41.55, 41.22, 40.01, 29.76, 29.08, 28.86, 28.49, 28.39, 21.13, 18.25.

3.4.9 Peak Assignment for 2i

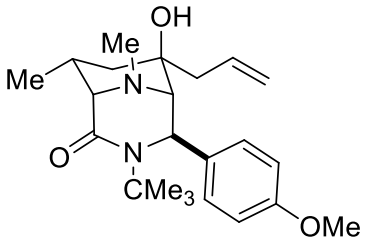

2i, 90%

Prepared in 1 mmol scale using General Procedure D. Purification: Flash chromatography on silica eluting with hexane/EtOAc (25:75). Yield = 347 mg, 90%, 95:5 dr. ^{1}H NMR (400 MHz, Chloroform-*d, rotamers*) δ δ 7.24 (s, 2H), 6.91 – 6.78 (m, 2H), 6.08 (dt, *J* = 16.7, 9.0 Hz, 1H), 5.34 –5.12 (m, 3H), 4.71 (s, 1H), 3.79 (s, 3H), 3.12 (d, *J* = 4.2 Hz, 1H), 2.68 (s, 1H), 2.49 – 2.37 (m, 6H), 1.65 (dd, *J* = 14.2, 4.4 Hz, 1H), 1.55 – 1.42 (m, 1H), 1.38 (s, 9H), 0.98 (d, *J* = 6.9 Hz, 3H). ^{13}C NMR (101 MHz, $CDCl_3$) δ 169.54, 158.58, 136.55, 133.24, 128.55, 118.91, 113.32, 72.51, 69.27, 67.09, 59.25, 57.67, 55.29, 44.35, 44.15, 40.04, 29.23, 28.84, 18.23.

3.4.10 Peak Assignment for 2j

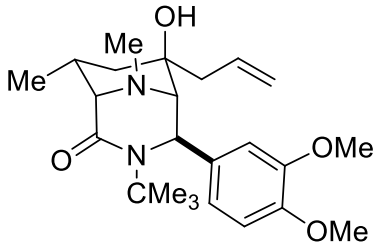

2j, 86%

Prepared in 1 mmol scale using General Procedure D. Purification: Flash chromatography on silica eluting with hexane/EtOAc (25:75). Yield = 358 mg, 86%, 95:5 dr. ^{1}H NMR (400 MHz, Chloroform-*d, rotamers*) δ 6.89 – 6.81 (m, 2H), 6.75 (d, J = 8.3 Hz, 1H), 6.18 – 6.03 (m, 1H), 5.31 – 5.21 (m, 2H), 4.67 (s, 1H), 3.82 (d, J = 9.9 Hz, 6H), 3.49 (s, 1H), 3.09 (d, J = 4.2 Hz, 1H), 2.71 (d, J = 1.7 Hz, 1H), 2.50 – 2.35 (m, 5H), 2.30 (ddt, J = 17.0, 8.6, 3.5 Hz, 1H), 1.62 (dd, J = 13.9, 4.4 Hz, 1H), 1.52 –1.37 (m, 10H), 0.95 (d, J = 7.0 Hz, 3H). ^{13}C NMR (101 MHz, $CDCl_3$) δ 169.53, 148.50, 147.96, 137.22, 133.66, 119.71, 118.45, 110.78, 110.55, 72.47, 69.13, 67.09, 59.34, 57.78, 55.94, 55.92, 44.29, 44.21, 40.15, 28.90, 18.21.

3.4.11 Peak Assignment for 2k

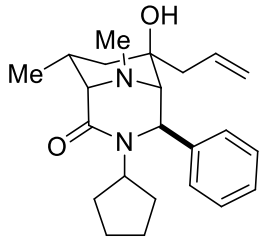

2k; 73%

Prepared in 1 mmol scale using General Procedure D. Purification: Flash chromatography on silica eluting with hexane/EtOAc (50:50). Yield = 269 mg, 73%, 95:5 dr. ^{1}H NMR (400 MHz, Chloroform-*d, rotamers*) δ 7.30 – 7.21 (m, 5H), 6.05 (dq, *J* = 16.1, 7.5 Hz, 1H), 5.28 – 5.19 (m, 2H), 4.45 (s, 1H), 3.89 (s, 1H), 3.63 – 3.44 (m, 1H), 3.07 (d, *J* = 5.1 Hz, 1H), 2.82 – 2.42 (m, 5H), 2.27 (dq, *J* = 13.1, 6.8, 6.2 Hz, 1H), 2.20 – 2.08 (m, 1H), 1.78 – 1.65 (m, 7H), 1.44 (tt, *J* = 16.0, 6.8 Hz, 1H), 1.36 – 1.12 (m, 2H), 0.97 (d, *J* = 7.0 Hz, 3H). ^{13}C NMR (101 MHz, $CDCl_3$) δ 169.03, 143.33, 133.18, 128.47, 127.21, 127.11, 118.64, 72.15, 68.99, 65.63, 61.88, 60.70, 44.39, 43.32, 38.72, 30.36, 29.82, 29.04, 24.67, 23.99, 18.22.

3.4.12 Peak Assignment for 2l

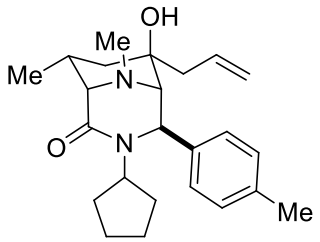

2l; 76%

Prepared in 1 mmol scale using General Procedure D. Purification: Flash chromatography on silica eluting with hexane/EtOAc (50:50). Yield = 290 mg, 76%, 95:5 dr. ^{1}H NMR (400 MHz, Chloroform-*d, rotamers*) δ 7.22 (d, *J* = 7.9 Hz, 2H), 7.22 – 7.10 (m, 2H), 6.08 (ddt, *J* = 18.3, 9.4, 7.0 Hz, 1H), 5.31 – 5.22 (m, 2H), 4.45 (s, 1H), 4.01 – 3.82 (br. s, 1H), 3.57 (p, *J* = 8.3 Hz, 1H), 3.10 (d, *J* = 4.6 Hz, 1H), 2.84 (s, 1H), 2.53 – 2.47 (m, 5H), 2.30 – 2.20 (m, 6H), 1.83 – 1.66 (m, 7H), 1.52 –1.16 (m, 4H), 1.01 (d, *J* = 7.0 Hz, 3H). ^{13}C NMR (101 MHz, $CDCl_3$) δ 168.96, 140.30, 136.84, 133.22, 129.15, 127.03, 118.56, 72.09, 69.09, 65.66, 61.94, 60.57, 44.47, 43.23, 38.65, 30.54, 29.81, 29.03, 24.73, 24.05, 21.05, 18.24.

3.4.13 Peak Assignment for 2m

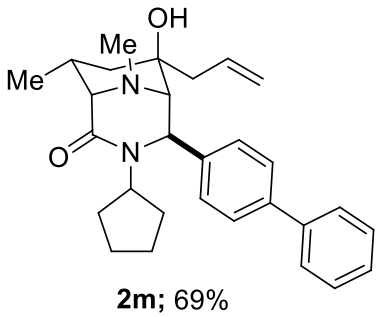

2m; 69%

Prepared in 1 mmol scale using General Procedure D. Purification: Flash chromatography on silica eluting with hexane/EtOAc (50:50). Yield = 306 mg, 69%, 95:5 dr. ^{1}H NMR (400 MHz, Chloroform-*d, rotamers*) δ 7.61 (ddd, *J* = 11.1, 7.8, 1.8 Hz, 4H), 7.50 – 7.33 (m, 5H), 6.21 – 6.06 (m, 1H), 5.36 – 5.27 (m, 2H), 4.55 (s, 1H), 4.00 (s, 1H), 3.65 (p, *J* = 8.3 Hz, 1H), 3.15 (d, *J* = 4.6 Hz, 1H), 2.93 (s, 1H), 2.59 – 2.52 (m, 5H), 2.40 – 2.20 (m, 2H), 1.96 –1.52 (m, 6H), 1.44 – 1.22 (m, 1H), 1.05 (d, *J* = 7.0 Hz, 3H), 0.95 (s, 3H). ^{13}C NMR (101 MHz, $CDCl_3$) δ 169.01, 142.43, 140.34, 140.07, 133.23, 128.90, 127.59, 127.53, 127.13, 127.02, 118.70, 76.79, 72.16, 69.08, 65.70, 62.06, 60.56, 44.56, 43.28, 38.72, 30.62, 29.90, 29.13, 24.75, 24.06, 18.26.

3.4.14 Peak Assignment for 2n

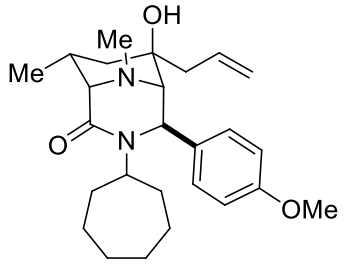

2n; 71%

Prepared in 1 mmol scale using General Procedure D. Purification: Flash chromatography on silica eluting with hexane/EtOAc (25:75). Yield = 302 mg, 71%, 95:5 dr. ^{1}H NMR (400 MHz, Chloroform-*d, rotamers*) δ 7.35 – 7.25 (m, 2H), 6.93 – 6.80 (m, 2H), 6.03 (ddt, *J* = 17.2, 10.2, 7.0 Hz, 1H), 5.31 – 5.19 (m, 2H), 4.33 (s, 1H), 3.88 – 3.76 (m, 5H), 3.12 (d, *J* = 4.8 Hz, 2H), 2.88 – 2.79 (m, 3H), 2.59 (s, 3H), 2.54 – 2.48 (m, 1H), 2.50 – 2.39 (m, 1H), 2.42 – 2.25 (m, 1H), 2.16 (qd, *J* = 12.1, 10.4, 4.5 Hz, 1H), 1.92 (ddt, *J* = 14.3, 7.2, 3.5 Hz, 1H), 1.79 – 1.62 (m, 5H), 1.54 – 1.30 (m, 2H), 1.27 (s, 1H), 1.25 – 1.09 (m, 1H), 1.13 – 1.00 (m, 3H). ^{13}C NMR (101 MHz, $CDCl_3$)

δ 168.78, 158.68, 134.79, 133.01, 128.43, 118.70, 113.97, 72.18, 68.90, 65.43, 63.60, 60.88, 55.34, 44.42, 43.10, 38.33, 33.97, 30.87, 30.22, 28.81, 26.99, 26.40, 26.36, 18.23.

3.4.15 Peak Assignment for 2o

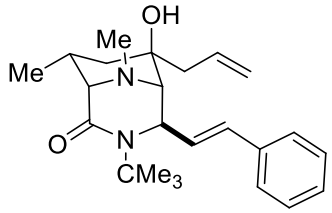

2o; 75%

Prepared in 1 mmol scale using General Procedure D. Purification: Flash chromatography on silica eluting with hexane/EtOAc (50:50). Yield = 287 mg, 75%, 95:5 dr. ^{1}H NMR (400 MHz, Chloroform-*d, rotamers*) δ 7.44 – 7.20 (m, 5H), 6.50 – 6.35 (m, 2H), 6.11 (dddd, *J* = 16.9, 10.5, 8.7, 5.5 Hz, 1H), 5.34 – 5.25 (m, 2H), 4.47 (dd, *J* = 4.8, 2.2 Hz, 1H), 3.10 – 2.76 (m, 2H), 2.69 – 2.58 (m, 5H), 2.37– 2.20 (m, 2H), 1.70 – 1.60 (m, 1H), 1.52 – 1.36 (m, 10H), 0.94 (d, *J* = 7.0 Hz, 3H). ^{13}C NMR (101 MHz, $CDCl_3$) δ 168.78, 136.38, 134.92, 133.58, 129.38, 128.85, 127.97, 126.21, 118.25, 72.26, 69.75, 67.55, 58.66, 56.68, 45.47, 43.41, 39.45, 31.04, 29.00, 17.98.

3.4.16 Peak Assignment for 2p

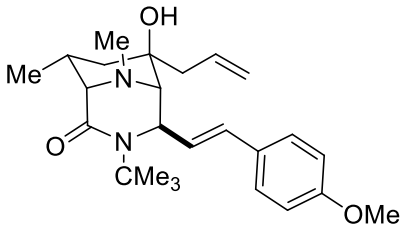

2p; 79%

Prepared in 1 mmol scale using General Procedure D. Purification: Flash chromatography on silica eluting with hexane/EtOAc (25:75). Yield = 325 mg, 79%, 95:5 dr. ^{1}H NMR (400 MHz, Chloroform-*d, rotamers*) δ 7.38 – 7.22 (m, 2H), 6.96 – 6.83 (m, 2H), 6.36 – 6.10 (m, 3H), 5.35 – 5.21 (m, 2H), 4.44 (d, *J* = 7.6 Hz, 1H), 4.07 (s, 1H), 3.83 (s, 3H), 3.09 – 2.95 (m, 1H), 2.72 – 2.57 (m, 5H), 2.42 – 2.19 (m, 3H), 1.65 – 1.15 (m, 10H), 0.94 (d, *J* = 6.9 Hz, 3H). ^{13}C NMR (101 MHz, $CDCl_3$) δ 168.76, 159.51, 133.57, 132.72, 129.13, 128.79, 127.36, 118.20, 114.26, 72.23, 69.78, 67.57, 58.62, 56.76, 55.42, 45.46, 43.38, 39.42, 30.78, 28.98, 17.98.

3.4.17 Peak Assignment for 5

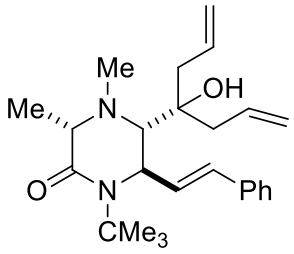

5; 92%

Prepared in 1 mmol scale using General Procedure D. Purification: Flash chromatography on silica eluting with hexane/EtOAc (0:100). Yield = 364 mg, 92%, 95:5 dr. ^{1}H NMR (400 MHz, Chloroform-*d, rotamers*) δ 7.34 – 7.26 (m, 6H), 6.42 – 6.30 (m, 2H), 5.90 (dddd, *J* = 27.8, 17.2, 13.2, 7.3 Hz, 2H), 5.18 (dq, *J* = 17.1, 8.9 Hz, 4H), 4.59 (d, *J* = 6.6 Hz, 1H), 3.71 (q, *J* = 6.8 Hz, 1H), 2.99 – 2.94 (m, 1H), 2.63 (s, 3H), 2.40 (d, *J* = 7.2 Hz, 4H), 1.51 (s, 9H), 1.43 (m, 3H). ^{13}C NMR (101 MHz, $CDCl_3$) δ 172.24, 136.75, 134.22, 133.55, 133.41, 130.11, 128.73, 127.73, 126.38, 119.46, 119.38, 78.27, 77.42, 77.10, 68.17, 60.22, 58.43, 55.65, 43.14, 42.56, 41.29, 28.56, 18.90.

3.4.18 Peak Assignment for 6

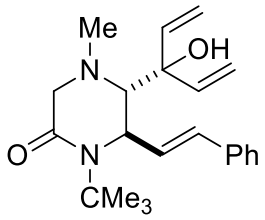

6, 85%

Prepared in 1 mmol scale using General Procedure D. Purification: Flash chromatography on silica eluting with hexane/EtOAc (0:100). Yield = 301 mg, 85%, 95:5 dr. ^{1}H NMR (400 MHz, Chloroform-*d, rotamers*) δ 7.42 - 7.28 (m, 5H), 6.42 (d, *J* = 16.0 Hz, 1H), 6.18 – 6.04 (m, 3H), 5.48 (d, *J* = 17.2 Hz, 1H), 5.37 (d, *J* = 17.2 Hz, 1H), 5.27 (d, *J* = 10.8 Hz, 1H), 5.18 (d, *J* = 10.6 Hz, 1H), 4.74 (d, *J* = 6.6 Hz, 1H), 3.44 – 3.33 (m, 2H), 3.02 (s, 1H), 2.83 (s, 1H), 2.49 (s, 3H), 1.45 (s, 9H). ^{13}C NMR (101 MHz, $CDCl_3$) δ 169.14, 141.88, 139.72, 136.24, 132.01, 130.56, 128.81, 128.03, 126.39, 114.37, 113.78, 78.66, 72.22, 58.88, 58.12, 55.58, 47.54, 28.88.

CITATIONS

(1) Taylor, R. D.; Maccoss, M.; Lawson, A. D. G. Rings in Drugs. *J. Med. Chem.* **2014**, *57* (14), 5845–5859.

(2) Vitaku, E.; Smith, D. T.; Njardarson, J. T. Analysis of the Structural Diversity, Substitution Patterns, and Frequency of Nitrogen Heterocycles among U.S. FDA Approved Pharmaceuticals. *J. Med. Chem.* **2014**, *57* (24), 10257–10274.

(3) Matib, M.; Zoubida, L. Effects of Piperazine on Removal of Hydrogen Sulfide from Liquefied Petroleum Gas (LPG) Using Aqueous Methyl Diethanol Amine (MDEA). *ChemXpress* **2017**, *11* (1), 131–143.

(4) Bishnoi, S.; Rochelle, G. T. Absorption of Carbon Dioxide into Aqueous Piperazine: Reaction Kinetics, Mass Transfer and Solubility. *Chem. Eng. Sci.* **2000**, *55* (22), 5531–5543.

(5) Baumann, M.; Baxendale, I. R. An Overview of the Synthetic Routes to the Best Selling Drugs Containing 6-Membered Heterocycles. *Beilstein J. Org. Chem.* **2013**, *9*, 2265–2319.

(6) Di Sciascio, G.; Riva, M. A. Aripiprazole: From Pharmacological Profile to Clinical Use. *Neuropsychiatr. Dis. Treat.* **2015**, *11*, 2635–2647.

(7) Casey, A. B.; Canal, C. E. Classics in Chemical Neuroscience: Aripiprazole. *ACS Chem. Neurosci.* **2017**, *8* (6), 1135–1146.

(8) Corbin, J. D.; Francis, S. H. Cyclic GMP Phosphodiesterase-5: Target of Sildenafil. *J. Biol. Chem.* **1999**, *274* (20), 13729–13732.

(9) Goldstein, I.; Burnett, A. L.; Rosen, R. C.; Park, P. W.; Stecher, V. J. The Serendipitous Story of Sildenafil: An Unexpected Oral Therapy for Erectile Dysfunction. *Sex. Med. Rev.* **2019**, *7* (1), 115–128.

(10) Keating, G. M. Dasatinib: A Review in Chronic Myeloid Leukaemia and Ph+ Acute Lymphoblastic Leukaemia. *Drugs* **2017**, *77* (1), 85–96.

(11) Lombardo, L. J.; Lee, F. Y.; Chen, P.; Norris, D.; Barrish, J. C.; Behnia, K.; Castaneda, S.; Cornelius, L. A. M.; Das, J.; Doweyko, A. M.; et al. Discovery of N-(2-Chloro-6-Methylphenyl)-2-(6-(4-(2-Hydroxyethyl)- Piperazin-1-Yl)-2-Methylpyrimidin-4-Ylamino)Thiazole-5-Carboxamide (BMS-354825), a Dual Src/Abl Kinase Inhibitor with Potent Antitumor Activity in Preclinical Assays. *J. Med. Chem.* **2004**, *47* (27), 6658–6661.

(12) Aguilera, D. G.; Tsimberidou, A. M. Dasatinib in Chronic Myeloid Leukemia: A Review. *Ther. Clin. Risk Manag.* **2009**, *5* (1), 281–289.

(13) Dinsmore, C. J.; Beshore, D. C. Syntheses and Transformations of Piperazinone Rings. A Review. *Org. Prep. Proced. Int.* **2002**, *34* (4), 367–404.

(14) Singer, B. H.; Utzinger, J.; Raso, G.; De Savigny, D.; N'Goran, E. K.; Tanner, M.; Ørnbjerg, N.; Brooker, S. Schistosomiasis and Neglected Tropical Diseases: Towards

Integrated and Sustainable Control and a Word of Caution. *Parasitology* **2009**, *136* (13), 1859.

(15) Erko, B.; Degarege, A.; Tadesse, K.; Mathiwos, A.; Legesse, M. Efficacy and Side Effects of Praziquantel in the Treatment of Schistosomiasis Mansoni in Schoolchildren in Shesha Kekele Elementary School, Wondo Genet, Southern Ethiopia. *Asian Pac. J. Trop. Biomed.* **2012**, *2* (3), 235–239.

(16) Kimani, B. W.; Mbugua, A. K.; Kihara, J. H.; Ng'ang'a, M.; Njomo, D. W. Safety, Efficacy and Acceptability of Praziquantel in the Treatment of Schistosoma Haematobium in Pre-School Children of Kwale County, Kenya. *PLoS Negl. Trop. Dis.* **2018**, *12* (10).

(17) Meister, I.; Ingram-Sieber, K.; Cowan, N.; Todd, M.; Robertson, M. N.; Meli, C.; Patra, M.; Gasser, G.; Keiser, J. Activity of Praziquantel Enantiomers and Main Metabolites against Schistosoma Mansoni. *Antimicrob. Agents Chemother.* **2014**, *58* (9), 5466–5472.

(18) Silberstein, S. D.; McCrory, D. C. Ergotamine and Dihydroergotamine: History, Pharmacology, and Efficacy. *Headache* **2003**, *43* (2), 144–166.

(19) Oda, Y.; Sato, T.; Chida, N. Direct Chemoselective Allylation of Inert Amide Carbonyls. *Org. Lett.* **2012**, *14* (3), 950–953.

(20) Nako, A. E.; Oyamada, J.; Nishiura, M.; Hou, Z. Scandium-Catalysed Intermolecular Hydroaminoalkylation of Olefins with Aliphatic Tertiary Amines. *Chem. Sci.* **2016**, *7* (10), 6429–6434.

(21) Andrade, C. Ketamine for Depression, 3: Does Chirality Matter? *J. Clin. Psychiatry* **2017**, *78* (6), e674–e677.

(22) Kim, J. H.; Scialli, A. R. Thalidomide: The Tragedy of Birth Defects and the Effective Treatment of Disease. *Toxicol. Sci.* **2011**, *122* (1), 1–6.

(23) Henderson, W. R.; Banerjee, E. R.; Chi, E. Y. Differential Effects of (S)- and (R)-Enantiomers of Albuterol in a Mouse Asthma Model. *J. Allergy Clin. Immunol.* **2005**, *116* (2), 332–340.

(24) Dubin, A.; Lattanzio, B.; Gatti, L. The Spectrum of Cardiovascular Effects of Dobutamine - from Healthy Subjects to Septic Shock Patients. *Rev. Bras. Ter. Intensiva* **2017**, *29* (4), 490–498.

(25) FDA Approves New Nasal Spray Medication for Treatment-Resistant Depression; Available Only at a Certified Doctor's Office or Clinic. *Case Medical Research*. 2019, pp 3–5.

(26) Tyler, M. W.; Yourish, H. B.; Ionescu, D. F.; Haggarty, S. J. Classics in Chemical Neuroscience: Ketamine. *ACS Chem. Neurosci.* **2017**, *8* (6), 1122–1134.

(27) Zhang, J. C.; Li, S. X.; Hashimoto, K. R (-)-Ketamine Shows Greater Potency and Longer Lasting Antidepressant Effects than S (+)-Ketamine. *Pharmacol. Biochem. Behav.* **2014**, *116*, 137–141.

(28) Molero, P.; Ramos-Quiroga, J. A.; Martin-Santos, R.; Calvo-Sánchez, E.; Gutiérrez-Rojas,

L.; Meana, J. J. Antidepressant Efficacy and Tolerability of Ketamine and Esketamine: A Critical Review. *CNS Drugs* **2018**, *32* (5), 411–420.

(29) Muller, J.; Pentyala, S.; Dilger, J.; Pentyala, S. Ketamine Enantiomers in the Rapid and Sustained Antidepressant Effects. *Ther. Adv. Psychopharmacol.* **2016**, *6* (3), 185–192.

(30) Goldfogel, M. J.; Meek, S. J. Diastereoselective Synthesis of Vicinal Tertiary and: N - Substituted Quaternary Stereogenic Centers by Catalytic Hydroalkylation of Dienes. *Chem. Sci.* **2016**, *7* (7), 4079–4084.

(31) Dow, D. E.; Bartlett, J. A. Dolutegravir, the Second-Generation of Integrase Strand Transfer Inhibitors (INSTIs) for the Treatment of HIV. *Infect. Dis. Ther.* **2014**, *3* (2), 83–102.

(32) Perryman, A. L.; Forli, S.; Morris, G. M.; Burt, C.; Cheng, Y.; Palmer, M. J.; Whitby, K.; McCammon, J. A.; Phillips, C.; Olson, A. J. A Dynamic Model of HIV Integrase Inhibition and Drug Resistance. *J. Mol. Biol.* **2010**, *397* (1), 600–615.

(33) Hughes, D. L. Review of Synthetic Routes and Final Forms of Integrase Inhibitors Dolutegravir, Cabotegravir, and Bictegravir. *Org. Process Res. Dev.* **2019**, *6*.

(34) Bruzzese, E.; Lo Vecchio, A.; Smarrazzo, A.; Tambaro, O.; Palmiero, G.; Bonadies, G.; Guarino, A. Dolutegravir-Based Anti-Retroviral Therapy Is Effective and Safe in HIV-Infected Paediatric Patients. *Ital. J. Pediatr.* **2018**, *44* (1), 1–5.

(35) Pinnetti, C.; Tintoni, M.; Ammassari, A.; Tamburrini, E.; Bernardi, S.; Liuzzi, G.; Scambia, G.; Perno, C. F.; Floridia, M.; Antinori, A.; et al. Successful Prevention of HIV Mother-to-Child Transmission with Dolutegravir-Based Combination Antiretroviral Therapy in a Vertically Infected Pregnant Woman with Multiclass Highly Drug-Resistant HIV-1. *Aids* **2015**, *29* (18), 2534–2537.

(36) Castagna, A.; Ferrara, M.; Galli, L.; Comi, L.; Sterrantino, G.; Cenderello, G.; Zaccarelli, M.; Foca, E.; Roncadori, A.; Lazzarin, A. Long-Term Efficacy of Dolutegravir in Treatment-Experienced Subjects Failing Therapy with HIV-1 Integrase Strand Inhibitor-Resistant Virus. *J. Antimicrob. Chemother.* **2017**, *73* (October 2017), 177–182.

(37) Markham, A. Bictegravir: First Global Approval. *Drugs* **2018**, *78* (5), 601–606.

(38) Hassounah, S. A.; Alikhani, A.; Oliveria, M.; Bharaj, S.; Ibanescu, R.-I.; Osman, N.; Xu, H.-T.; Brenner, B. G.; Mesplede, T.; Wainberg, M. A. Antiviral Activity of Bictegravir and Cabotegravir against Integrase Inhibitor- Resistant SIVmac239 and HIV-1. *Antimicrob. Agents Chemother.* **2017**, *61* (12), 1–9.

(39) Whitfield, T.; Torkington, A.; van Halsema, C. Profile of Cabotegravir and Its Potential in the Treatment and Prevention of HIV-1 Infection: Evidence to Date. *HIV/AIDS - Res. Palliat. Care* **2016**, *8*, 157–164.

(40) Spreen, W.; Min, S.; Ford, S. L.; Chen, S.; Lou, Y.; Bomar, M.; St Clair, M.; Piscitelli, S.; Fujiwara, T. Pharmacokinetics, Safety, and Monotherapy Antiviral Activity of GSK1265744, an HIV Integrase Strand Transfer Inhibitor. *HIV Clin. Trials* **2013**, *14* (5), 192–203.

(41) Min, S.; Sloan, L.; Dejesus, E.; Hawkins, T.; McCurdy, L.; Song, I.; Stroder, R.; Chen, S.; Underwood, M.; Fujiwara, T.; et al. Antiviral Activity, Safety, and Pharmacokinetics/Pharmacodynamics of Dolutegravir as 10-Day Monotherapy in HIV-1-Infected Adults. *Aids* **2011**, *25* (14), 1737–1745.

(42) Gallant, J. E.; Thompson, M.; DeJesus, E.; Voskuhl, G. W.; Wei, X.; Zhang, H.; White, K.; Cheng, A.; Quirk, E.; Martin, H. Antiviral Activity, Safety, and Pharmacokinetics of Bictegravir as 10-Day Monotherapy in HIV-1-Infected Adults. *J. Acquir. Immune Defic. Syndr.* **2017**, *75* (1), 61–66.

(43) Ye, Z.; Gettys, K. E.; Dai, M. Opportunities and Challenges for Direct C-H Functionalization of Piperazines. *Beilstein J. Org. Chem.* **2016**, *12*, 702–715.

(44) Luescher, M. U.; Vo, C. V. T.; Bode, J. W. SnAP Reagents for the Synthesis of Piperazines and Morpholines. *Org. Lett.* **2014**, *16* (4), 1236–1239.

(45) Siau, W. Y.; Bode, J. W. One-Step Synthesis of Saturated Spirocyclic N-Heterocycles with Stannyl Amine Protocol (SnAP) Reagents and Ketones. *J. Am. Chem. Soc.* **2014**, *136* (51), 17726–17729.

(46) Hsieh, S. Y.; Bode, J. W. Silicon Amine Reagents for the Photocatalytic Synthesis of Piperazines from Aldehydes and Ketones. *Org. Lett.* **2016**, *18* (9), 2098–2101.

(47) Yar, M.; McGarrigle, E. M.; Aggarwal, V. K. Bromoethylsulfonium Salt-a More Effective Annulation Agent for the Synthesis of 6- and 7-Membered 1,4-Heterocyclic Compounds. *Org. Lett.* **2009**, *11* (2), 257–260.

(48) Matlock, J. V.; Svejstrup, T. D.; Songara, P.; Overington, S.; McGarrigle, E. M.; Aggarwal, V. K. Synthesis of 6- and 7-Membered N-Heterocycles Using α-Phenylvinylsulfonium Salts. *Org. Lett.* **2015**, *17* (20), 5044–5047.

(49) Nakhla, J. S.; Wolfe, J. P. A Concise Asymmetric Synthesis of Cis-2,6-Disubstituted N-Aryl Piperazines via Pd-Catalyzed Carboamination Reactions. *Org. Lett.* **2007**, *9* (17), 3279–3282.

(50) James, T.; Simpson, I.; Grant, J. A.; Sridharan, V.; Nelson, A. Modular, Gold-Catalyzed Approach to the Synthesis of Lead-like Piperazine Scaffolds. *Org. Lett.* **2013**, *15* (23), 6094–6097.

(51) Zarganes-Tzitzikas, T.; Patil, P.; Khoury, K.; Herdtweck, E.; Dömling, A. Concise Synthesis of Tetrazole-Ketopiperazines by Two Consecutive Ugi Reactions. *European J. Org. Chem.* **2015**, *2015* (1), 51–55.

(52) Viso, A.; Fernández De La Pradilla, R.; Flores, A.; García, A.; Tortosa, M.; López-Rodríguez, M. L. Synthesis of Highly Substituted Enantiopure Piperazines and Ketopiperazines from Vicinal N-Sulfinyl Diamines. *J. Org. Chem.* **2006**, *71* (4), 1442–1448.

(53) Ben Haj Salah, K.; Legrand, B.; Bibian, M.; Wenger, E.; Fehrentz, J. A.; Denoyelle, S. Synthesis of [1,2,4]Triazolo[4,3- a]Piperazin-6-Ones: An Approach to the Triazole-Fused Ketopiperazine Scaffold. *Org. Lett.* **2018**, *20* (11), 3250–3254.

(54) Procopiou, P. A.; Ancliff, R. A.; Bamford, M. J.; Browning, C.; Connor, H.; Davies, S.; Fogden, Y. C.; Hodgson, S. T.; Holmes, D. S.; Looker, B. E.; et al. 4-Acyl-1-(4-Aminoalkoxyphenyl)-2-Ketopiperazines as a Novel Class of Non-Brain-Penetrant Histamine H3receptor Antagonists. *J. Med. Chem.* **2007**, *50* (26), 6706–6717.

(55) Powell, N. A.; Ciske, F. L.; Clay, E. C.; Cody, W. L.; Downing, D. M.; Blazecka, P. G.; Holsworth, D. D.; Edmunds, J. J. Practical Synthesis of 1-Aryl-6-(Hydroxymethyl)-2-Ketopiperazines via a 6-Exo Amide-Epoxide Cyclization. *Org. Lett.* **2004**, *6* (22), 4069–4072.

(56) Kaplaneris, N.; Spyropoulos, C.; Kokotou, M. G.; Kokotos, C. G. Enantioselective Organocatalytic Synthesis of 2-Oxopiperazines from Aldehydes: Identification of the Elusive Epoxy Lactone Intermediate. *Org. Lett.* **2016**, *18* (22), 5800–5803.

(57) Ruider, S. A.; Müller, S.; Carreira, E. M. Ring Expansion of 3-Oxetanone-Derived Spirocycles: Facile Synthesis of Saturated Nitrogen Heterocycles. *Angew. Chemie - Int. Ed.* **2013**, *52* (45), 11908–11911.

(58) Payne, P. R.; Garcia, P.; Eisenberger, P.; Yim, J. C. H.; Schafer, L. L. Tantalum Catalyzed Hydroaminoalkylation for the Synthesis of α- And β-Substituted N-Heterocycles. *Org. Lett.* **2013**, *15* (9), 2182–2185.

(59) McDermott, B. P.; Campbella, A. D.; Ertanb, A. First Example of S-BuLi/(-)-Sparteine-Mediated Chiral Deprotonation of a Piperazine and Proof of the Sense of Induction. *Synlett* **2008**, No. 6, 875–879.

(60) Firth, J. D.; O'Brien, P.; Ferris, L. Synthesis of Enantiopure Piperazines via Asymmetric Lithiation-Trapping of N-Boc Piperazines: Unexpected Role of the Electrophile and Distal N-Substituent. *J. Am. Chem. Soc.* **2016**, *138* (2), 651–659.

(61) Firth, J. D.; O'Brien, P.; Ferris, L. General Procedures for the Lithiation/Trapping of N-Boc Piperazines. *J. Org. Chem.* **2017**, *82* (13), 7023–7031.

(62) Mcnally, A.; Prier, C. K.; Macmillan, D. W. C. Discovery of an A-Amino C-H Arylation Reaction Using the Strategy of Accelerated Serendipity. *Science* **2011**, *334* (11), 1114–1117.

(63) Anxionnat, B.; Robert, B.; George, P.; Ricci, G.; Perrin, M. A.; Gomez Pardo, D.; Cossy, J. Ring Expansion of Cyclic β-Amino Alcohols Induced by Diethylaminosulfur Trifluoride: Synthesis of Cyclic Amines with a Tertiary Fluorine at C3. *J. Org. Chem.* **2012**, *77* (14), 6087–6099.

(64) Korch, K. M.; Eidamshaus, C.; Behenna, D. C.; Nam, S.; Horne, D.; Stoltz, B. M. Enantioselective Synthesis of α-Secondary and α-Tertiary Piperazin-2- Ones and Piperazines by Catalytic Asymmetric Allylic Alkylation. *Angew. Chemie - Int. Ed.* **2015**, *54* (1), 179–183.

(65) Sun, A.; Hess, S.; Stoltz, B. M. Enantioselective Synthesis of Gem-Disubstituted N-Boc Diazaheterocycles via Decarboxylative Asymmetric Allylic Alkylation. *Chem. Sci.* **2019**.

(66) Hagmann, W. K. The Many Roles for Fluorine in Medicinal Chemistry. *Journal of Medicinal Chemistry*. 2008, pp 4359–4369.

(67) Shah, P.; Westwell, A. D. The Role of Fluorine in Medicinal Chemistry. *J. Enzyme Inhib. Med. Chem.* **2007**, *22* (5), 527–540.

(68) Dallumal, R. M.; Chua, S. S.; Wu, D. B. C.; Vethakkan, S. R. Sitagliptin: Is It Effective in Routine Clinical Practice? *Int. J. Endocrinol.* **2015**, *2015*, 1–9.

(69) Green, J. B.; Bethel, M. A.; Armstrong, P. W.; Buse, J. B.; Engel, S. S.; Garga, J.; Josse, R.; Kaufman, K. D.; Koglin, J.; Korn, S.; et al. Effect of Sitagliptin on Cardiovascular Outcomes in Type 2 Diabetes. *N. Engl. J. Med.* **2015**, *373* (3), 232–242.

(70) Herman, G. A.; Bergman, A.; Liu, F.; Stevens, C.; Wang, A. Q.; Zeng, W.; Chen, L.; Snyder, K.; Hilliard, D.; Tanen, M.; et al. Pharmacokinetics and Pharmacodynamic Effects of the Oral DPP-4 Inhibitor Sitagliptin in Middle-Aged Obese Subjects. *J. Clin. Pharmacol.* **2006**, *46* (8), 876–886.

(71) Ratti, E.; Carpenter, D. J.; Zamuner, S.; Fernandes, S.; Squassante, L.; Danker-Hopfe, H.; Archer, G.; Robertson, J.; Alexander, R.; Trist, D. G.; et al. Efficacy of Vestipitant, A Neurokinin-1 Receptor Antagonist, in Primary Insomnia. *Sleep* **2013**, *36* (12), 1823–1830.

(72) Swain, S. K.; Nayak, S.; Ravan, J. R.; Sahu, M. C. Tinnitus and Its Current Treatment-Still an Enigma in Medicine. *J. Formos. Med. Assoc.* **2016**, *115* (3), 139–144.

(73) Sánchez-Roselló, M.; Delgado, O.; Mateu, N.; Trabanco, A. A.; Van Gool, M.; Fustero, S. Diastereoselective Synthesis of 2-Phenyl-3-(Trifluoromethyl)Piperazines as Building Blocks for Drug Discovery. *J. Org. Chem.* **2014**, *79* (12), 5887–5894.

(74) Wang, J.; Sánchez-Roselló, M.; Aceña, J. L.; Del Pozo, C.; Sorochinsky, A. E.; Fustero, S.; Soloshonok, V. A.; Liu, H. Fluorine in Pharmaceutical Industry: Fluorine-Containing Drugs Introduced to the Market in the Last Decade (2001-2011). *Chem. Rev.* **2014**, *114* (4), 2432–2506.

(75) Yar, M.; McGarrigle, E. M.; Aggarwal, V. K. An Annulation Reaction for the Synthesis of Morpholines, Thiomorpholines, and Piperazines from β-Heteroatom Amino Compounds and Vinyl Sulfonium Salts. *Angew. Chemie - Int. Ed.* **2008**, *47* (20), 3784–3786.

(76) Cushman, M.; Gentry, J.; Dekow, F. W. Condensation of Imines with Homophthalic Anhydrides. A Convergent Synthesis of Cis-and Trans-13-Methyltetrahydroprotoberberines. *J. Org. Chem.* **1977**, *42* (7), 1111–1116.

(77) Castagnoli, N. The Condensation of Succinic Anhydride with Benzylidinemethylamine. A Stereoselective Synthesis of Trans- and Cis-1-Methyl-4-Carboxy-5-Phenyl-2-Pyrrolidinone. *J. Org. Chem.* **1969**, *34* (10), 3187–3189.

(78) Sorto, N. A.; Di Maso, M. J.; Muñoz, M. A.; Dougherty, R. J.; Fettinger, J. C.; Shaw, J. T. Diastereoselective Synthesis of γ- And δ-Lactams from Imines and Sulfone-Substituted Anhydrides. *J. Org. Chem.* **2014**, *79* (6), 2601–2610.

(79) Tan, D. Q.; Younai, A.; Pattawong, O.; Fettinger, J. C.; Cheong, P. H. Y.; Shaw, J. T. Stereoselective Synthesis of γ-Lactams from Imines and Cyanosuccinic Anhydrides. *Org. Lett.* **2013**, *15* (19), 5126–5129.

(80) Cushman, M.; Castagnoli, N. Synthesis of Pharmacologically Active Nitrogen Analogs of

the Tetrahydrocannabinols. *J. Org. Chem.* **1974**, *39* (11), 1546–1550.

(81) Dar'In, D.; Bakulina, O.; Chizhova, M.; Krasavin, M. New Heterocyclic Product Space for the Castagnoli-Cushman Three-Component Reaction. *Org. Lett.* **2015**, *17* (15), 3930–3933.

(82) Adamovskyi, M. I.; Ryabukhin, S. V.; Sibgatulin, D. A.; Rusanov, E.; Grygorenko, O. O. Beyond the Five and Six: Evaluation of Seven-Membered Cyclic Anhydrides in the Castagnoli-Cushman Reaction. *Org. Lett.* **2017**, *19* (1), 130–133.

(83) Farah, A. O.; Archibald, R.; Rodriguez, M. J.; Moreno, A.; Dondji, B.; Beng, T. K. Flexible Access to 2,3,5,6-Tetrasubstituted Dehydropiperidines by Ni- or Co-Catalyzed Site-Selective Cross-Coupling Using Vilsmeier-Haack-Derived α-Chloro-β-Formyltetrahydropyridines. *Tetrahedron Lett.* **2018**, *59* (38), 3495–3498.

(84) Beng, T. K.; Bauder, M.; Rodriguez, M. J.; Moreno, A. Copper-Catalyzed Regioselective Dehydrogenative Alkoxylation of Morpholinonyl Alkenols: Application to the Synthesis of Spirotricyclic Dihydropyrans and of Trans-Fused Bicyclic Morpholines. *New J. Chem.* **2018**, *42* (20), 16451–16455.

(85) Braunstein, H.; Langevin, S.; Khim, M.; Adamson, J.; Hovenkotter, K.; Kotlarz, L.; Mansker, B.; Beng, T. K. Modular Access to Vicinally Functionalized Allylic (Thio)Morpholinonates and Piperidinonates by Substrate-Controlled Annulation of 1,3-Azadienes with Hexacyclic Anhydrides. *Org. Biomol. Chem.* **2016**, *14* (37), 8864–8872.

(86) Hovenkotter, K.; Braunstein, H.; Langevin, S.; Beng, T. K. Expedient and Modular Access to 2-Azabicyclic Architectures by Iron-Catalyzed Dehydrative Coupling of Alcohol-Bearing Allylic Lactams. *Org. Biomol. Chem.* **2017**, *15* (5), 1217–1221.

(87) Mizuta, S.; Onomura, O. Diastereoselective Addition to N-Acyliminium Ions with Aryl- and Alkenyl Boronic Acids via a Petasis-Type Reaction. *RSC Adv.* **2012**, *2* (6), 2266–2269.

(88) Onomura, O. *Studies on Anodic Selective Functionalization of Cyclic Amine Derivatives*; 2012; Vol. 85.

(89) Libendi, S.; Demizu, Y.; Matsumura, Y.; Onomura, O. *High Regioselectivity in Electrochemical α-Methoxylation of N-Protected Cyclic Amines.*; 2008; Vol. 64.

(90) Onomura, O.; Kirira, P.; Tanaka, T.; Tsukada, S.; Matsumura, Y.; Demizu, Y. *Diastereoselective Arylation of L-Proline Derivatives at the 5-Position*; 2008; Vol. 64.

(91) Denmark, S. E.; Burk, M. T. Lewis Base Catalysis of Bromo- and Iodolactonization, and Cycloetherification. *Proc. Natl. Acad. Sci.* **2010**, *107* (48), 20655–20660.

(92) González-López, M.; Shaw, J. T. Cyclic Anhydrides in Formal Cycloadditions and Multicomponent Reactions. *Chem. Rev.* **2009**, *109* (1), 164–189.

(93) Gigant, N.; Claveau, E.; Bouyssou, P.; Gillaizeau, I. Diversity-Oriented Synthesis of Polycyclic Diazinic Scaffolds. *Org. Lett.* **2012**, *14* (3), 844–847.

(94) Kutama, I. U.; Jones, S. Enantioselective Desymmetrization of Glutarimides Catalyzed by

Oxazaborolidines Derived from Cis-1-Amino-Indan-2-Ol. *J. Org. Chem.* **2015**, *80* (22), 11468–11479.

(95) Schofield, M. M.; Jain, S.; Porat, D.; Dick, G. J.; Sherman, D. H. Identification and Analysis of the Bacterial Endosymbiont Specialized for Production of the Chemotherapeutic Natural Product ET-743. *Environ. Microbiol.* **2015**, *17* (10), 3964–3975.

(96) Barone, A.; Chi, D. C.; Theoret, M. R.; Chen, H.; He, K.; Kufrin, D.; Helms, W. S.; Subramaniam, S.; Zhao, H.; Patel, A.; et al. FDA Approval Summary: Trabectedin for Unresectable or Metastatic Liposarcoma or Leiomyosarcoma Following an Anthracycline-Containing Regimen. *Clin. Cancer Res.* **2017**, *23* (24), 7448–7453.

(97) Twigg, D. G.; Kondo, N.; Mitchell, S. L.; Galloway, W. R. J. D.; Sore, H. F.; Madin, A.; Spring, D. R. Partially Saturated Bicyclic Heteroaromatics as an Sp3-Enriched Fragment Collection. *Angew. Chemie - Int. Ed.* **2016**, *55* (40), 12479–12483.

(98) Hung, A. W.; Ramek, A.; Wang, Y.; Kaya, T.; Wilson, J. A.; Clemons, P. A.; Young, D. W. Route to Three-Dimensional Fragments Using Diversity-Oriented Synthesis. *Proc. Natl. Acad. Sci.* **2011**, *108* (17), 6799–6804.

(99) Nelson, A.; Foley, D. J.; Doveston, R. G.; Craven, P. G. E.; Churcher, I.; Marsden, S. P.; von Delft, F.; Aimon, A.; Talon, R.; Collins, P. M. Synthesis and Demonstration of the Biological Relevance of Sp 3 -Rich Scaffolds Distantly Related to Natural Product Frameworks . *Chem. - A Eur. J.* **2017**, *23* (60), 15227–15232.

(100) Lovering, F.; Bikker, J.; Humblet, C. Escape from Flatland: Increasing Saturation as an Approach to Improving Clinical Success. *J. Med. Chem.* **2009**, *52* (21), 6752–6756.

(101) Veerman, J. J. N.; Bon, R. S.; Hue, B. T. B.; Girones, D.; Rutjes, F. P. J. T.; Van Maarseveen, J. H.; Hiemstra, H. Synthesis of 2,6-Bridged Piperazine-3-Ones by N-Acyliminium Ion Chemistry. *J. Org. Chem.* **2003**, *68* (11), 4486–4494.

(102) Gauvreau, D.; Hughes, G. J.; Lau, S. Y. W.; McKay, D. J.; O'Shea, P. D.; Sidler, R. R.; Yu, B.; Davies, I. W. Practical Synthesis of a Renin Inhibitor via a Diastereoselective Dieckmann Cyclization. *Org. Lett.* **2010**, *12* (22), 5146–5149.

(103) Chatani, N.; Asaumi, T.; Yorimitsu, S.; Ikeda, T.; Kakiuchi, F.; Murai, S. Ru3(CO)12-Catalyzed Coupling Reaction of Sp3 C - H Bonds Adjacent to a Nitrogen Atom in Alkylamines with Alkenes. *J. Am. Chem. Soc.* **2001**, *123* (44), 10935–10941.

(104) Dénès, F.; Pérez-Luna, A.; Chemla, F. Addition of Metal Enolate Derivatives to Unactivated Carbon−Carbon Multiple Bonds. *Chem. Rev.* **2010**, *110* (4), 2366–2447.

(105) Eaton, P. E.; Lee, C. H.; Xiong, Y. Magnesium Amide Bases and Amido-Grignards. 1. Ortho Magnesiation. *J. Am. Chem. Soc.* **1989**, *111* (20), 8016–8018.

APPENDIX A: CHAPTER 2 SPECTROSCOPIC DATA

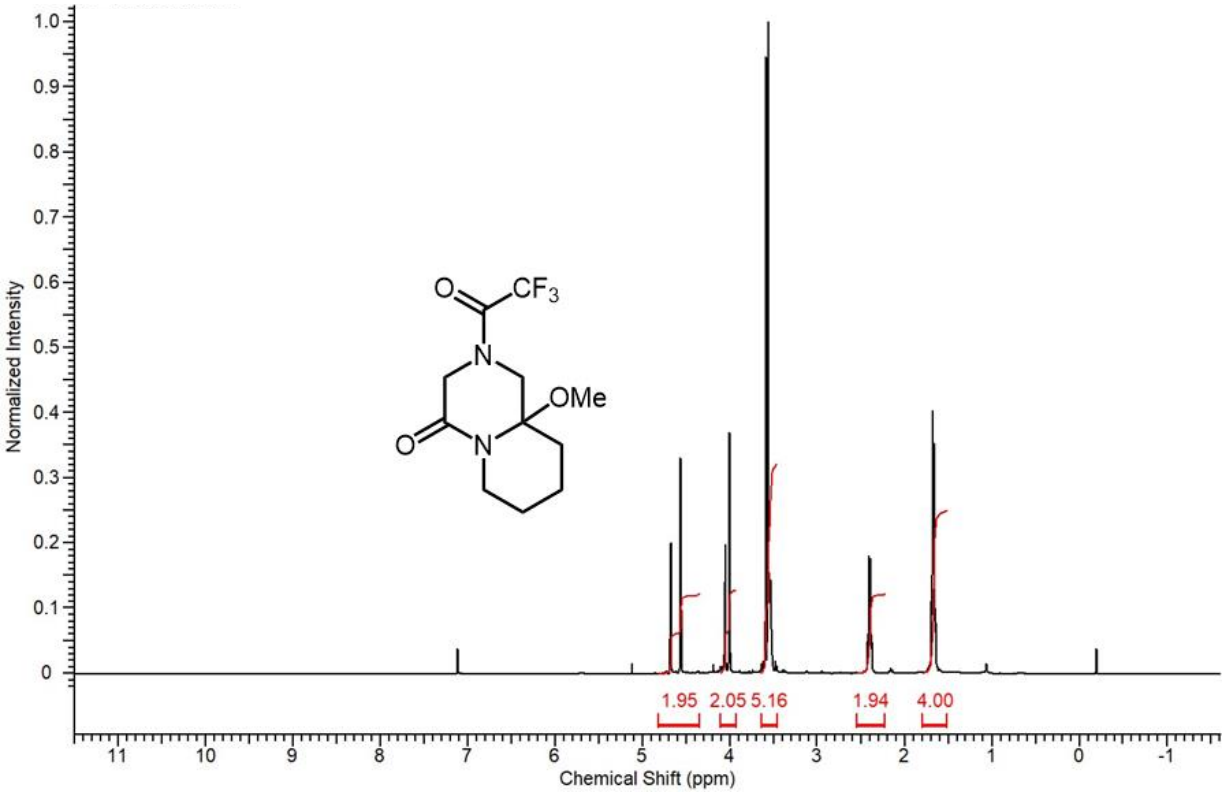

Spectra 1-1 Proton NMR spectrum of **8a.**

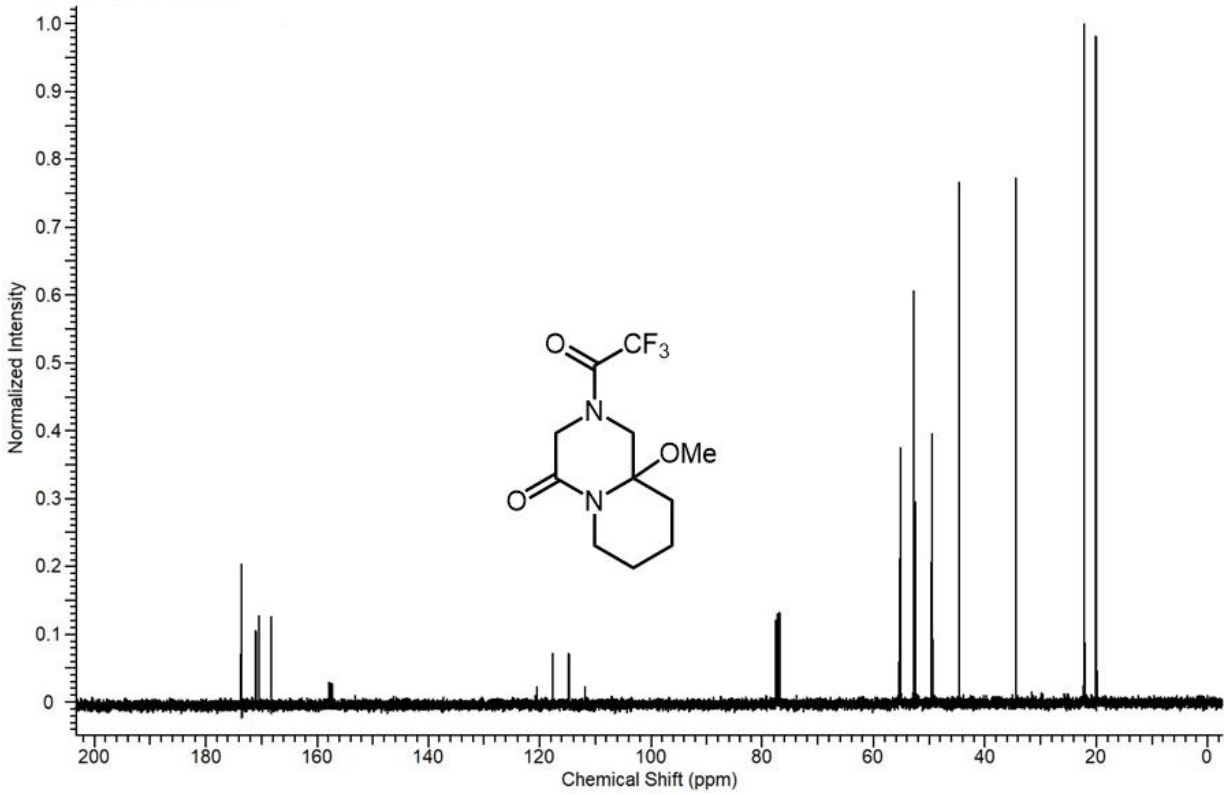

Spectra 1-2 Carbon NMR spectrum of **8a.**

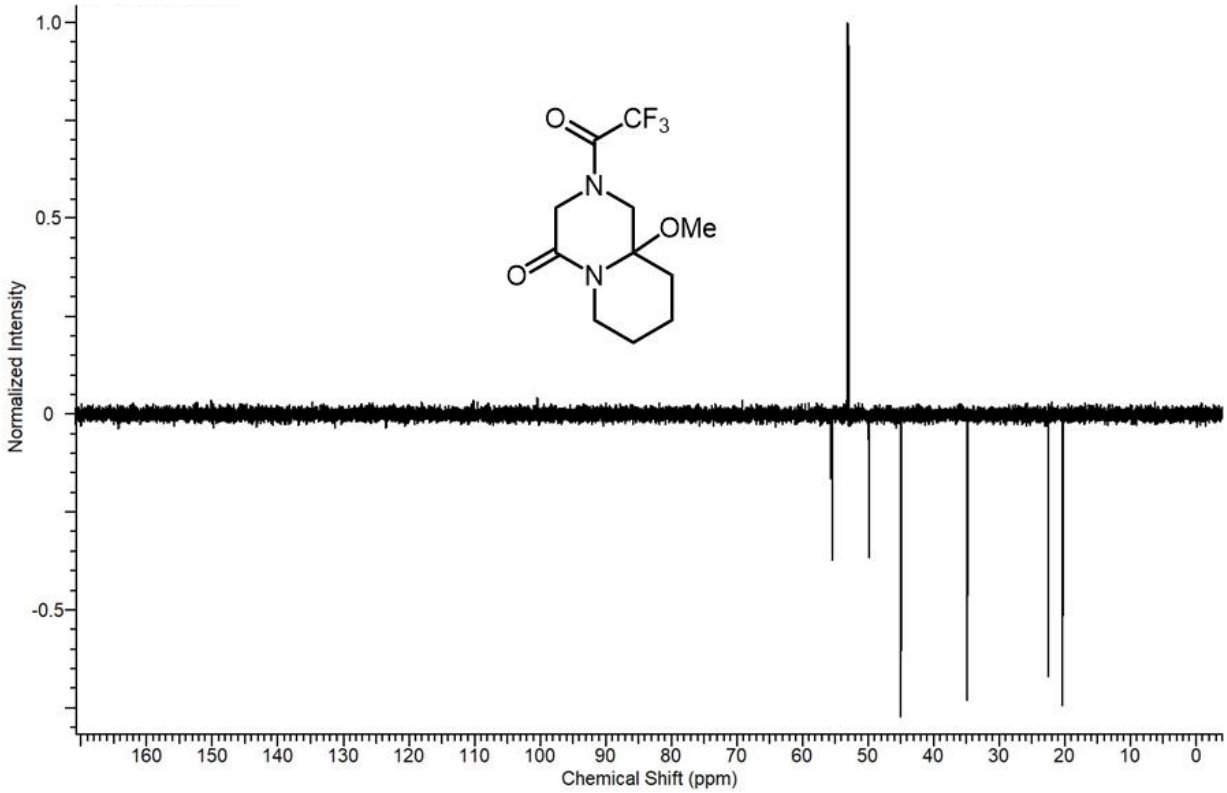

Spectra 1-3 DEPT-135 NMR spectrum of **8a.**

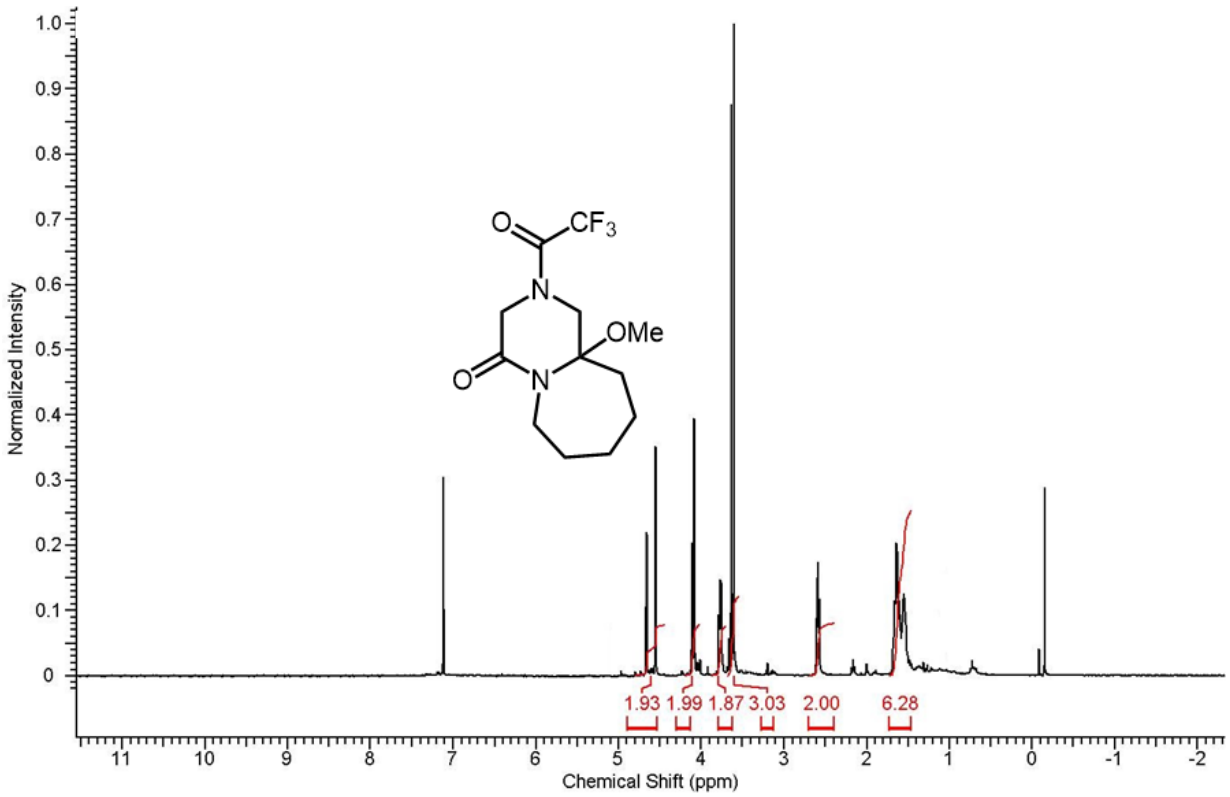

Spectra 1-4 Proton NMR spectrum of **8b.**

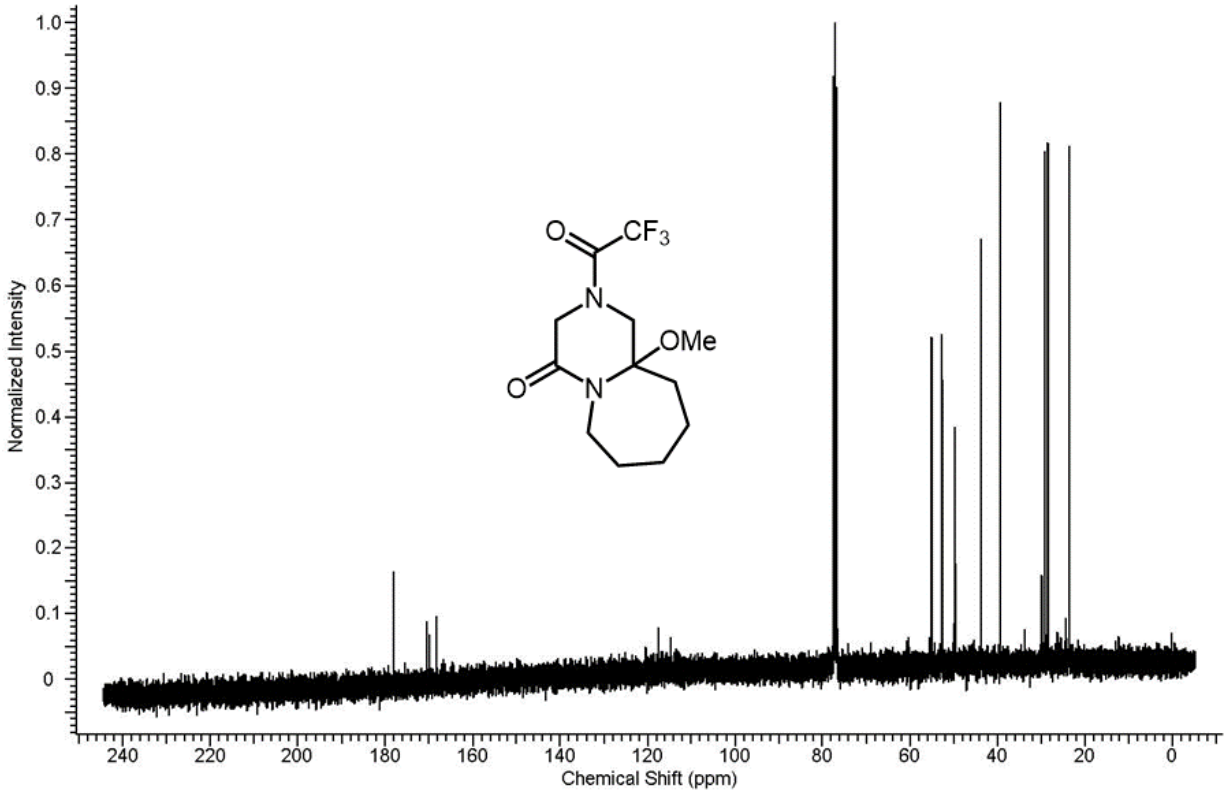

Spectra 1-5 Carbon NMR spectrum of **8b.**

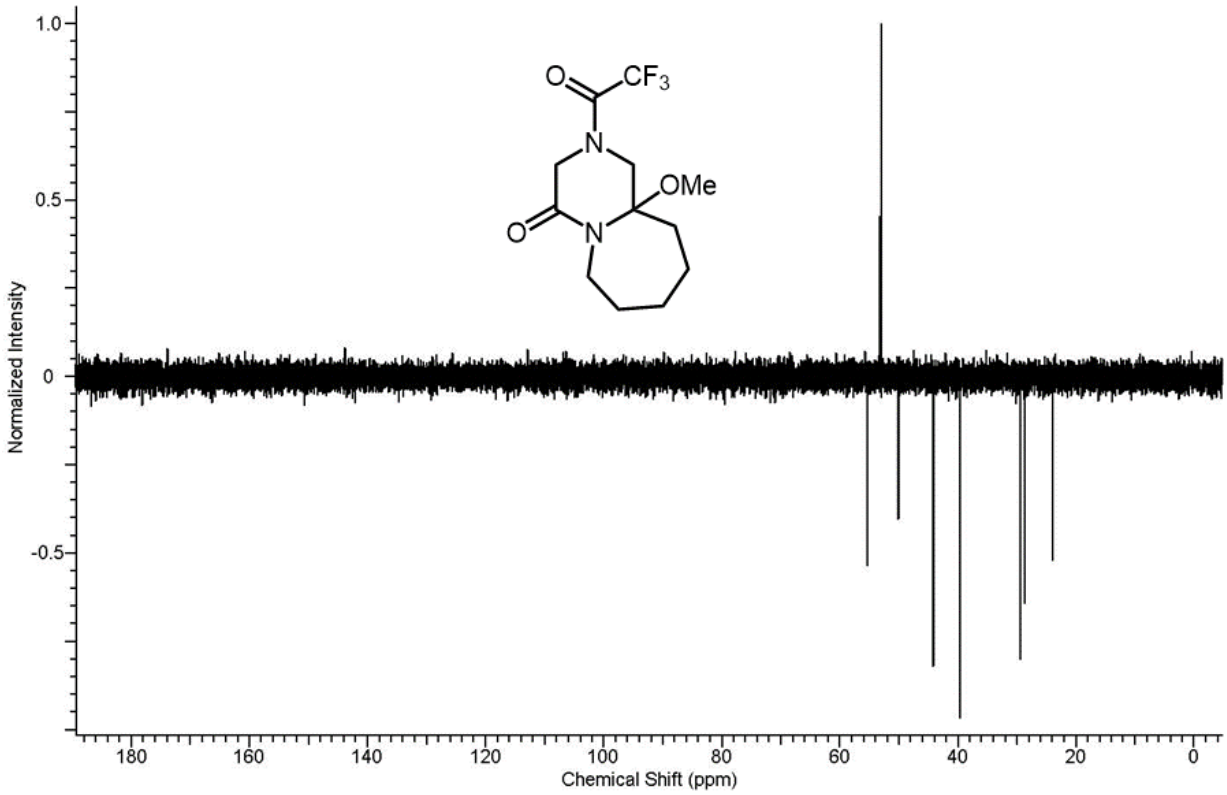

Spectra 1-6 DEPT-135 NMR spectrum of **8b.**

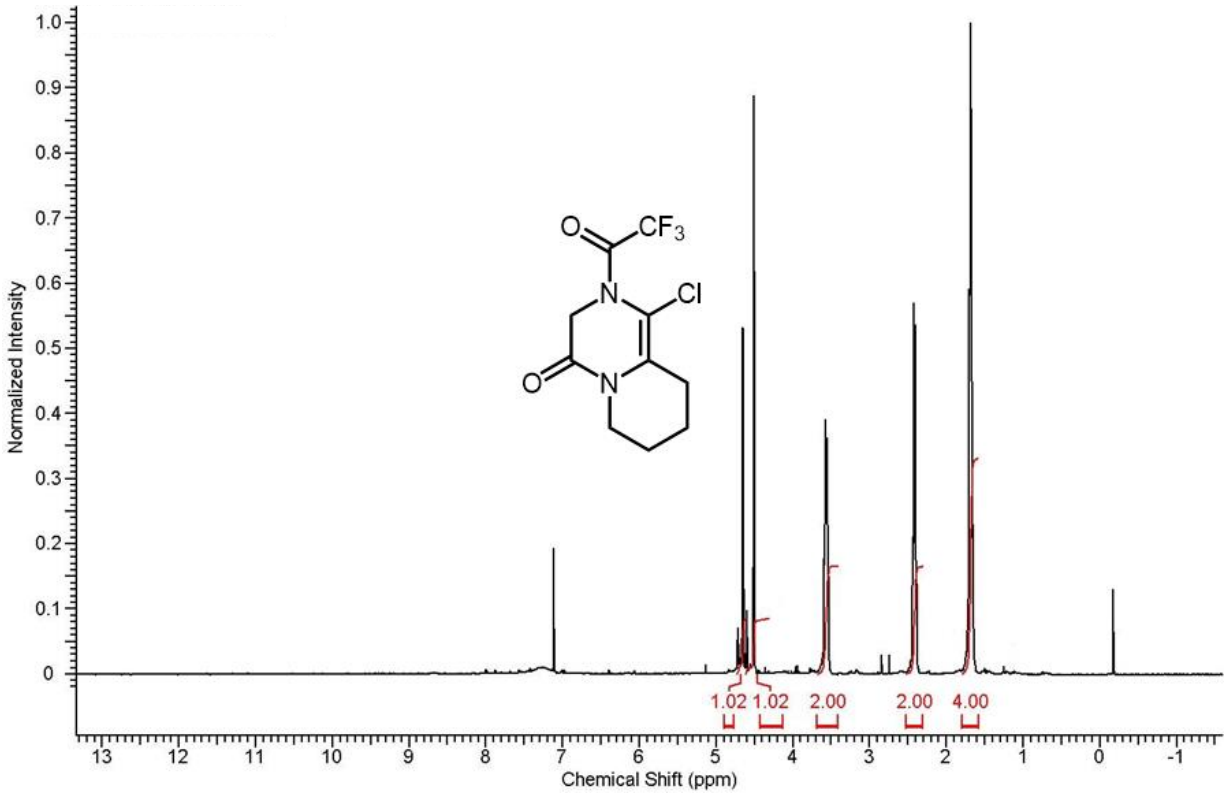

Spectra 1-7 Proton NMR spectrum of **8c.**

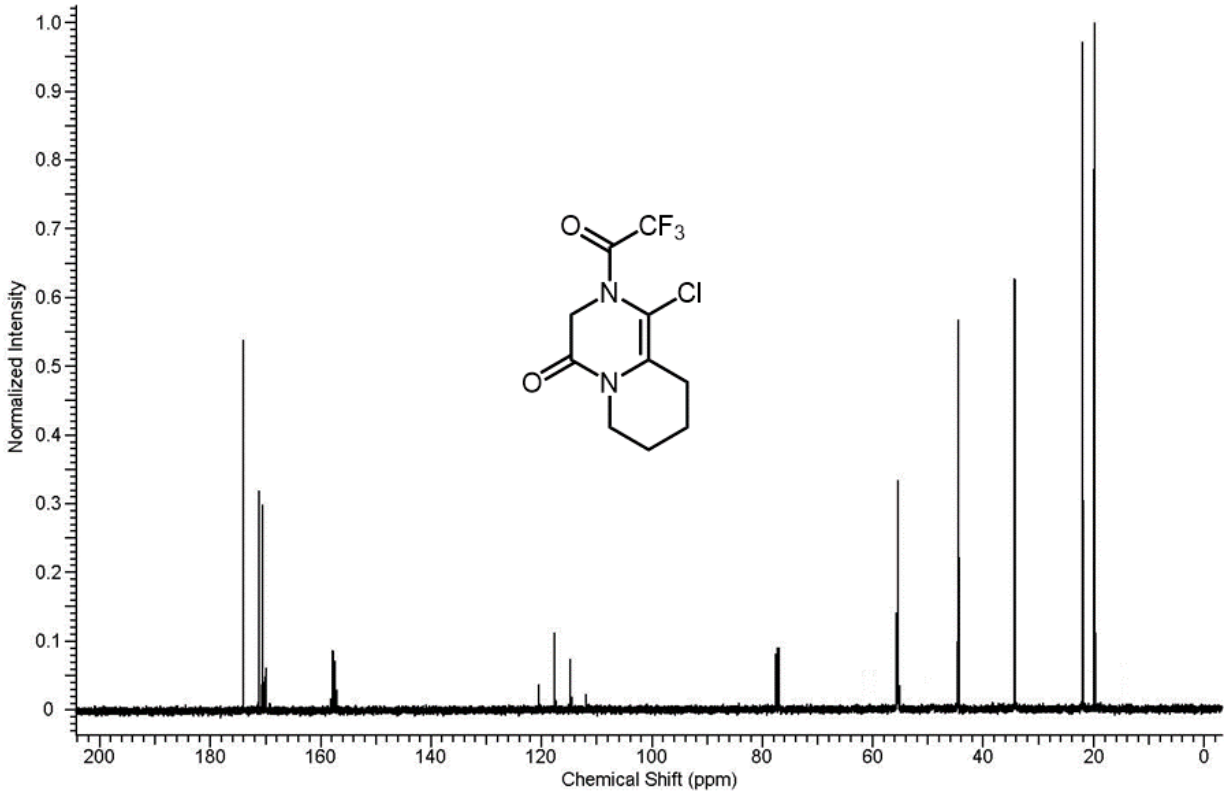

Spectra 1-8 Carbon NMR spectrum of **8c.**

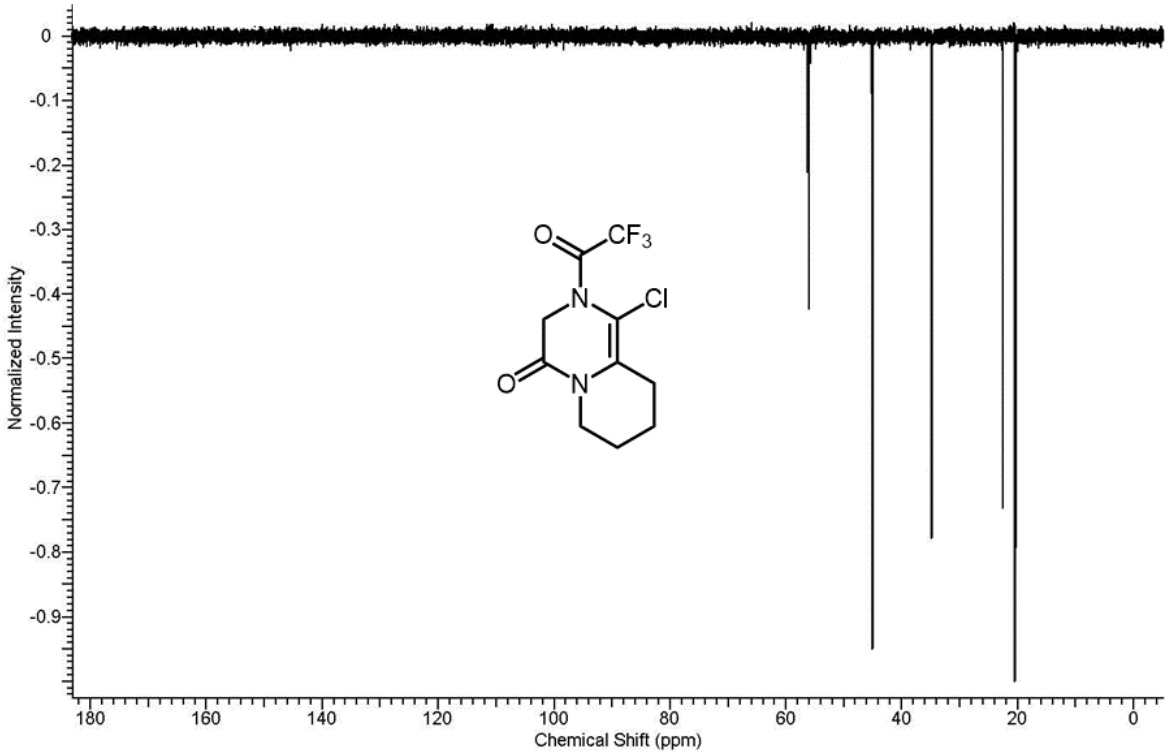

Spectra 1-9 DEPT-135 NMR spectrum of **8c.**

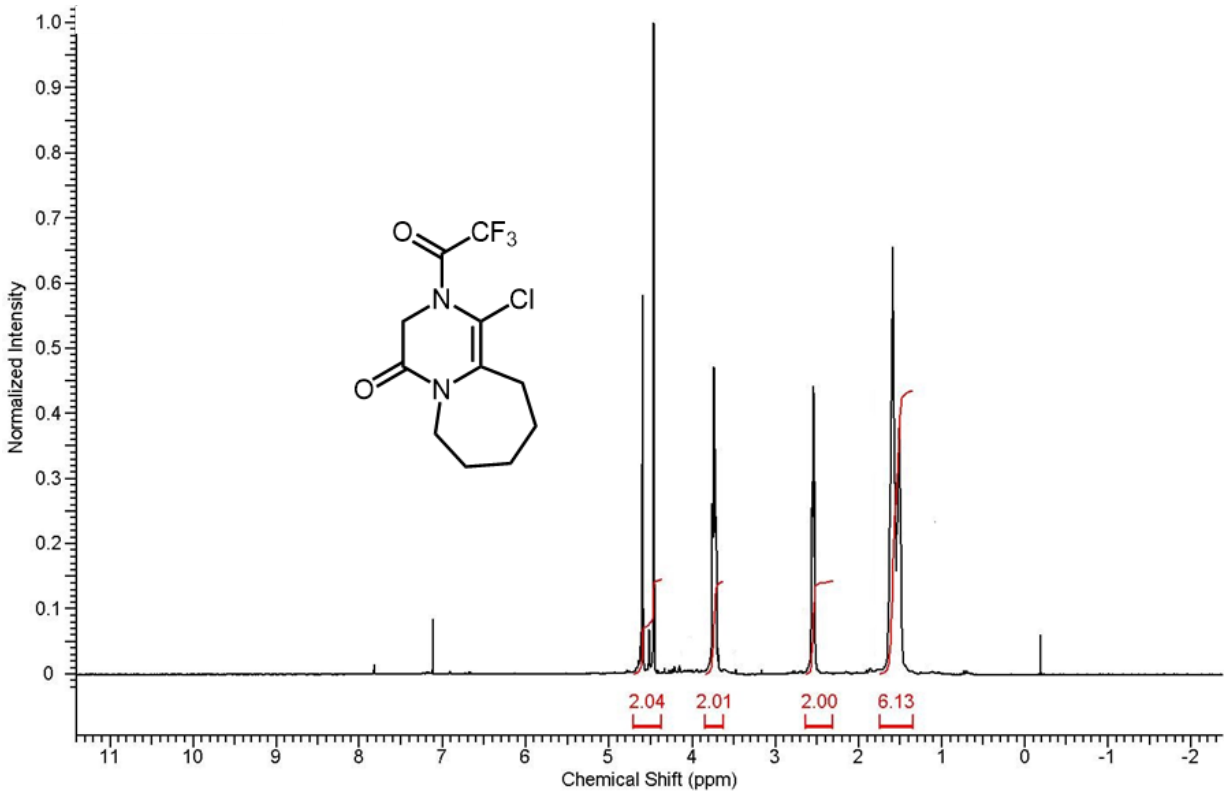

Spectra 1-10 Proton NMR spectrum of **8d.**

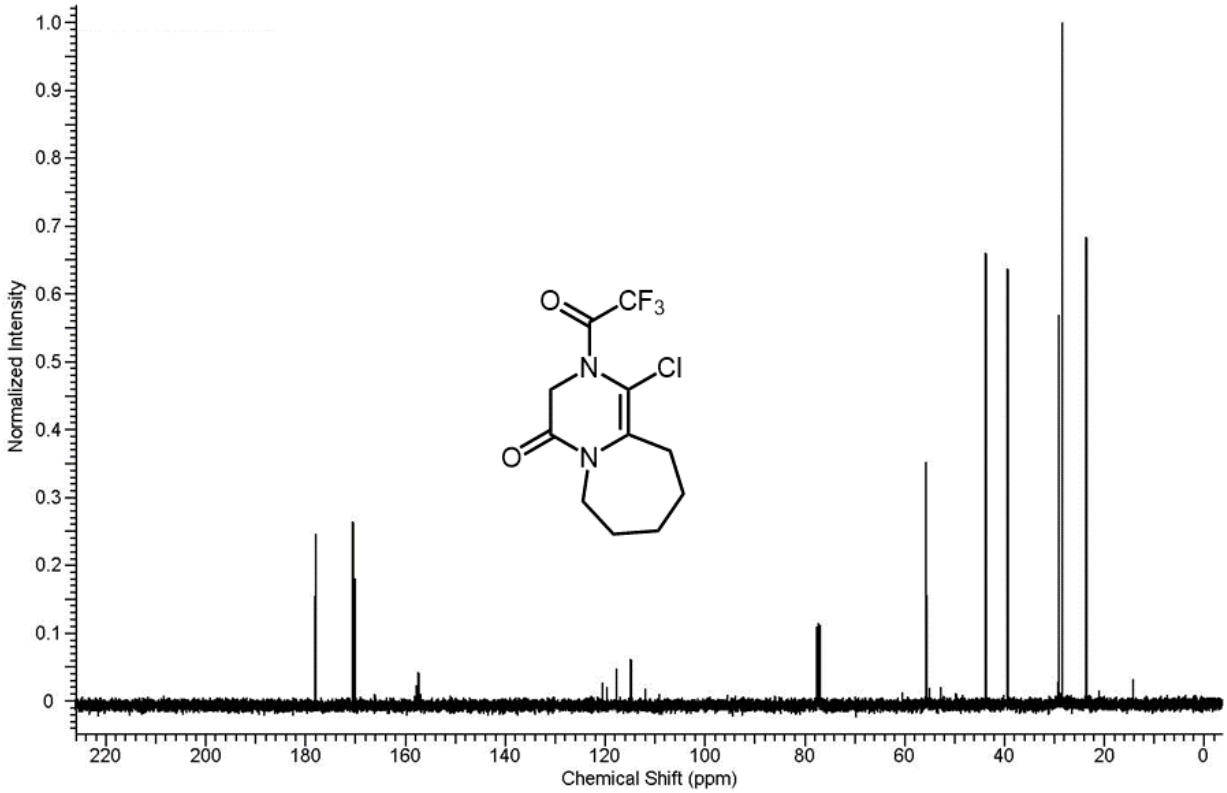

Spectra 1-11 Carbon NMR spectrum of **8d.**

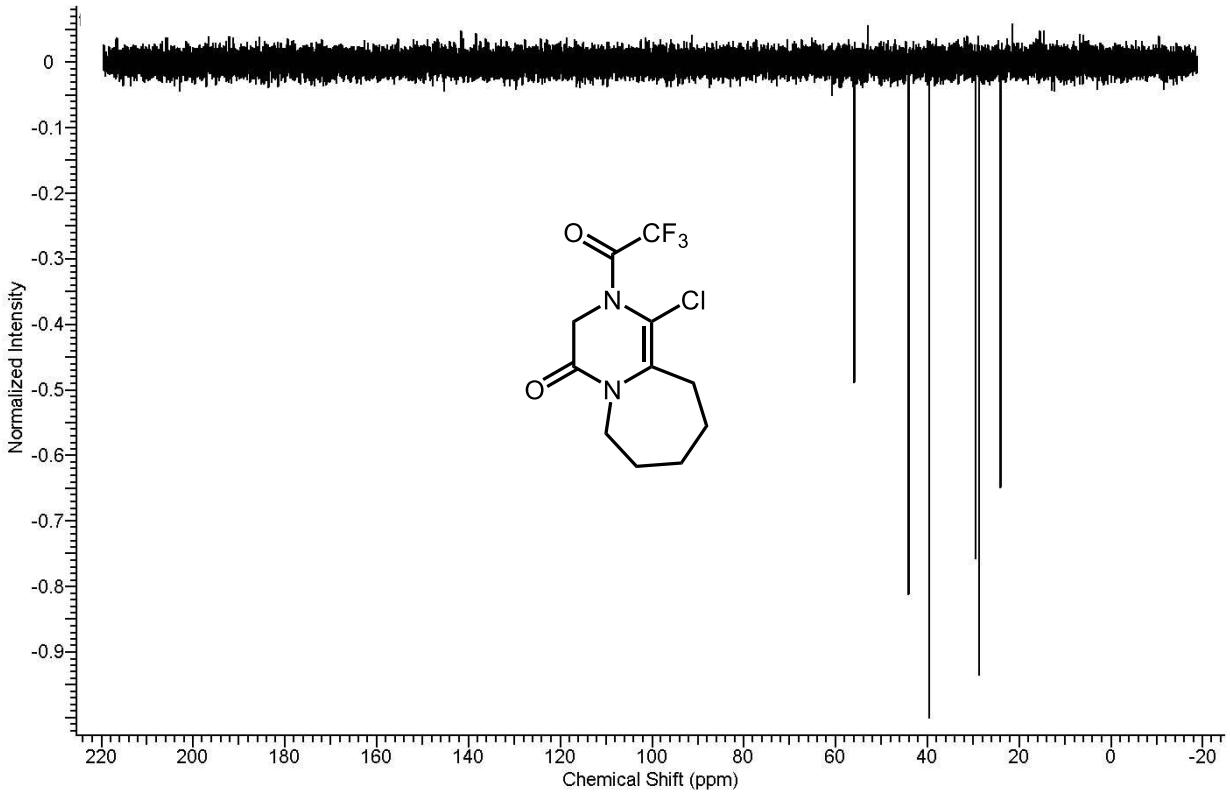

Spectra 1-12 DEPT-135 NMR spectrum of **8d.**

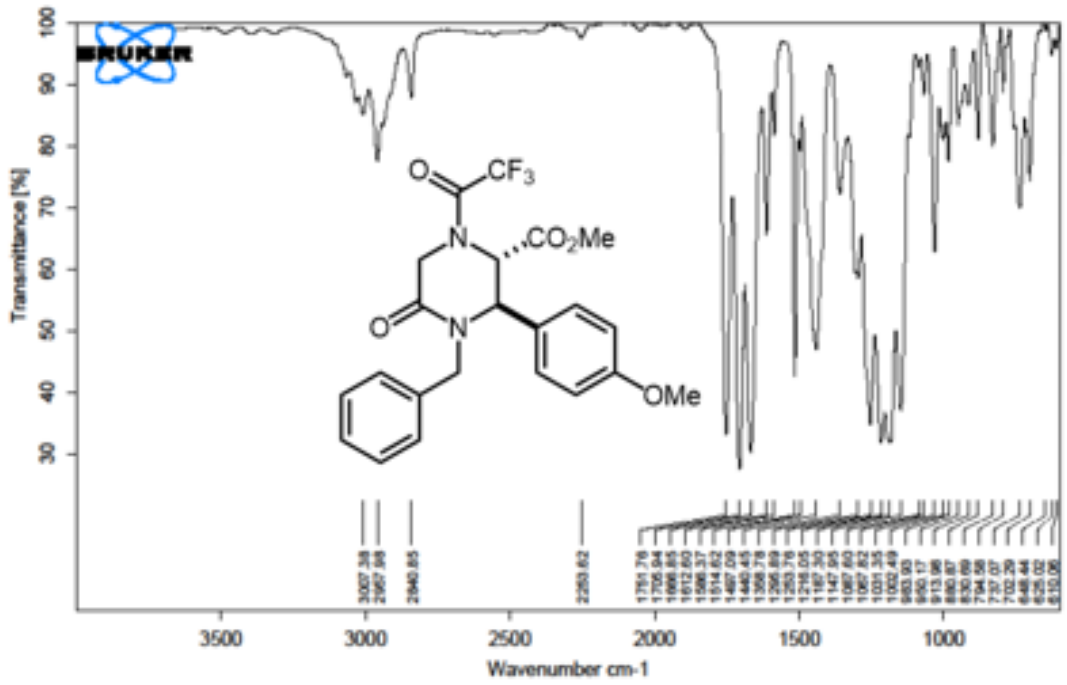

Spectra 1-13 IR spectrum of **10a**.

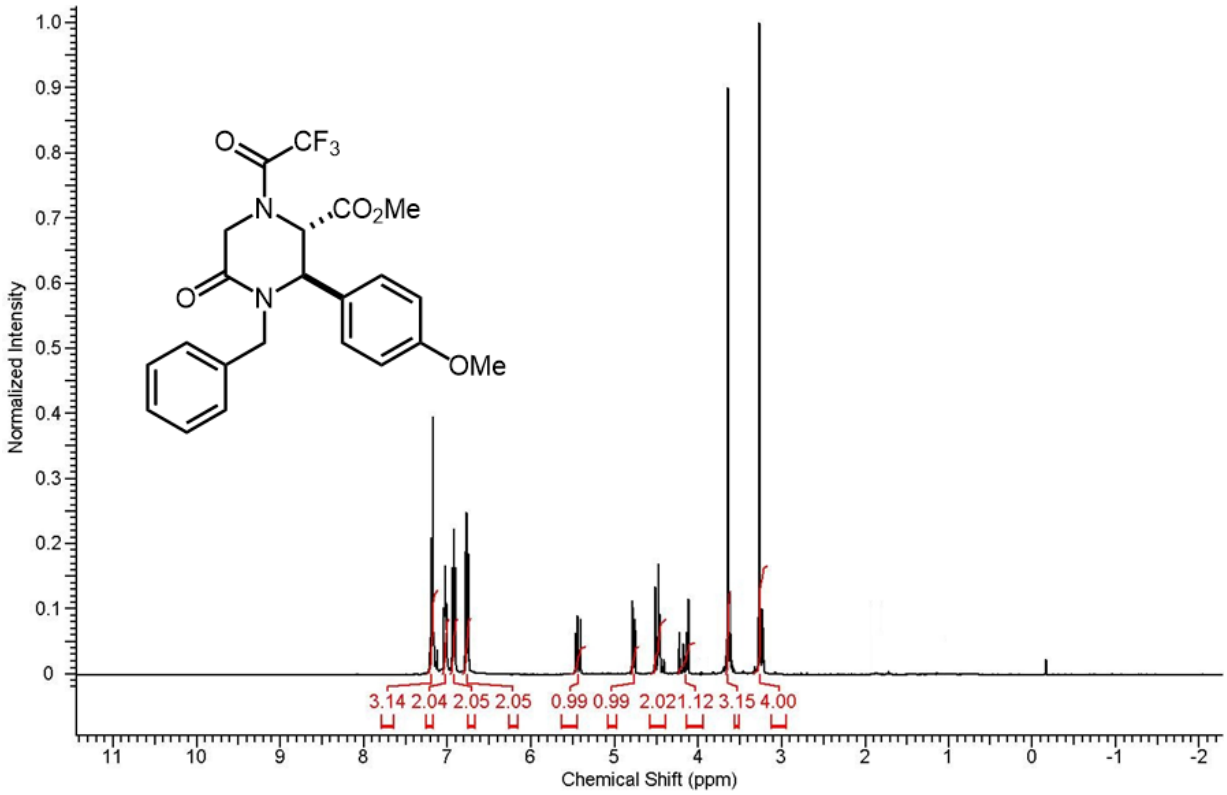

Spectra 1-14 Proton NMR spectrum of **10a.**

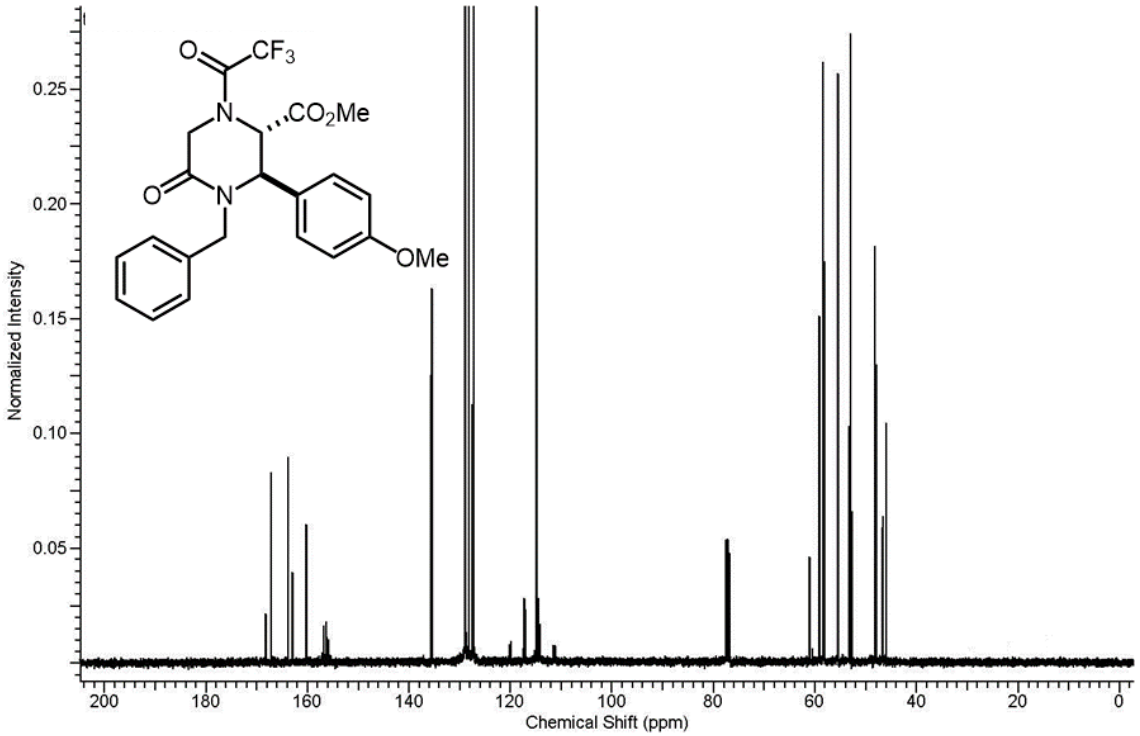

Spectra 1-15 Carbon NMR spectrum of **10a.**

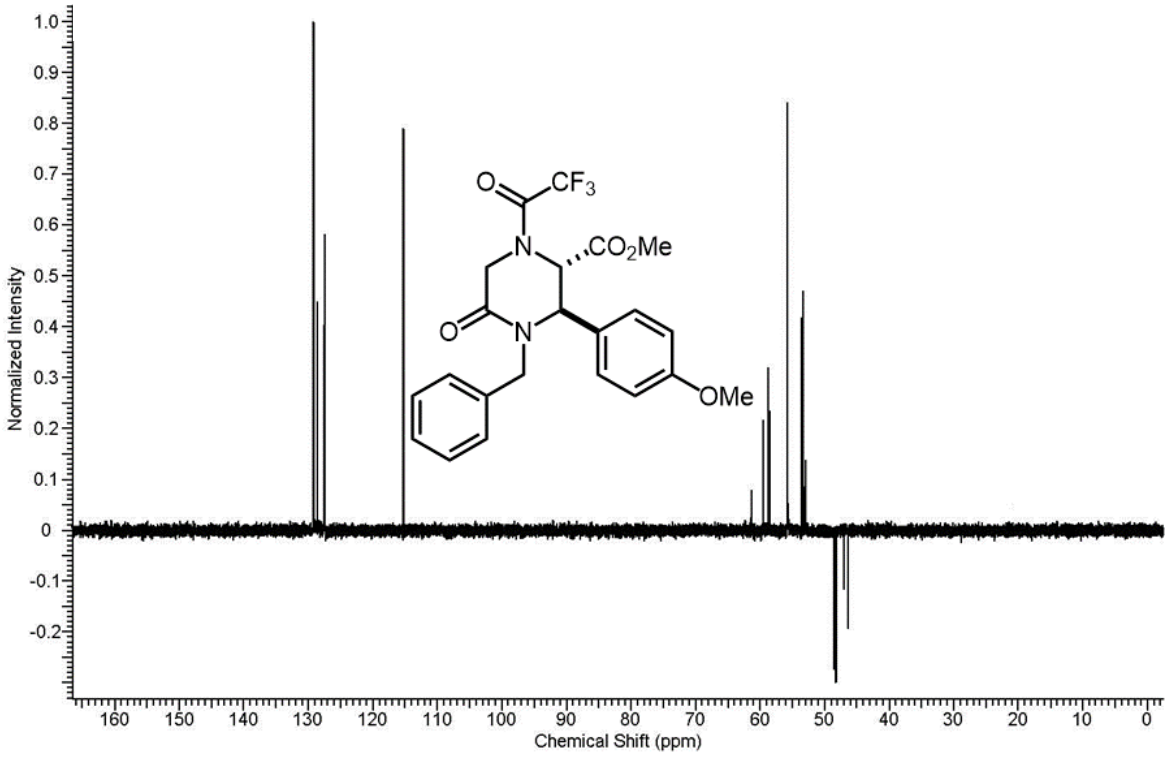

Spectra 1-16 DEPT-135 NMR spectrum of **10a.**

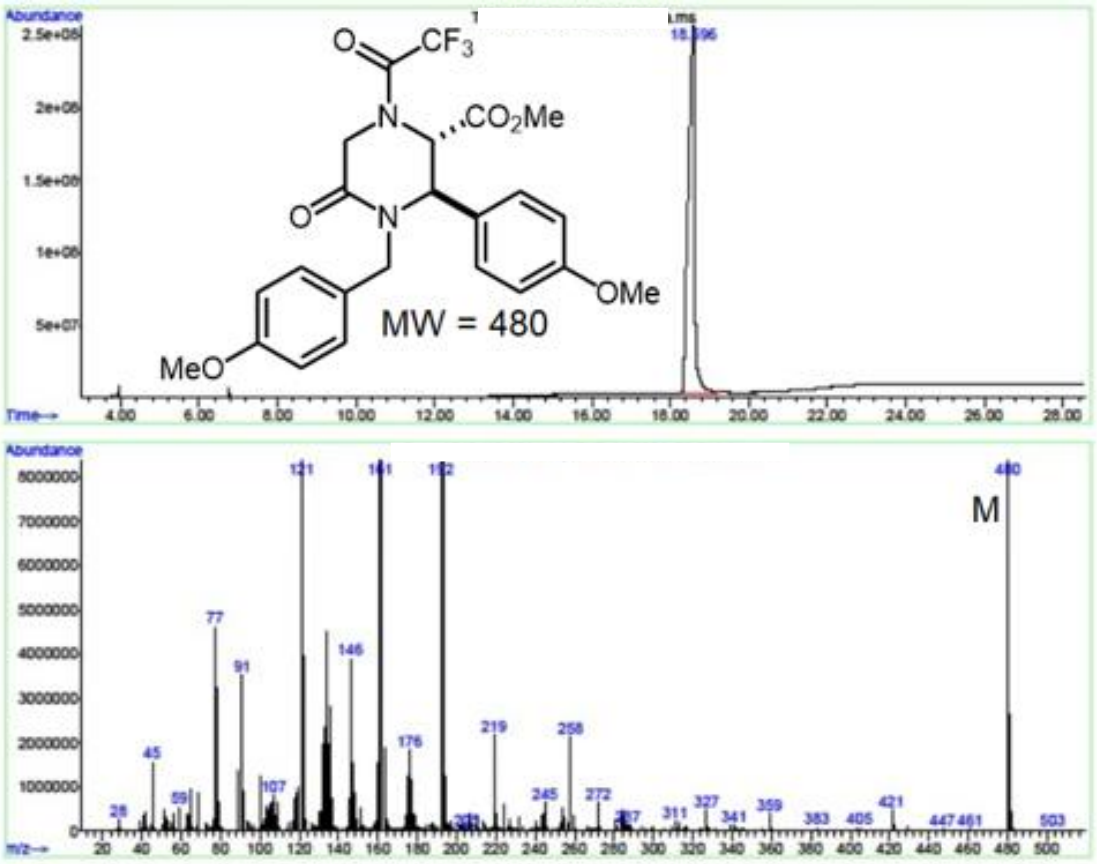

Spectra 1-17 GC-MS spectrum of **10b.**

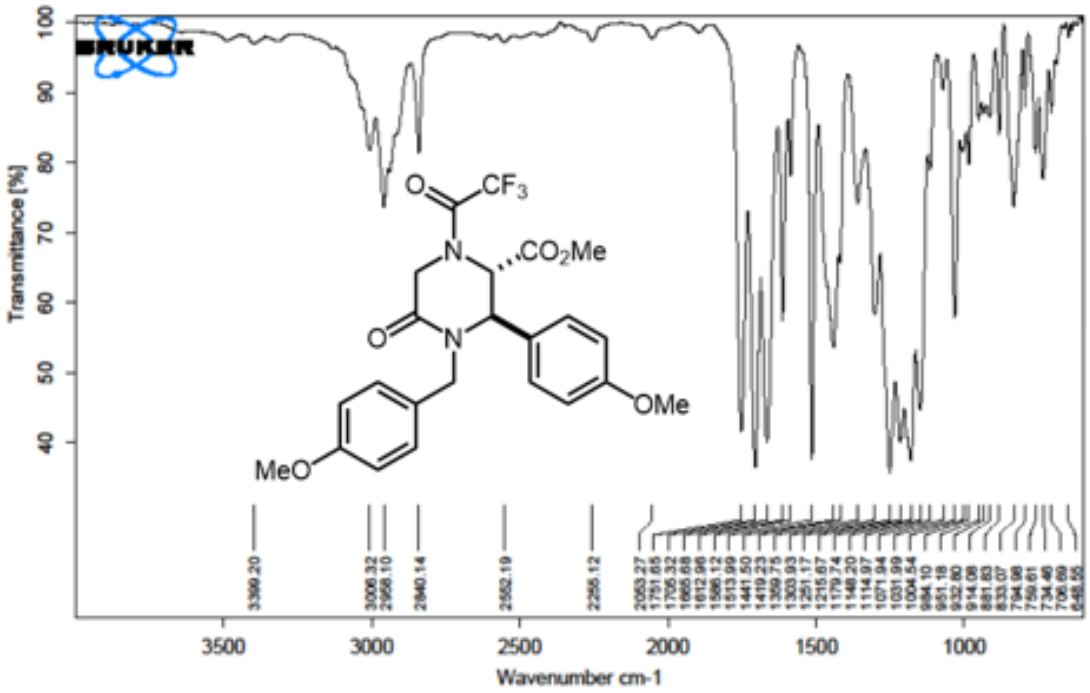

Spectra 1-18 IR spectrum of **10b.**

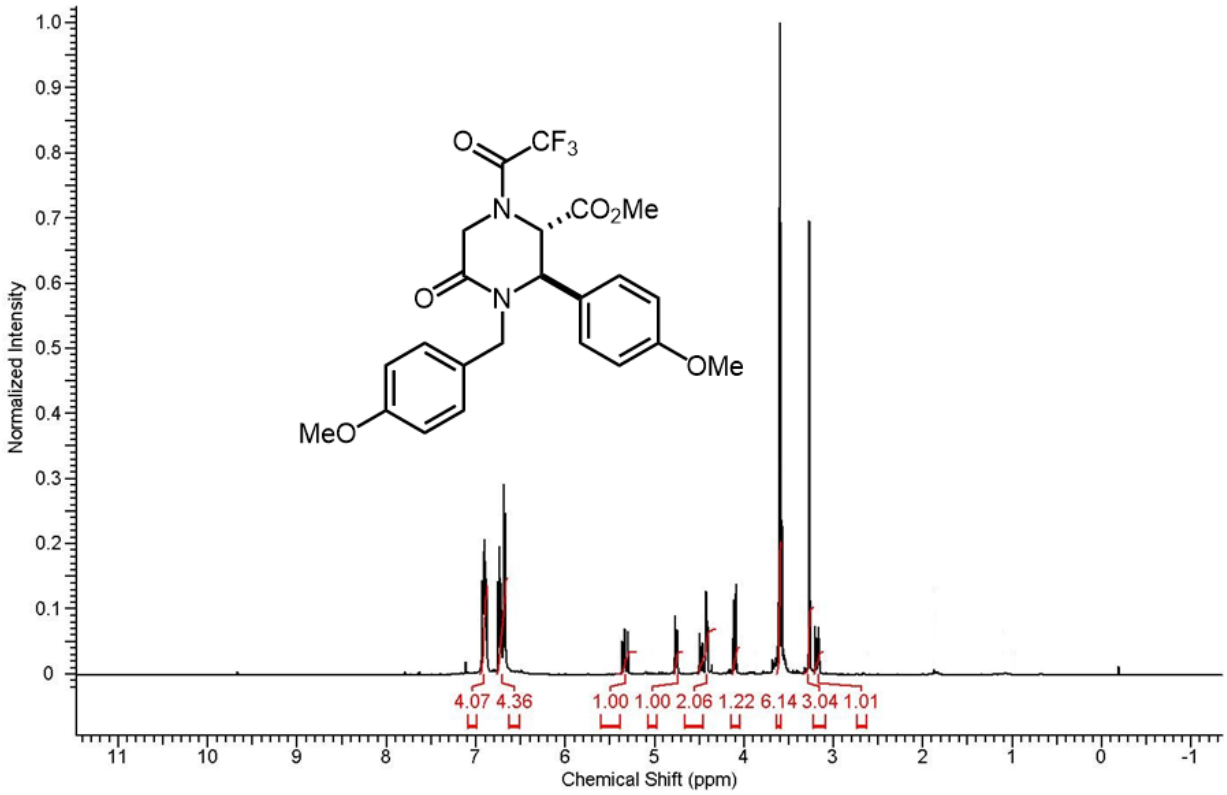

Spectra 1-19 Proton NMR spectrum of **10b.**

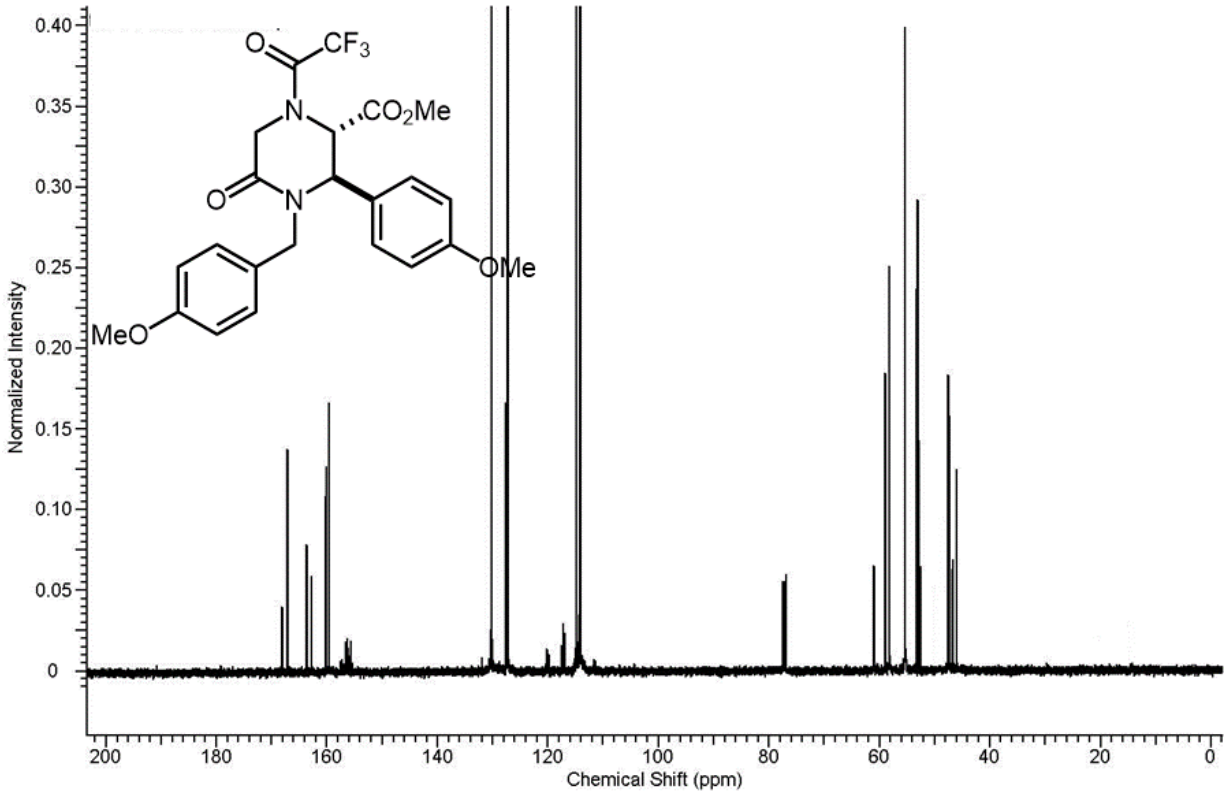

Spectra 1-20 Carbon NMR spectrum of **10b.**

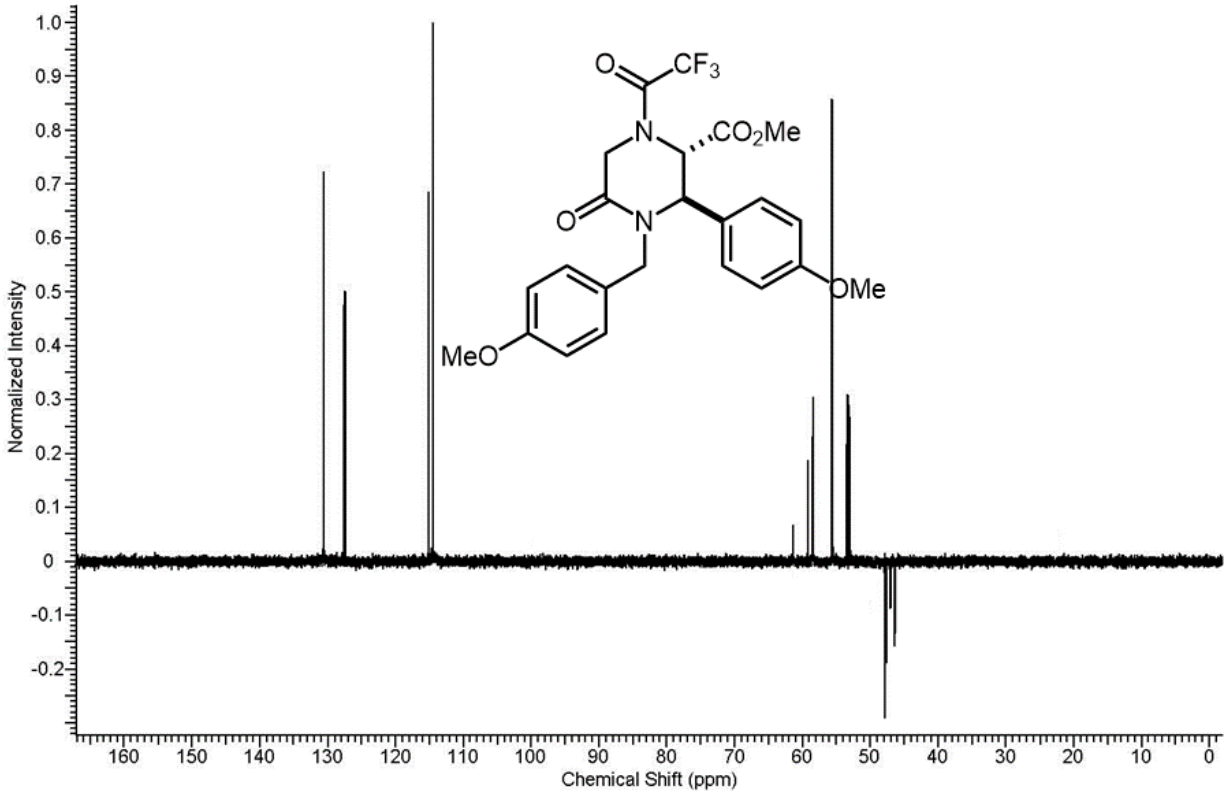

Spectra 1-21 DEPT-135 NMR spectrum of **10b.**

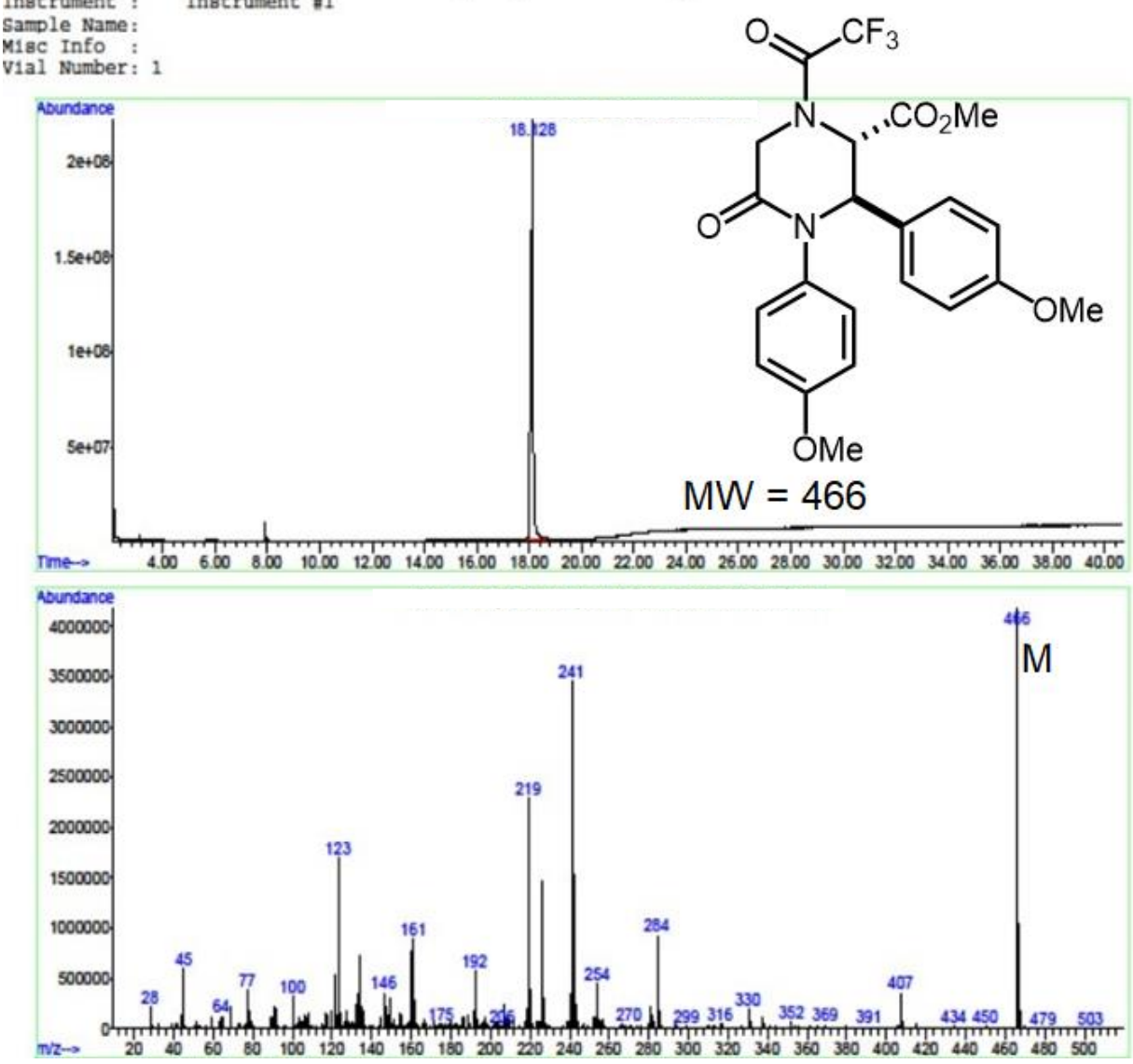

Spectra 1-22 GC-MS spectrum of **10c.**

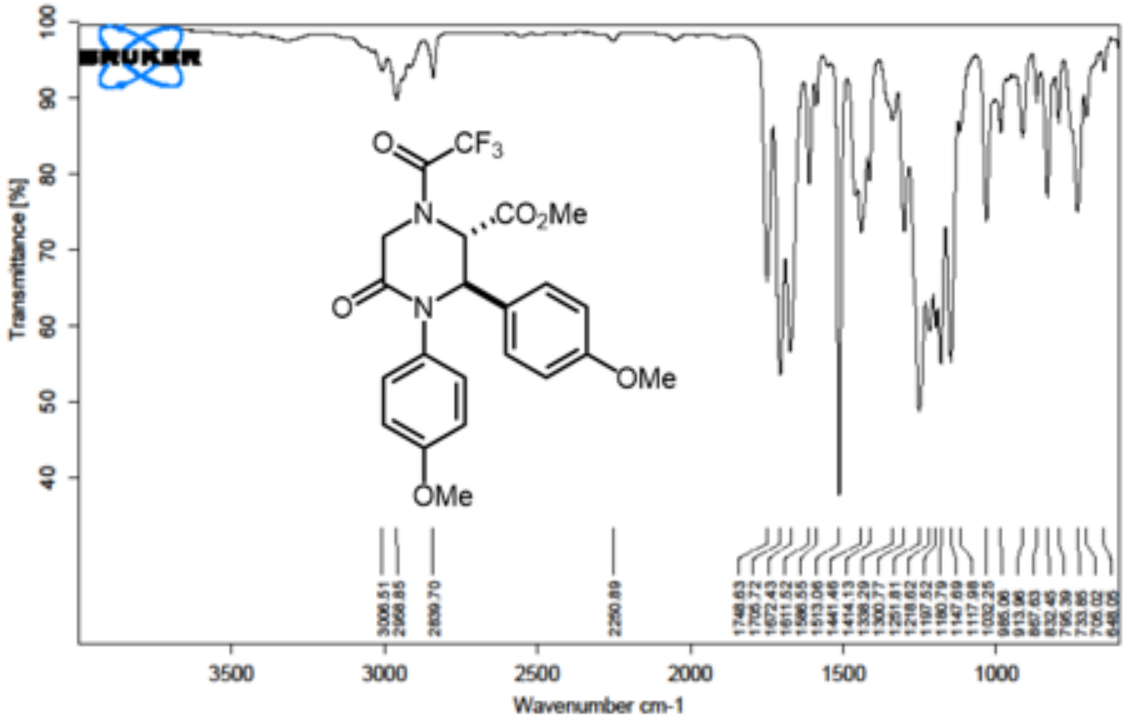

Spectra 1-23 IR spectrum of **10c.**

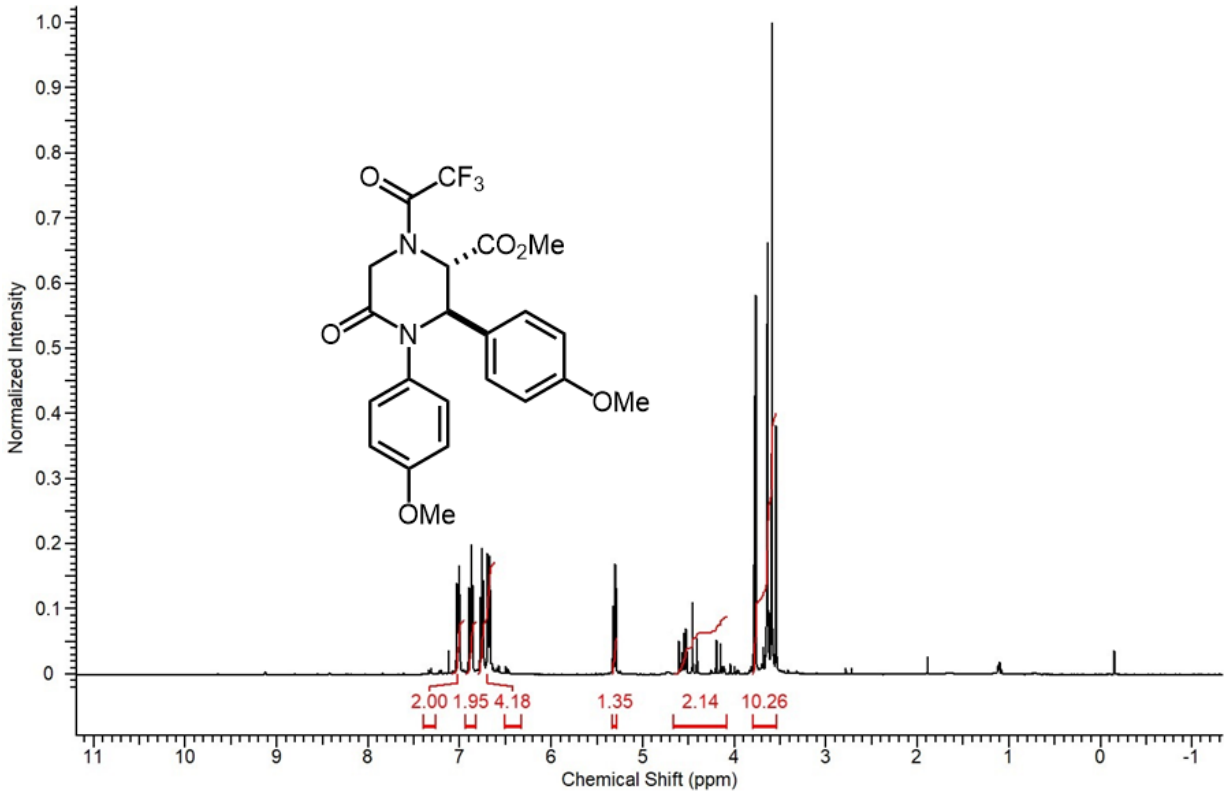

Spectra 1-24 Proton NMR spectrum of **10c.**

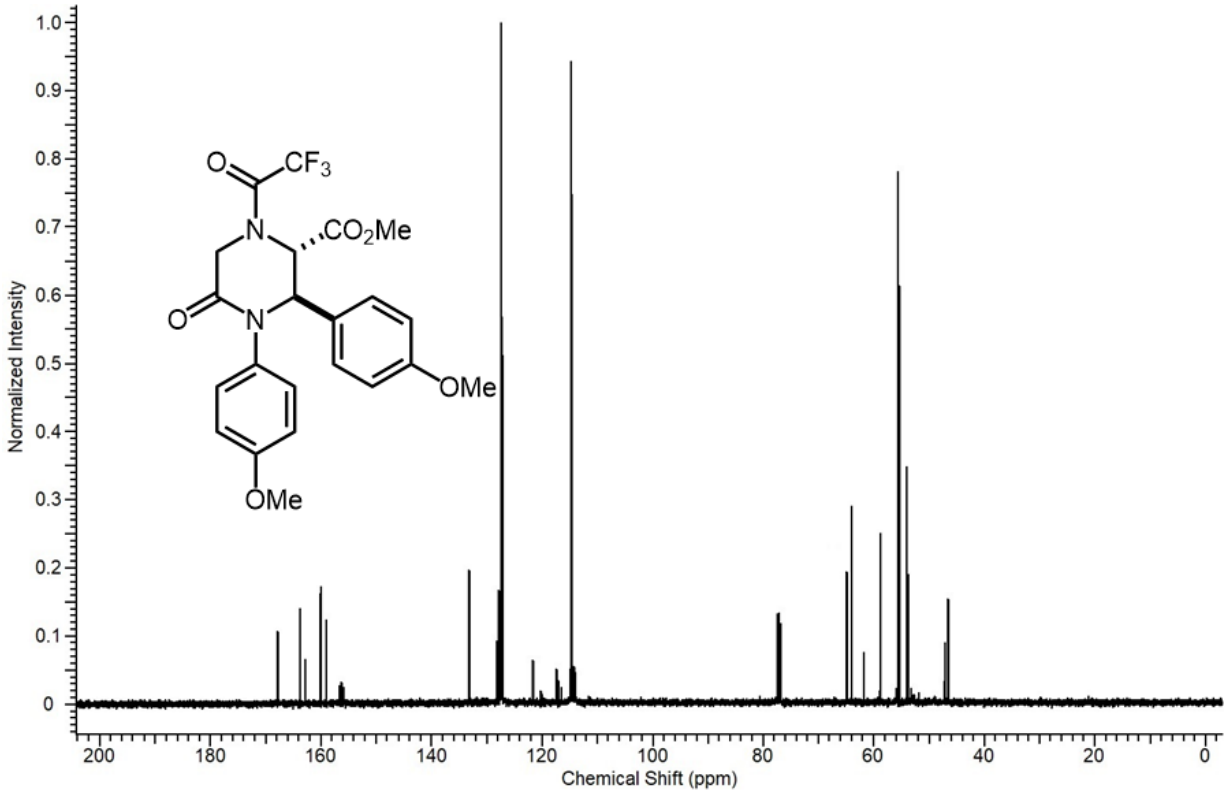

Spectra 1-25 Carbon NMR spectrum of **10c.**

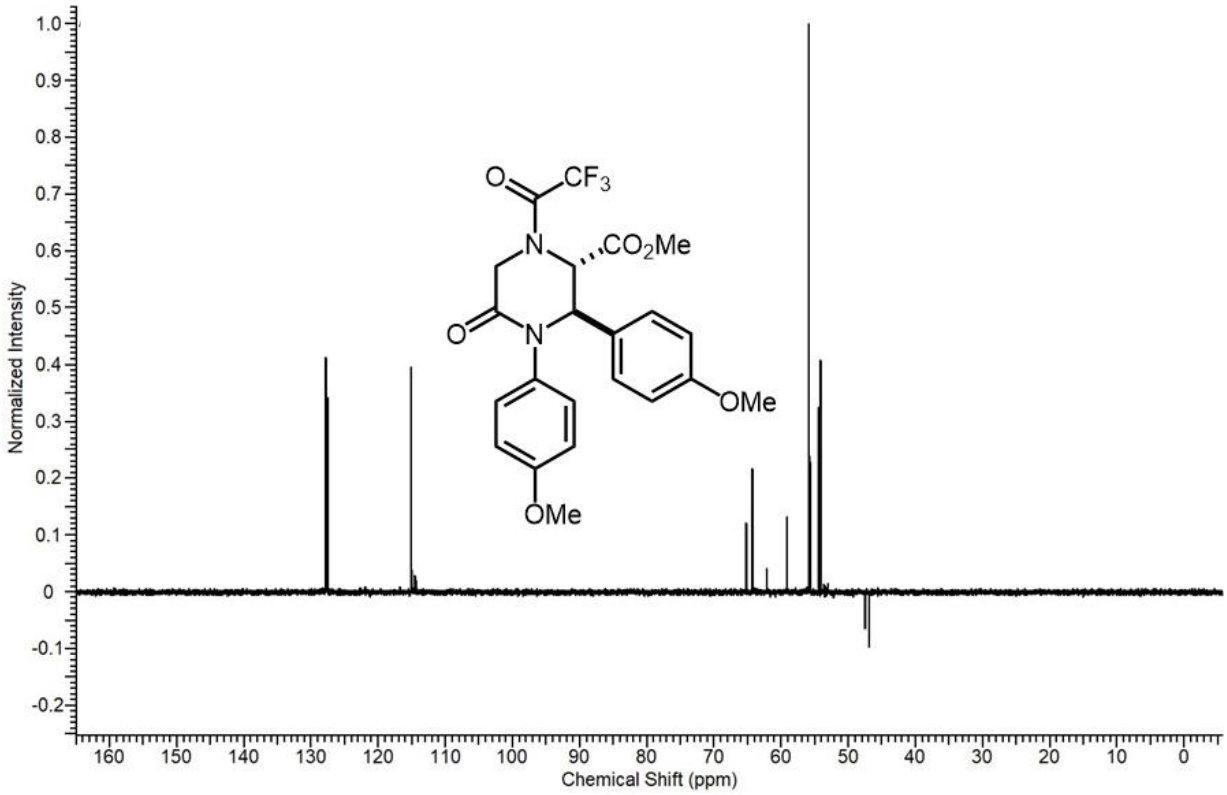

Spectra 1-26 DEPT-135 NMR spectrum of **10c.**

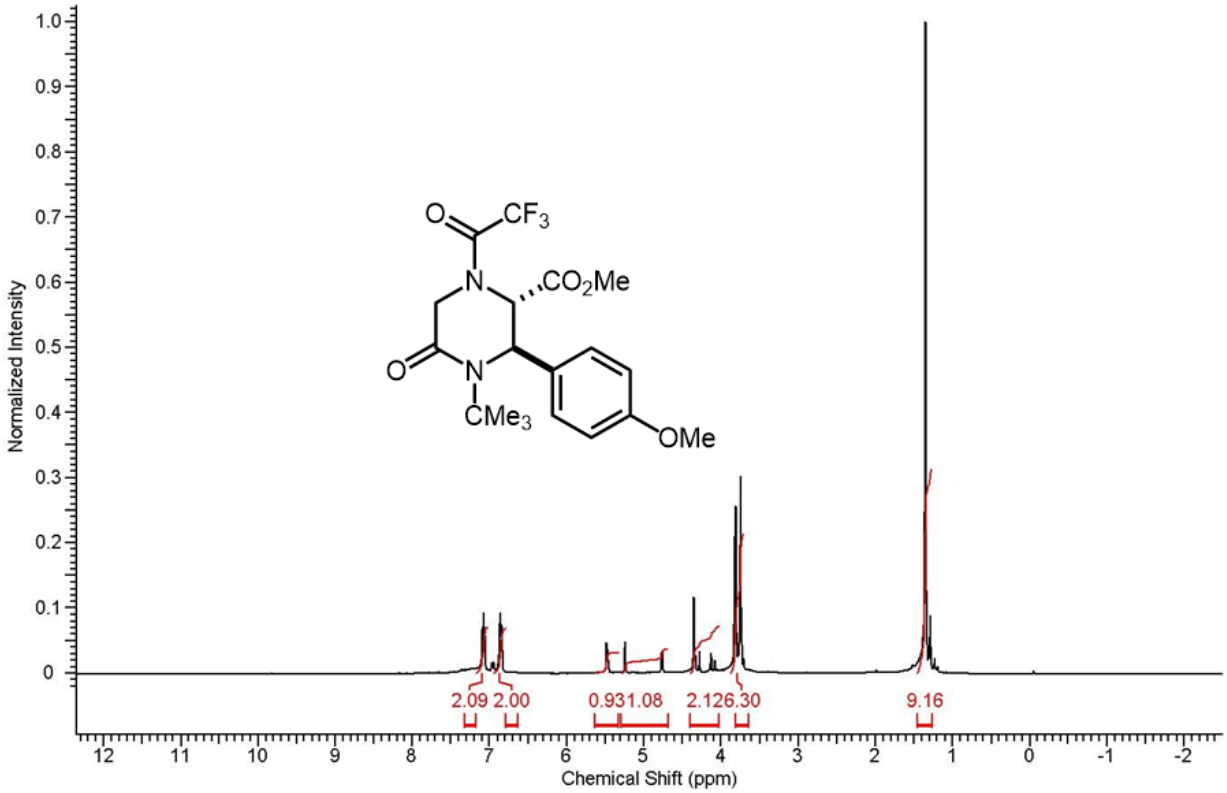

Spectra 1-27 Proton NMR spectrum of **10d.**

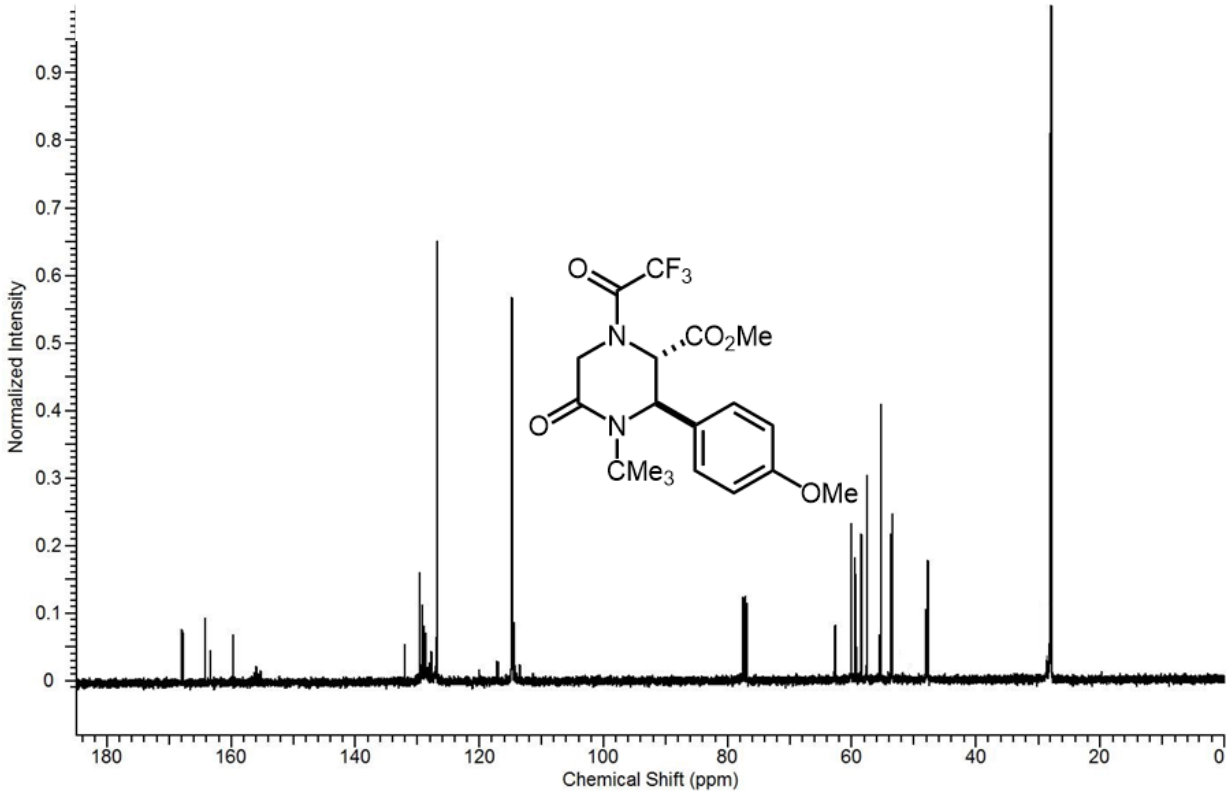

Spectra 1-28 Carbon NMR spectrum of **10d.**

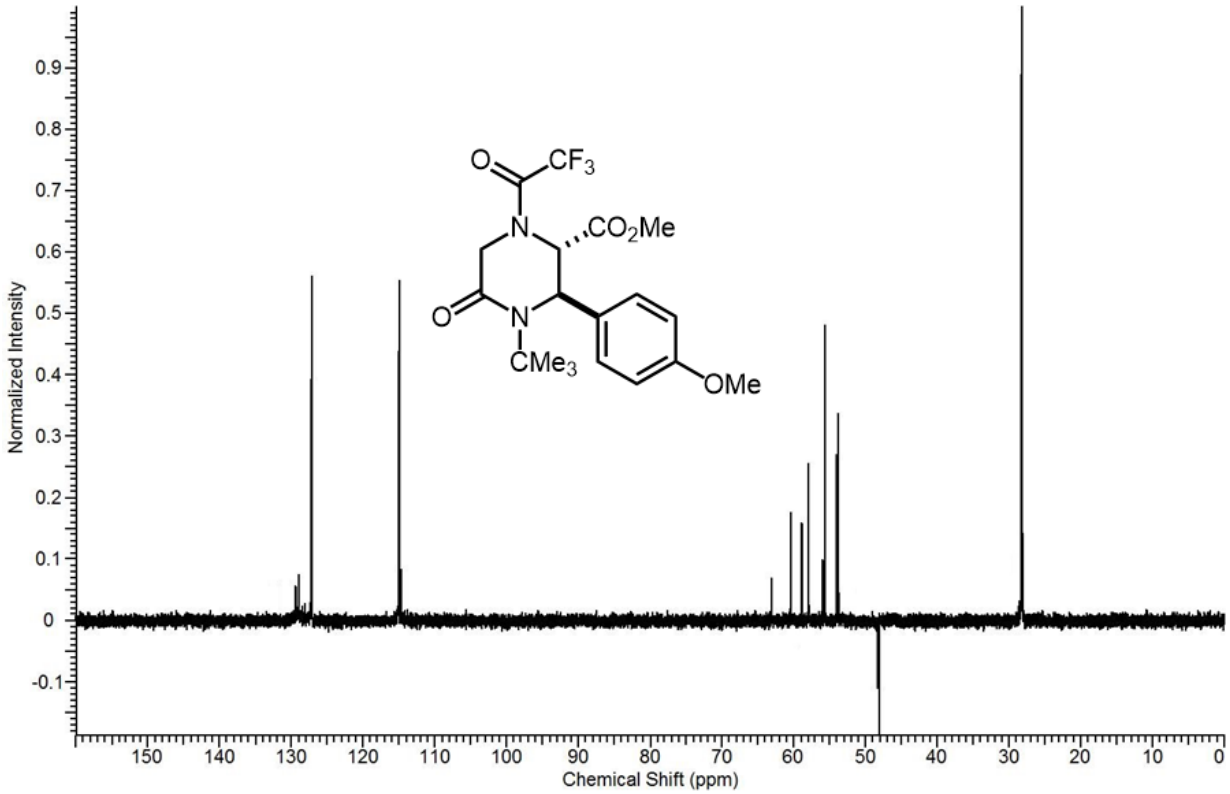

Spectra 1-29 DEPT-135 NMR spectrum of **10d.**

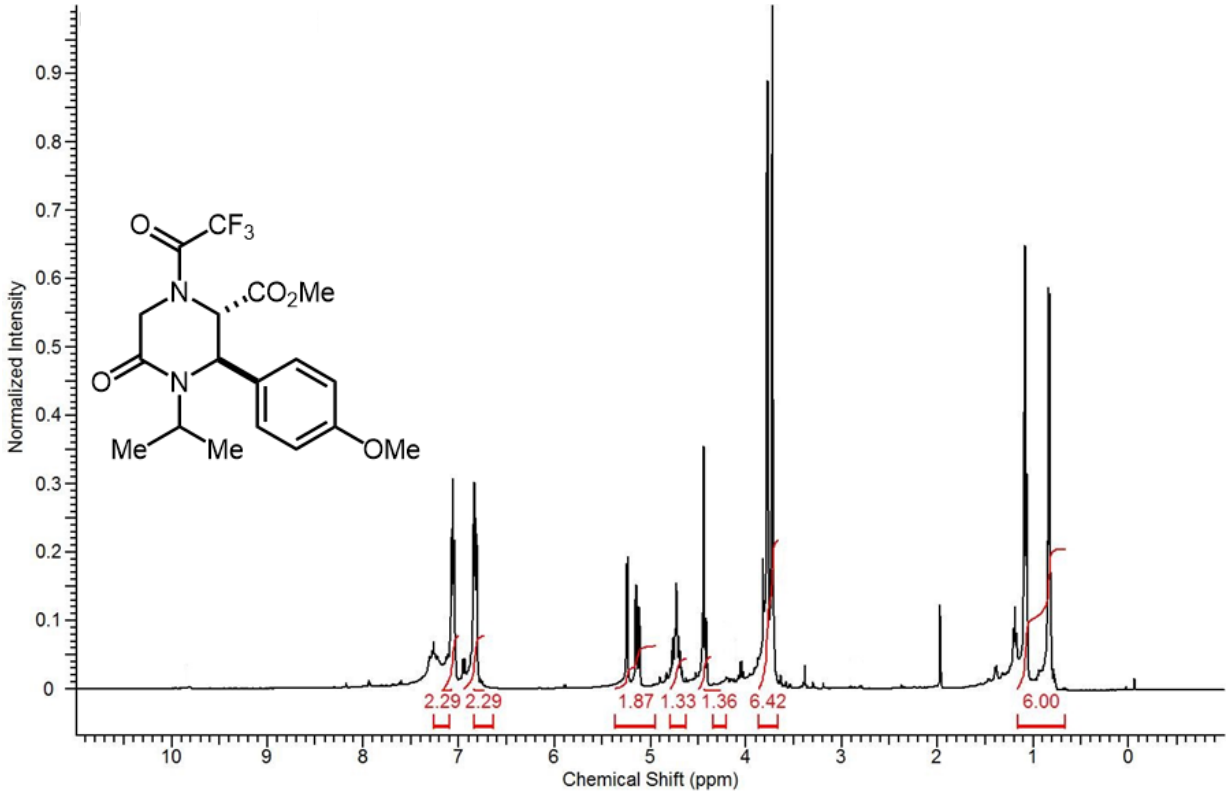

Spectra 1-30 Proton NMR spectrum of **10e.**

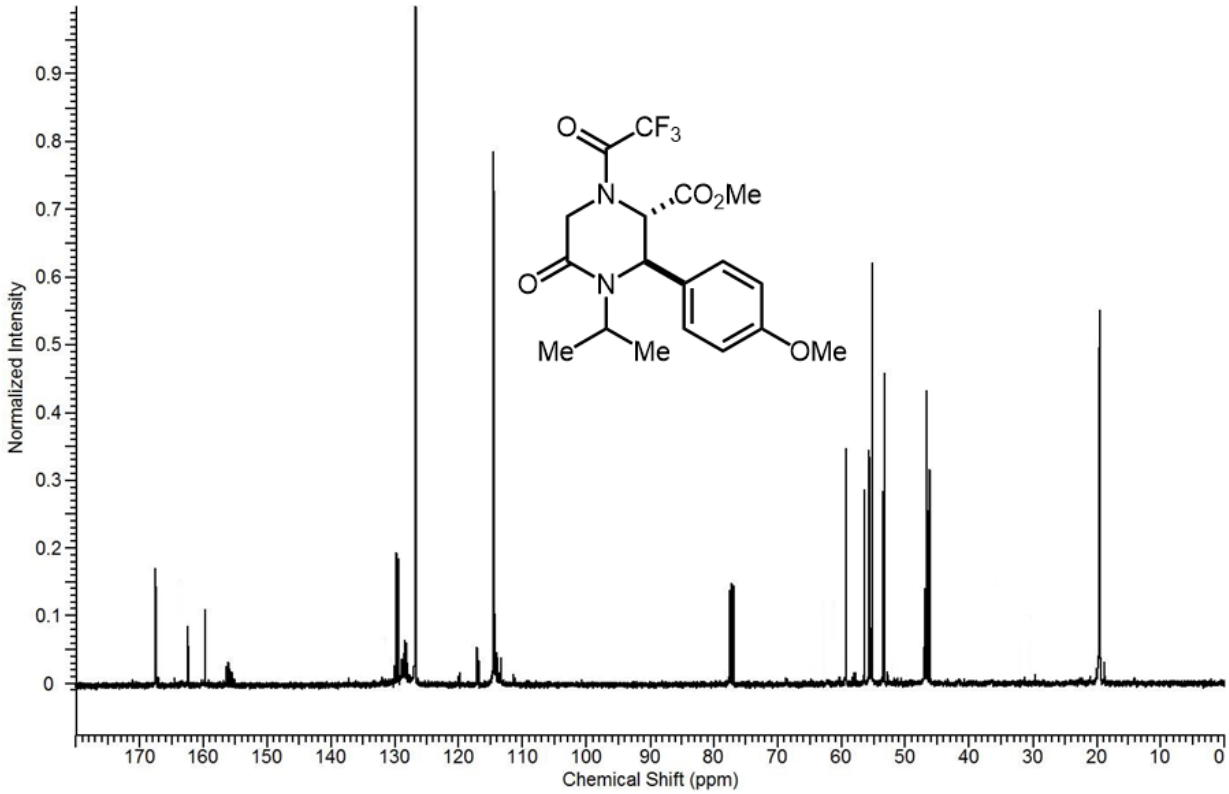

Spectra 1-31 Carbon NMR spectrum of **10e.**

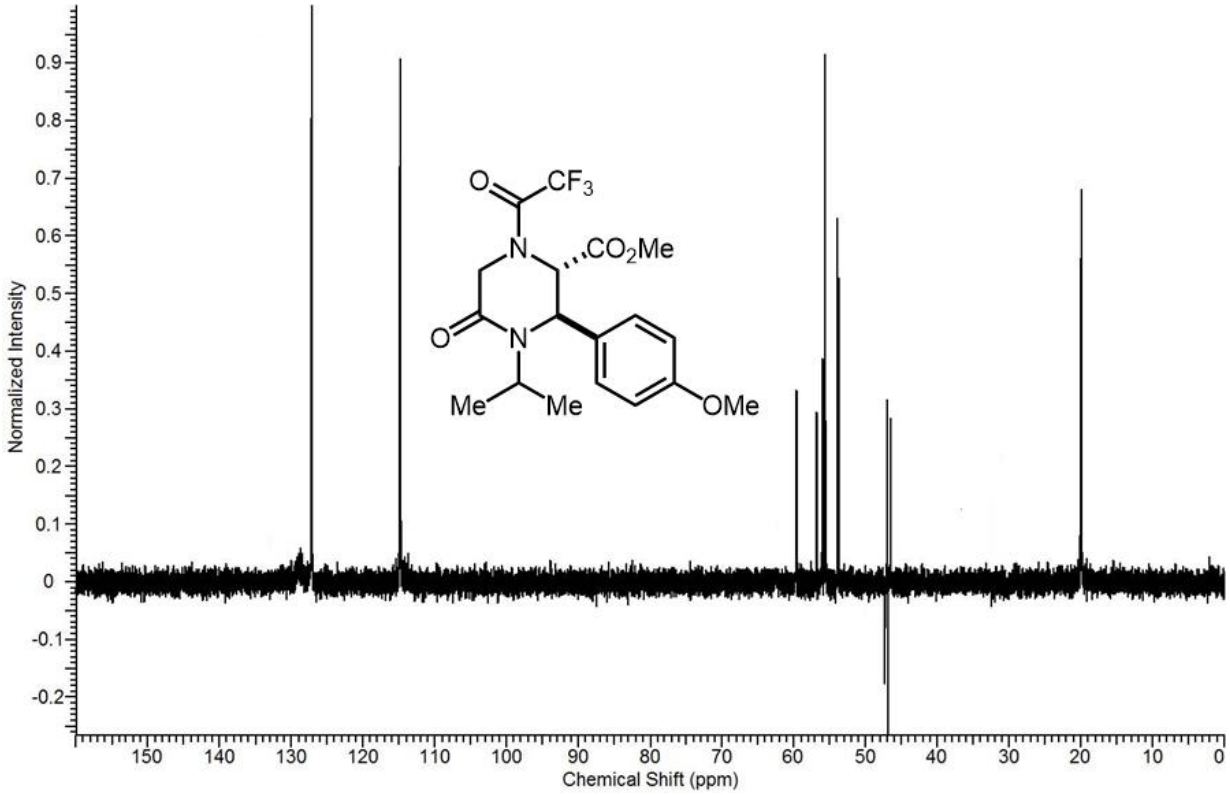

Spectra 1-32 DEPT-135 NMR spectrum of **10e.**

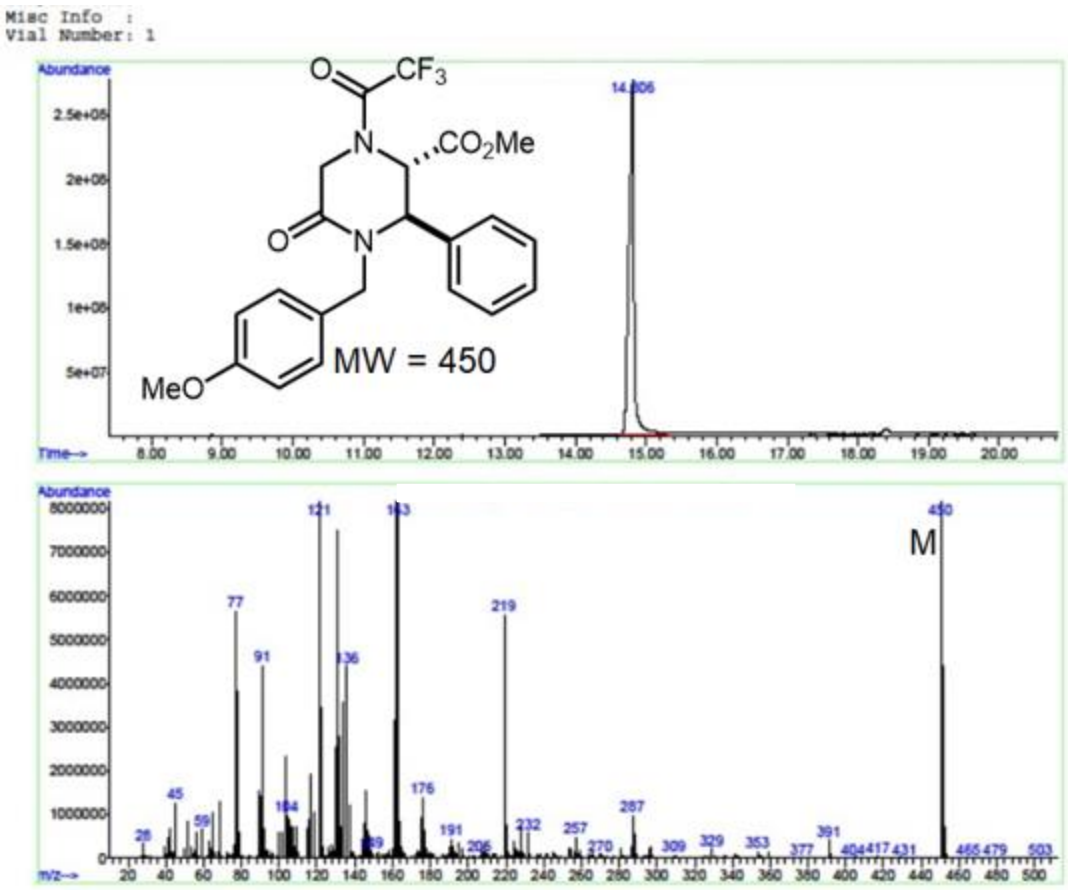

Spectra 1-33 GC-MS spectrum of **10f.**

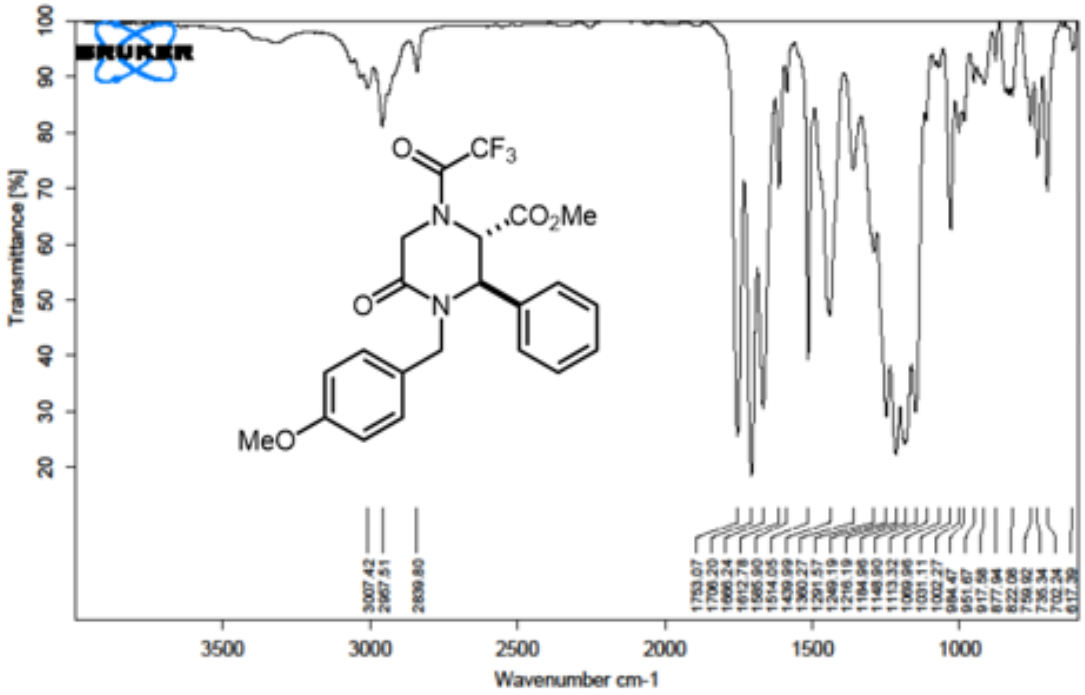

Spectra 1-34 IR spectrum of **10f.**

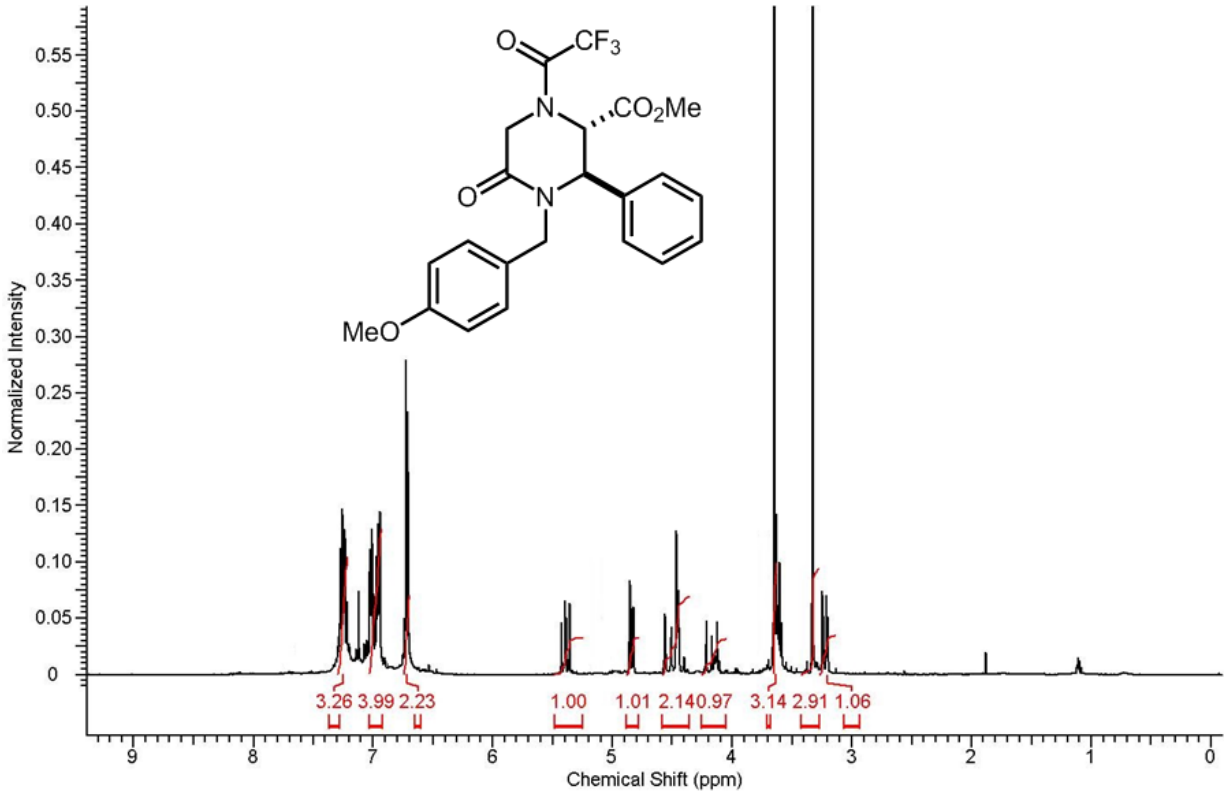

Spectra 1-35 Proton NMR spectrum of **10f.**

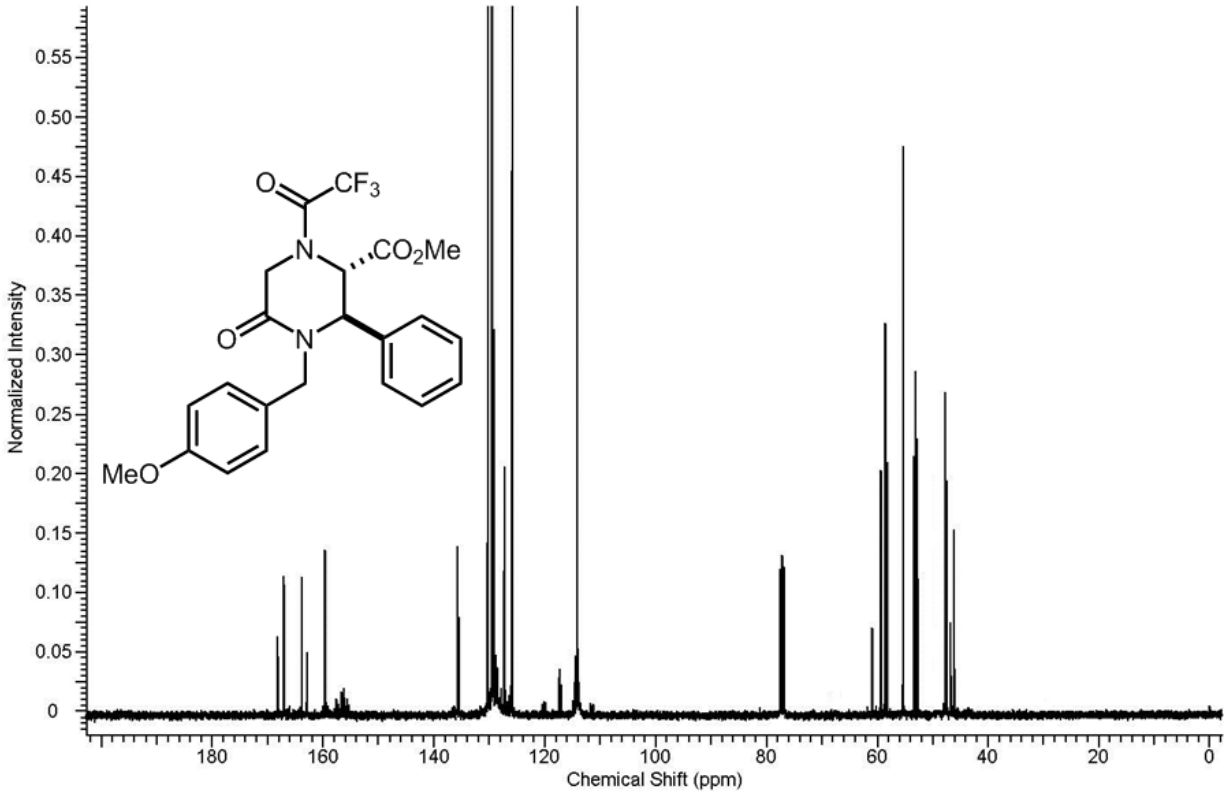

Spectra 1-36 Carbon NMR spectrum of **10f.**

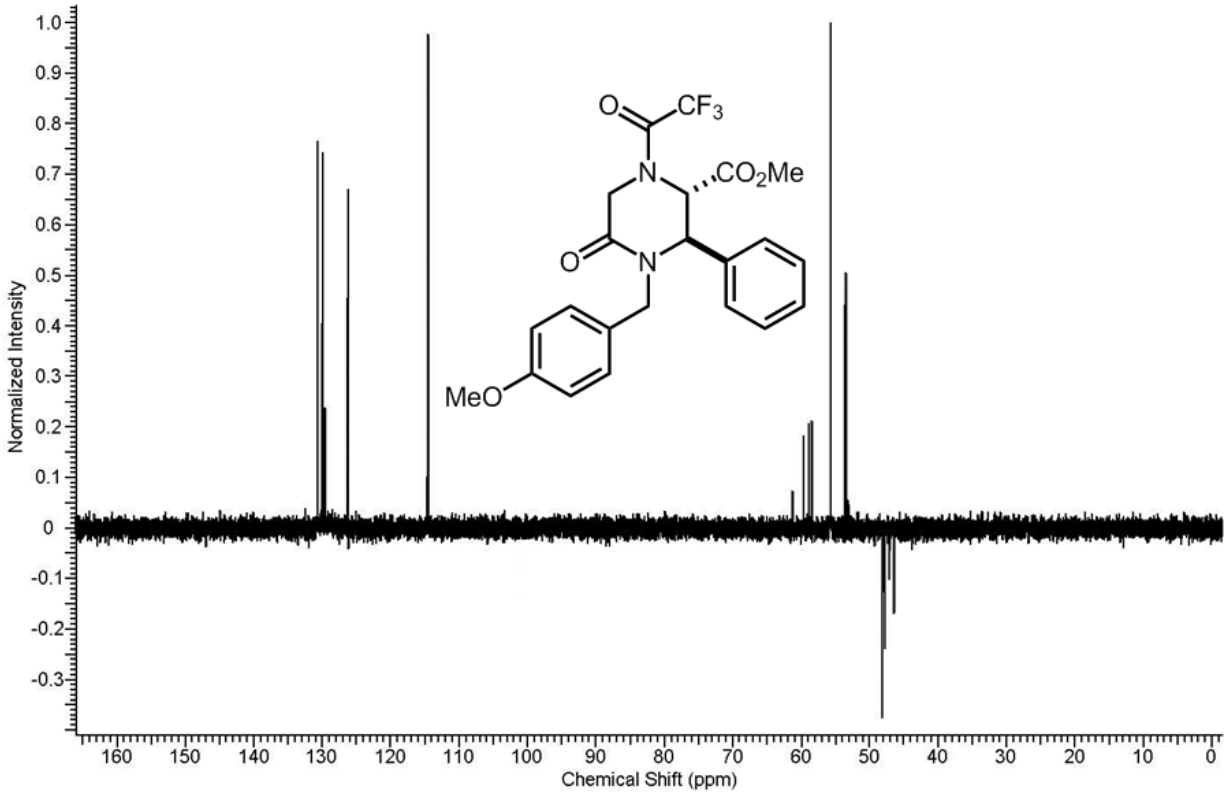

Spectra 1-37 DEPT-135 NMR spectrum of **10f.**

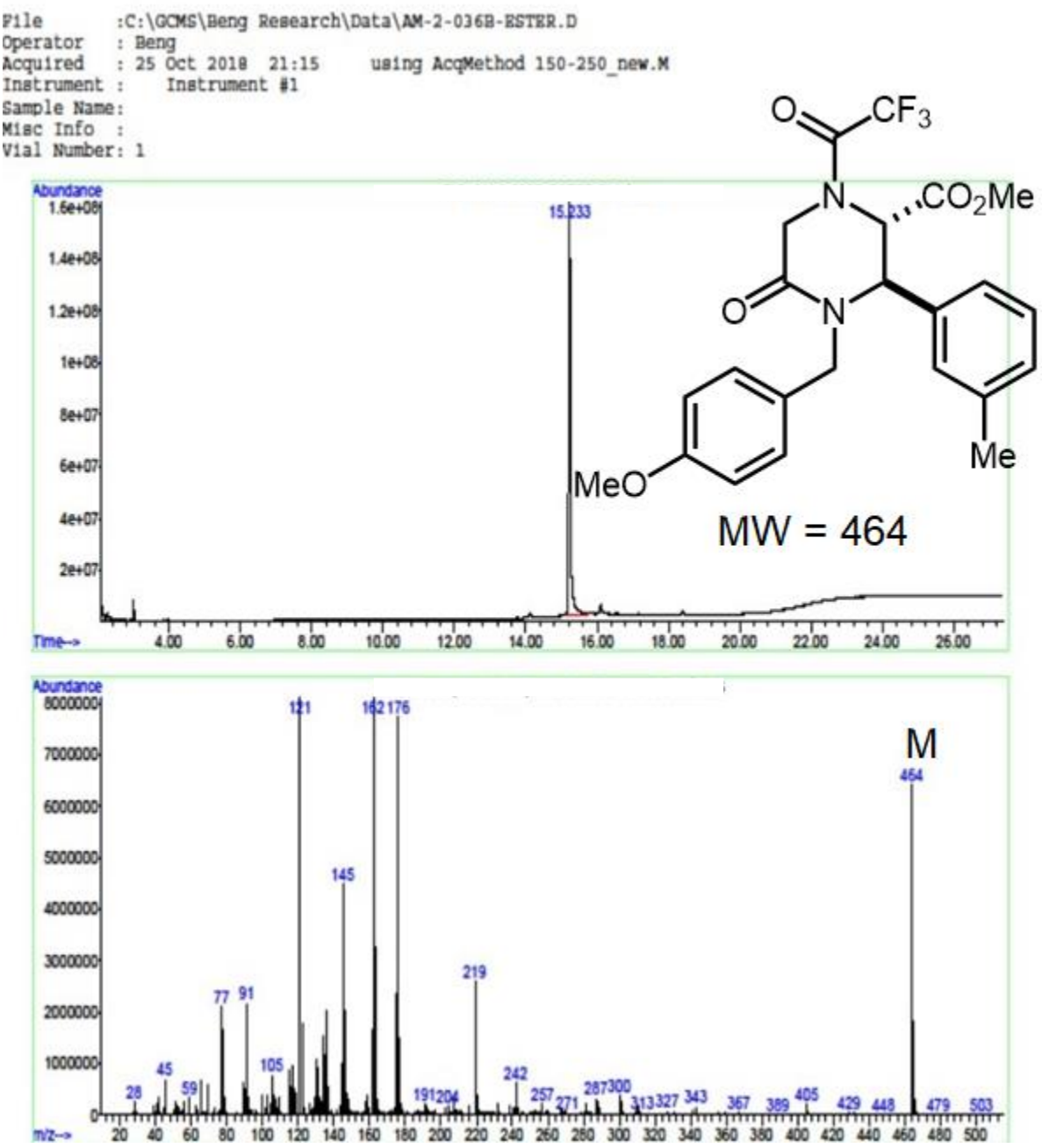

Spectra 1-38 GC-MS spectrum of **10g.**

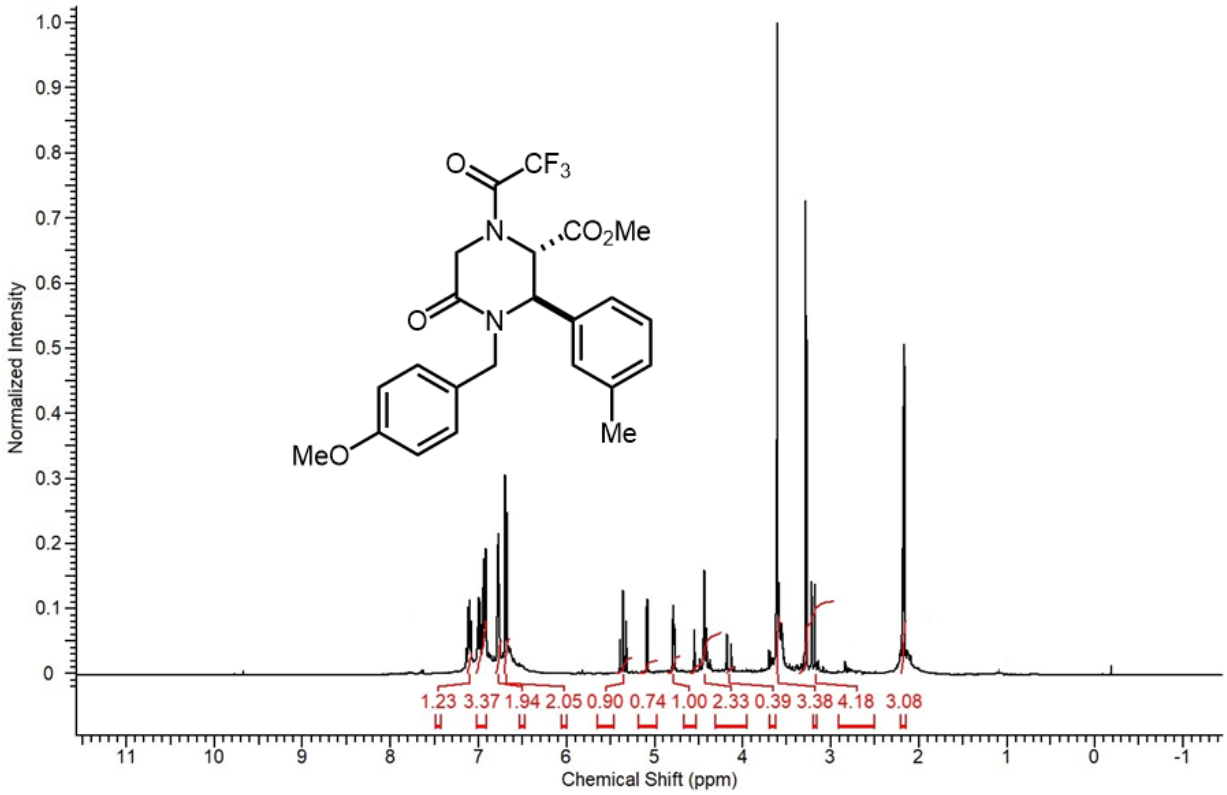

Spectra 1-39 Proton NMR spectrum of **10g.**

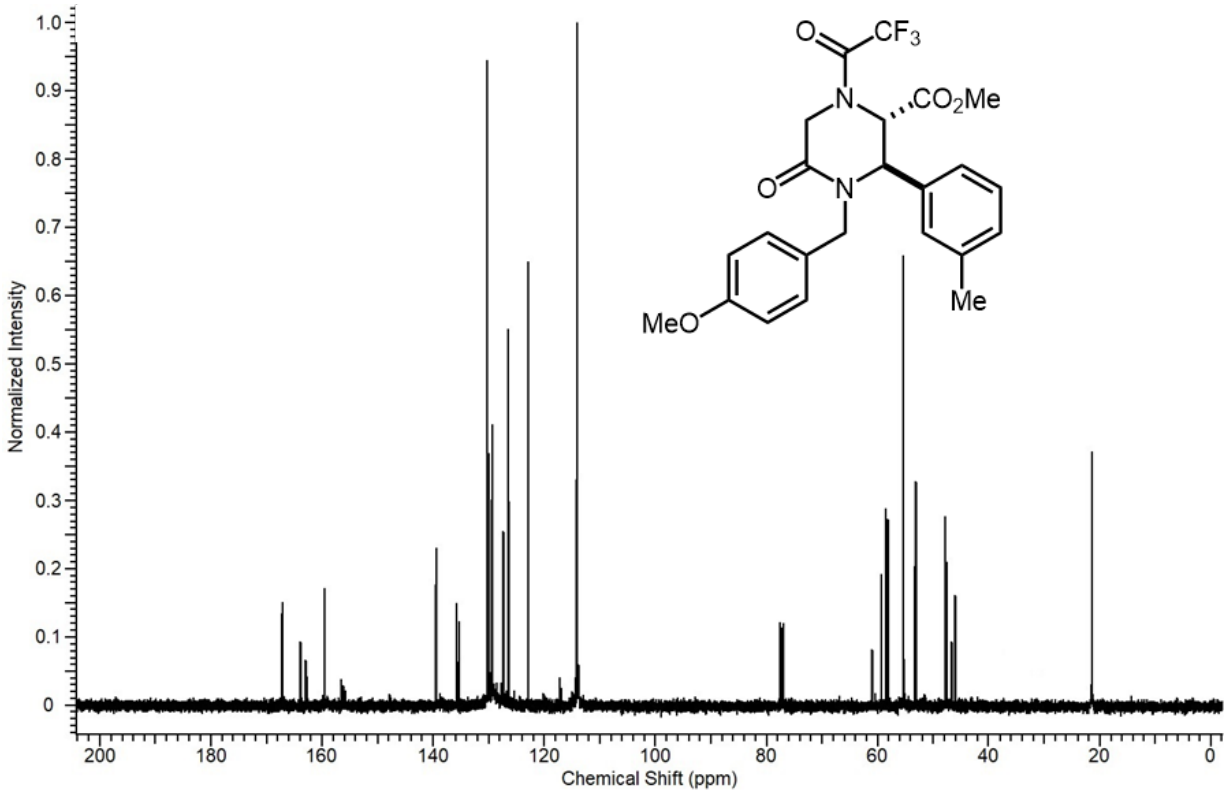

Spectra 1-40 Carbon NMR spectrum of **10g.**

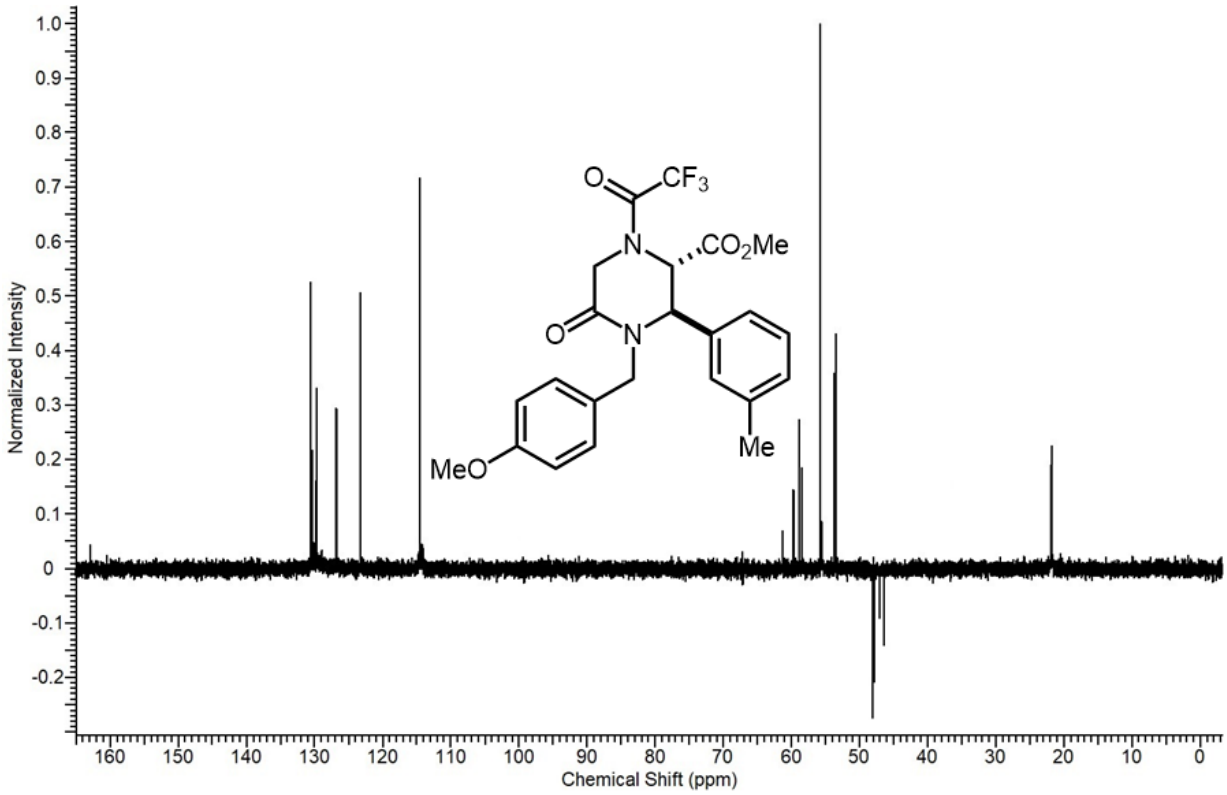

Spectra 1-41 DEPT-135 NMR spectrum of **10g.**

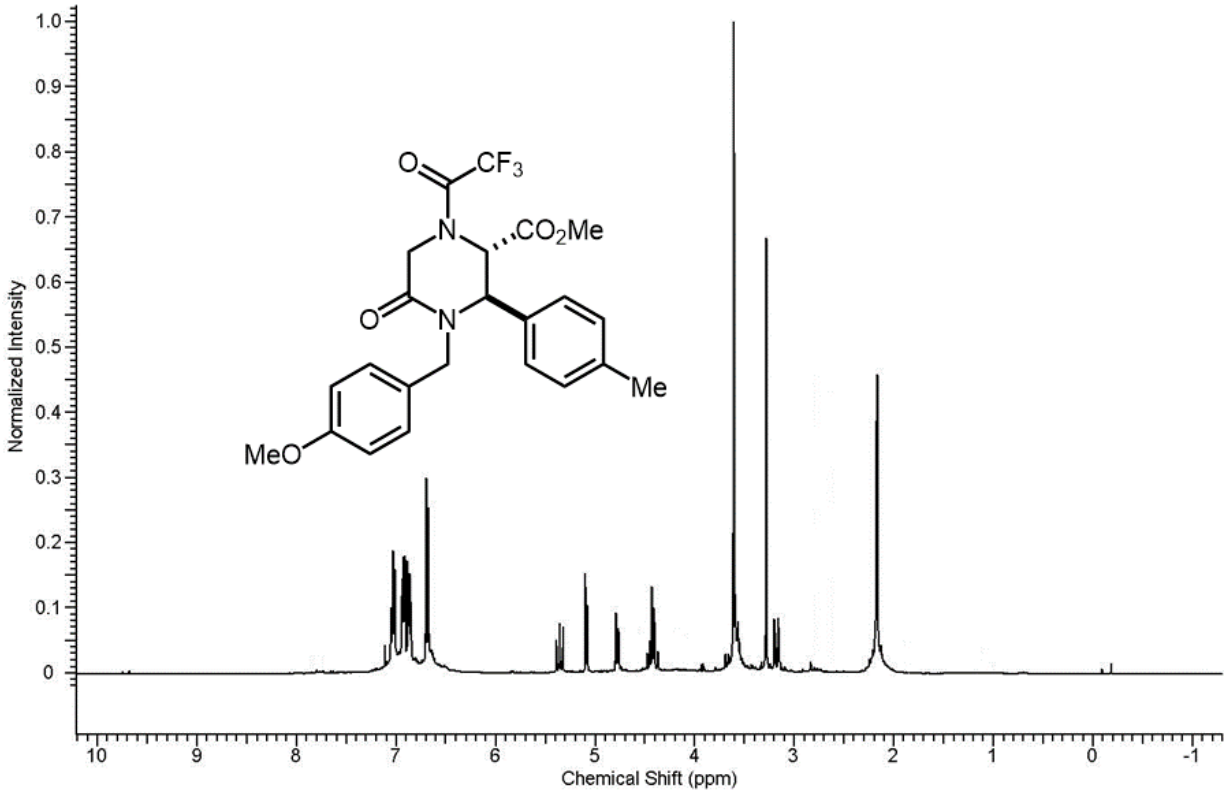

Spectra 1-42 Proton NMR spectrum of **10h.**

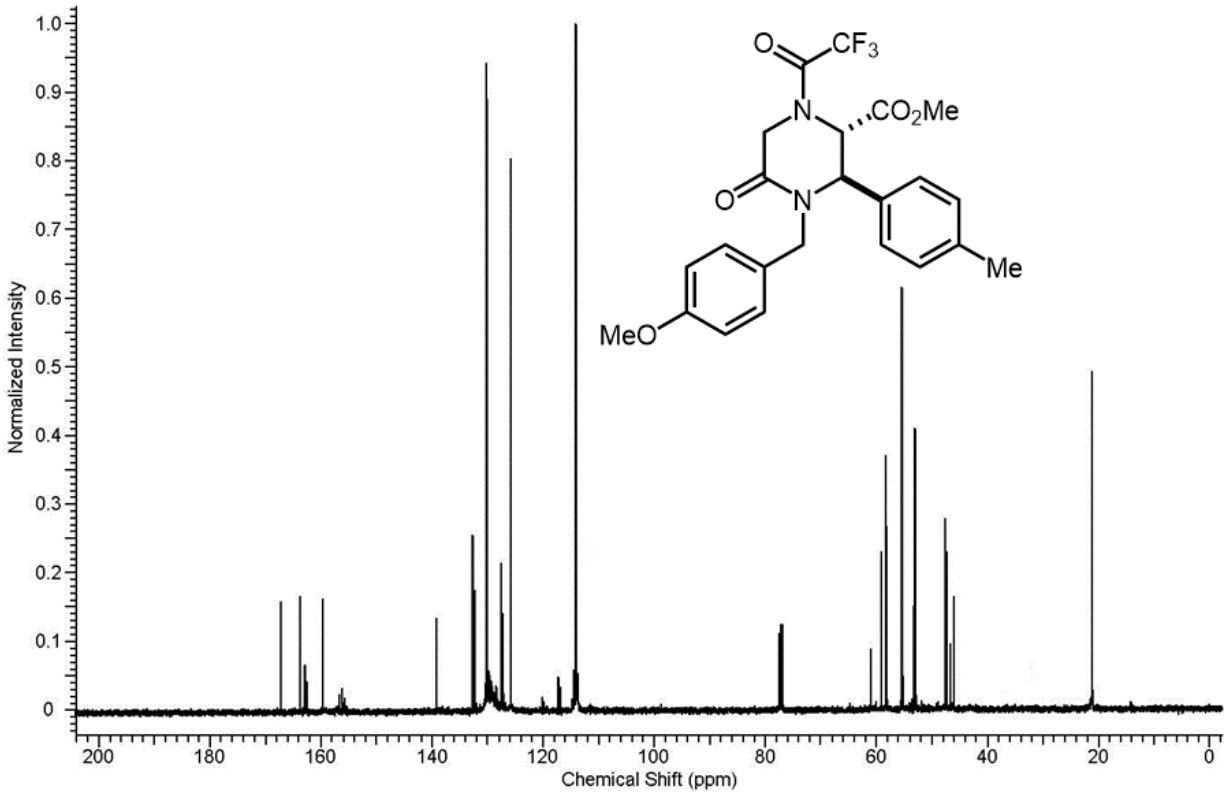

Spectra 1-43 Carbon NMR spectrum of **10h.**

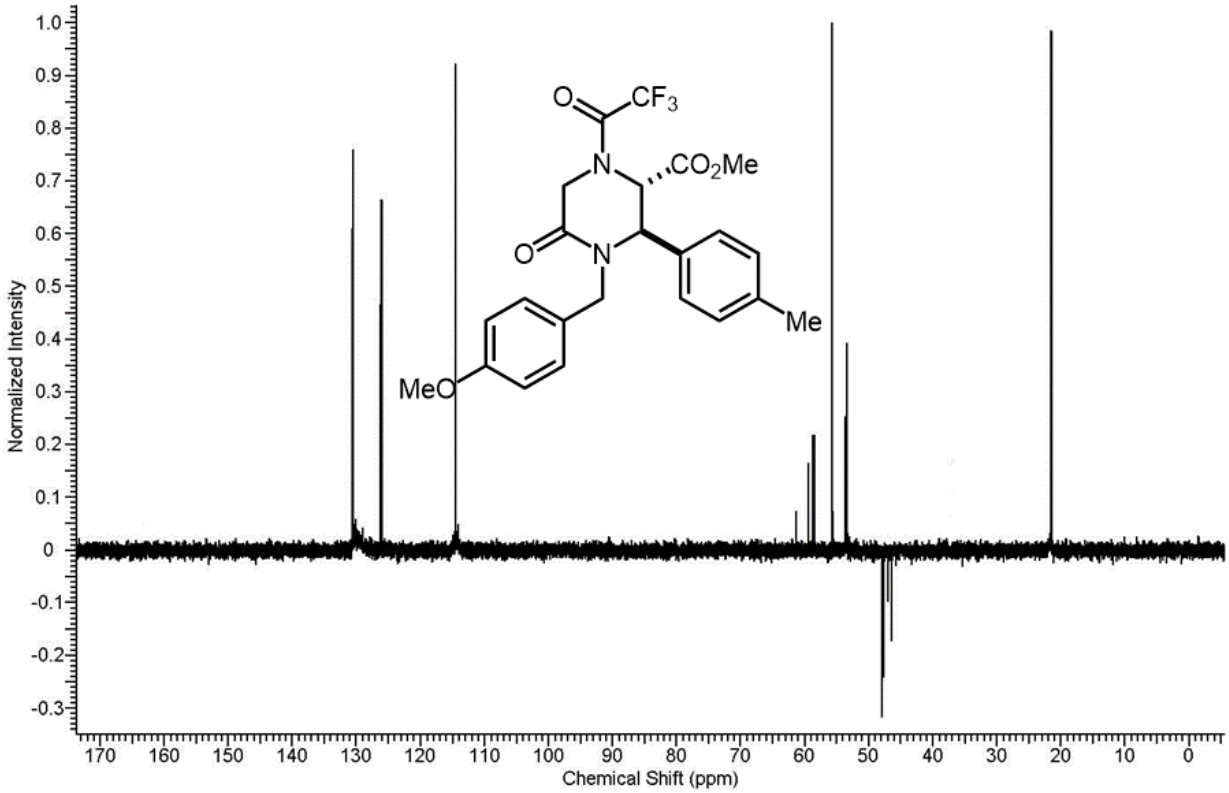

Spectra 1-44 DEPT-135 NMR spectrum of **10h.**

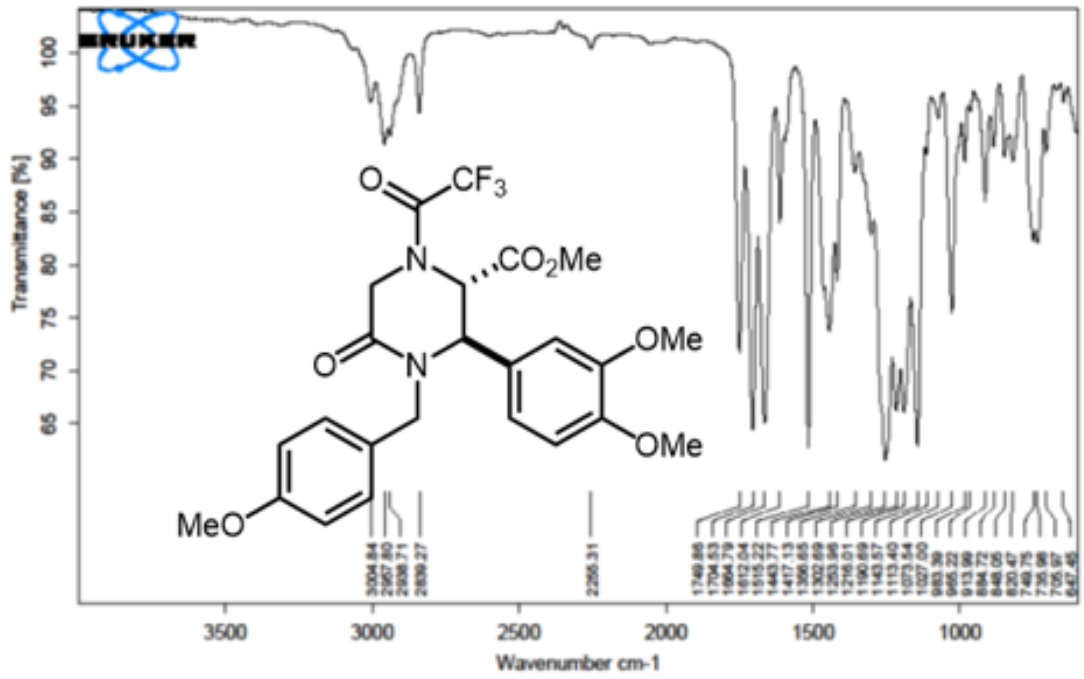

Spectra 1-45 IR spectrum of **10i.**

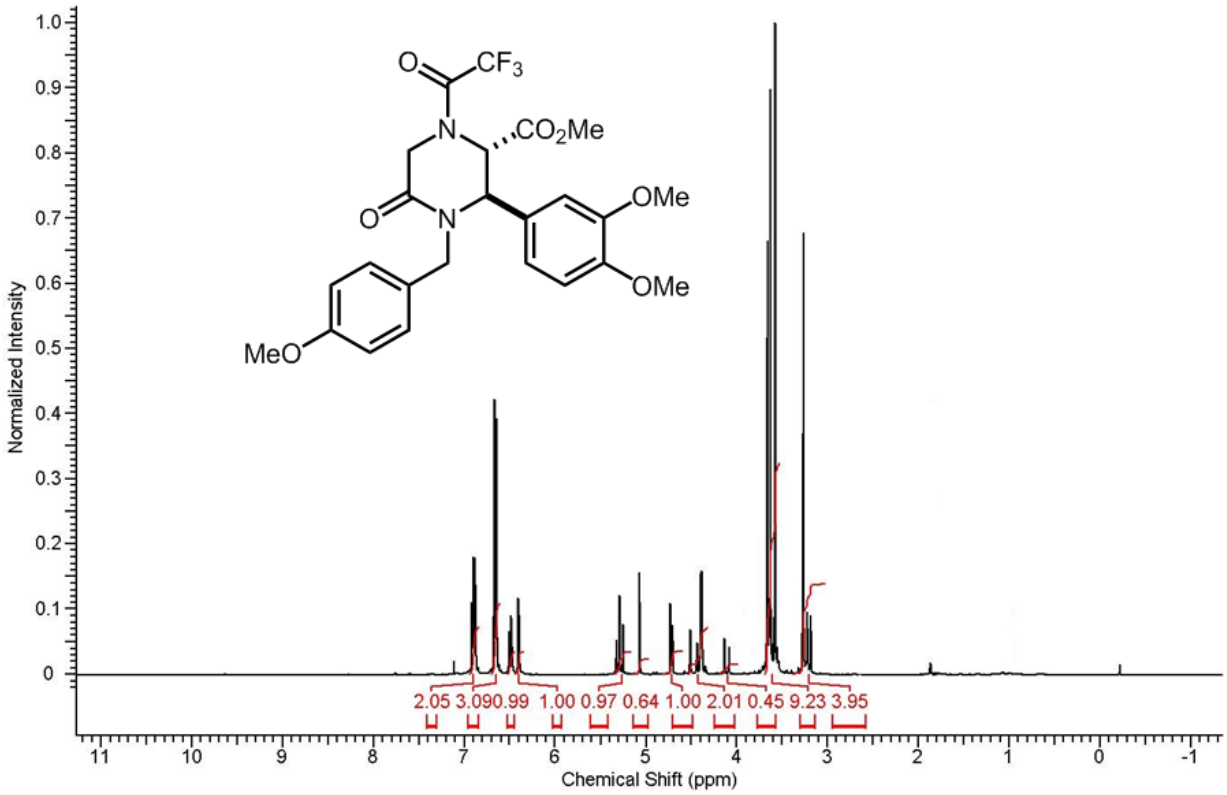

Spectra 1-46 Proton NMR spectrum of **10i.**

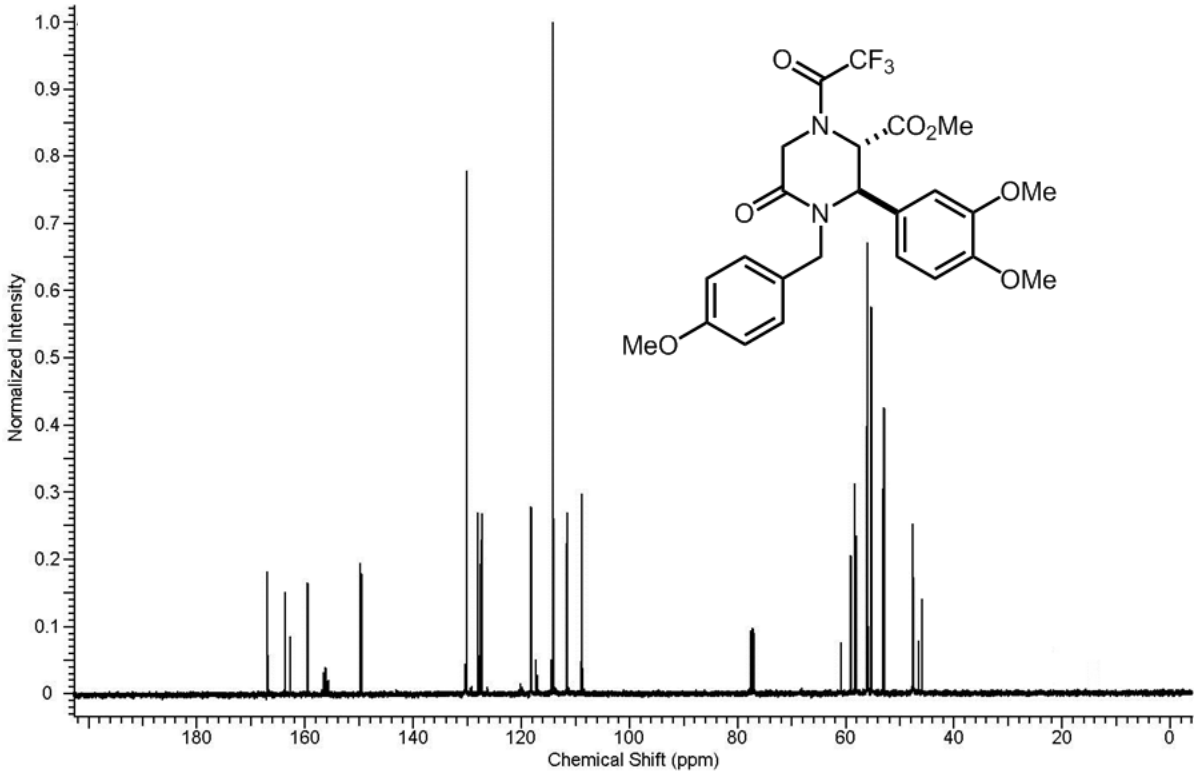

Spectra 1-47 Carbon NMR spectrum of **10i.**

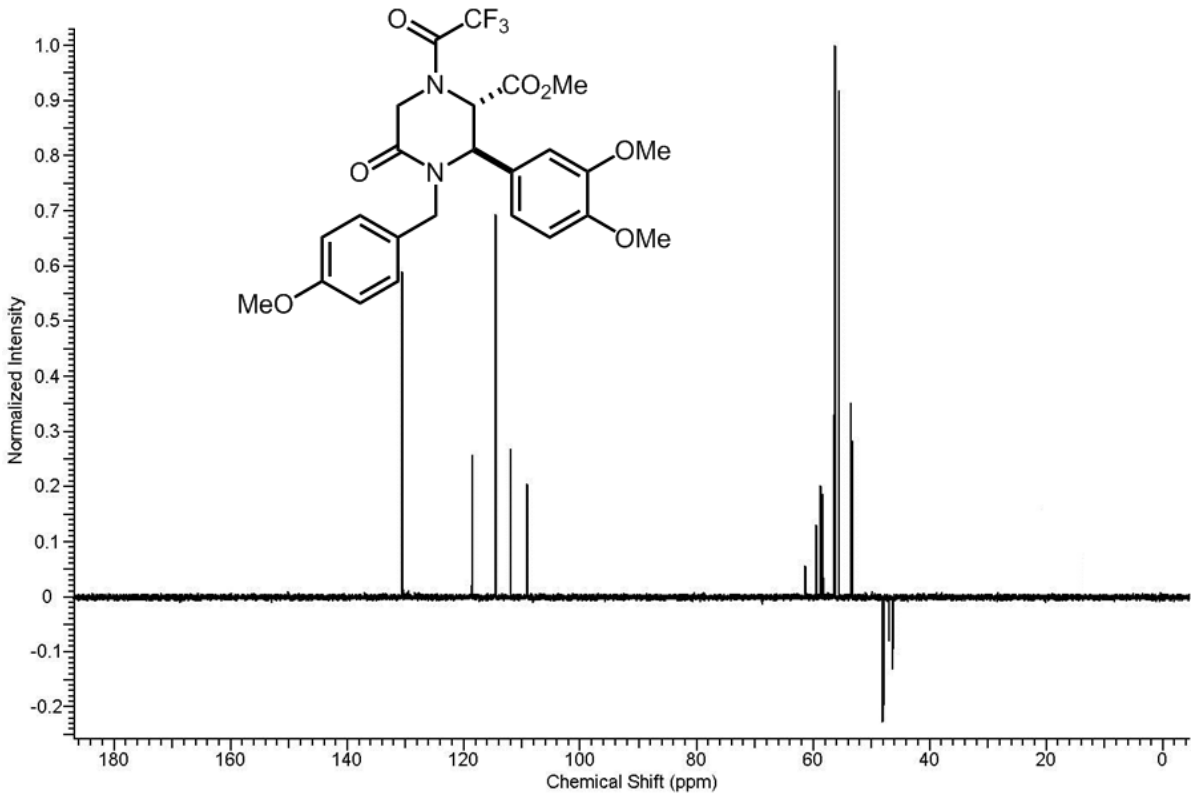

Spectra 1-48 DEPT-135 NMR spectrum of **10i.**

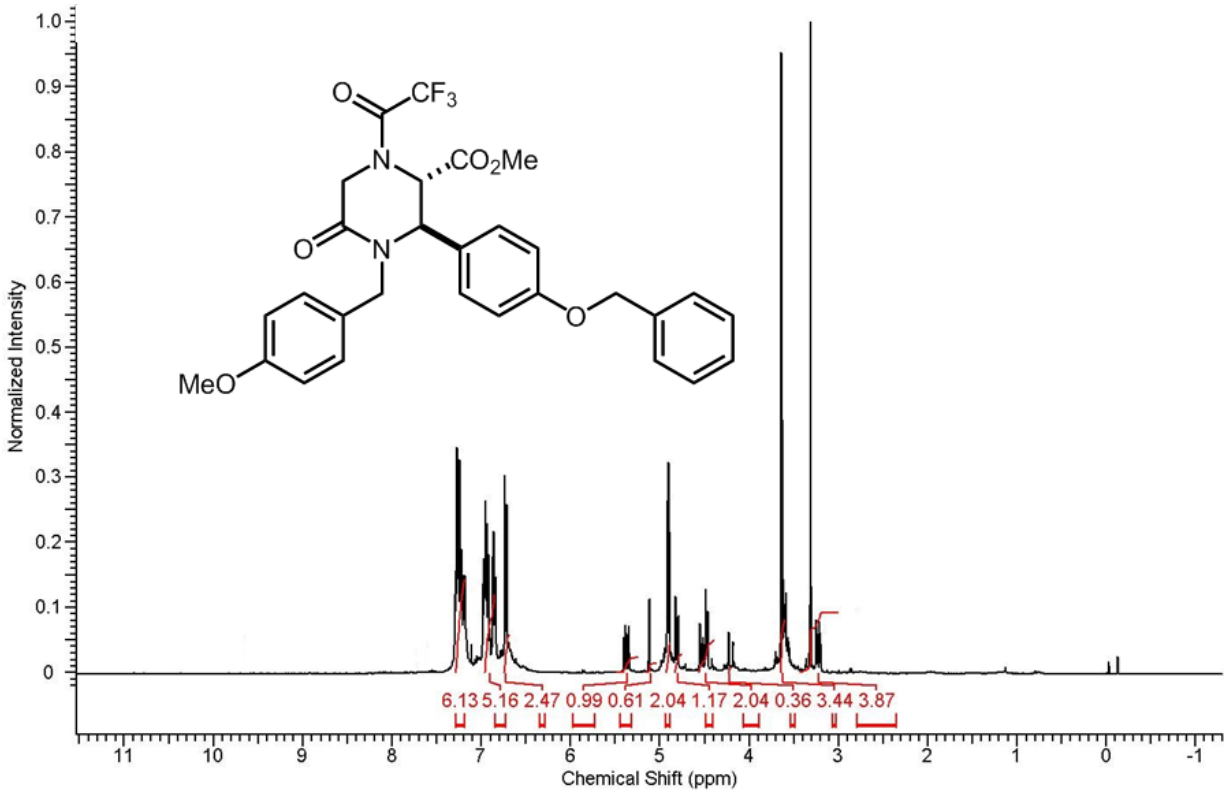

Spectra 1-49 Proton NMR spectrum of **10j.**

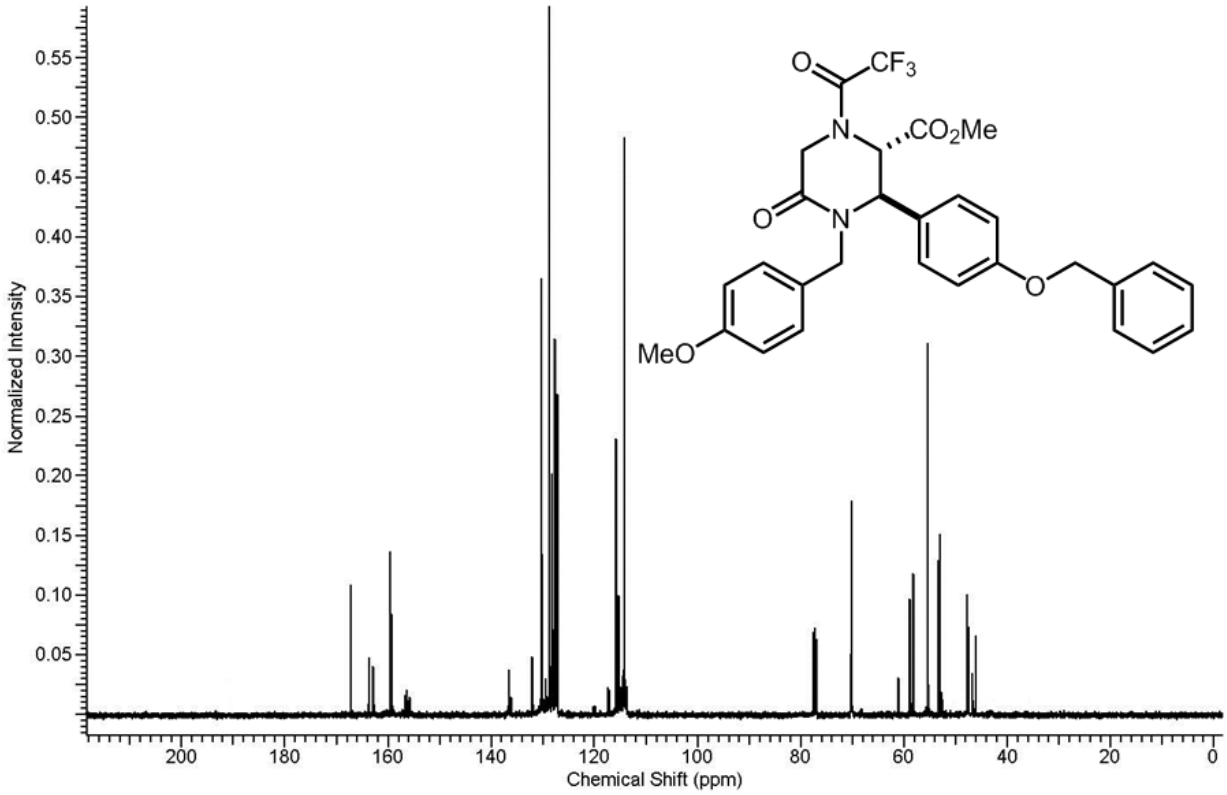

Spectra 1-50 Carbon NMR spectrum of **10j.**

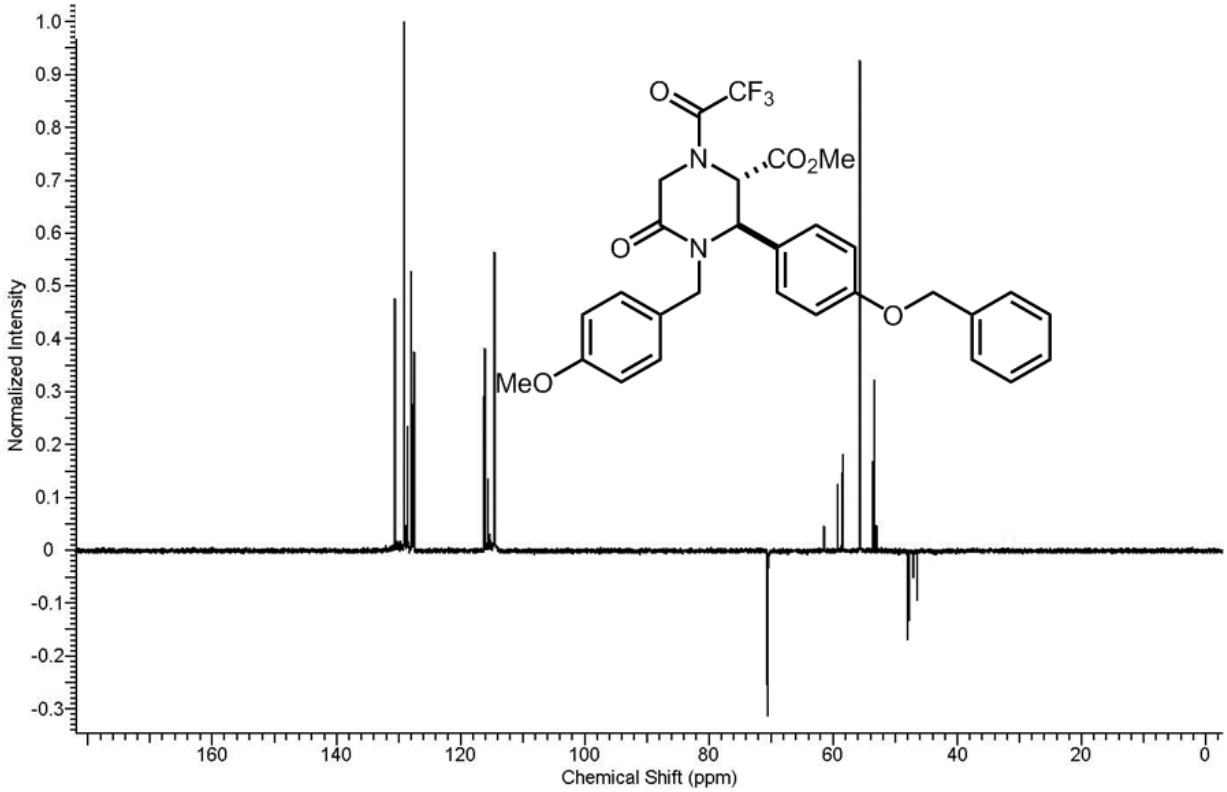

Spectra 1-51 DEPT-135 NMR spectrum of **10j.**

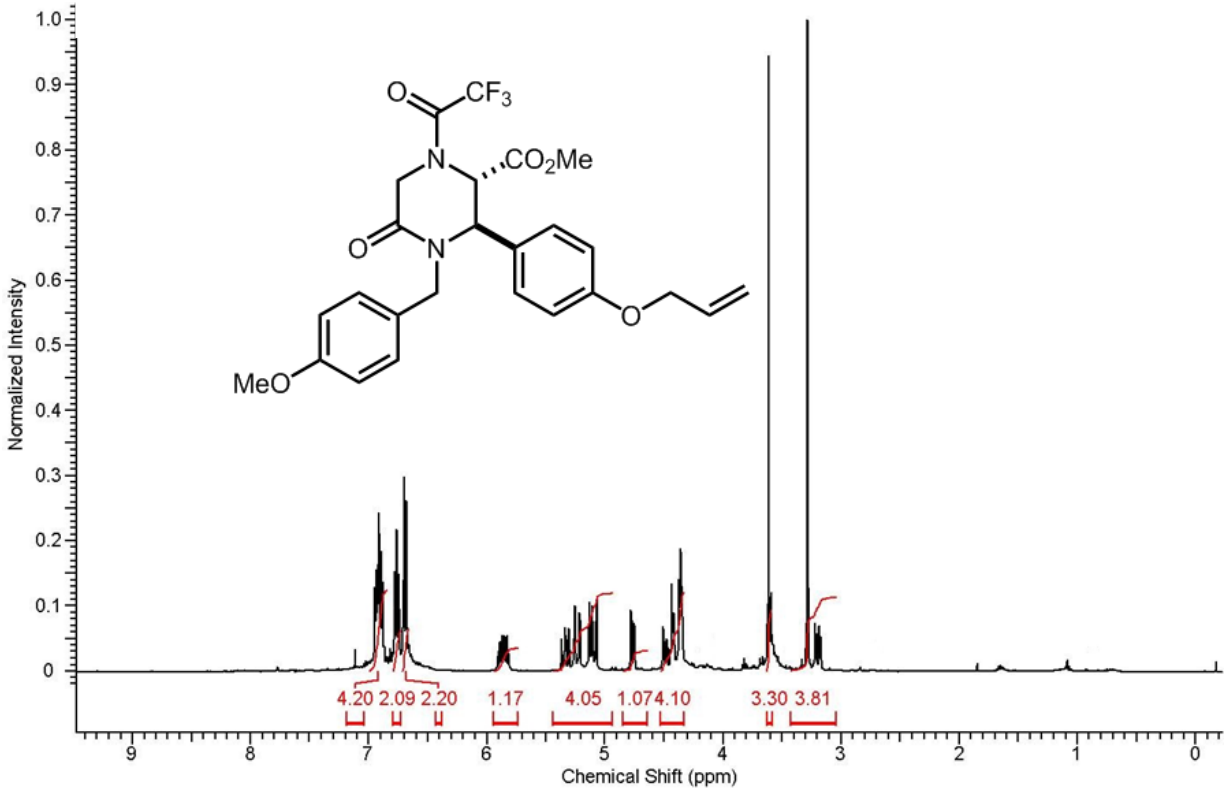

Spectra 1-52 Proton NMR spectrum of **10k.**

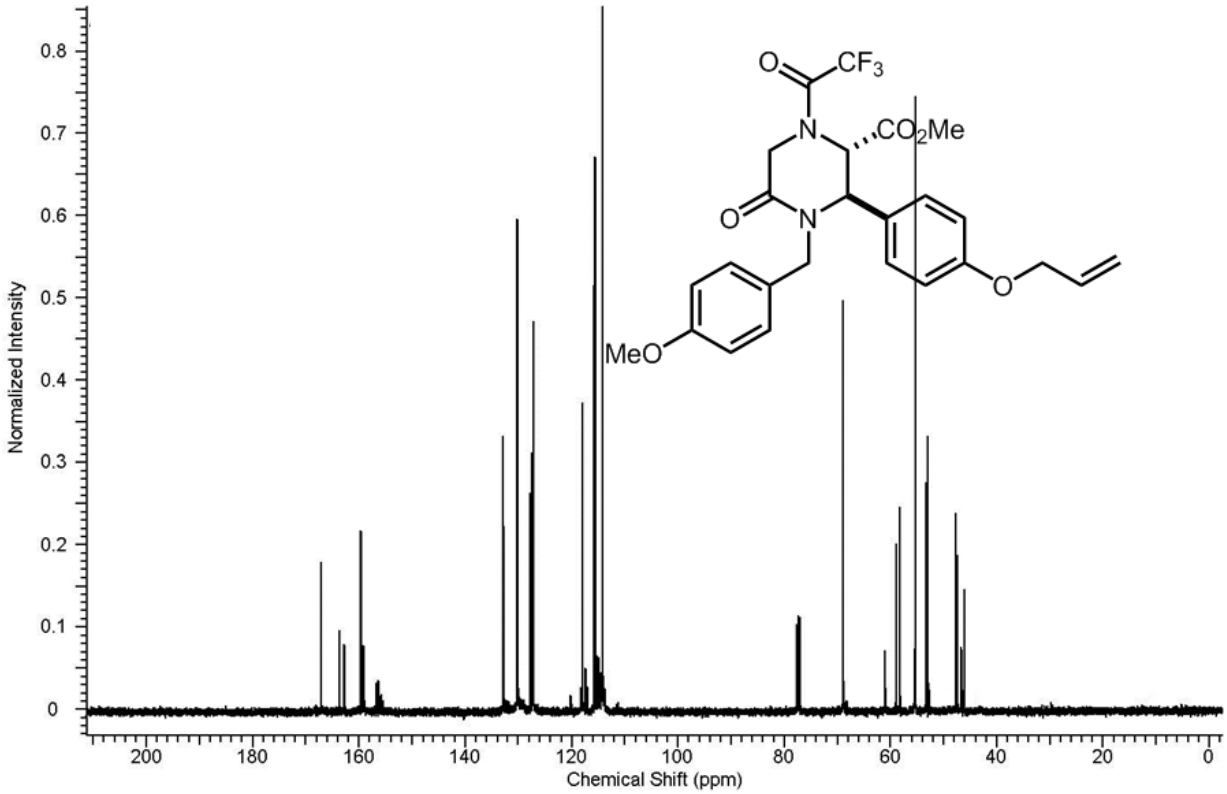

Spectra 1-53 Carbon NMR spectrum of **10k.**

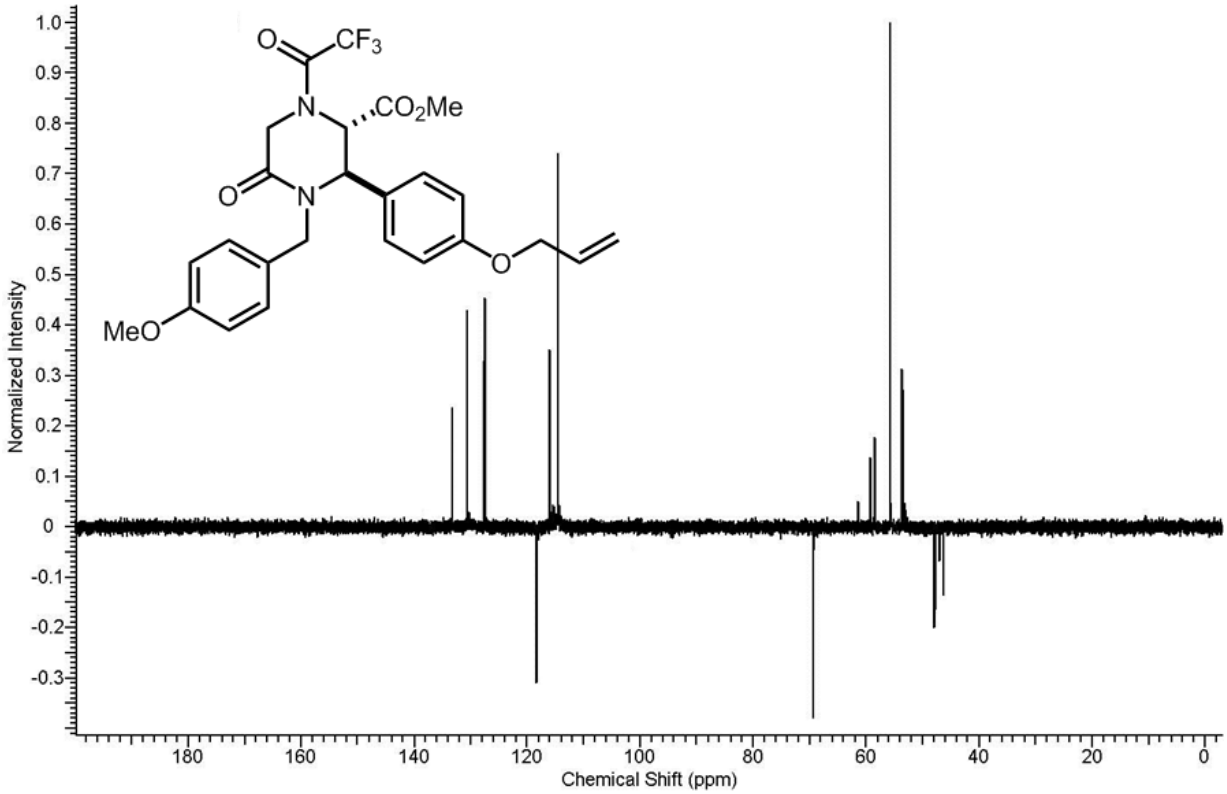

Spectra 1-54 DEPT-135 NMR spectrum of **10k.**

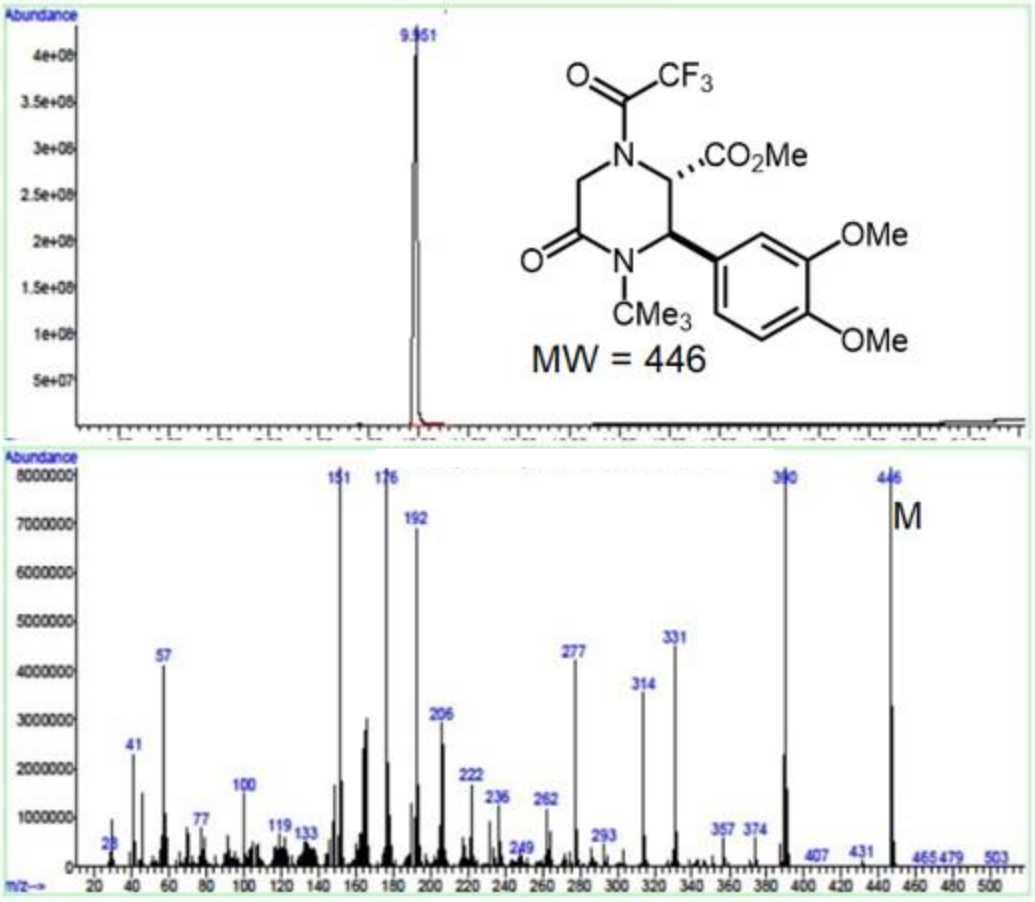

Spectra 1-55 GC-MS spectrum of **10l.**

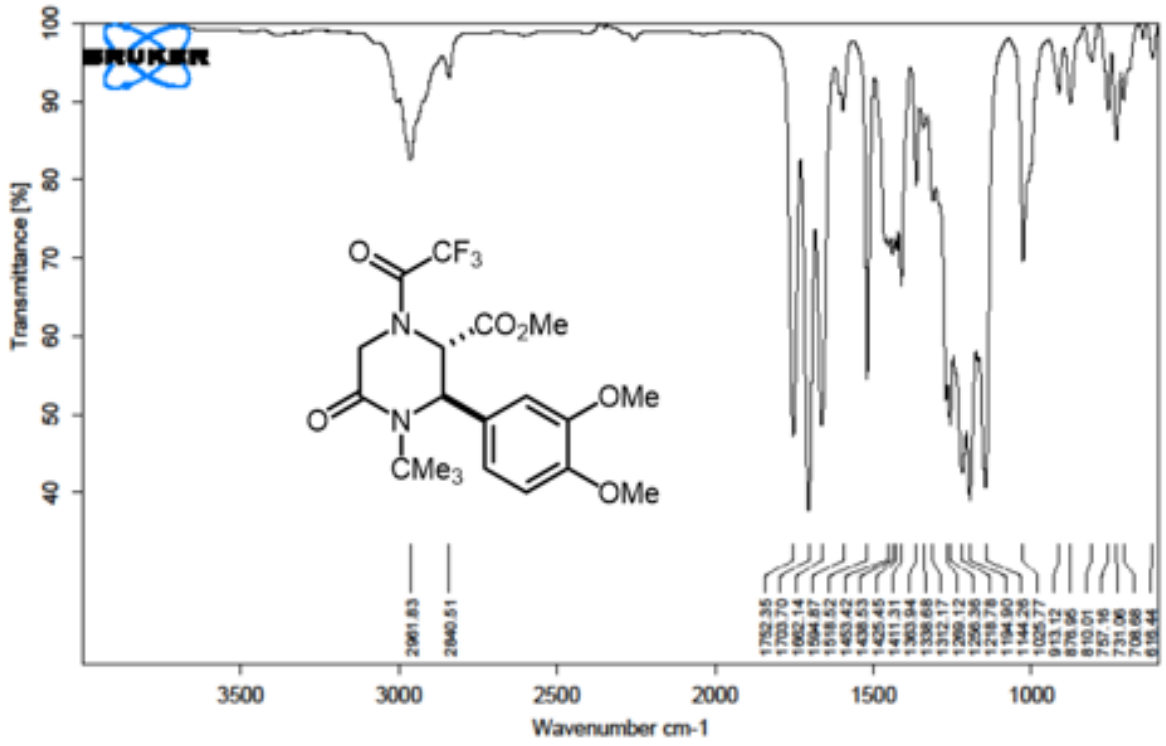

Spectra 1-56 IR NMR spectrum of **10l.**

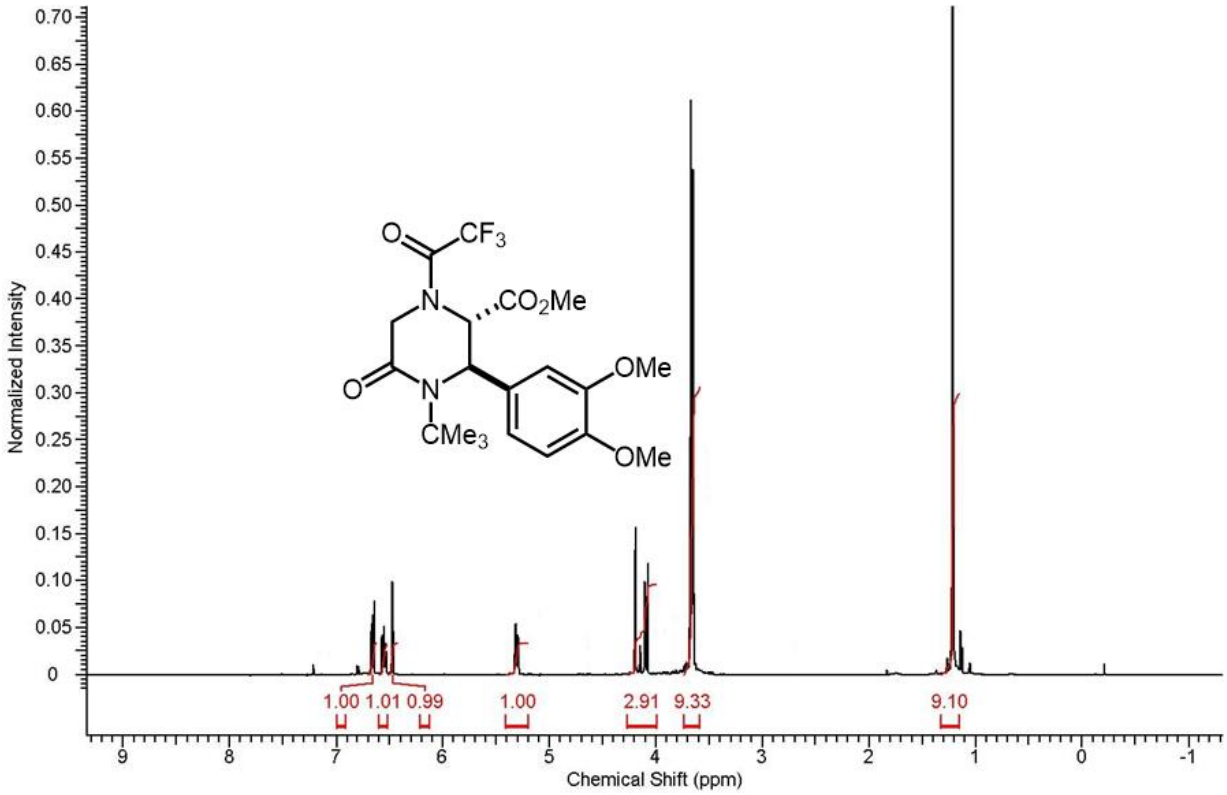

Spectra 1-57 Proton NMR spectrum of **10l.**

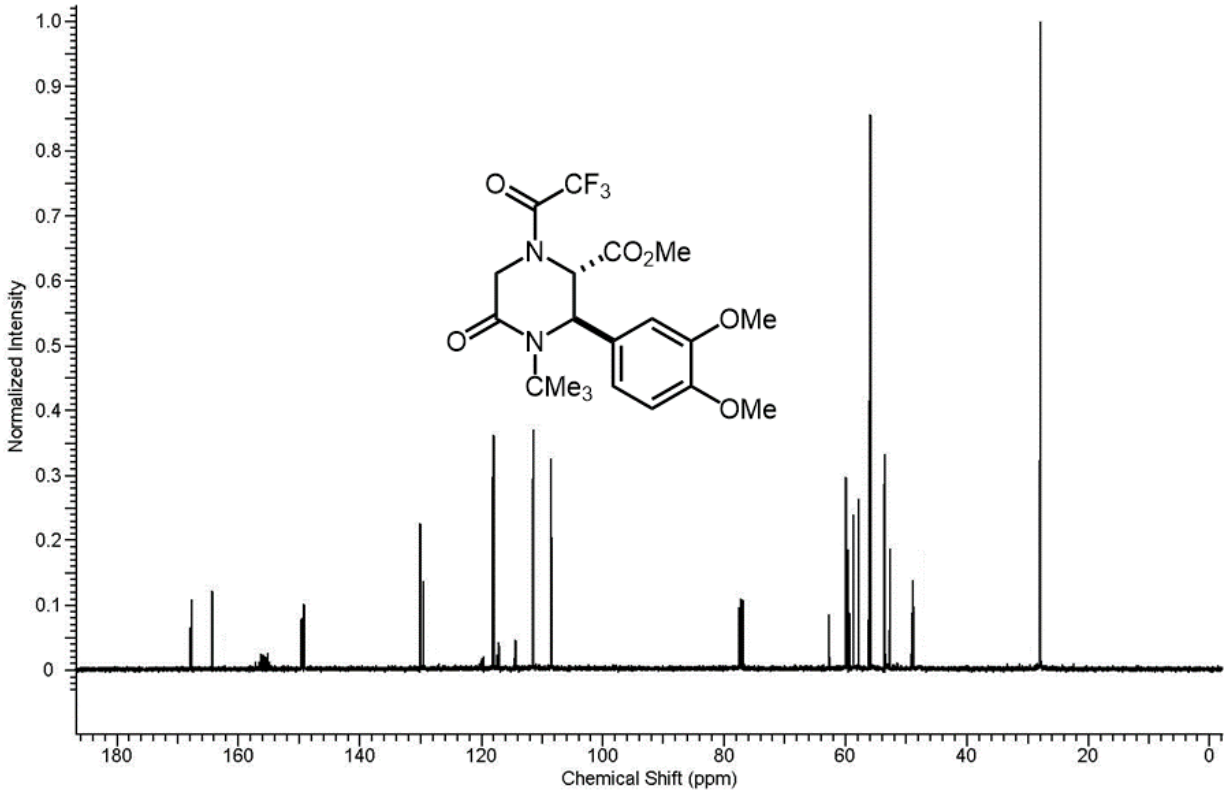

Spectra 1-58 Carbon NMR spectrum of **10l.**

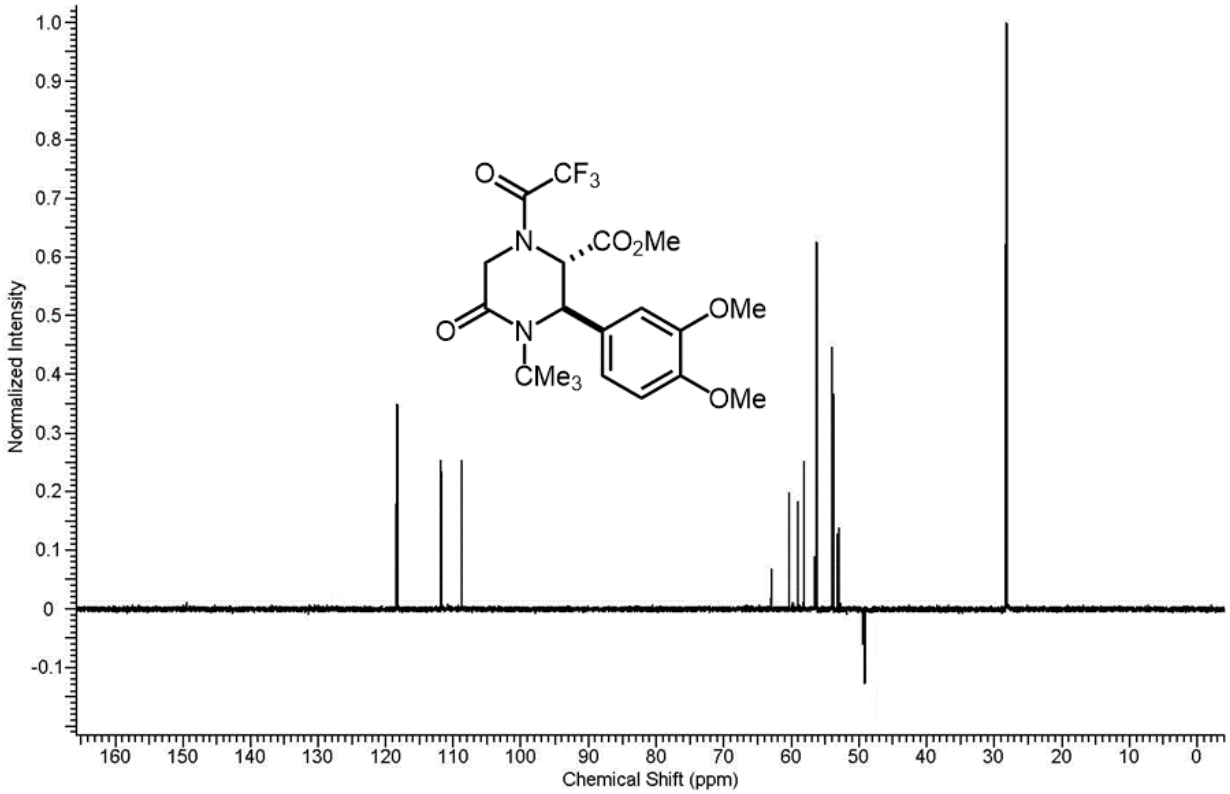

Spectra 1-59 DEPT-135 NMR spectrum of **10l.**

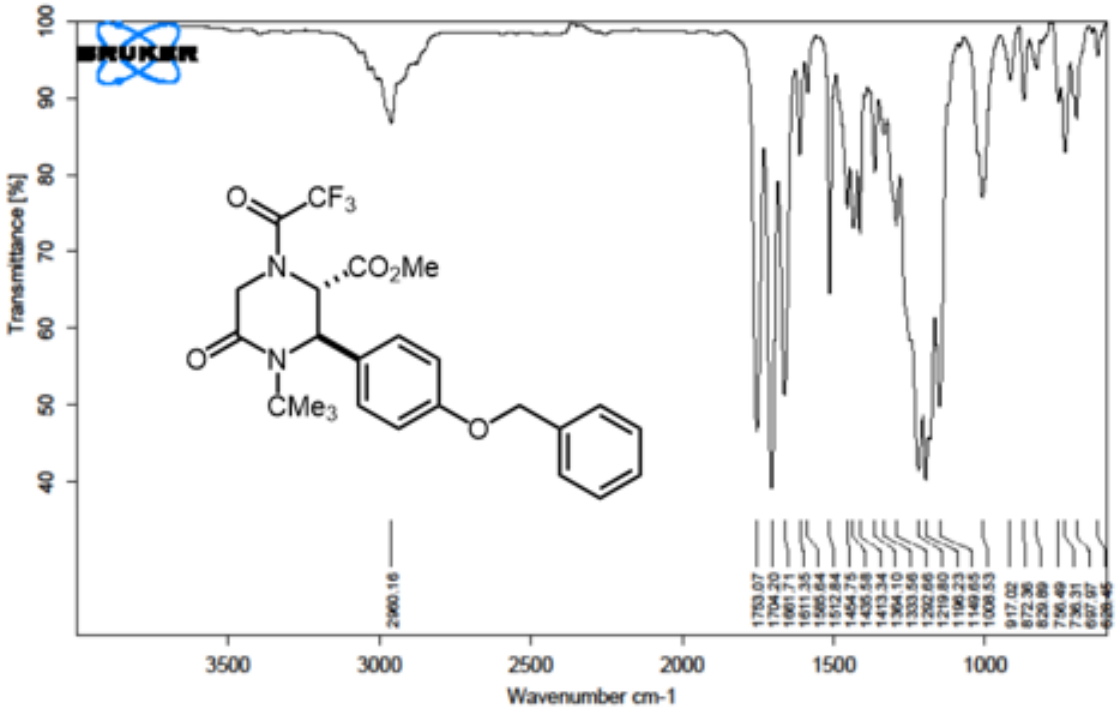

Spectra 1-60 IR spectrum of **10m.**

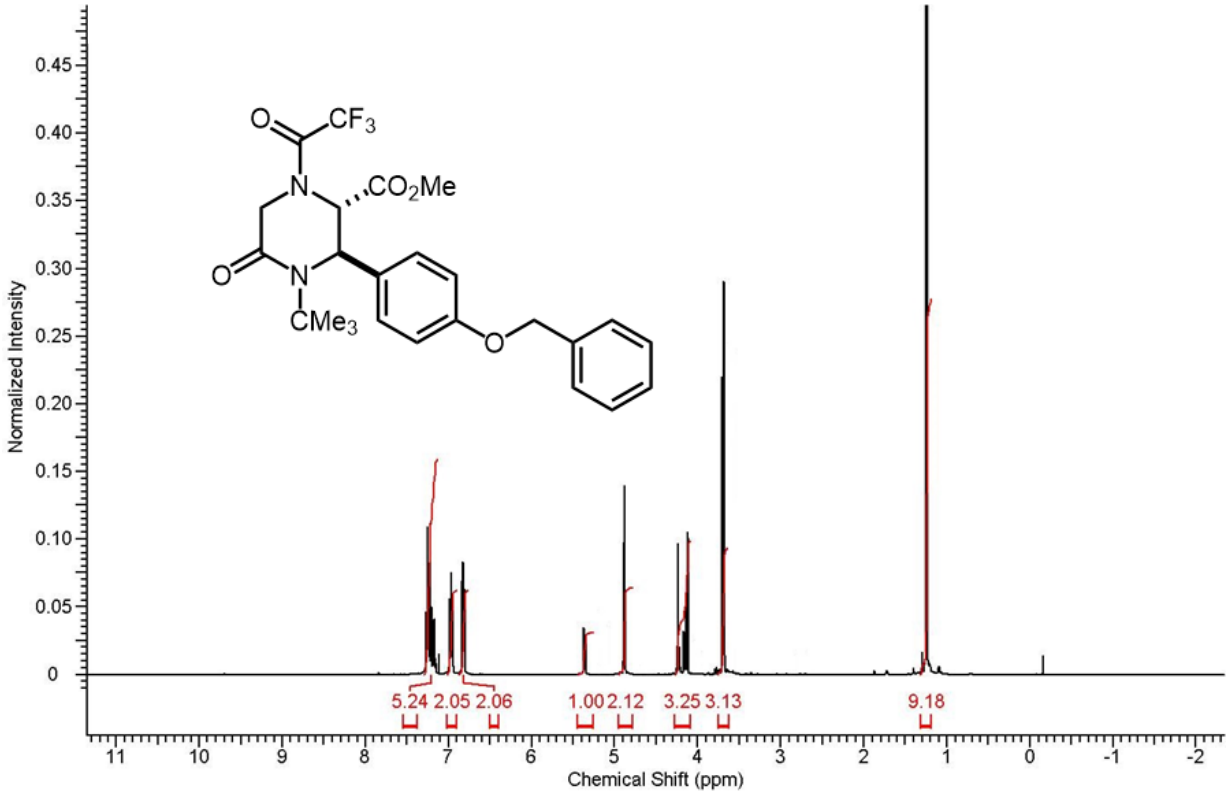

Spectra 1-61 Proton NMR spectrum of **10m.**

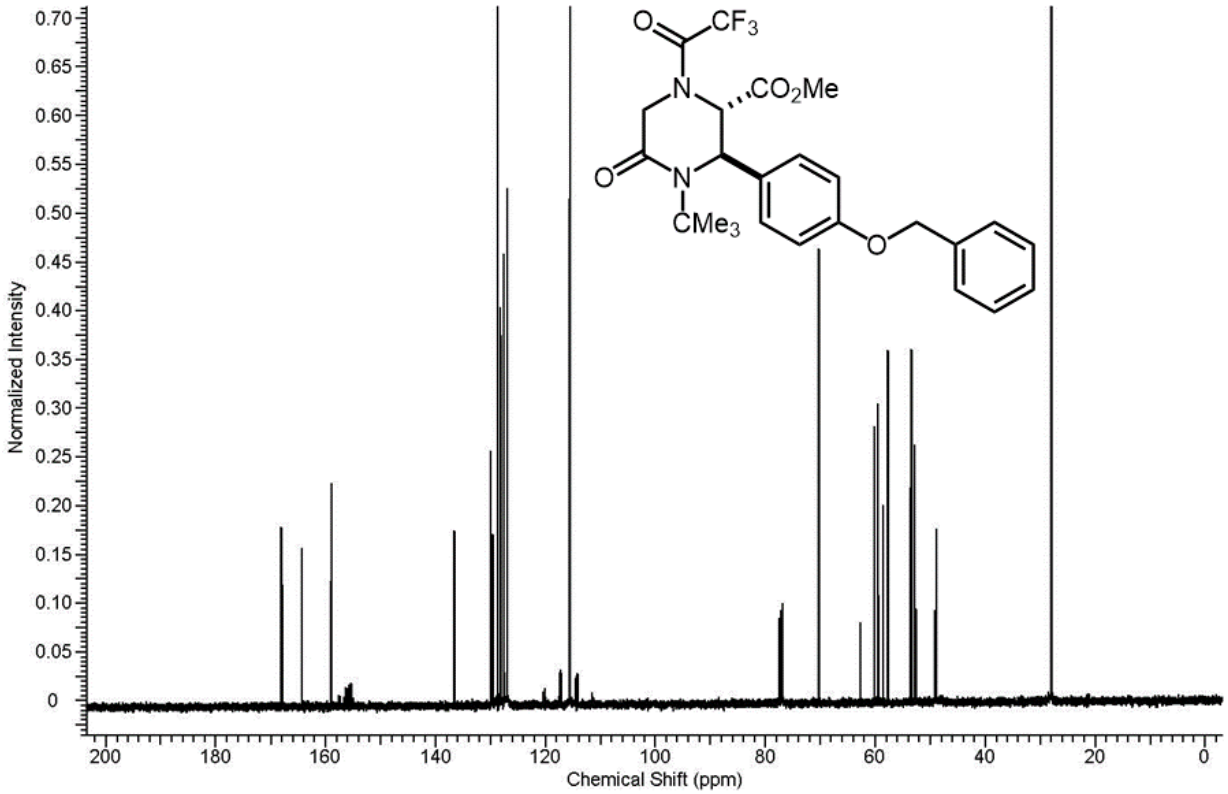

Spectra 1-62 Carbon NMR spectrum of **10m.**

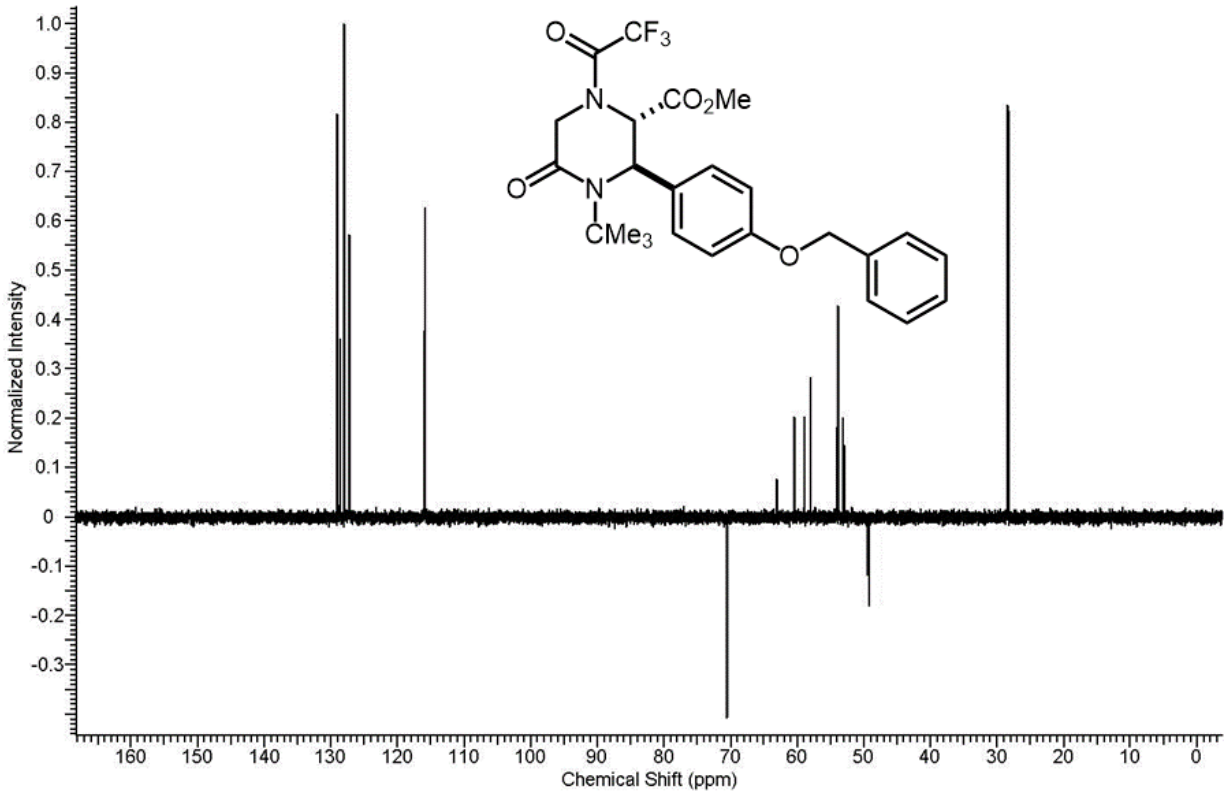

Spectra 1-63 DEPT-135 NMR spectrum of **10m.**

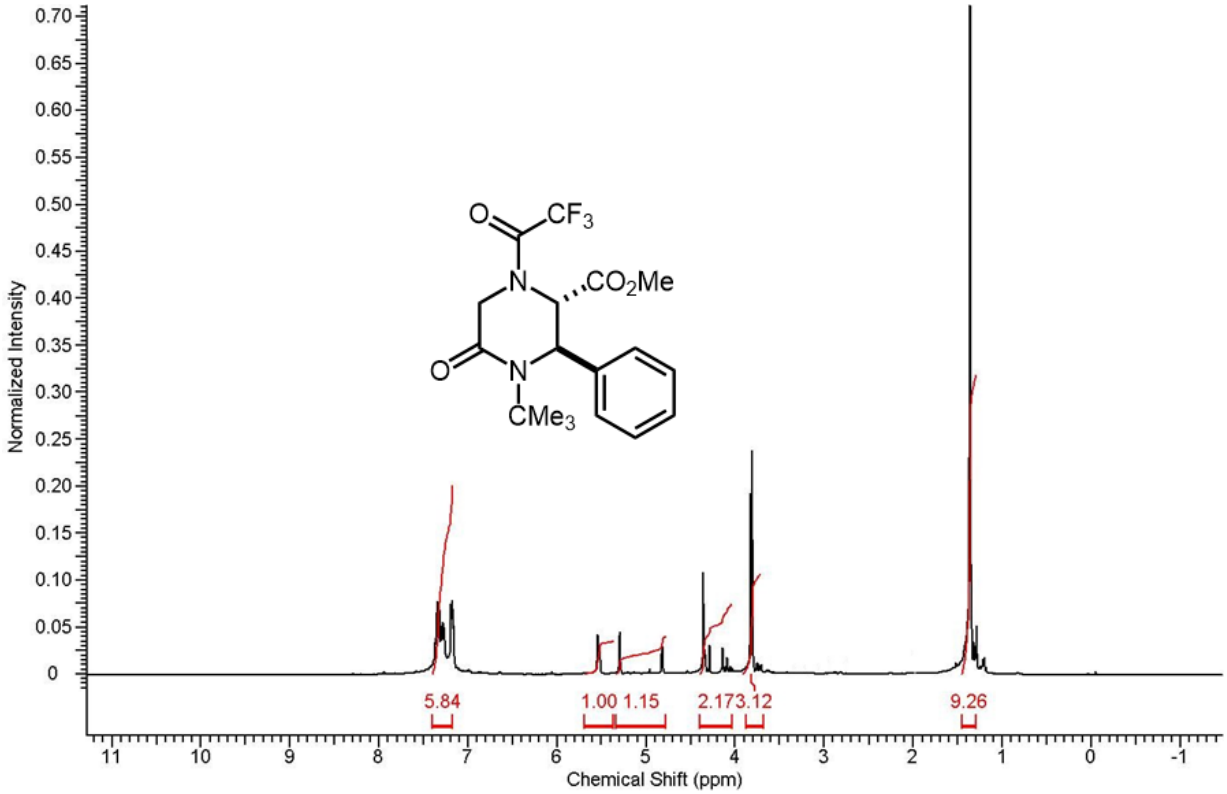

Spectra 1-64 Proton NMR spectrum of **10n.**

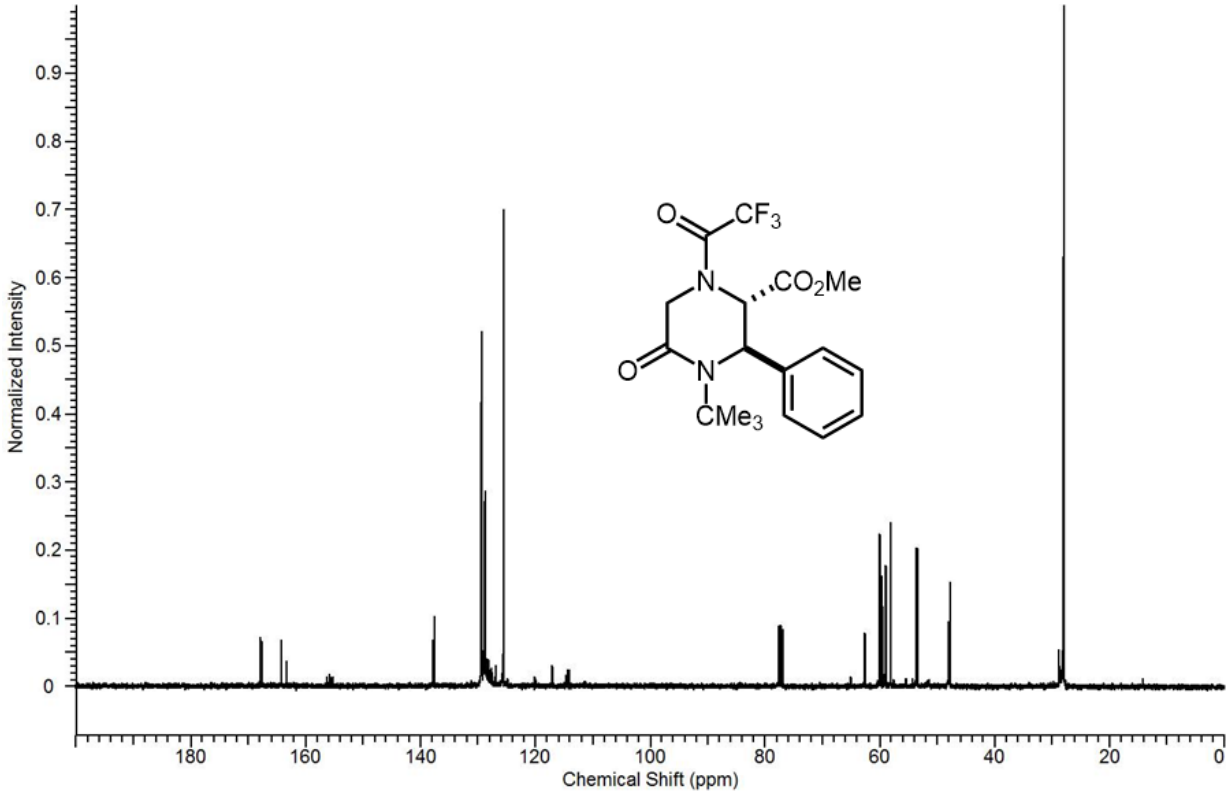

Spectra 1-65 Carbon NMR spectrum of **10n.**

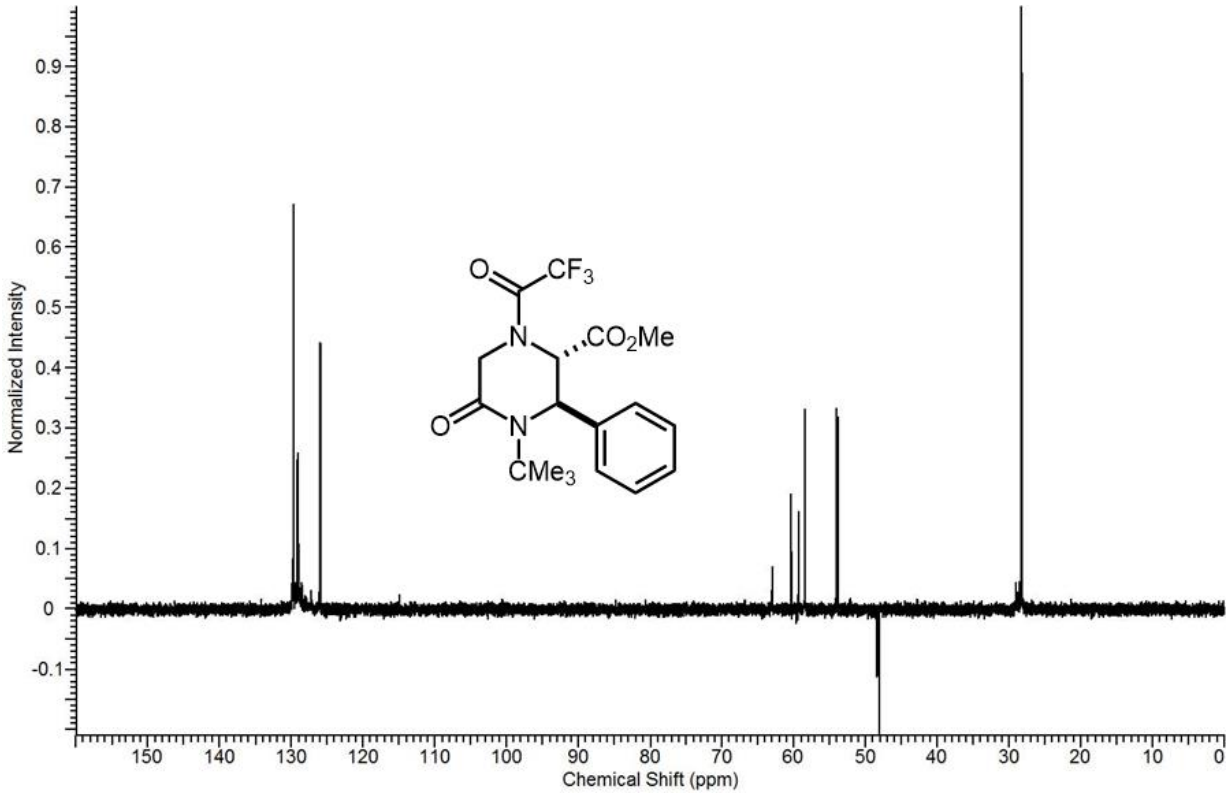

Spectra 1-66 DEPT-135 NMR spectrum of **10n.**

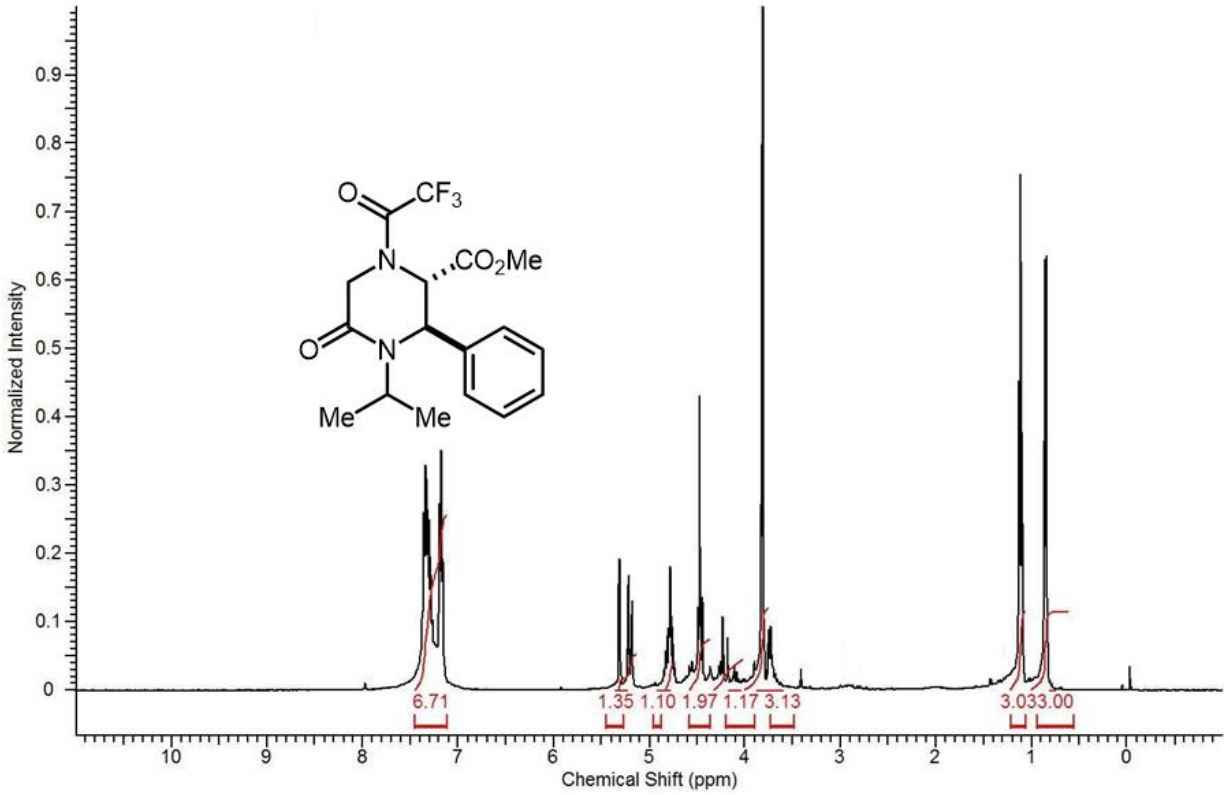

Spectra 1-67 Proton NMR spectrum of **10o.**

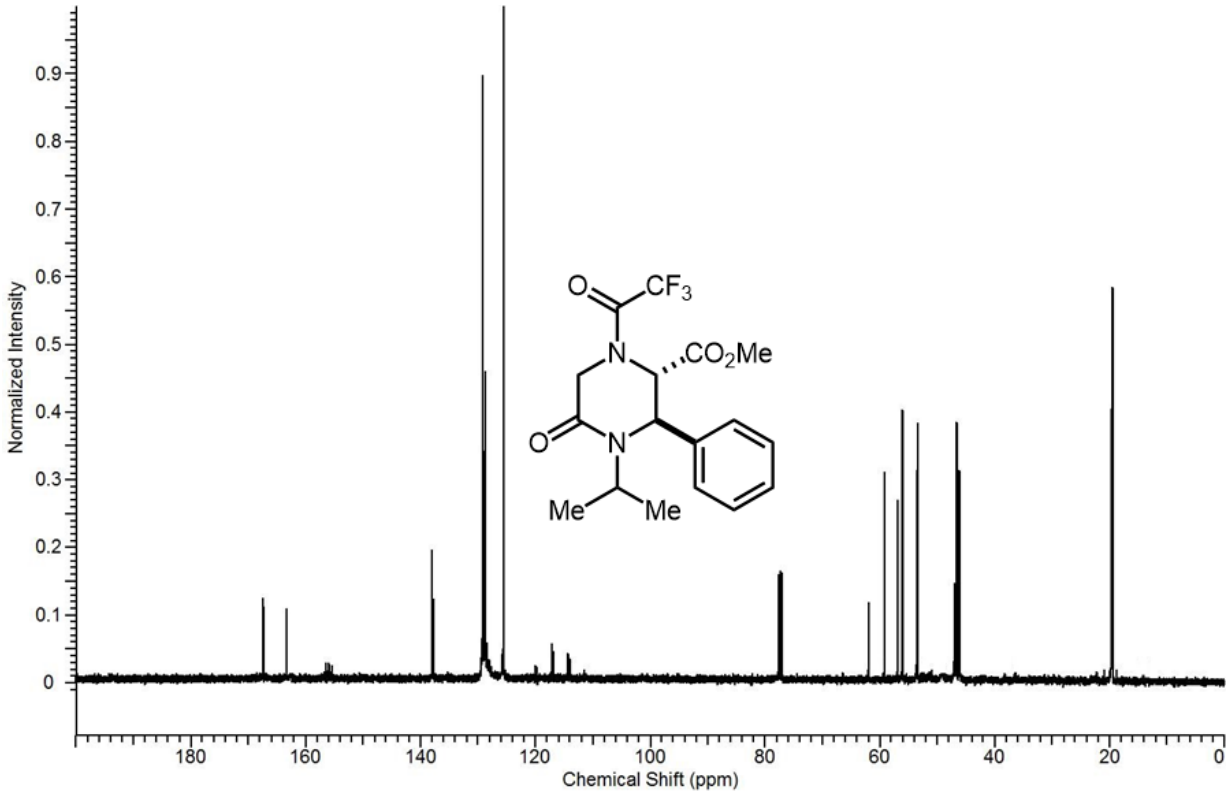

Spectra 1-68 Carbon NMR spectrum of **10o.**

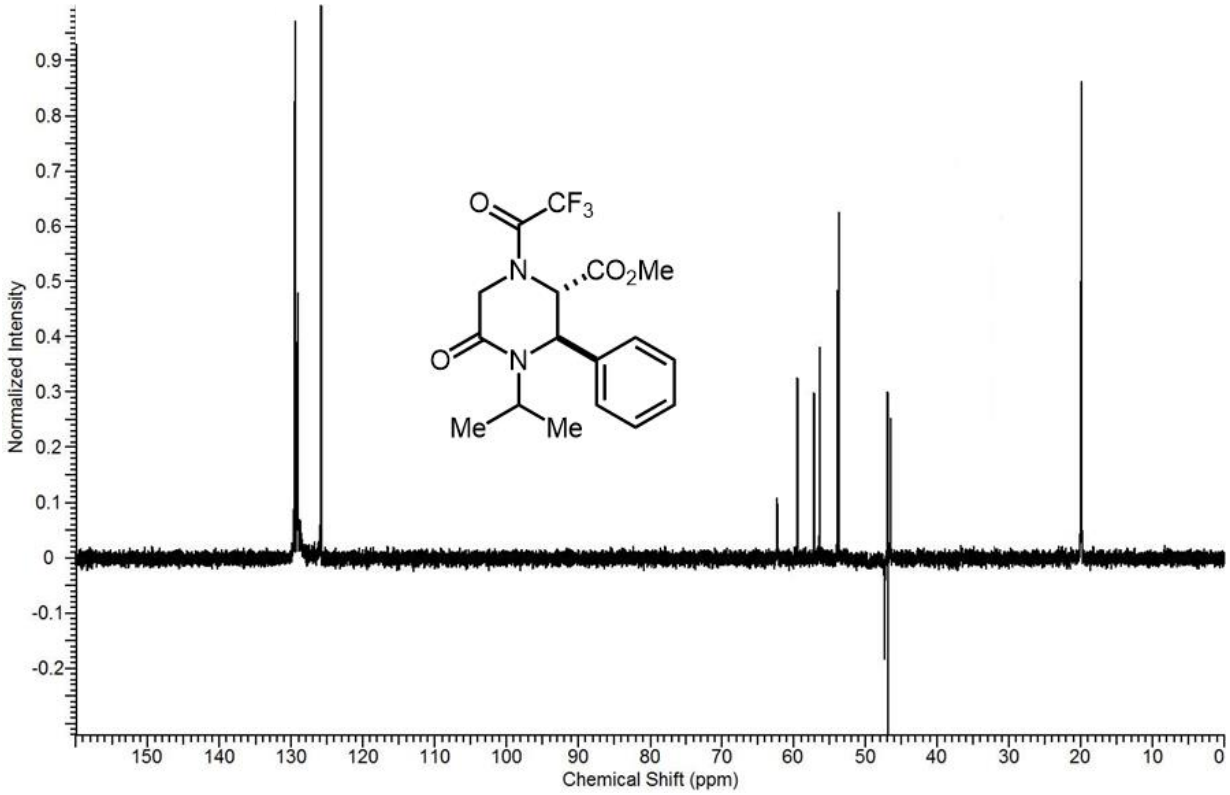

Spectra 1-69 DEPT-135 NMR spectrum of **10o.**

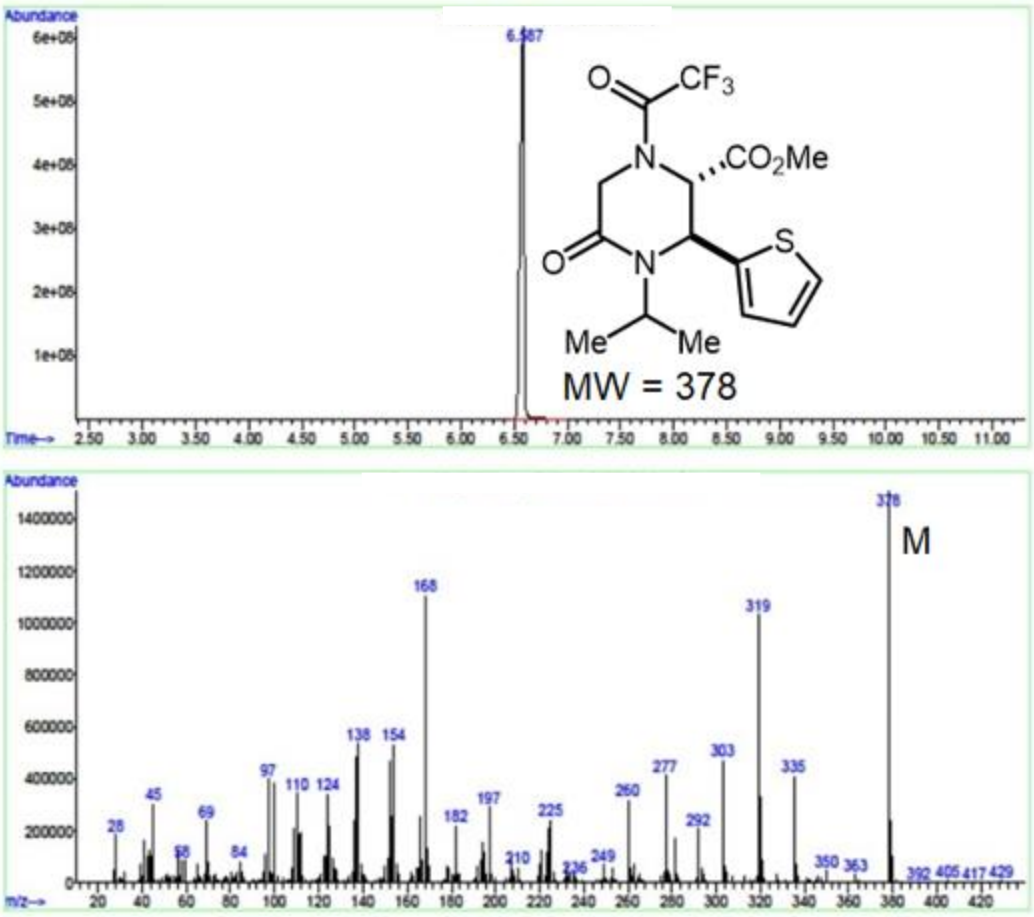

Spectra 1-70 GC-MS spectrum of **10p.**

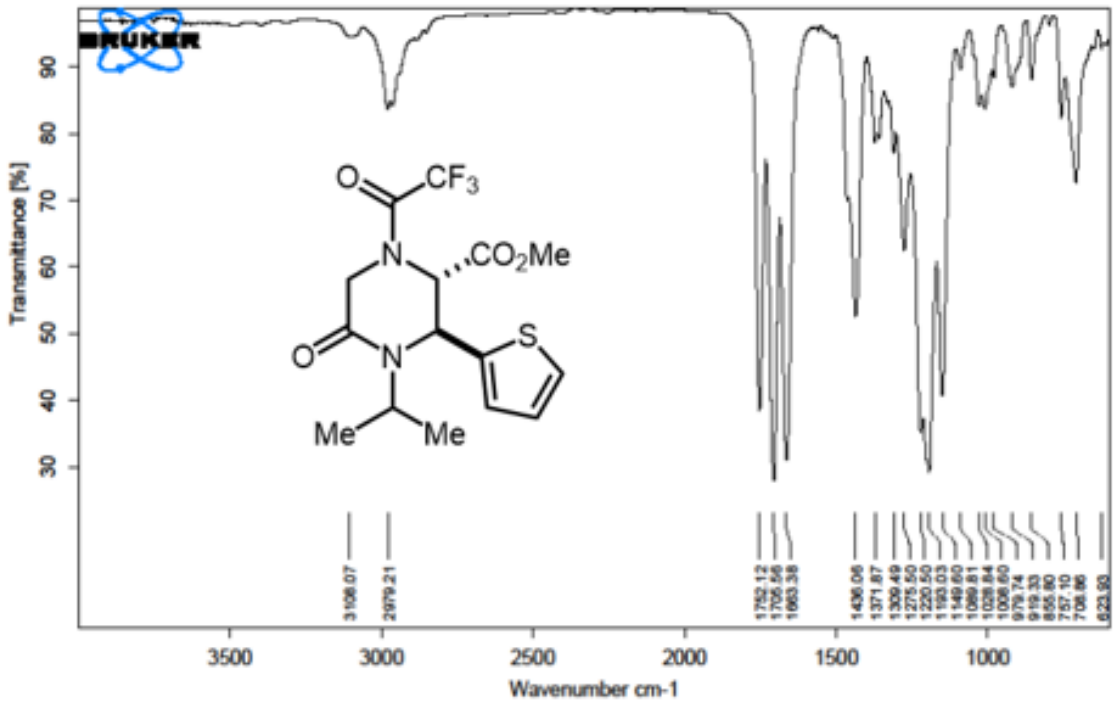

Spectra 1-71 IR spectrum of **10p.**

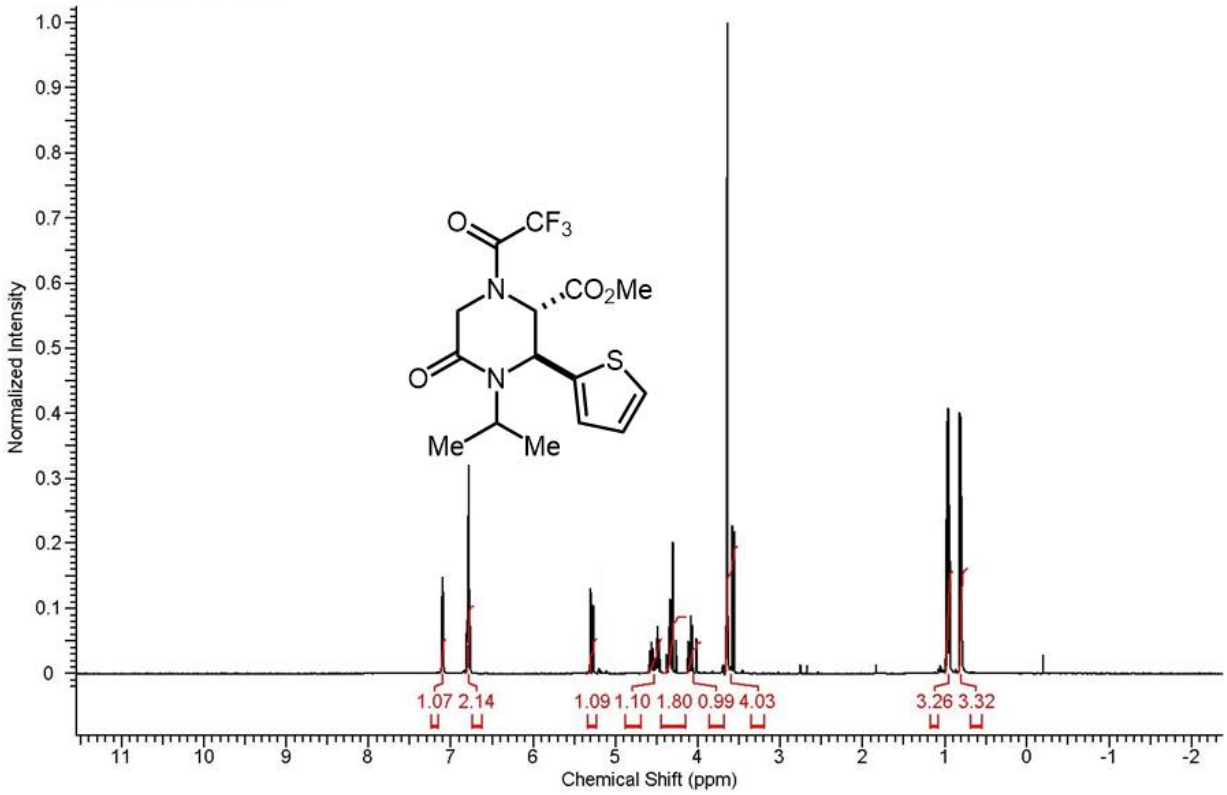

Spectra 1-72 Proton NMR spectrum of **10p.**

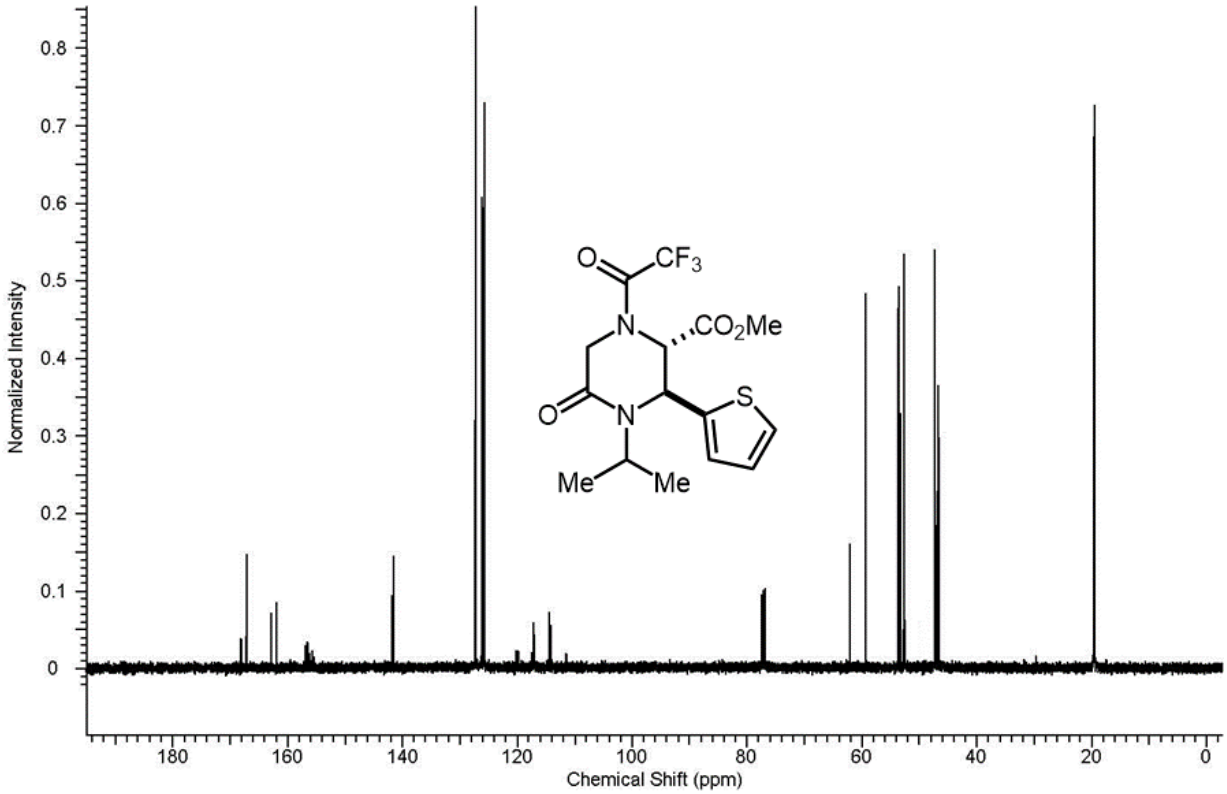

Spectra 1-73 Carbon NMR spectrum of **10p.**

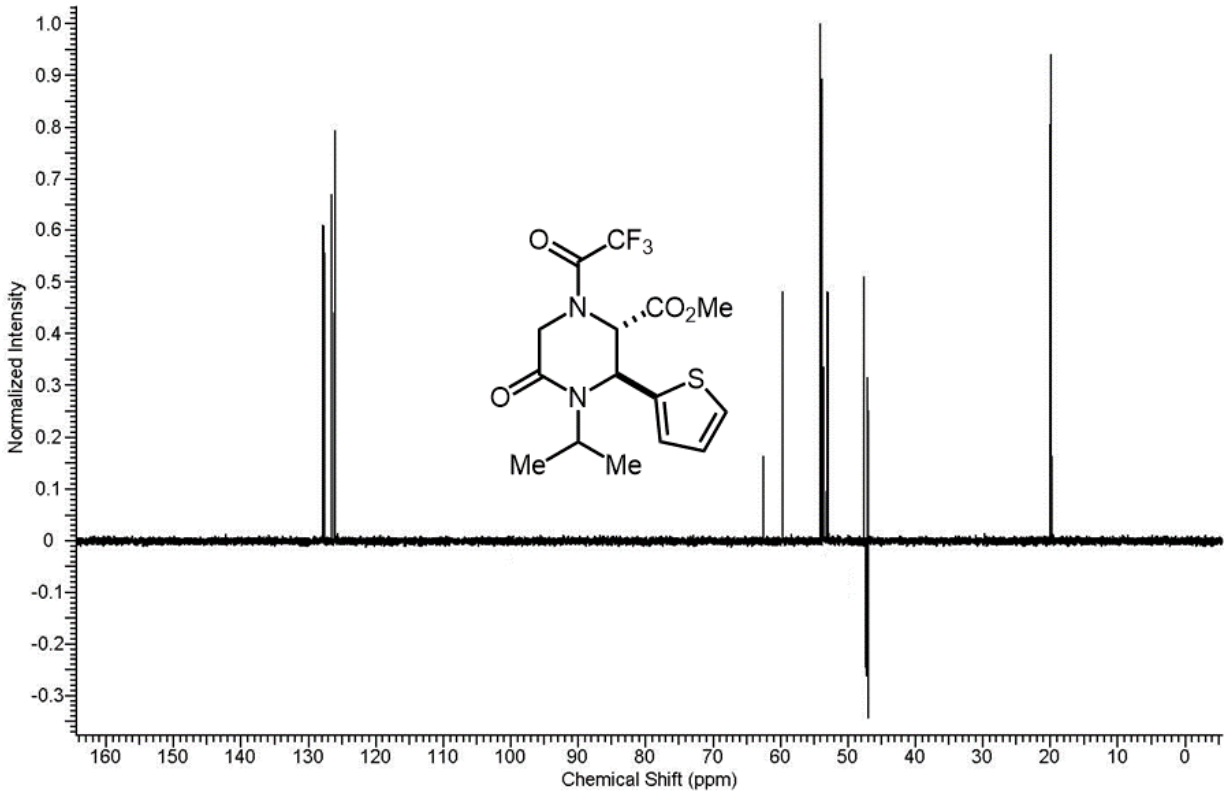

Spectra 1-74 DEPT-135 NMR spectrum of **10p.**

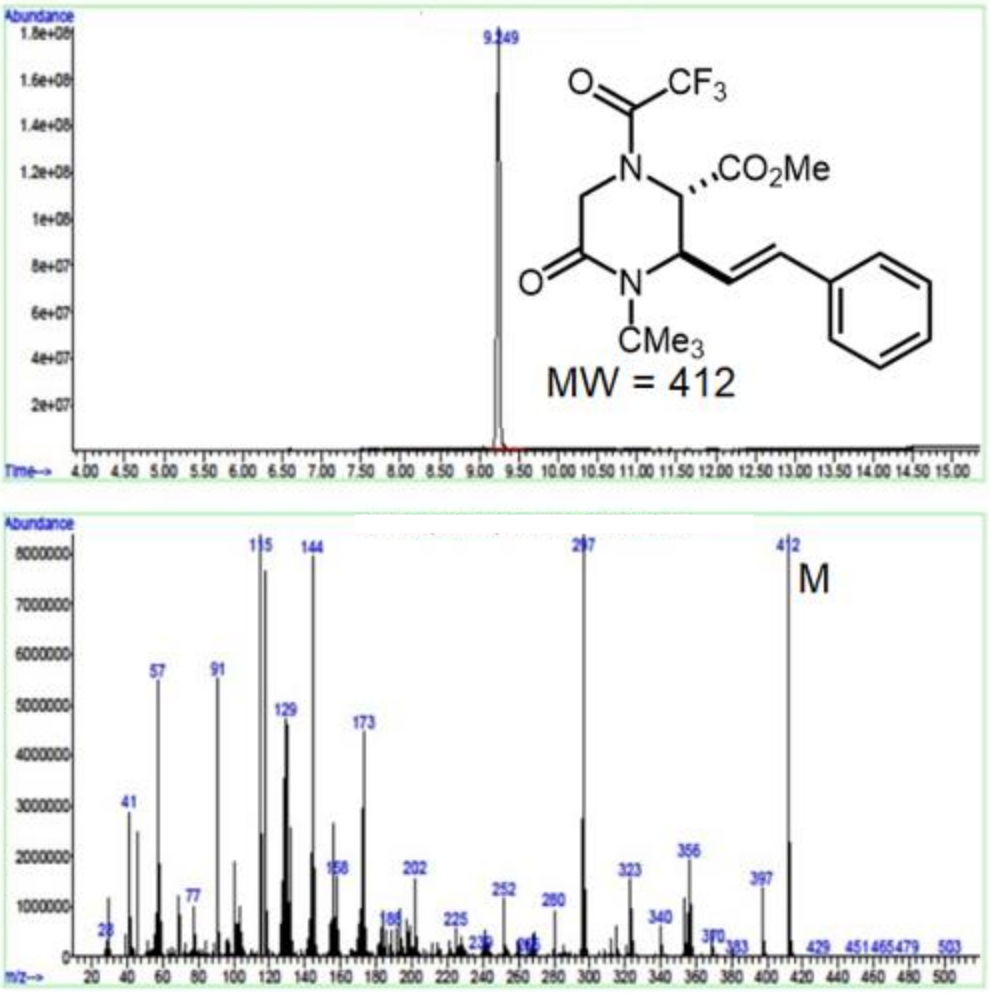

Spectra 1-75 GC-MS spectrum of **11a.**

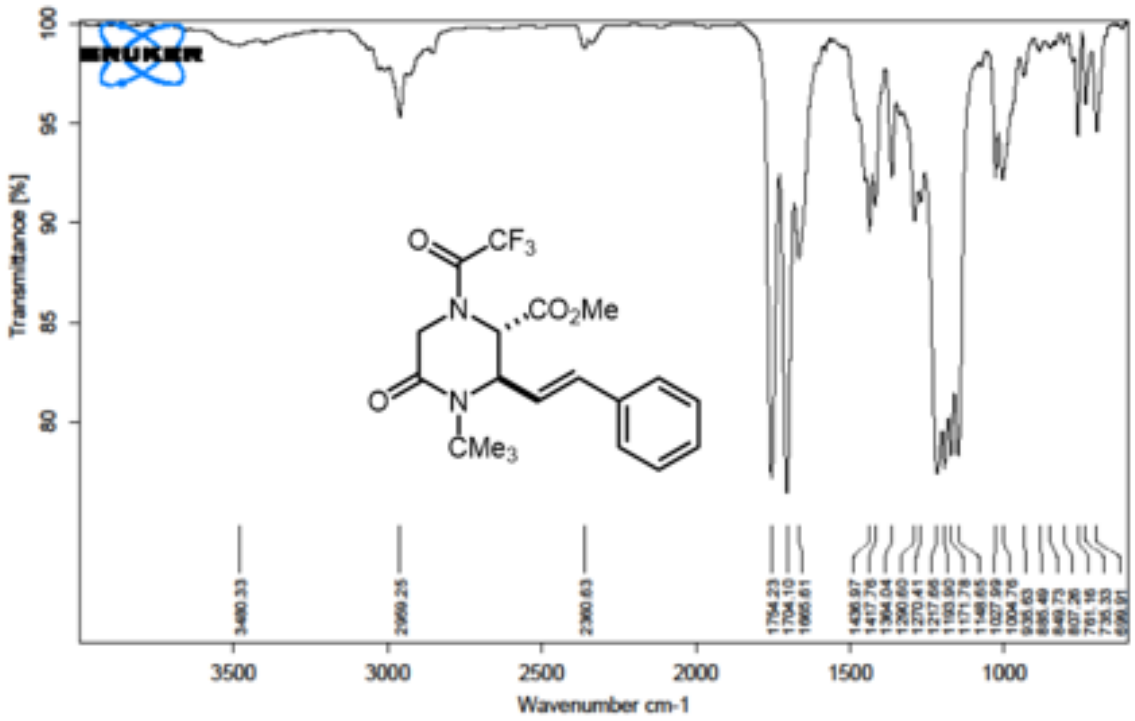

Spectra 1-76 IR spectrum of **11a.**

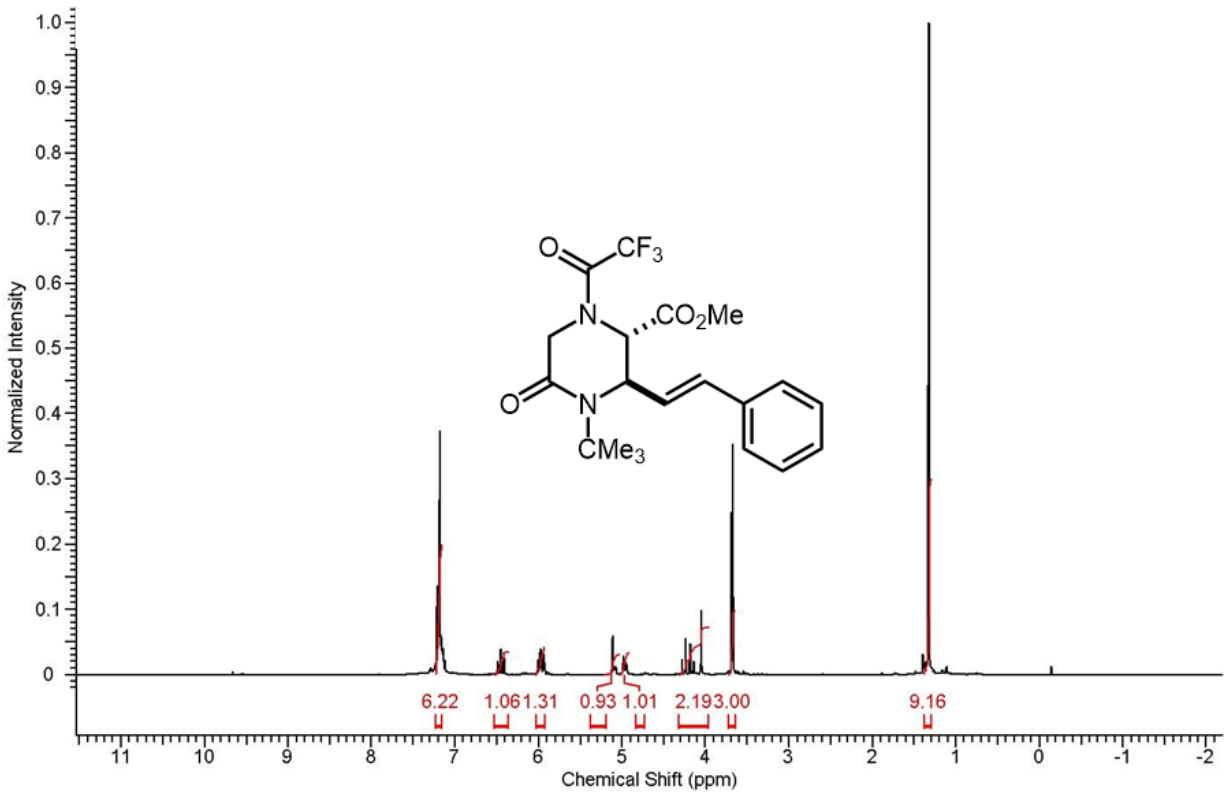

Spectra 1-77 Proton NMR spectrum of **11a.**

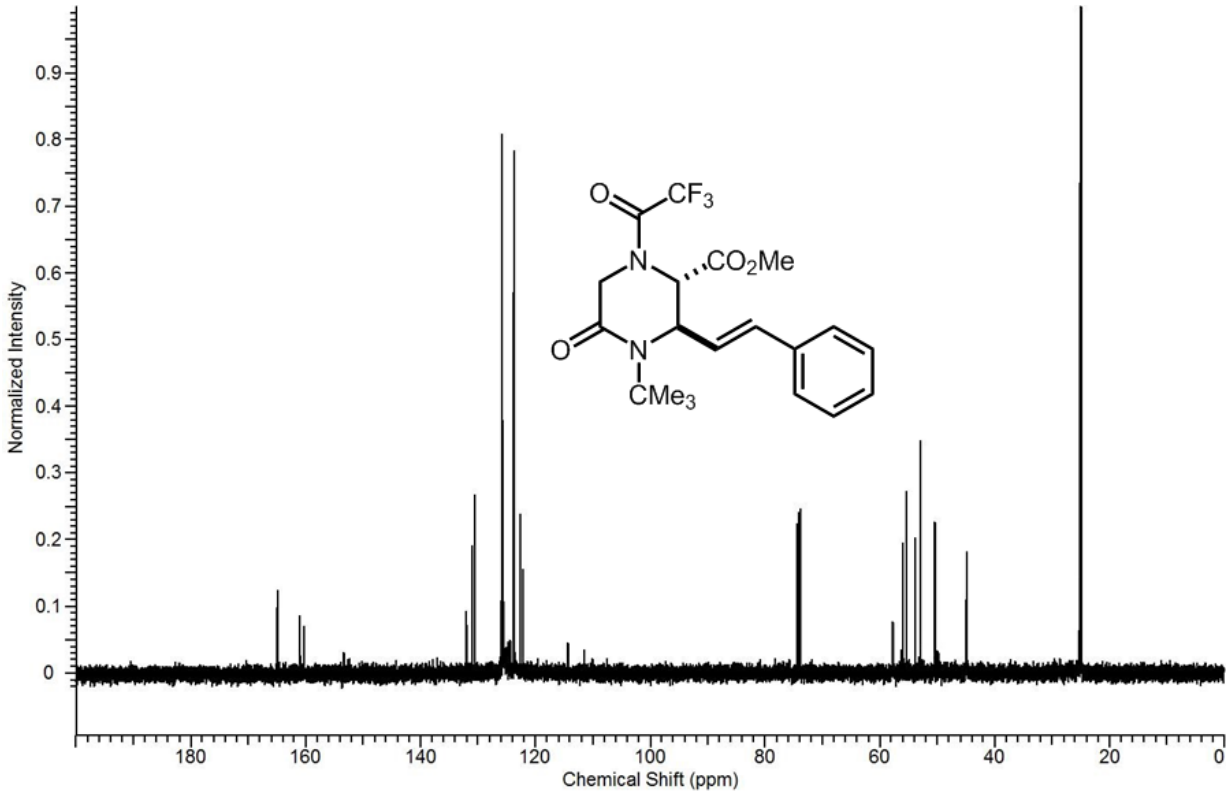

Spectra 1-78 Carbon NMR spectrum of **11a.**

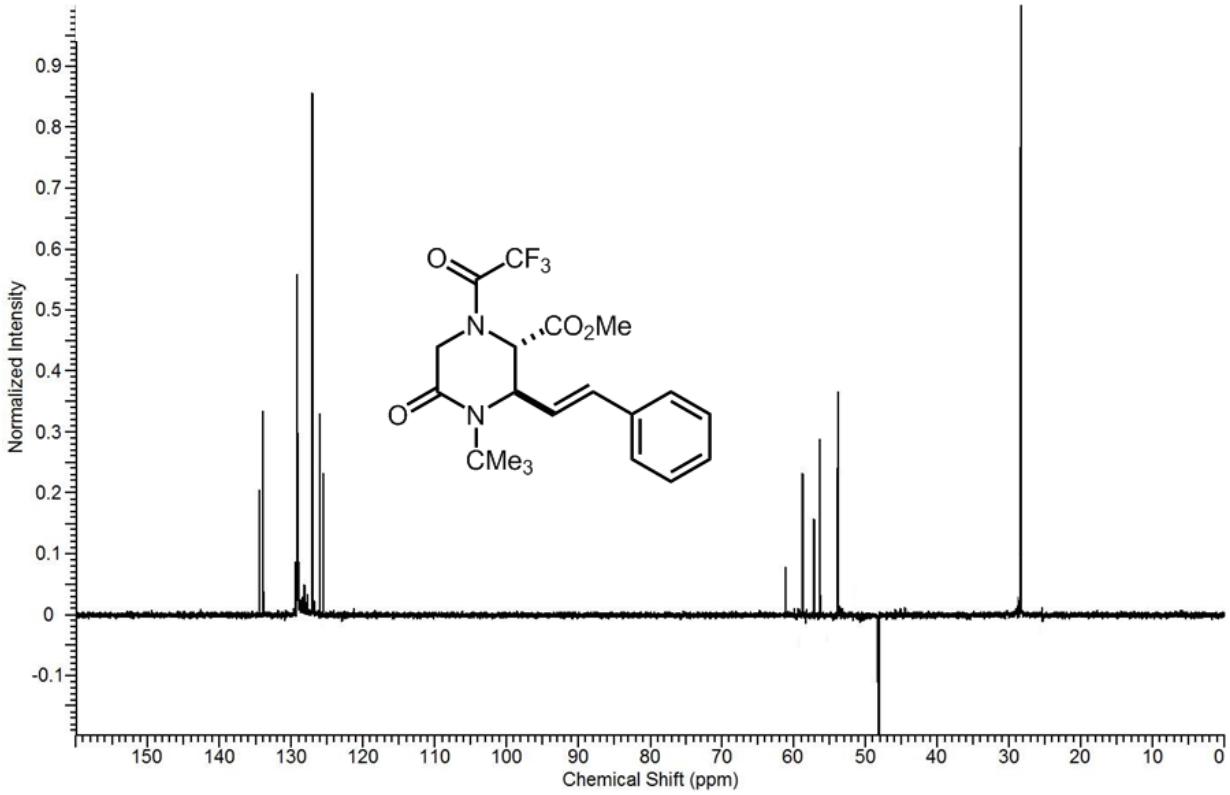

Spectra 1-79 DEPT-135 NMR spectrum of **11a.**

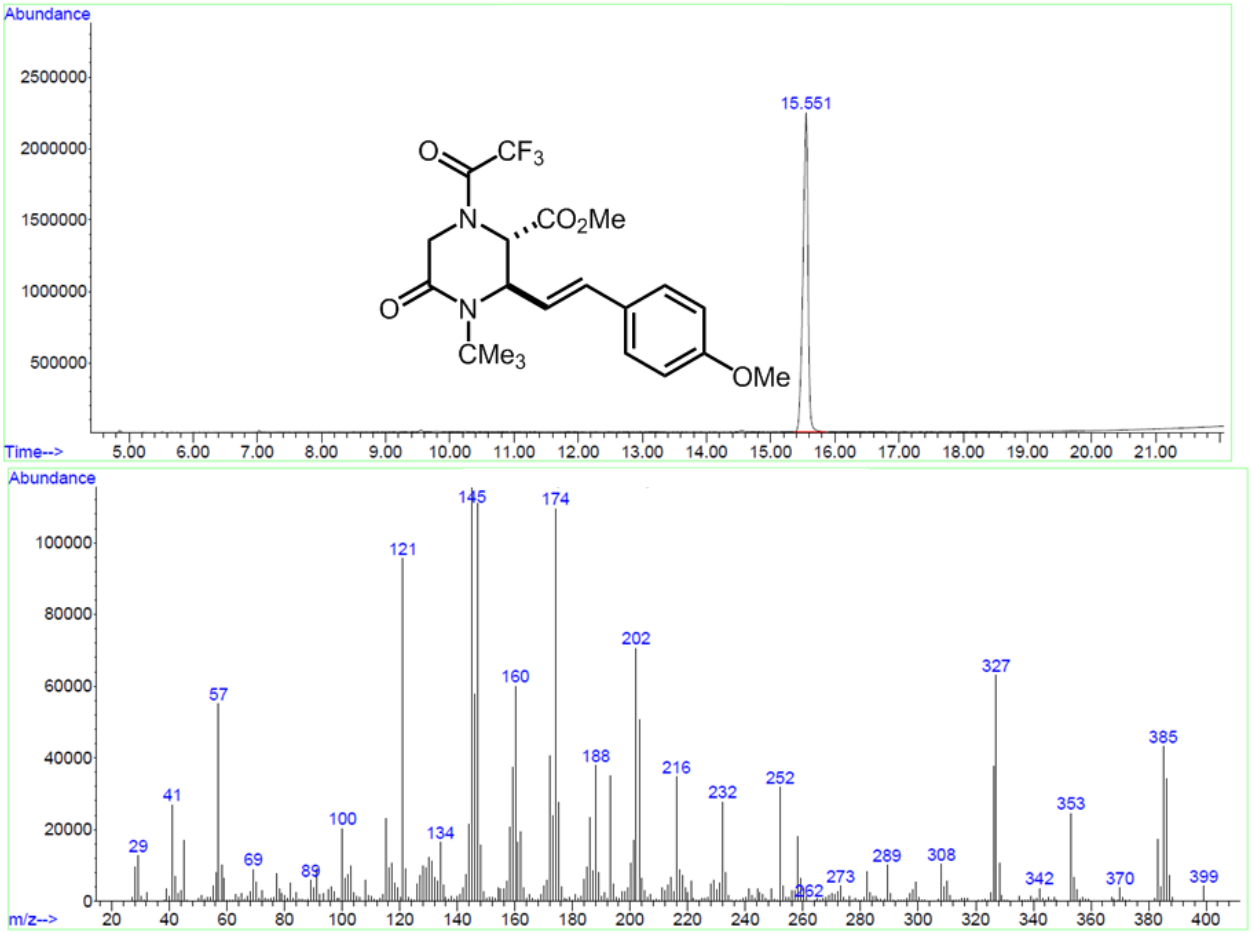

Spectra 1-80 GC-MS spectrum of **11b.**

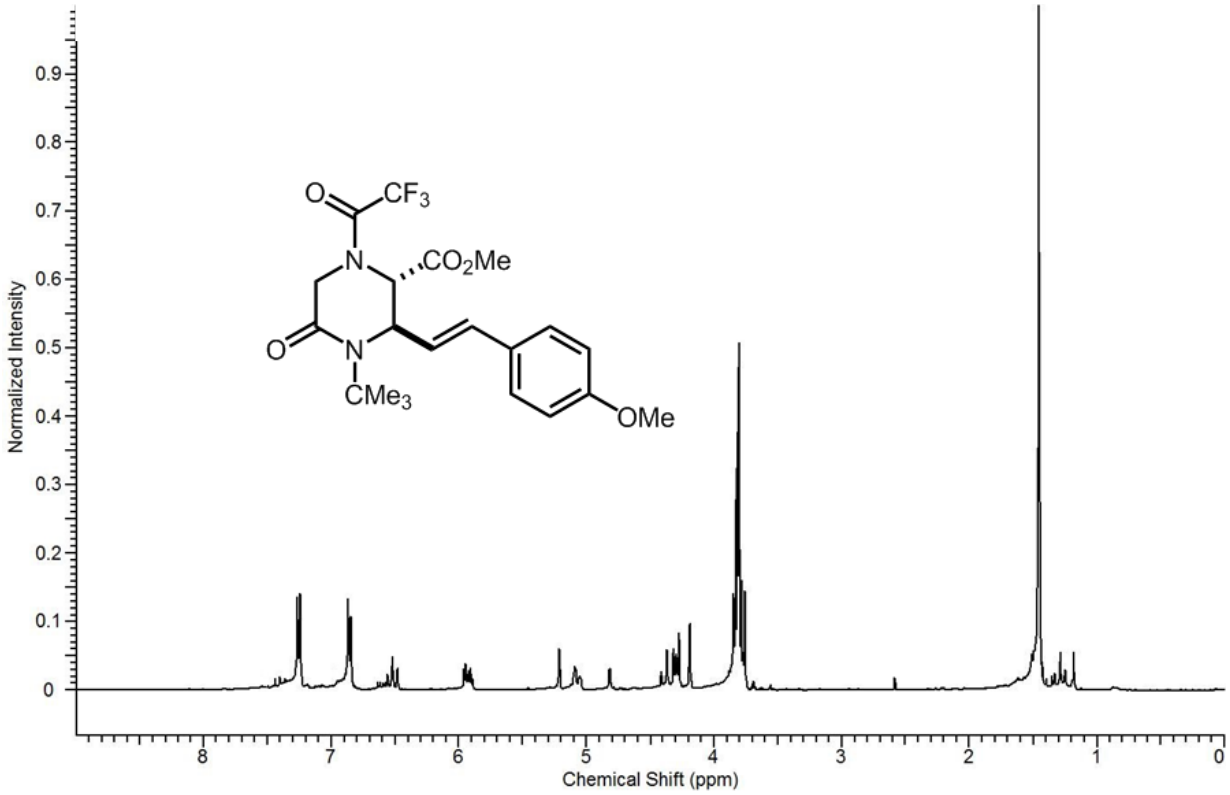

Spectra 1-81 Proton NMR spectrum of **11b.**

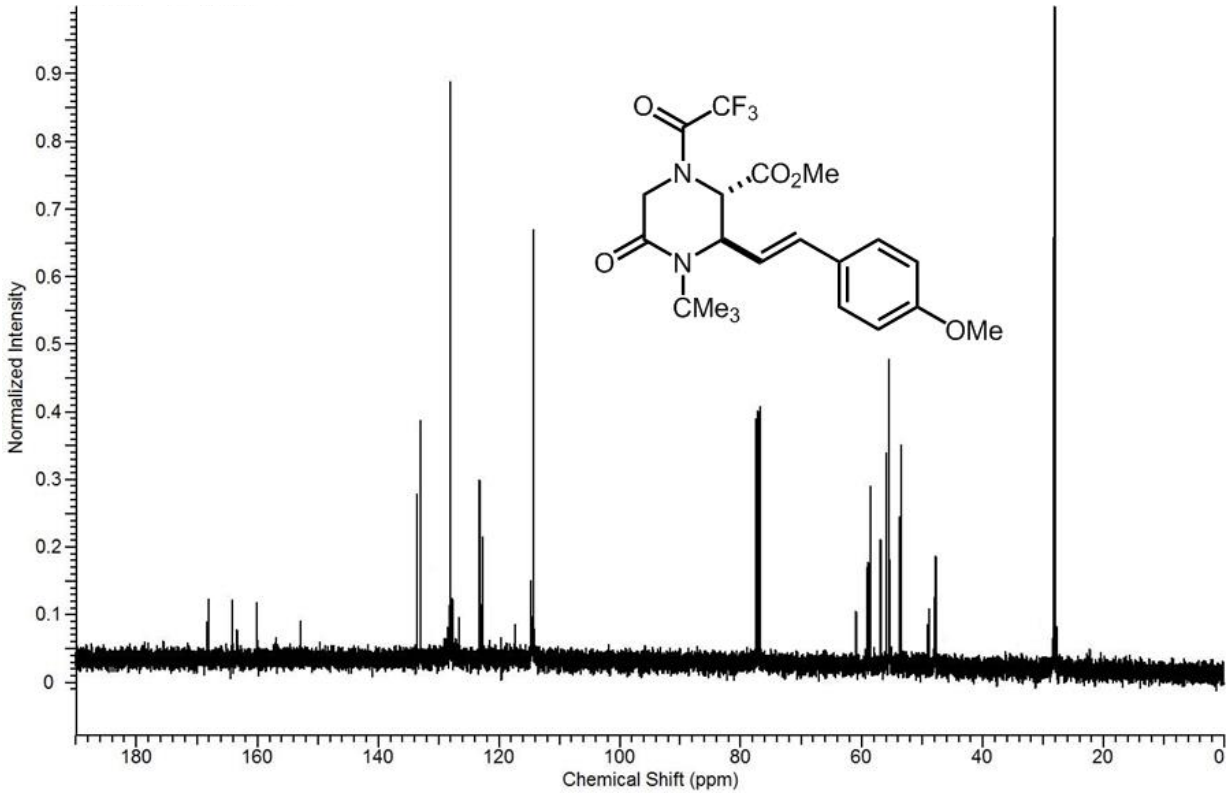

Spectra 1-82 Carbon NMR spectrum of **11b.**

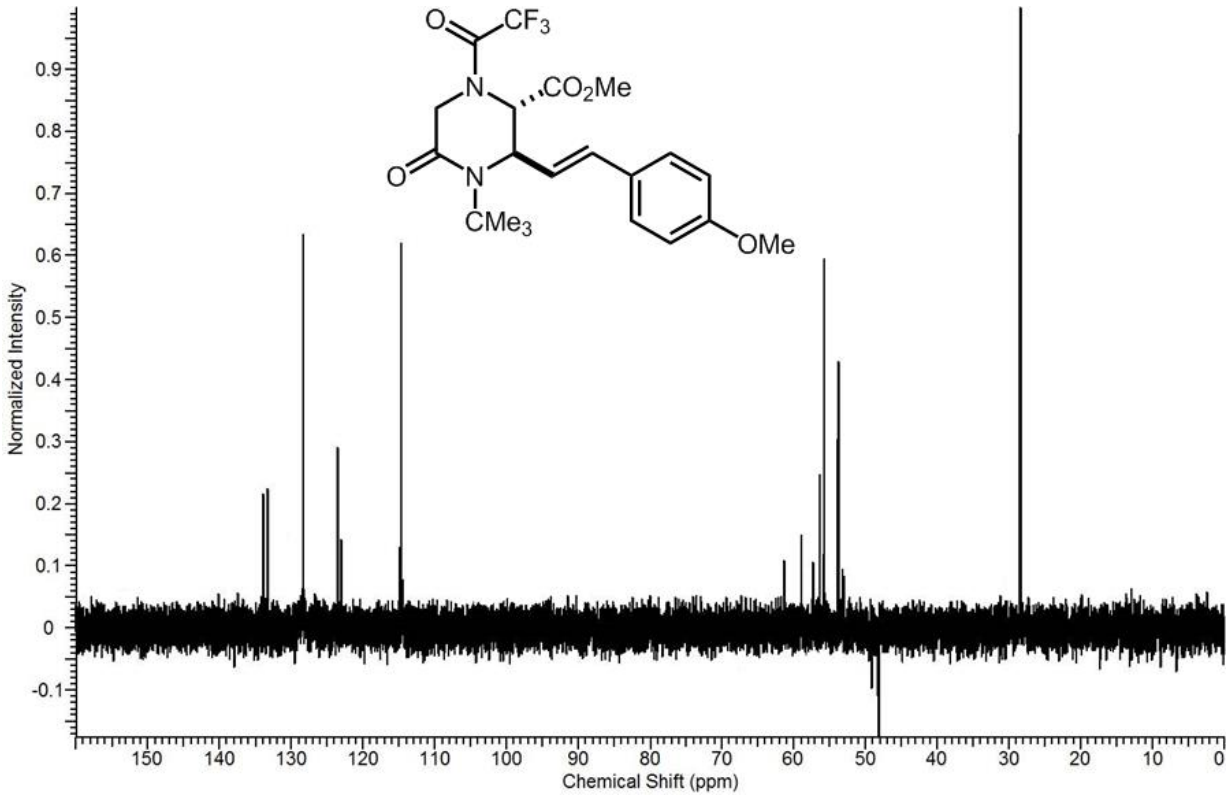

Spectra 1-83 DEPT-135 NMR spectrum of **11b.**

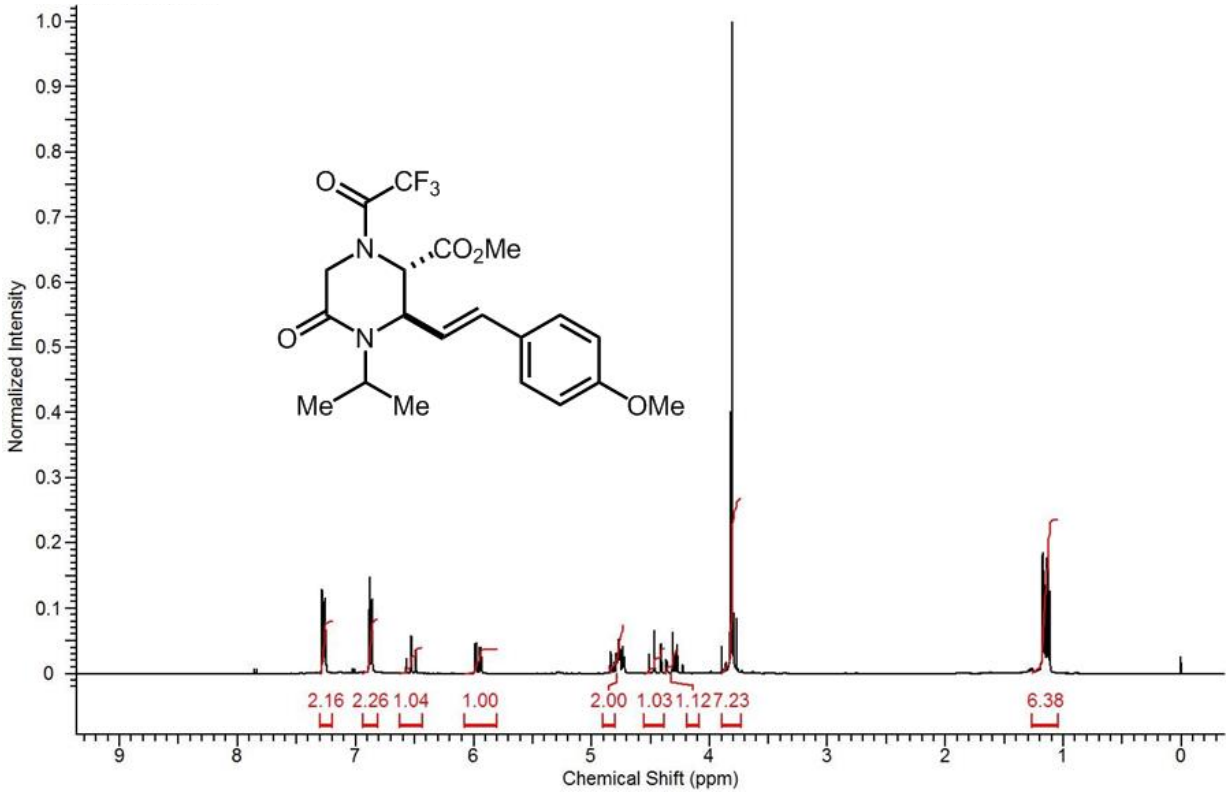

Spectra 1-84 Proton NMR spectrum of **11c.**

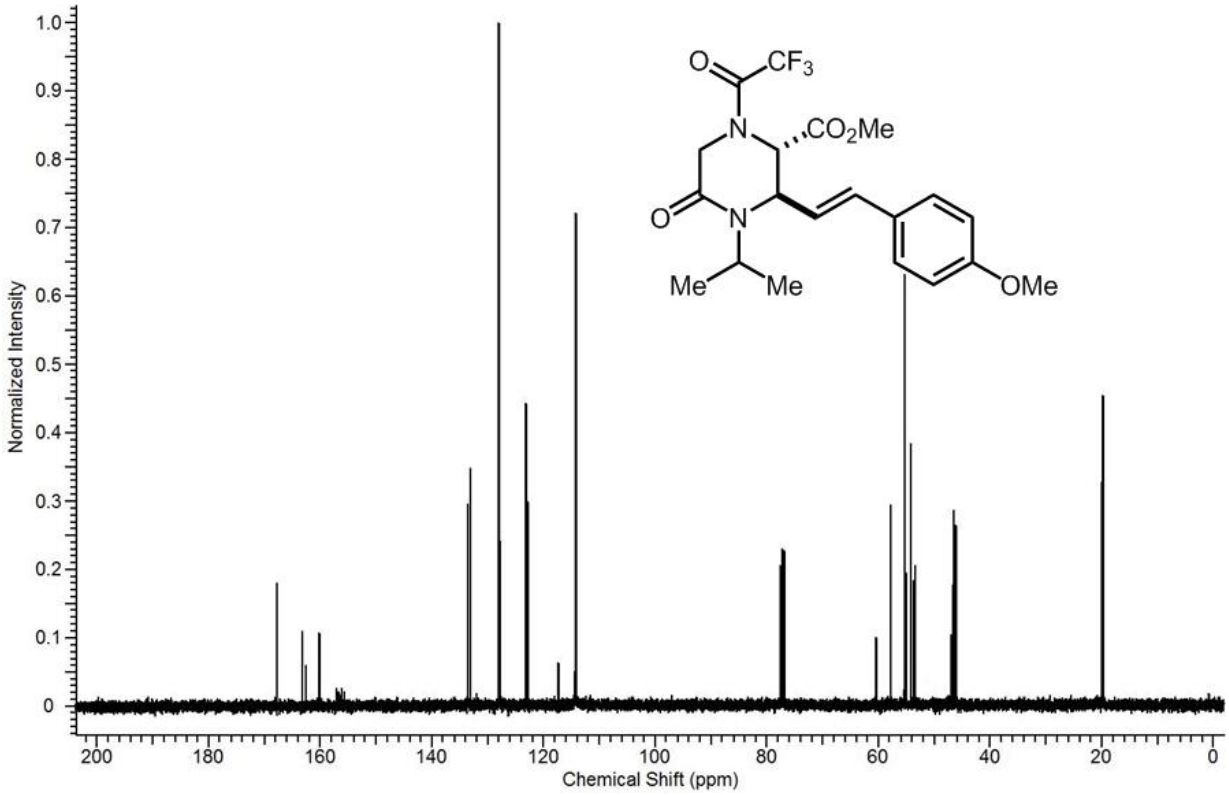

Spectra 1-85 Carbon NMR spectrum of **11c.**

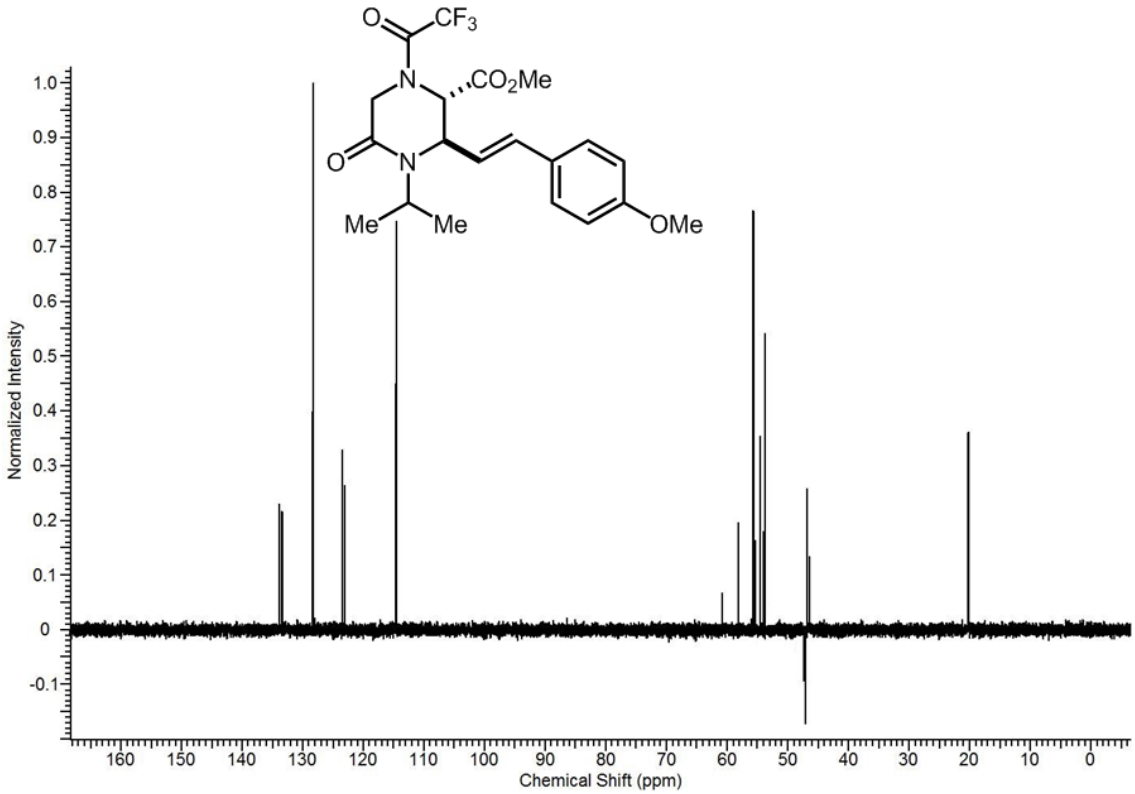

Spectra 1-86 DEPT-135 NMR spectrum of **11c.**

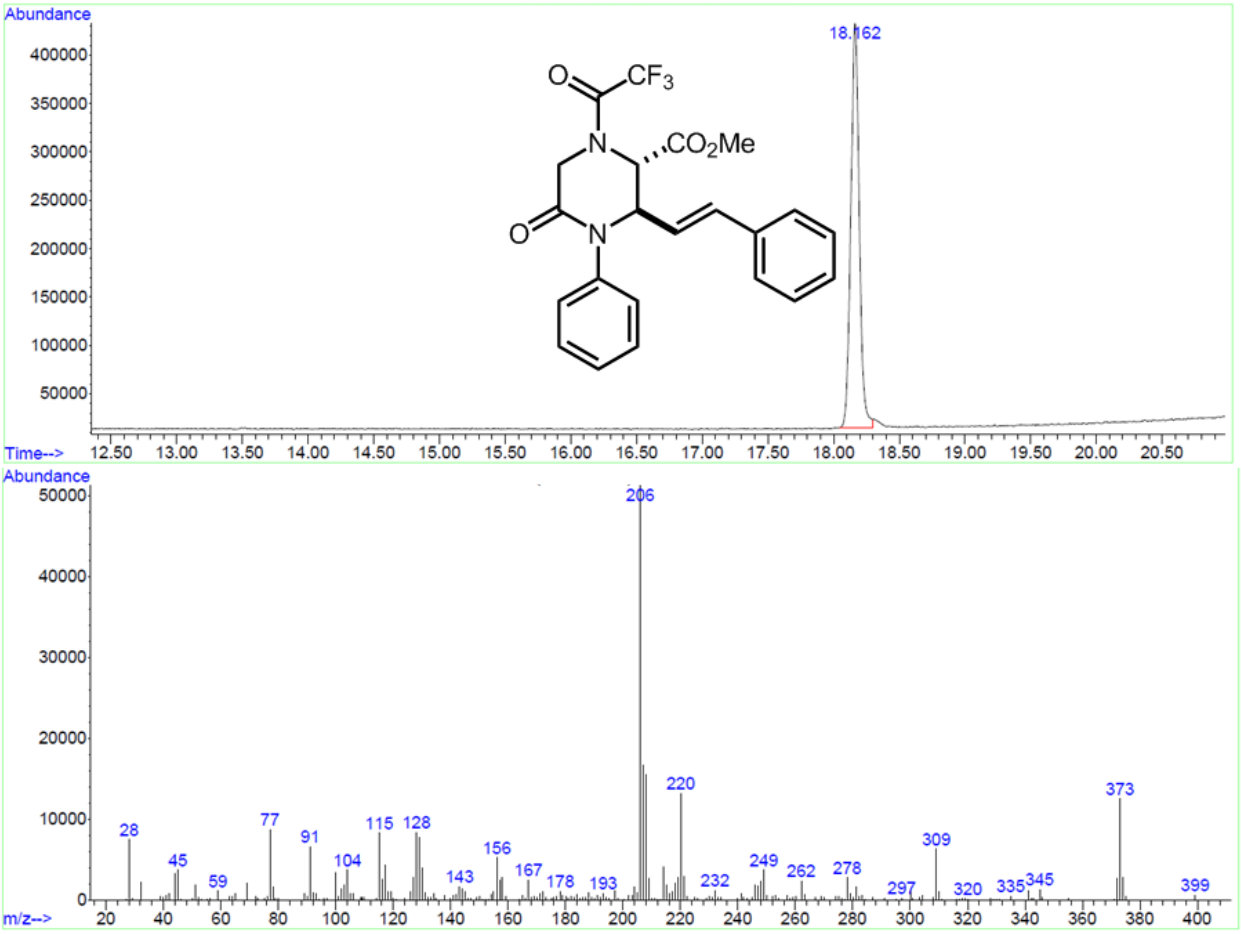

Spectra 1-87 GC-MS spectrum of **11d.**

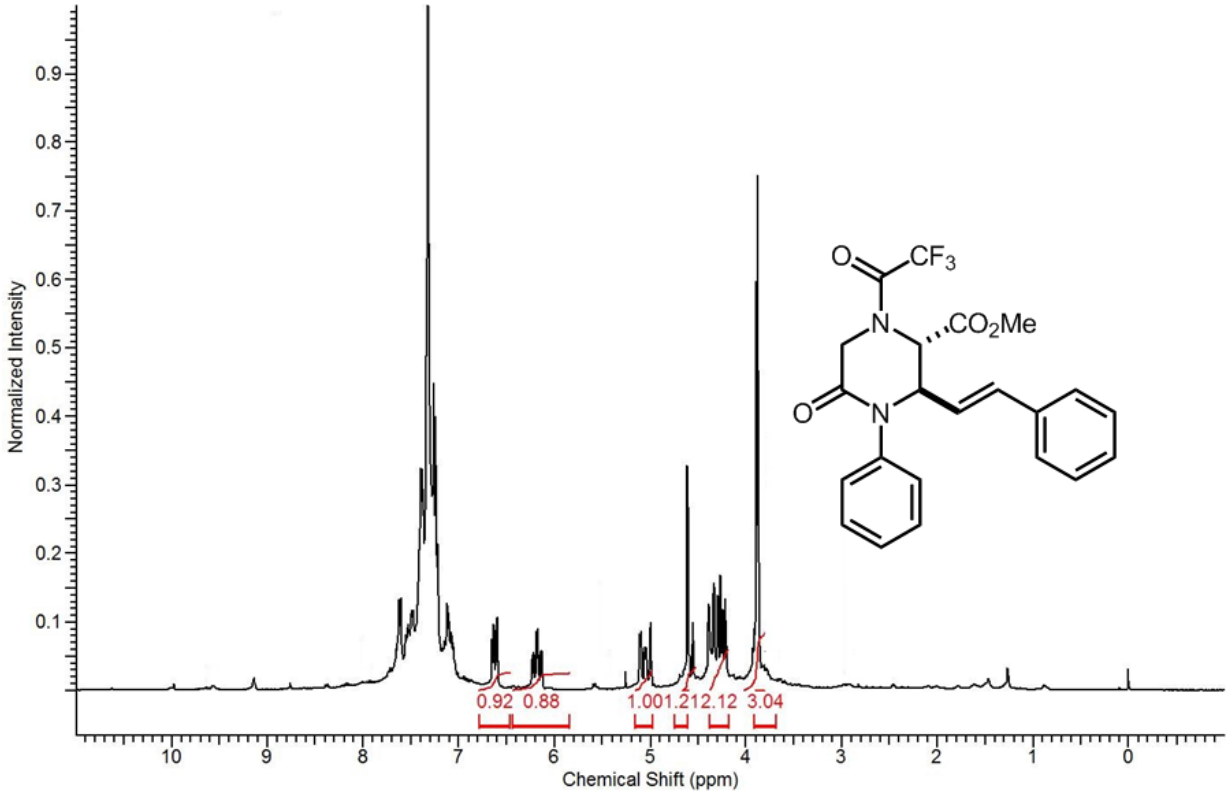

Spectra 1-88 Proton NMR spectrum of **11d.**

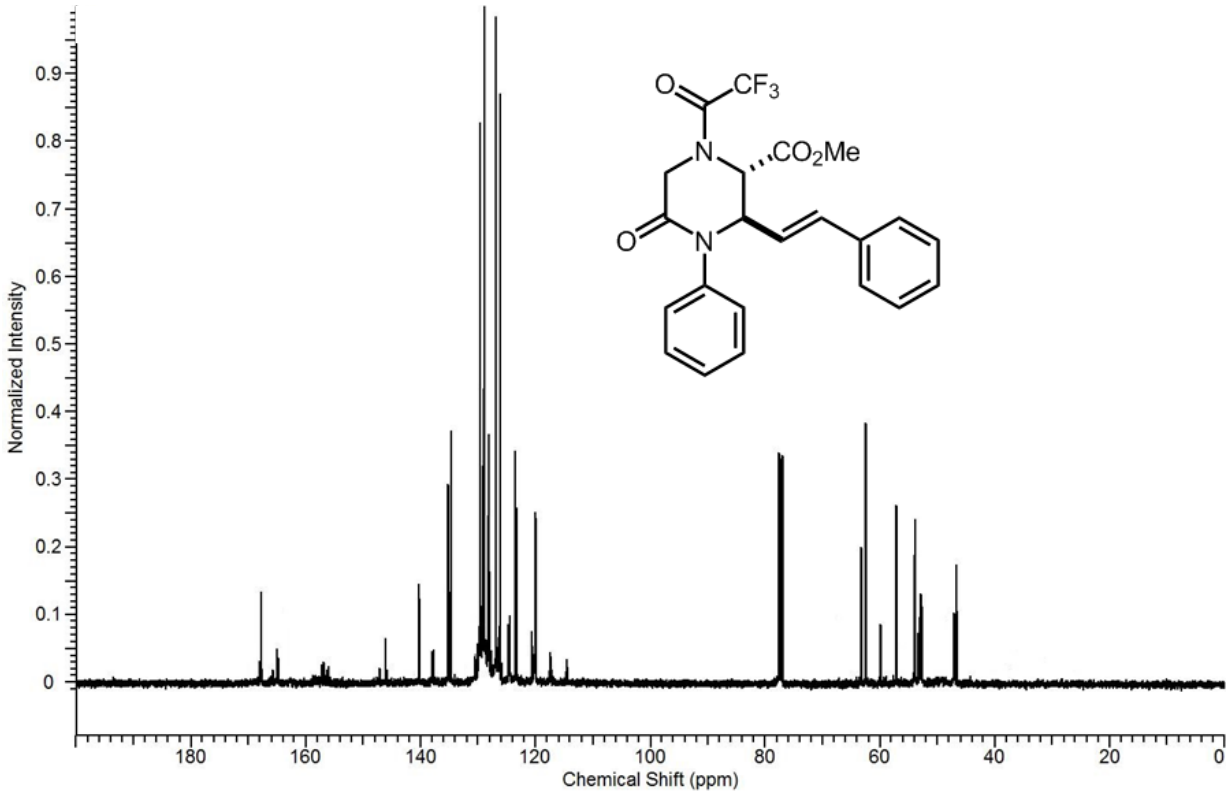

Spectra 1-89 Carbon NMR spectrum of **11d.**

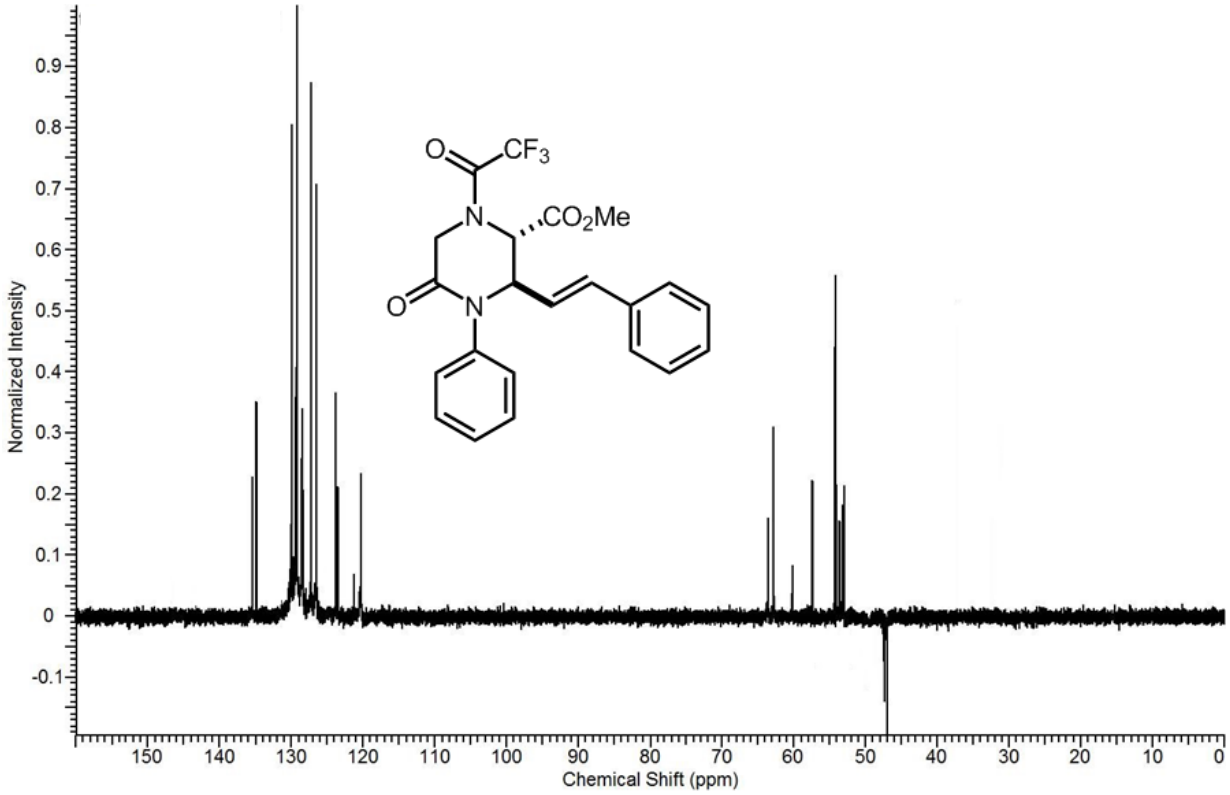

Spectra 1-90 DEPT-135 NMR spectrum of **11d.**

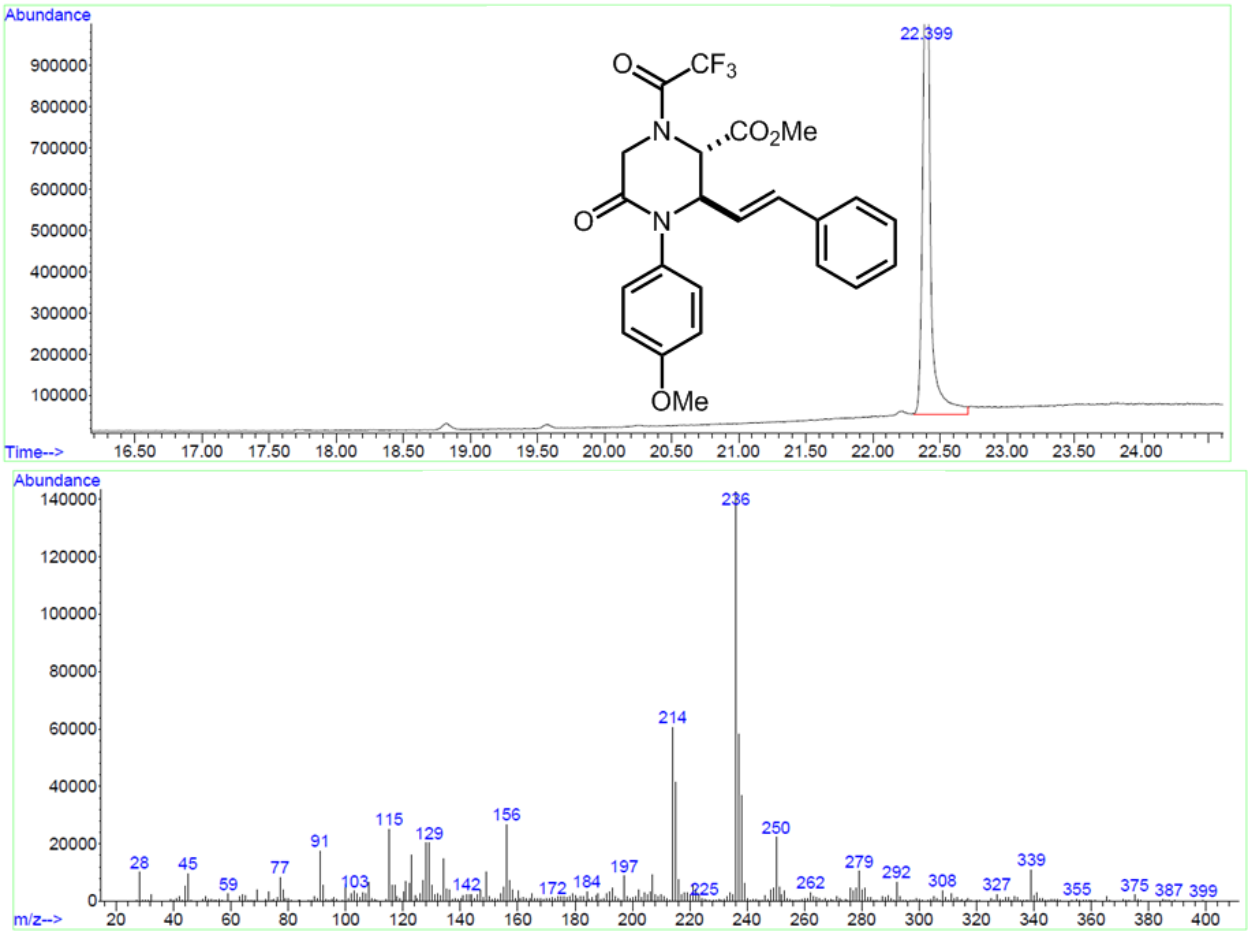

Spectra 1-91 GC-MS spectrum of **11e.**

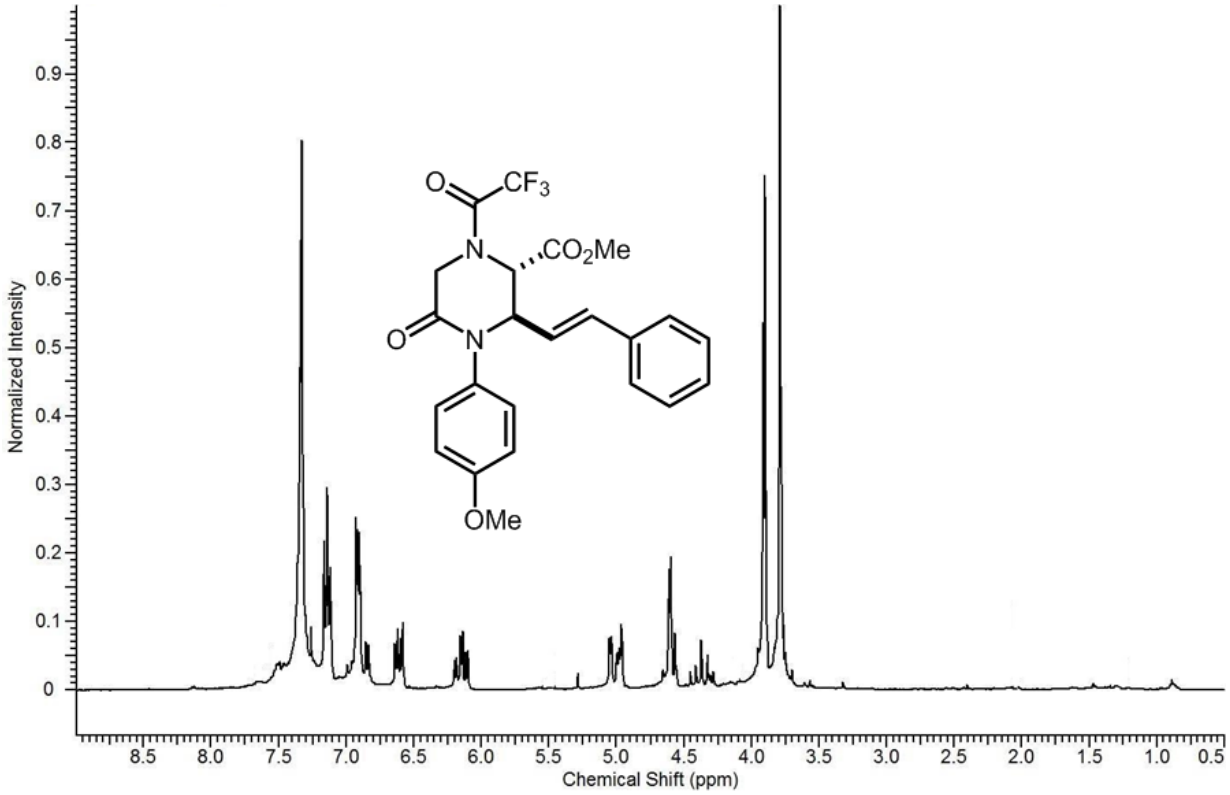

Spectra 1-92 Proton NMR spectrum of **11e.**

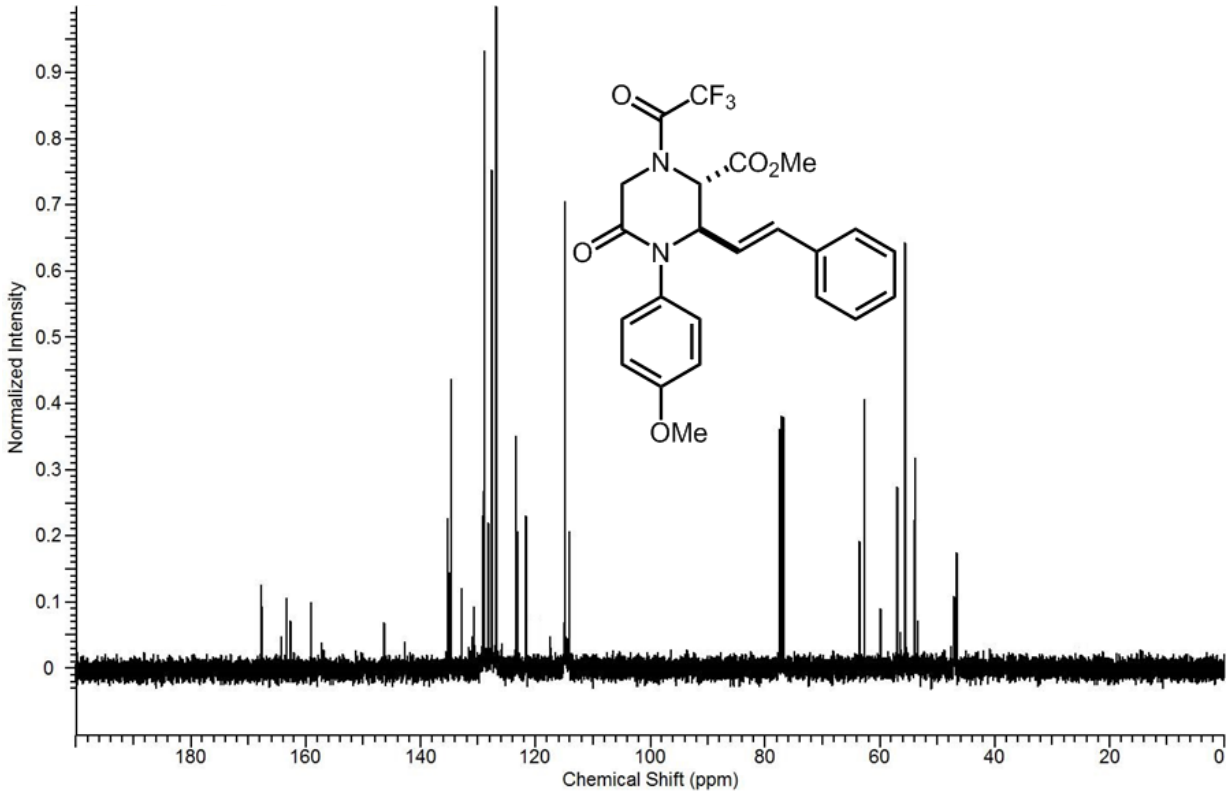

Spectra 1-93 Carbon NMR spectrum of **11e.**

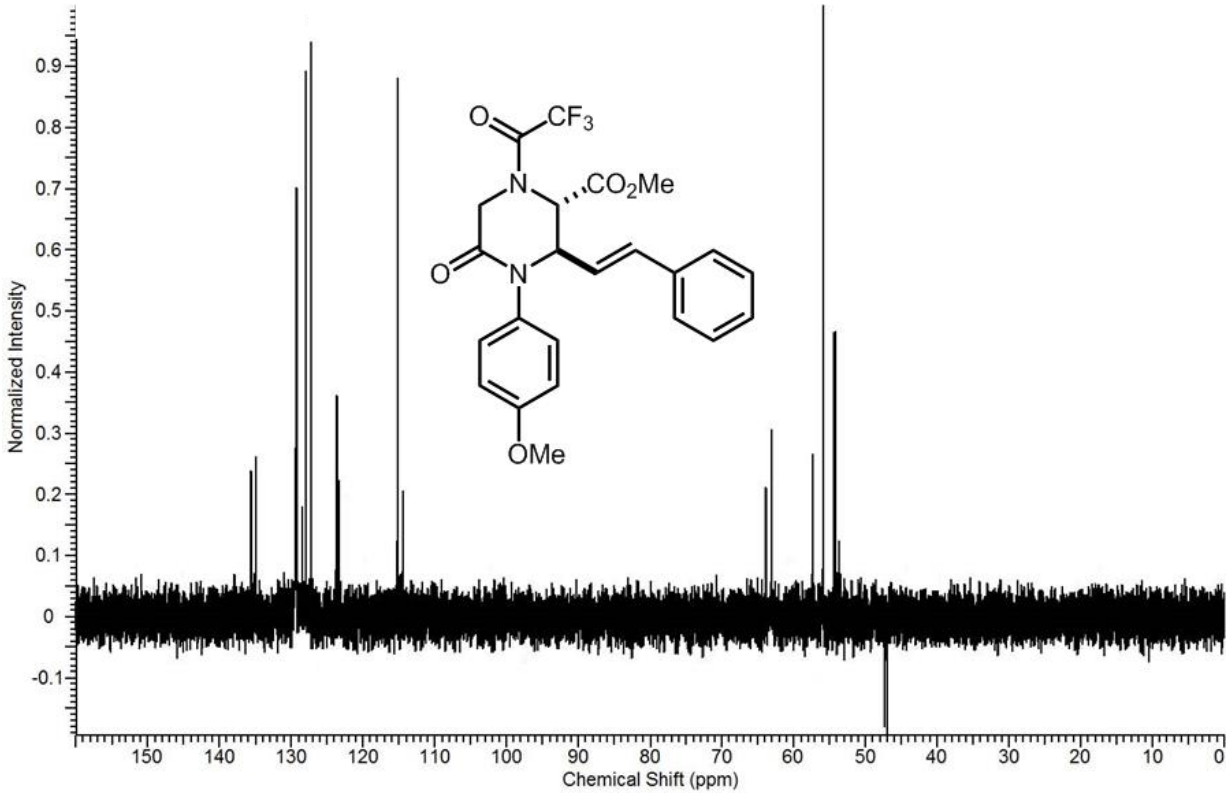

Spectra 1-94 DEPT-135 NMR spectrum of **11e.**

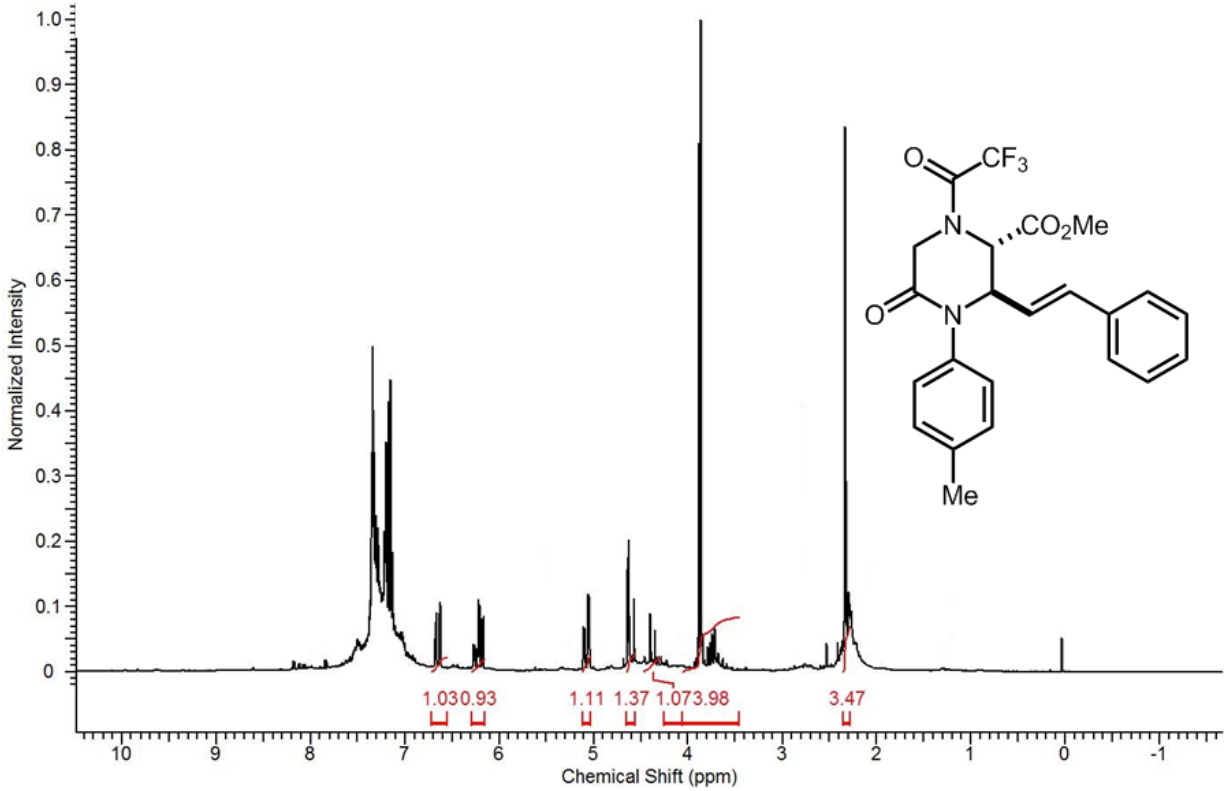

Spectra 1-95 Proton NMR spectrum of **11f.**

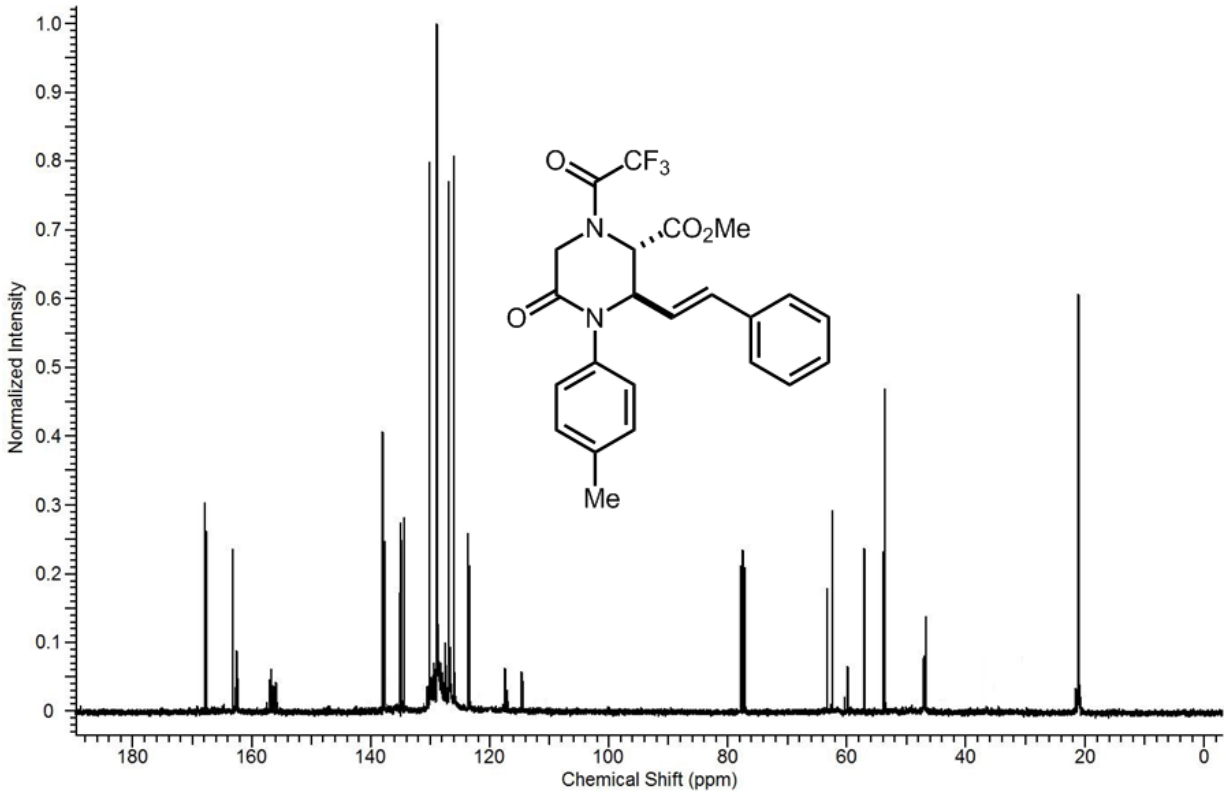

Spectra 1-96 Carbon NMR spectrum of **11f.**

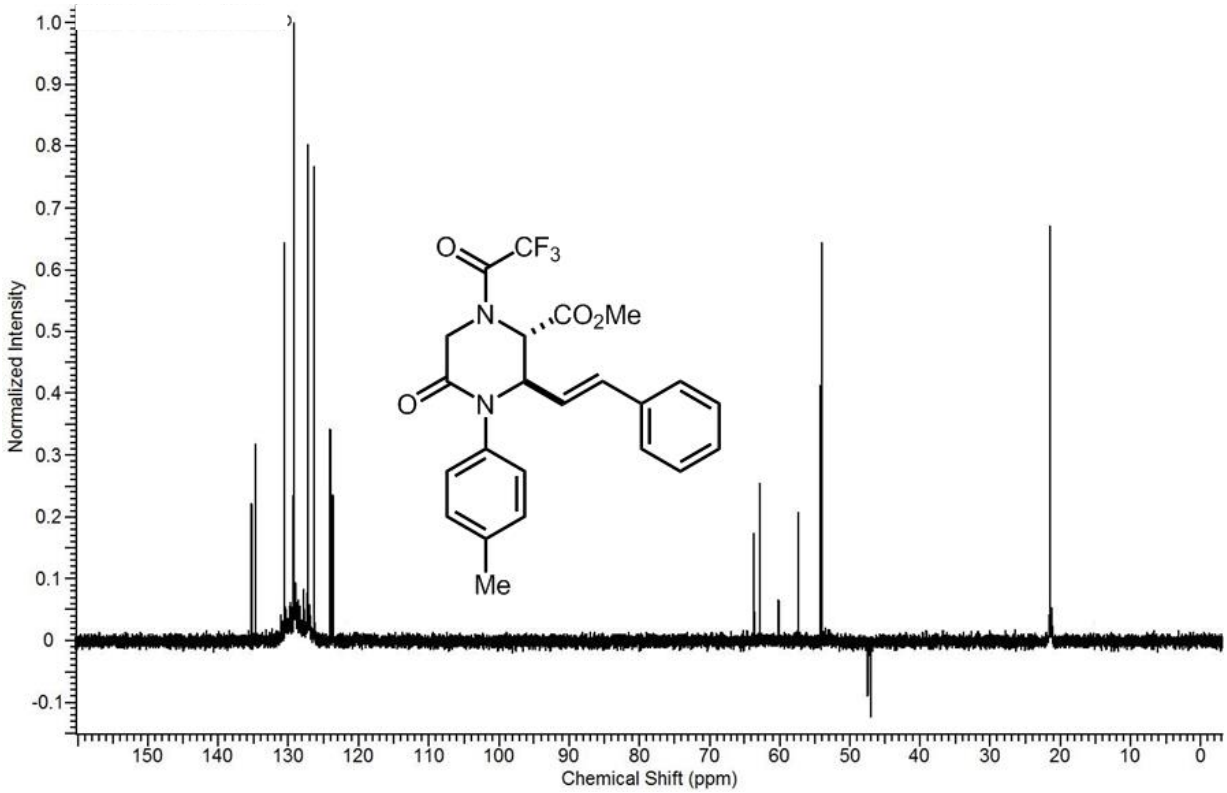

Spectra 1-97 DEPT-135 NMR spectrum of **11f.**

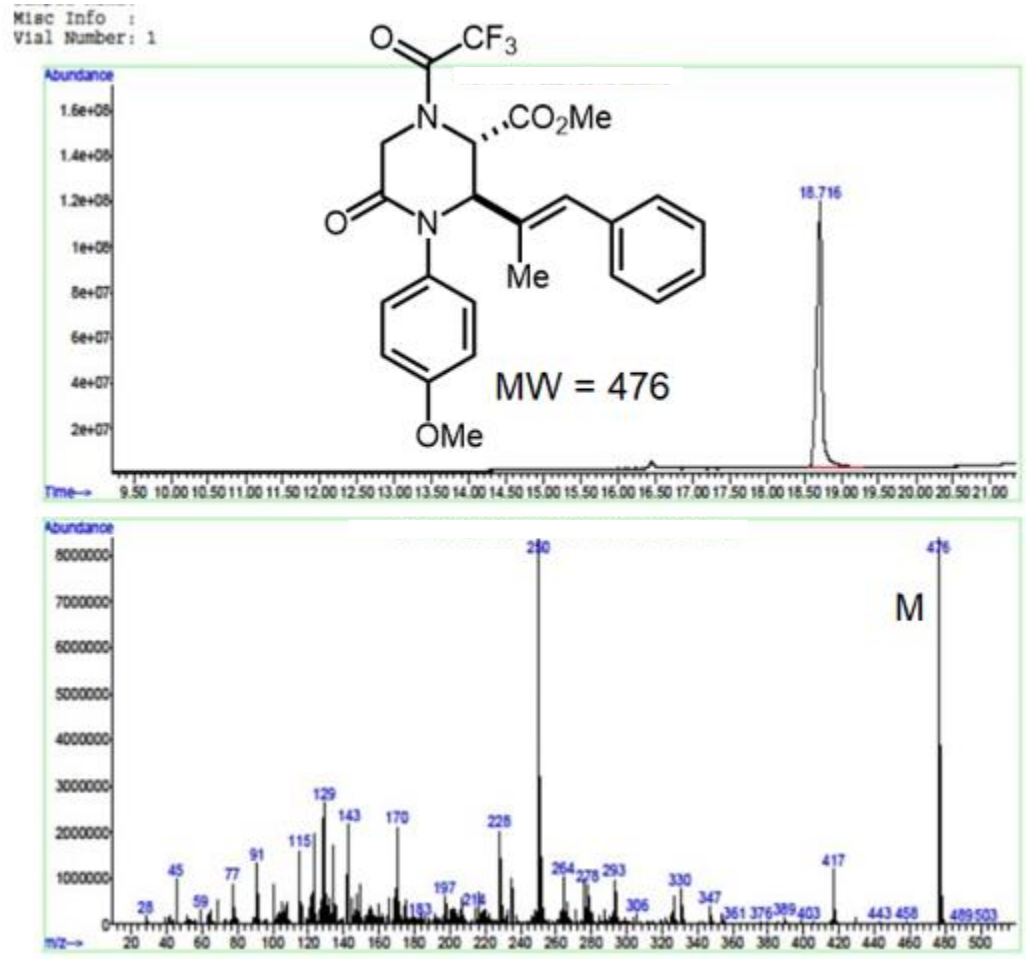

Spectra 1-98 GC-MS spectrum of **11g.**

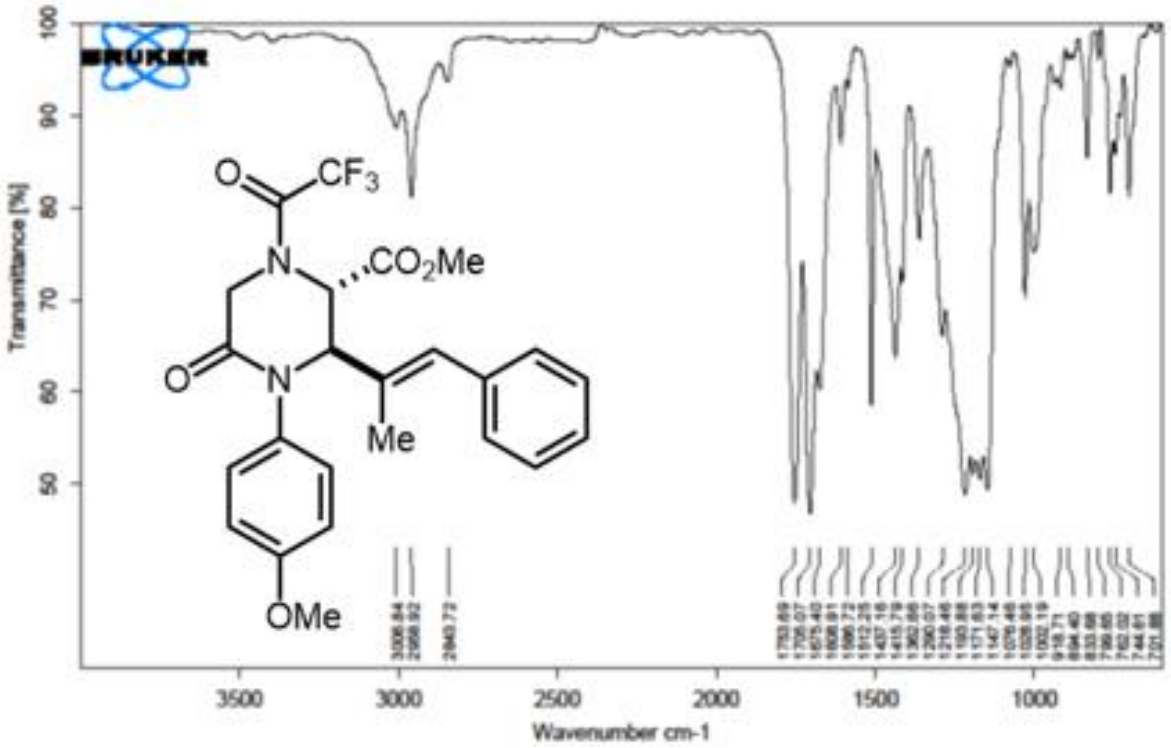

Spectra 1-99 IR spectrum of **10g.**

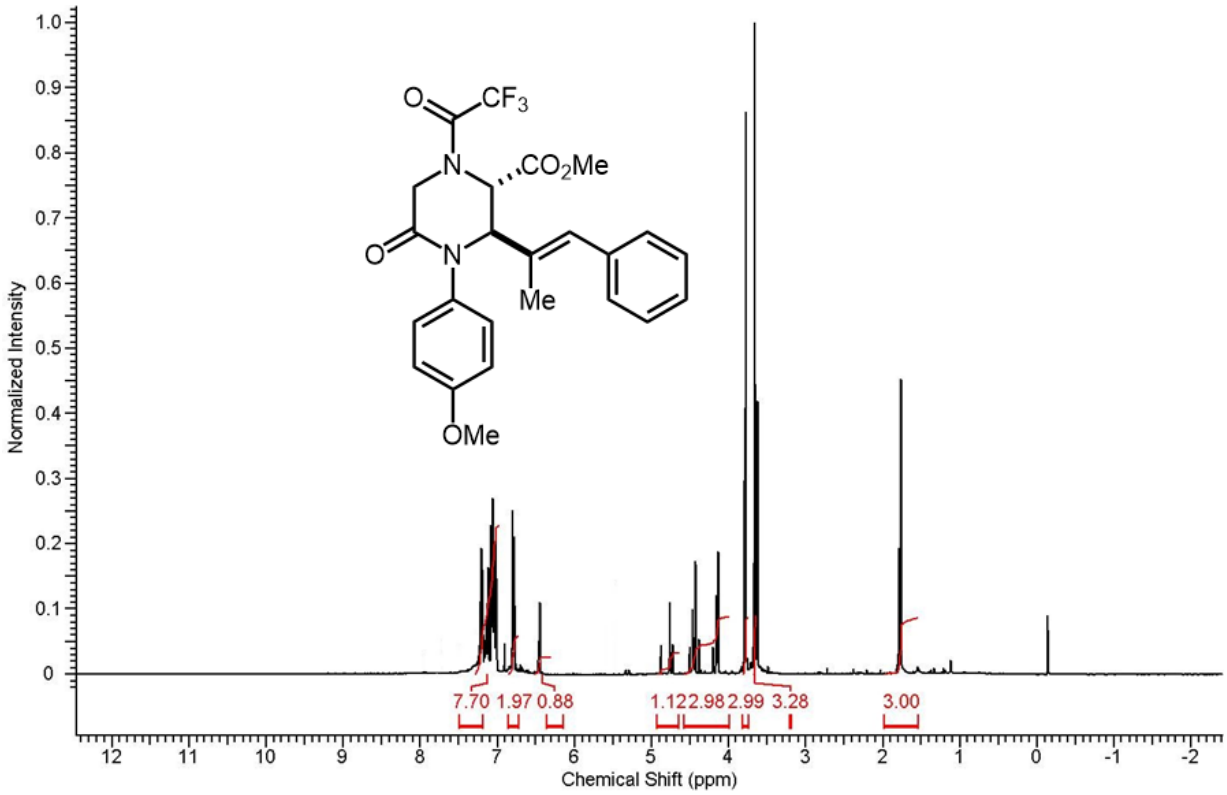

Spectra 1-100 Proton NMR spectrum of **11g.**

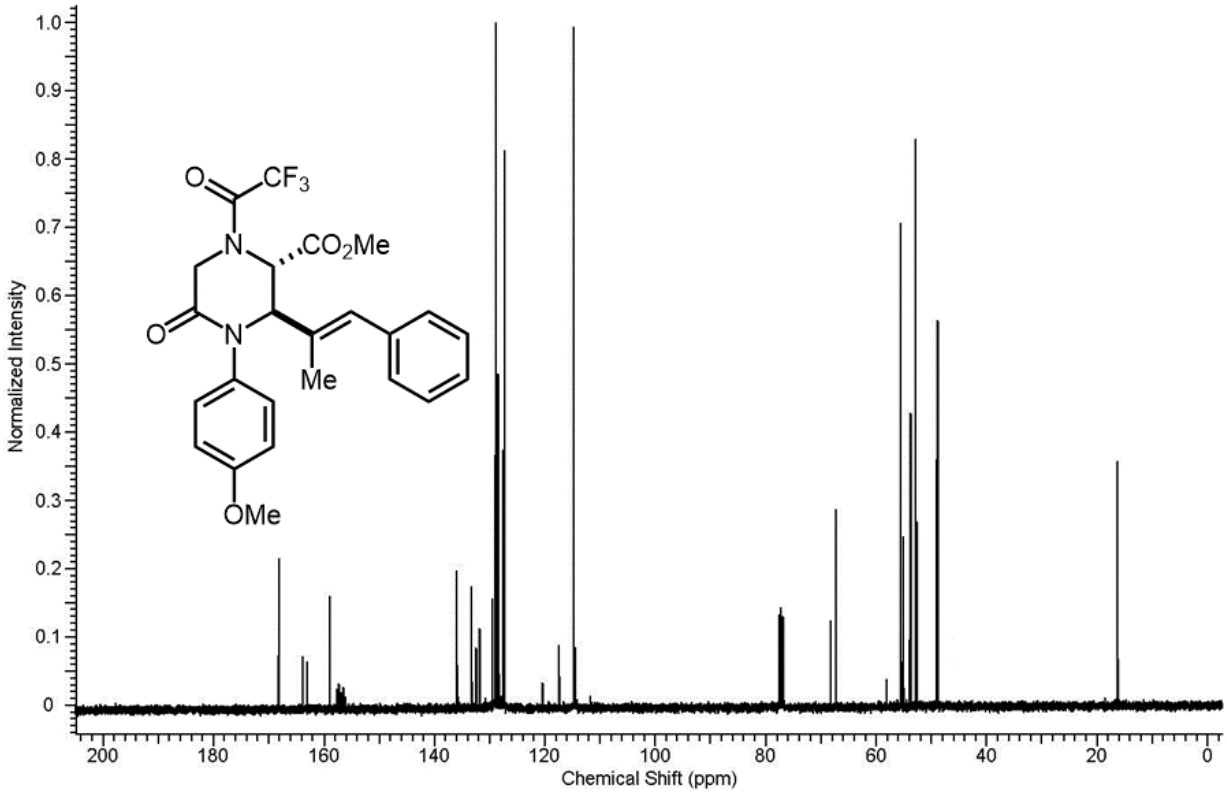

Spectra 1-101 Carbon NMR spectrum of **11g.**

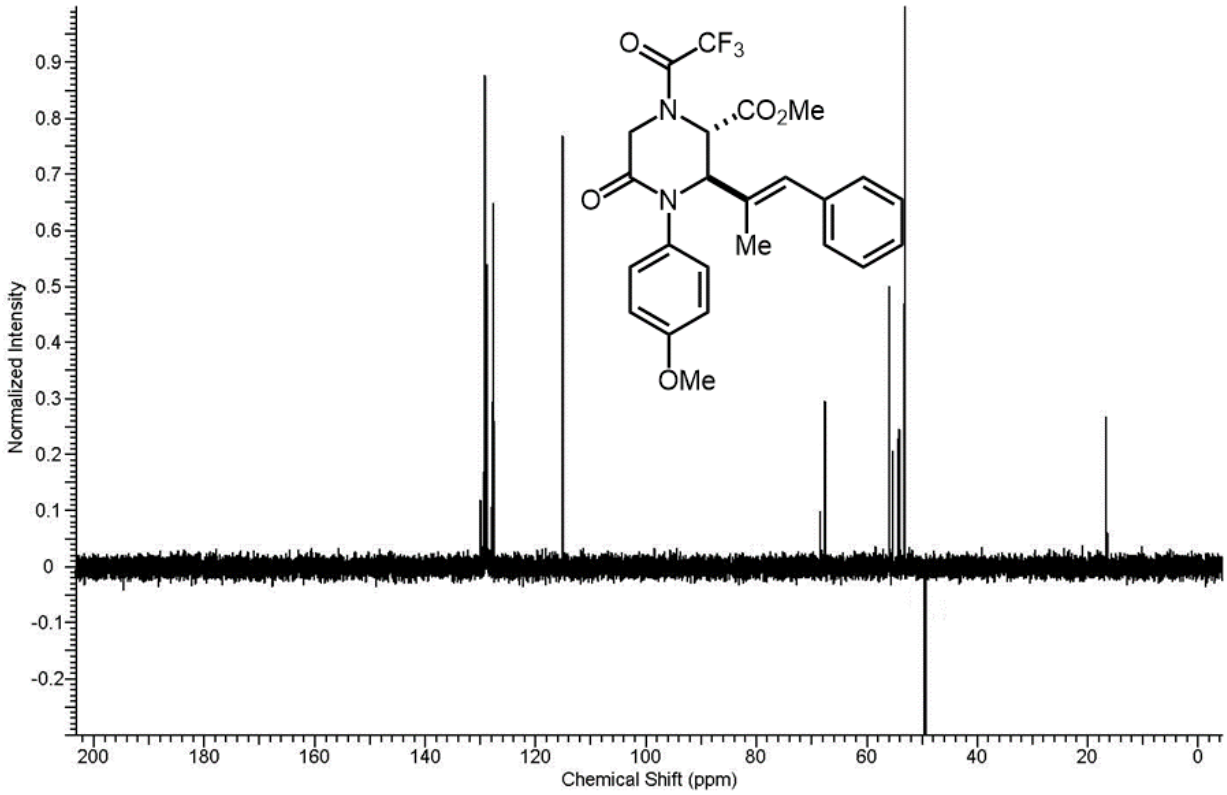

Spectra 1-102 DEPT-135 NMR spectrum of **11g.**

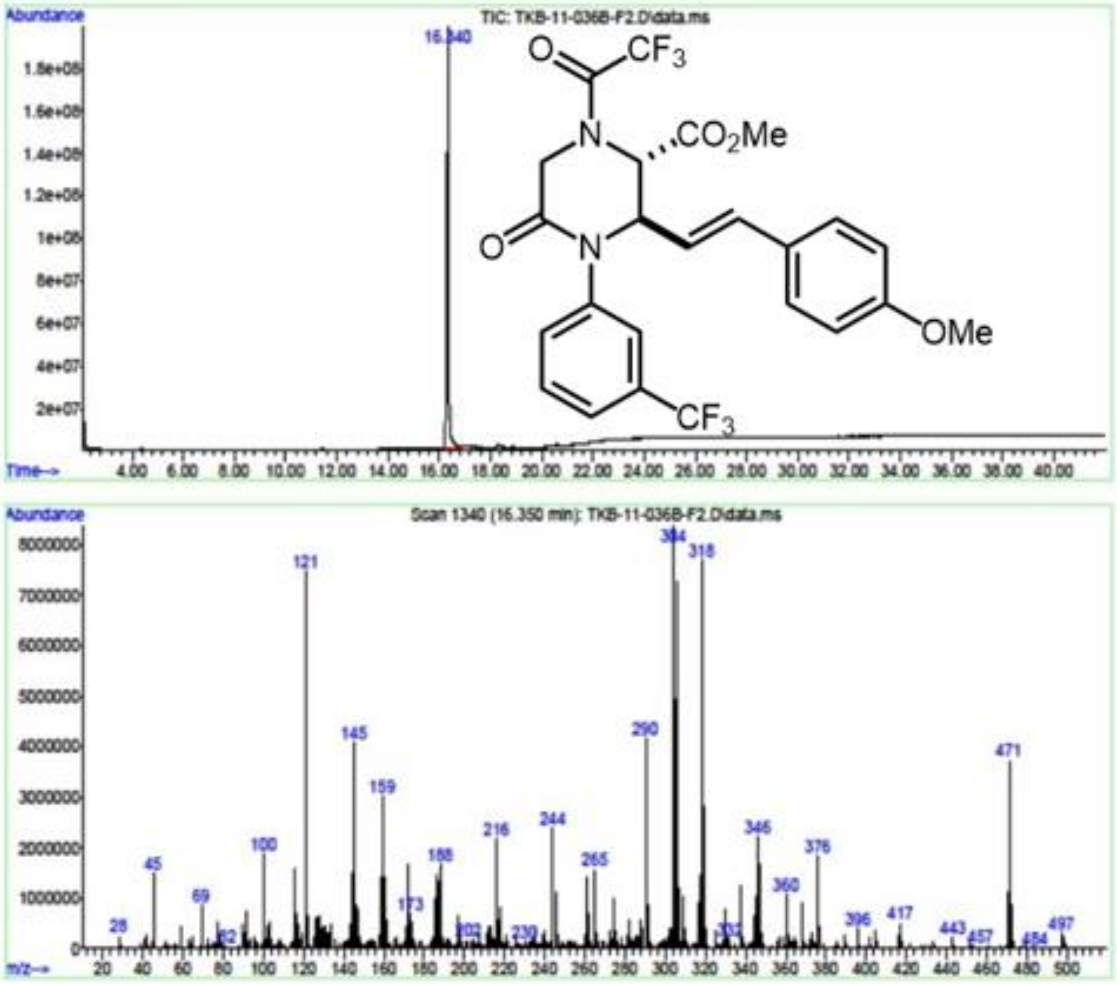

Spectra 1-103 GC-MS spectrum of **11h.**

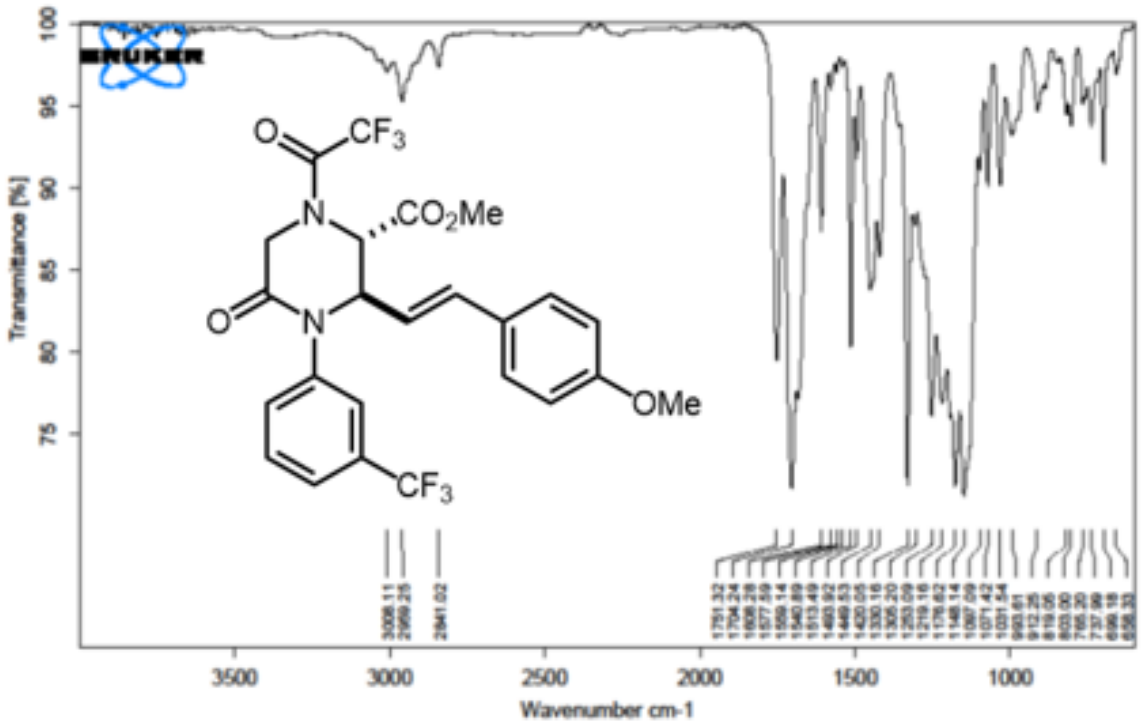

Spectra 1-104 IR spectrum of **11h.**

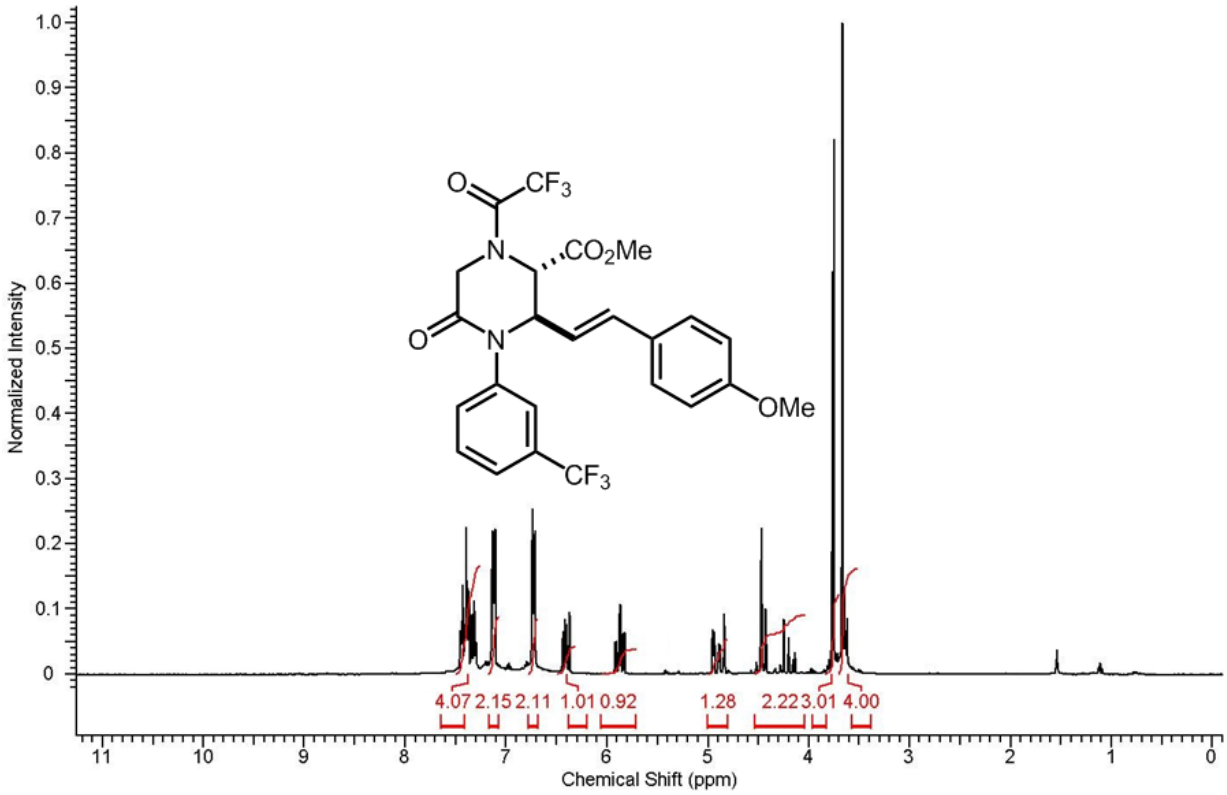

Spectra 1-105 Proton NMR spectrum of **11h.**

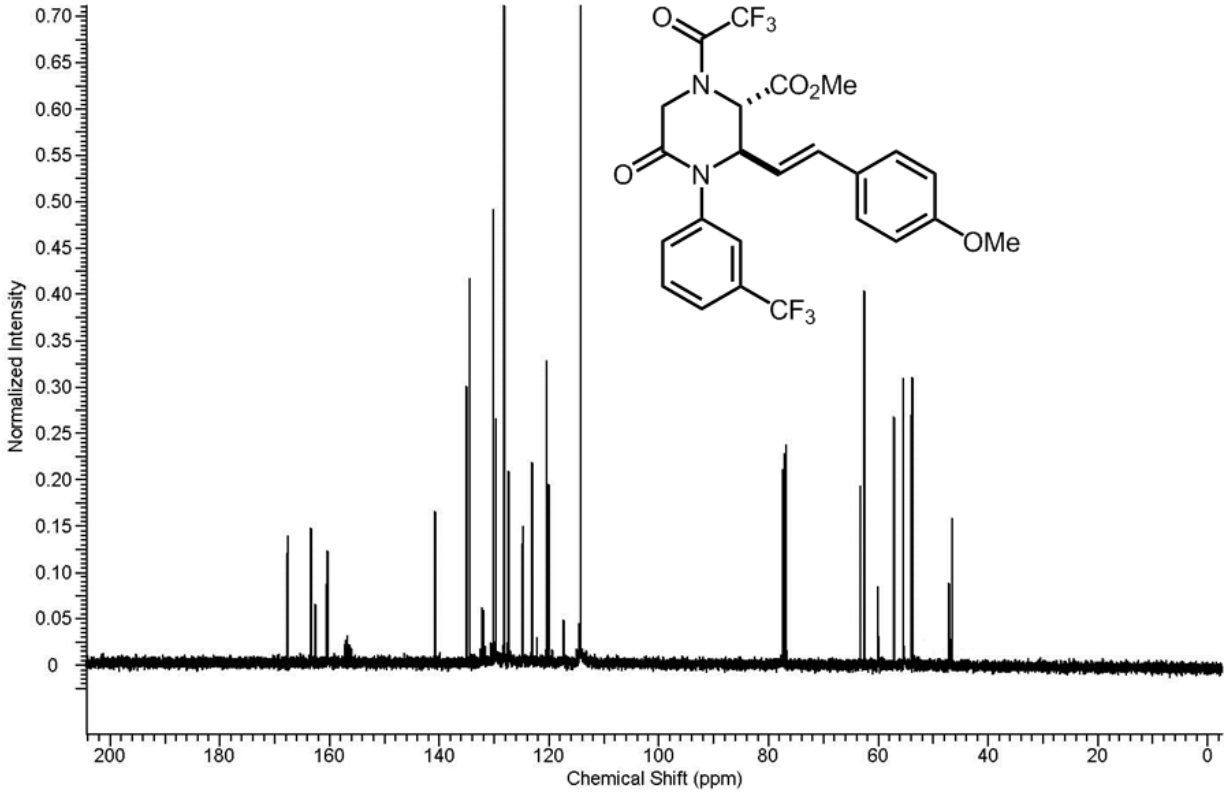

Spectra 1-106 Carbon NMR spectrum of **11h.**

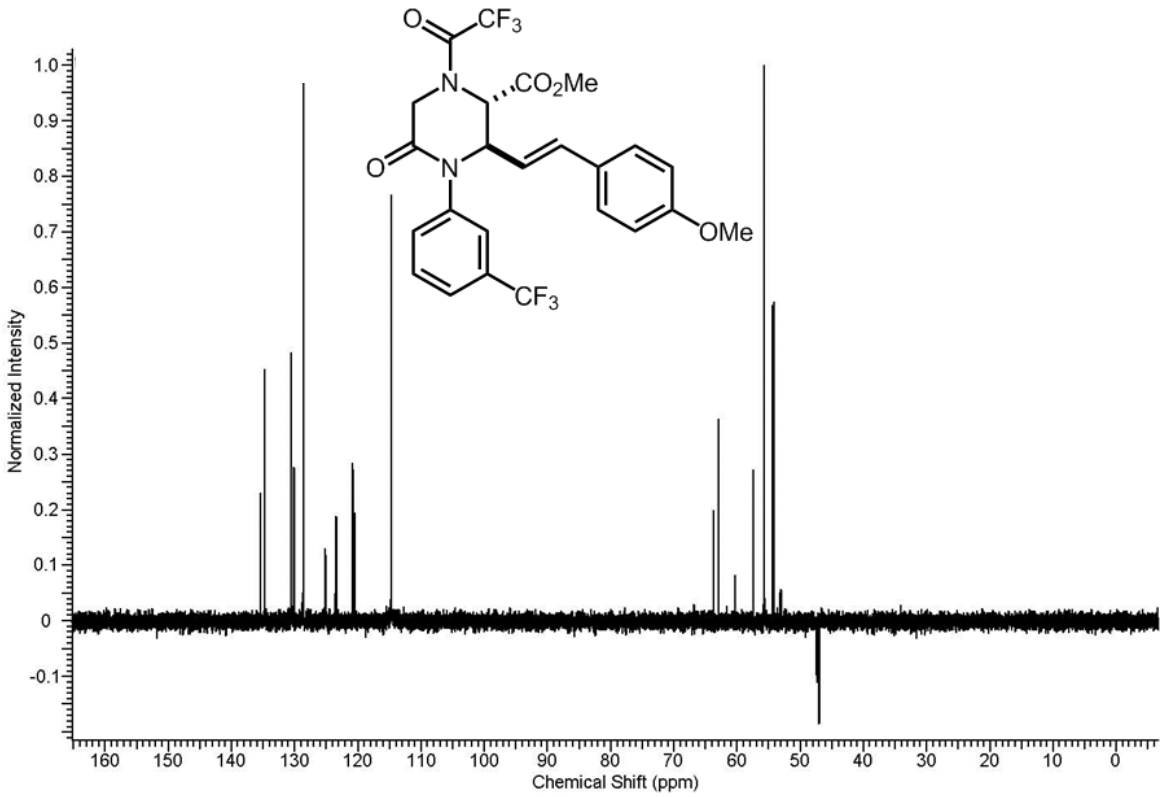

Spectra 1-107 DEPT-135 NMR spectrum of **11h.**

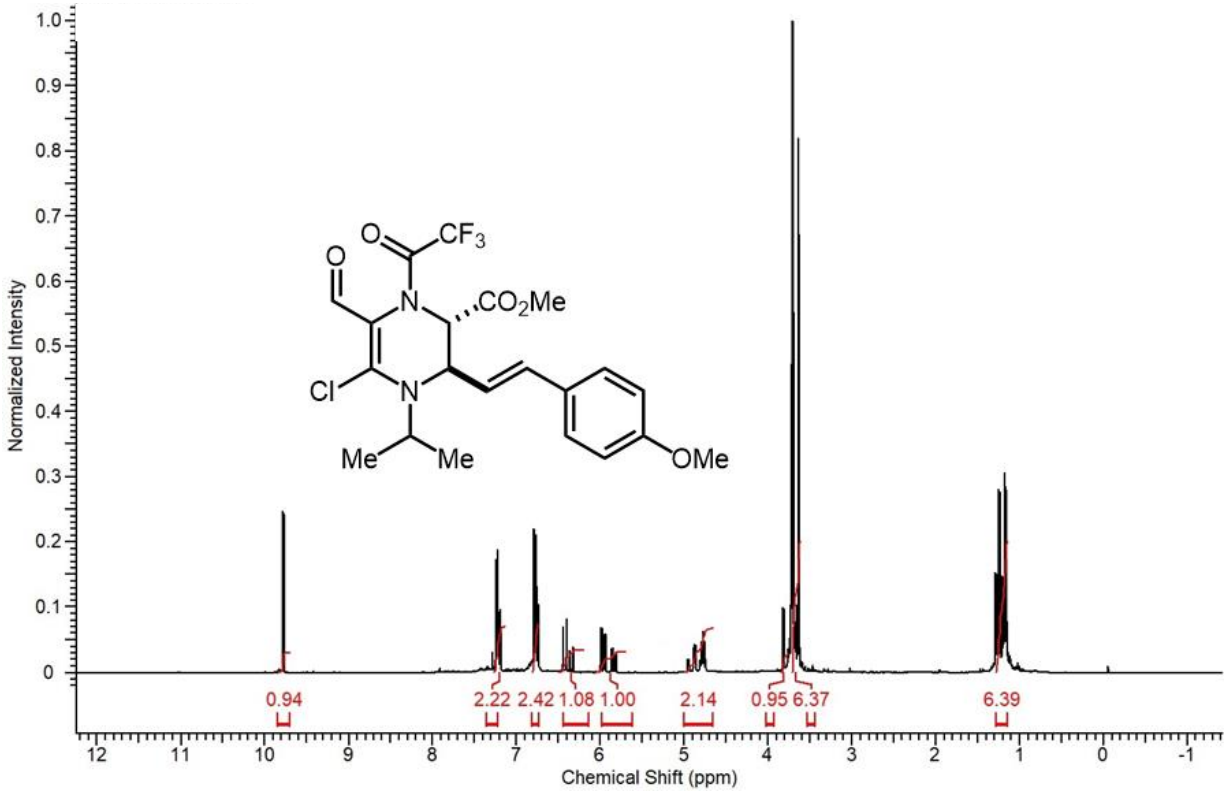

Spectra 1-108 Proton NMR spectrum of **12.**

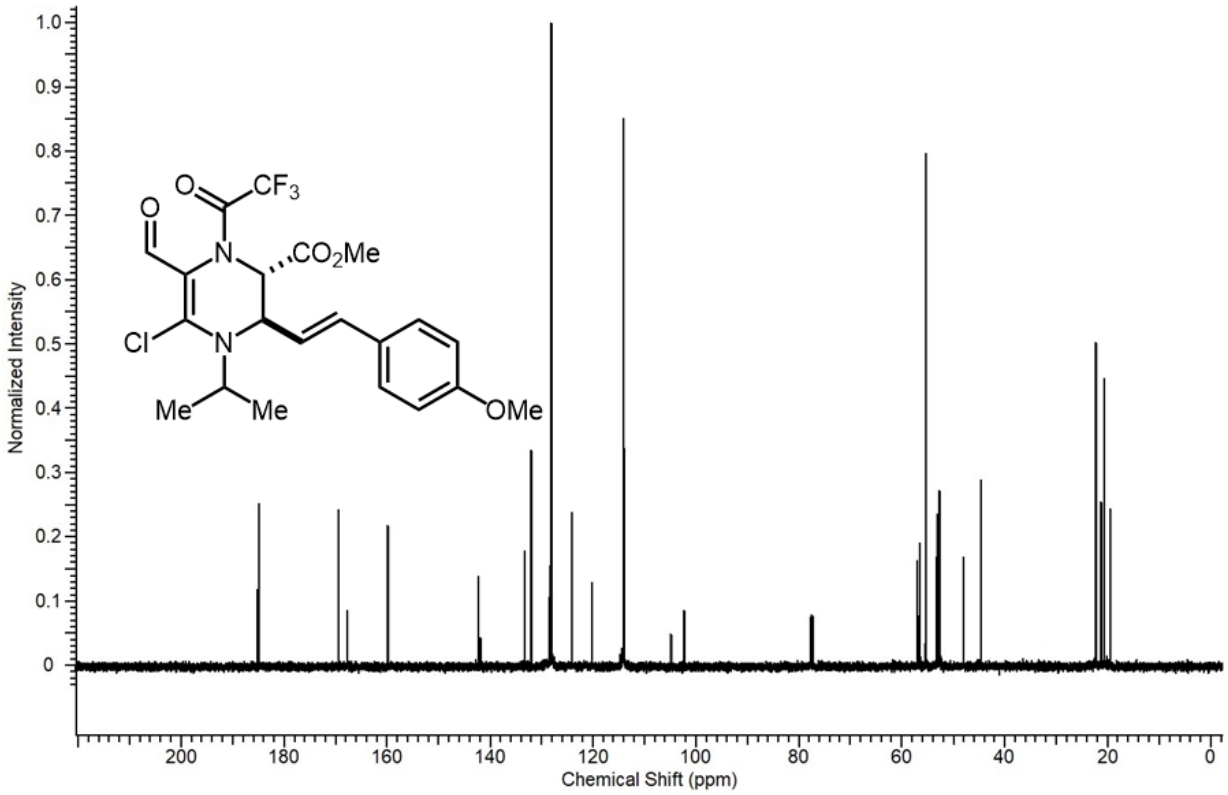

Spectra 1-109 Carbon NMR spectrum of **12.**

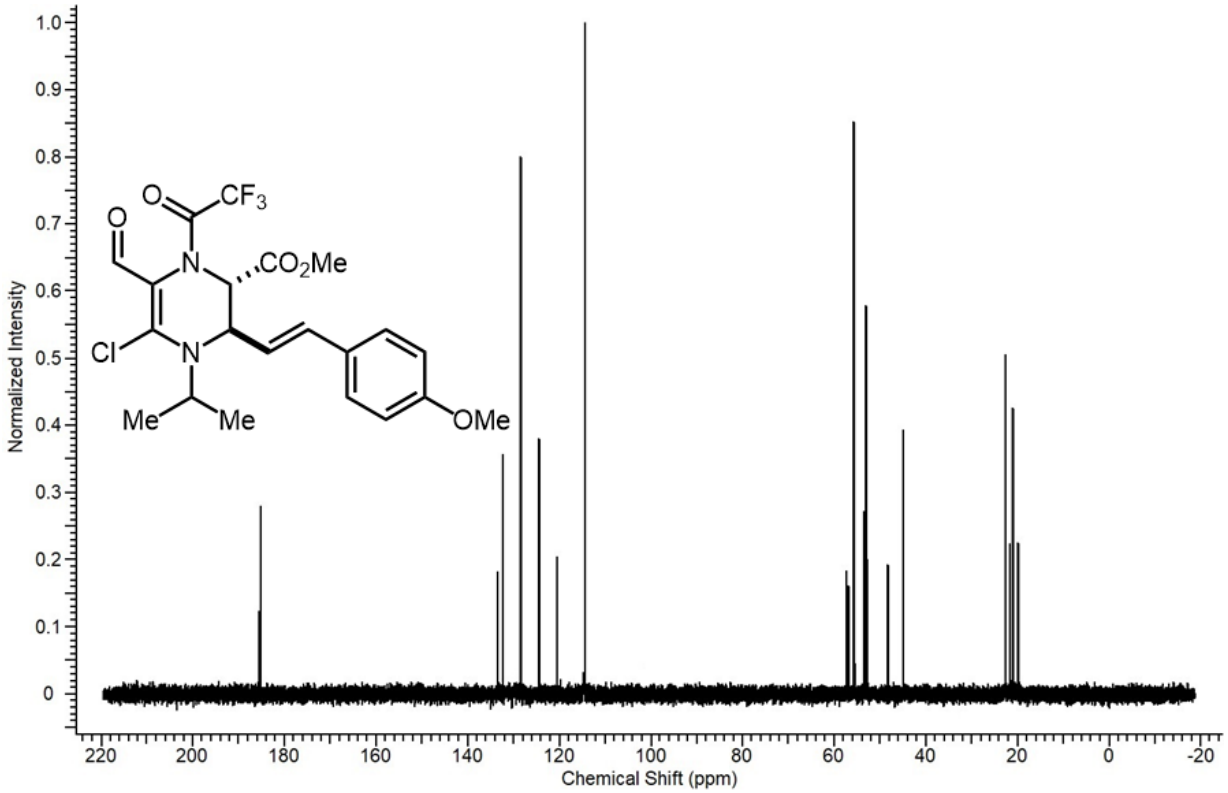

Spectra 1-110 DEPT-135 NMR spectrum of **12.**

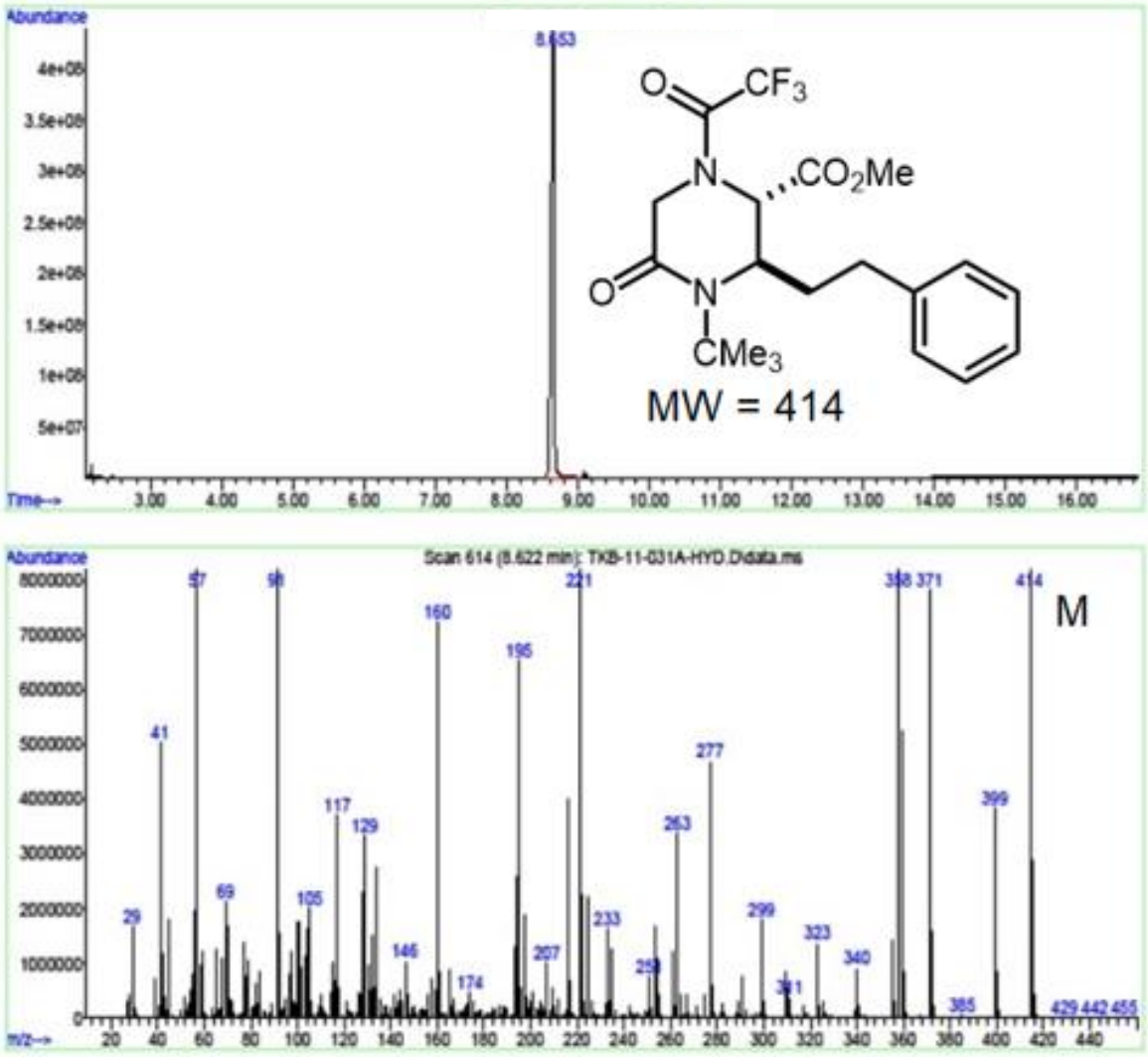

Spectra 1-111 GC-MS spectrum of **13.**

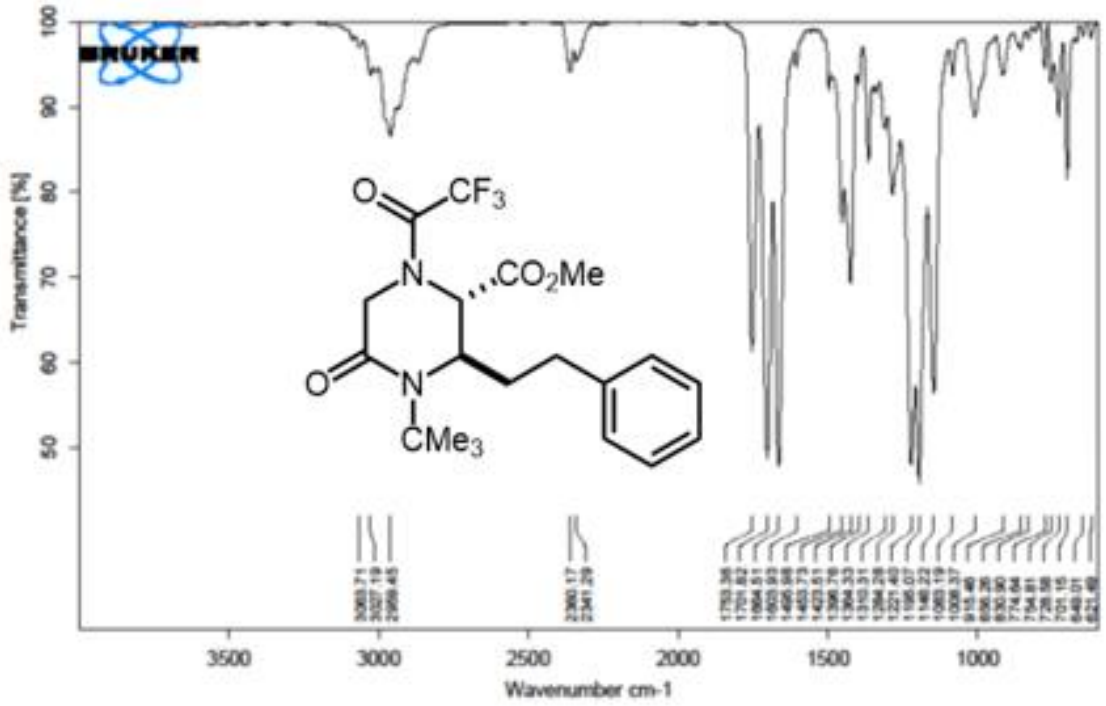

Spectra 1-112 IR spectrum of **13.**

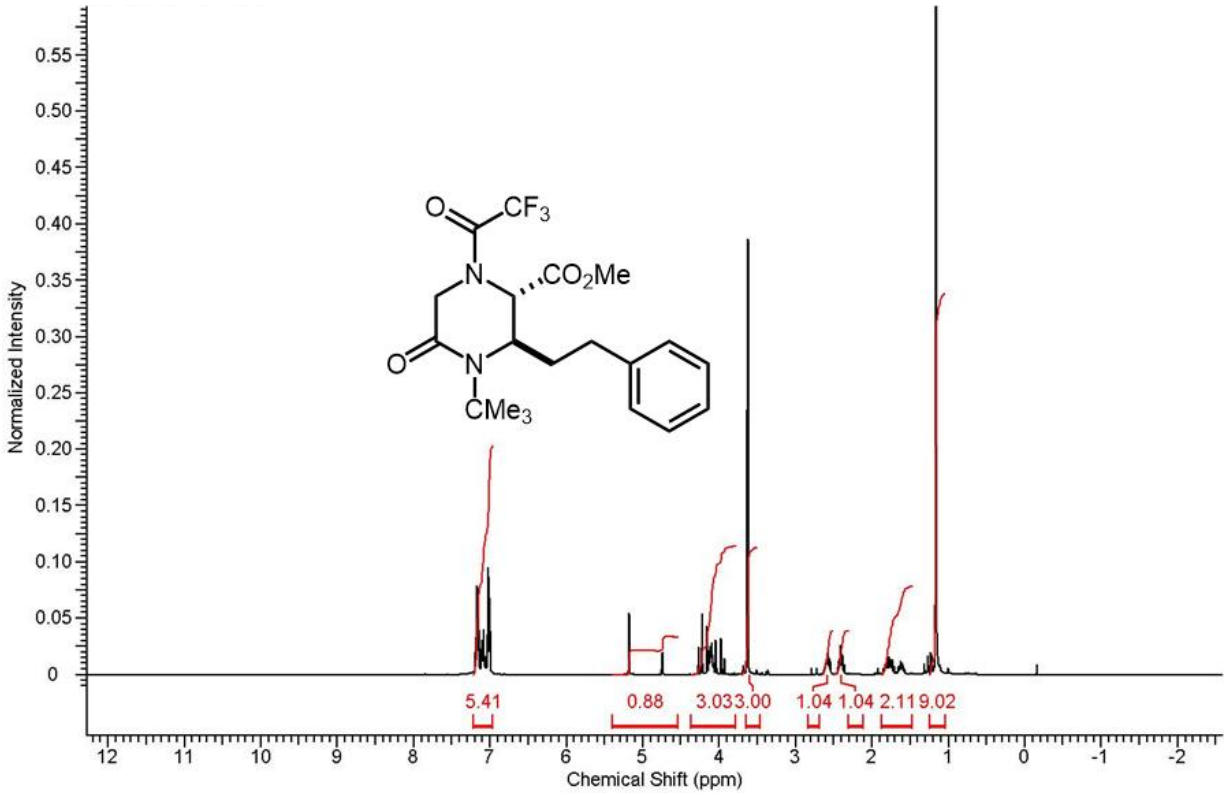

Spectra 1-113 Proton NMR spectrum of **13.**

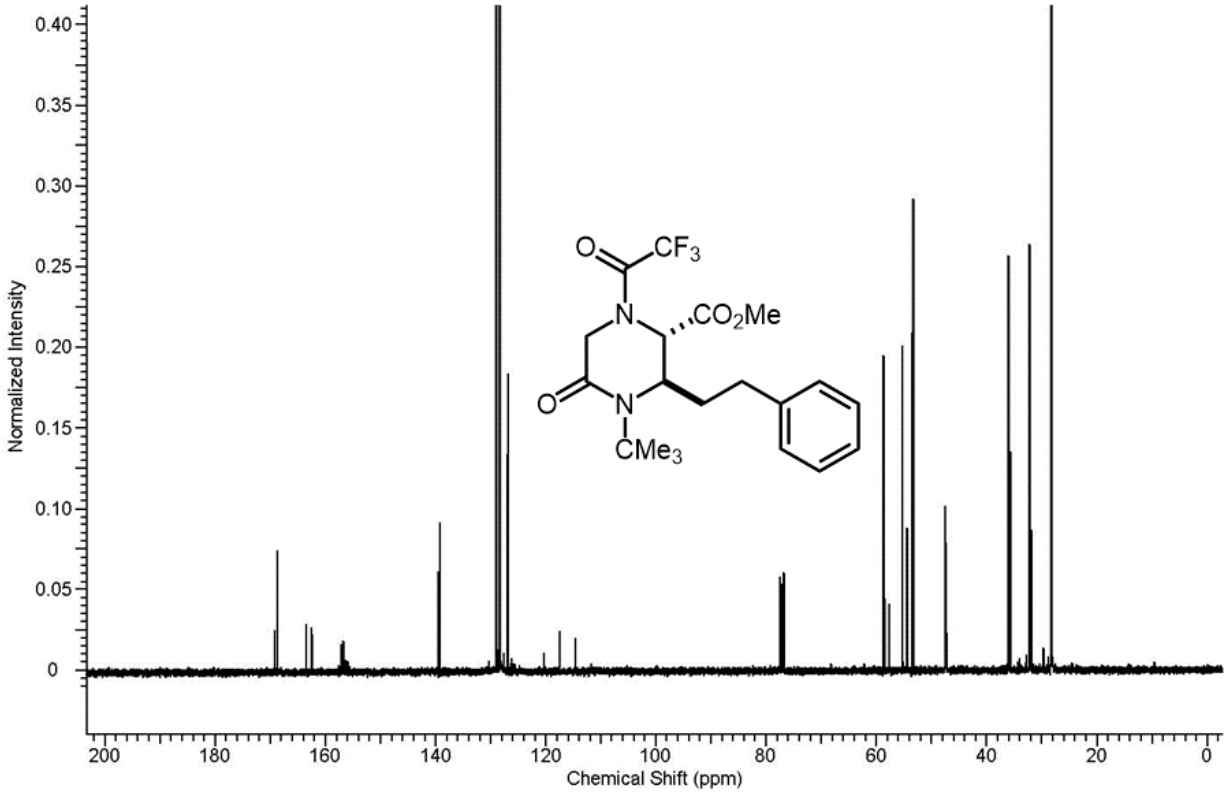

Spectra 1-114 Carbon NMR spectrum of **13.**

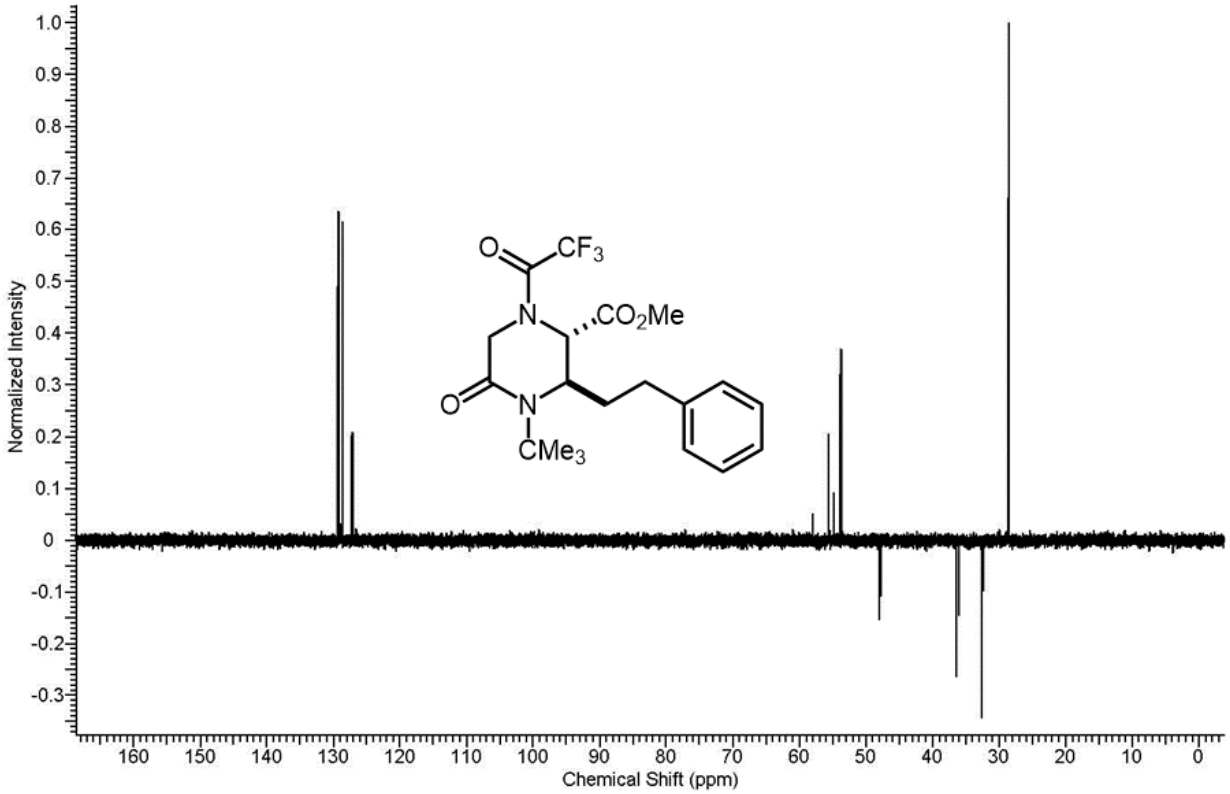

Spectra 1-115 DEPT-135 NMR spectrum of **13.**

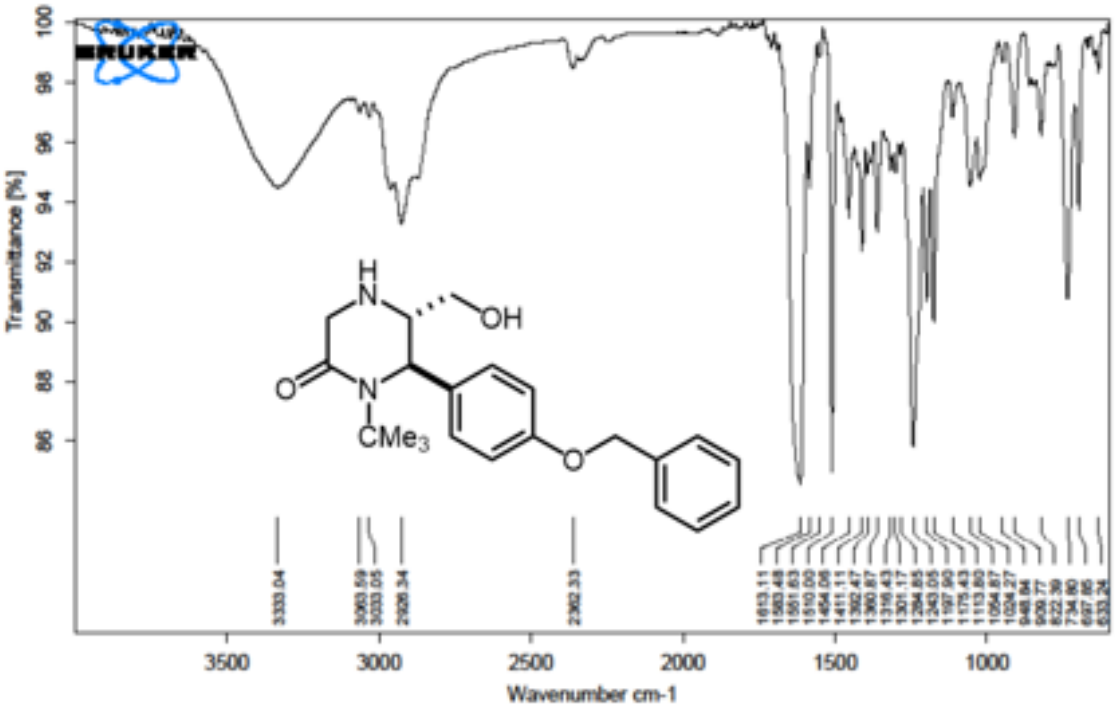

Spectra 1-116 IR spectrum of **14.**

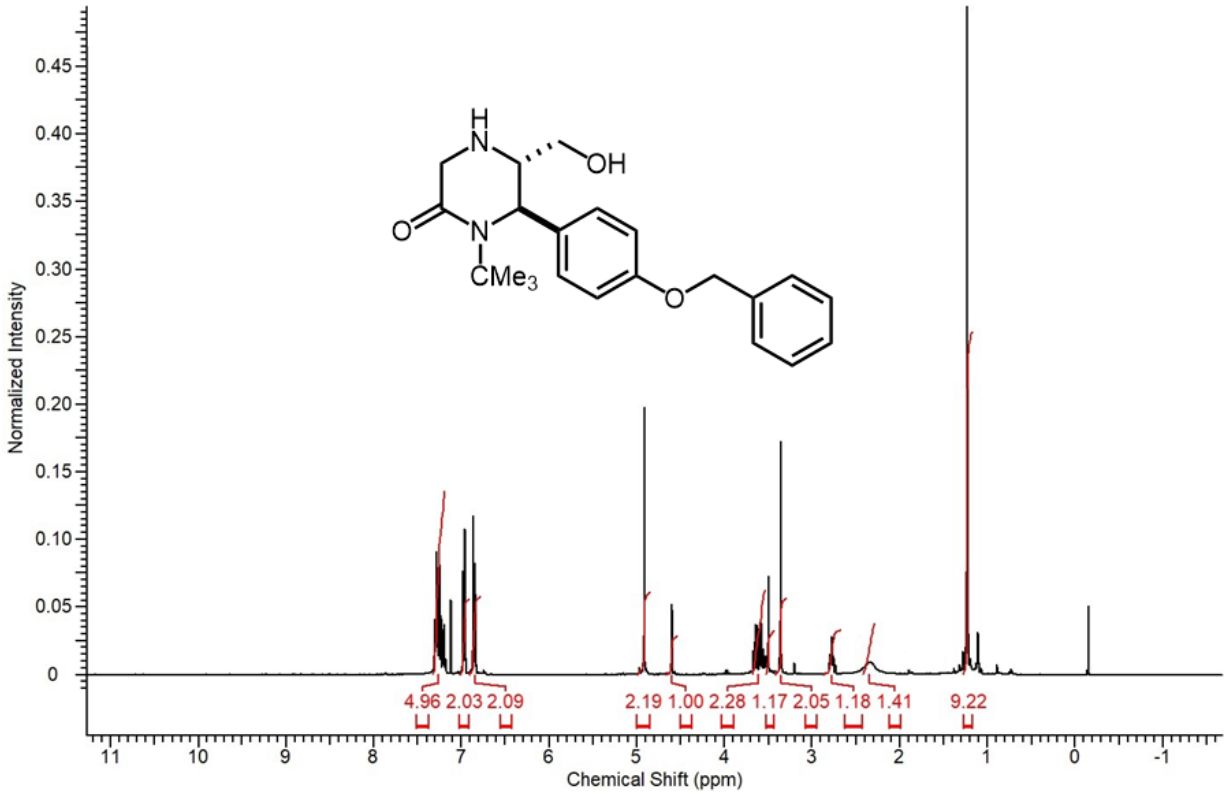

Spectra 1-117 Proton NMR spectrum of **14.**

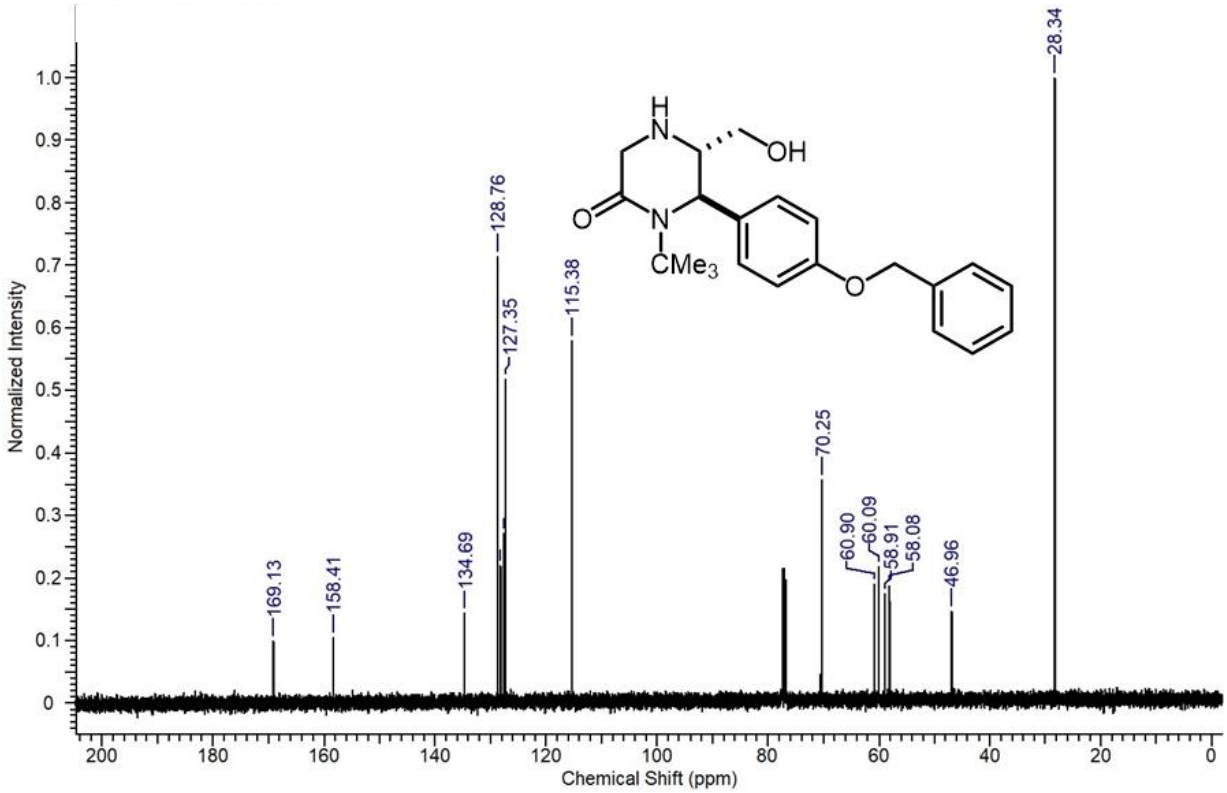

Spectra 1-118 Carbon NMR spectrum of **14.**

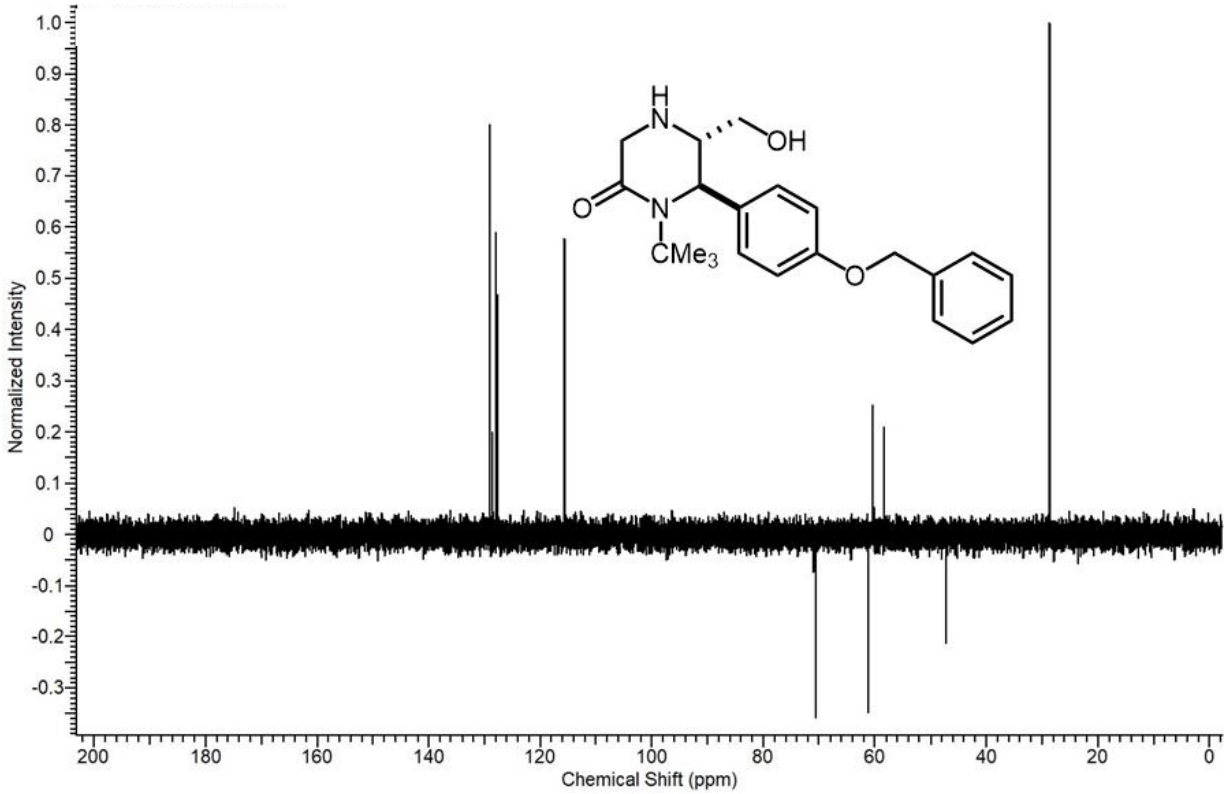

Spectra 1-119 DEPT-135 NMR spectrum of **14.**

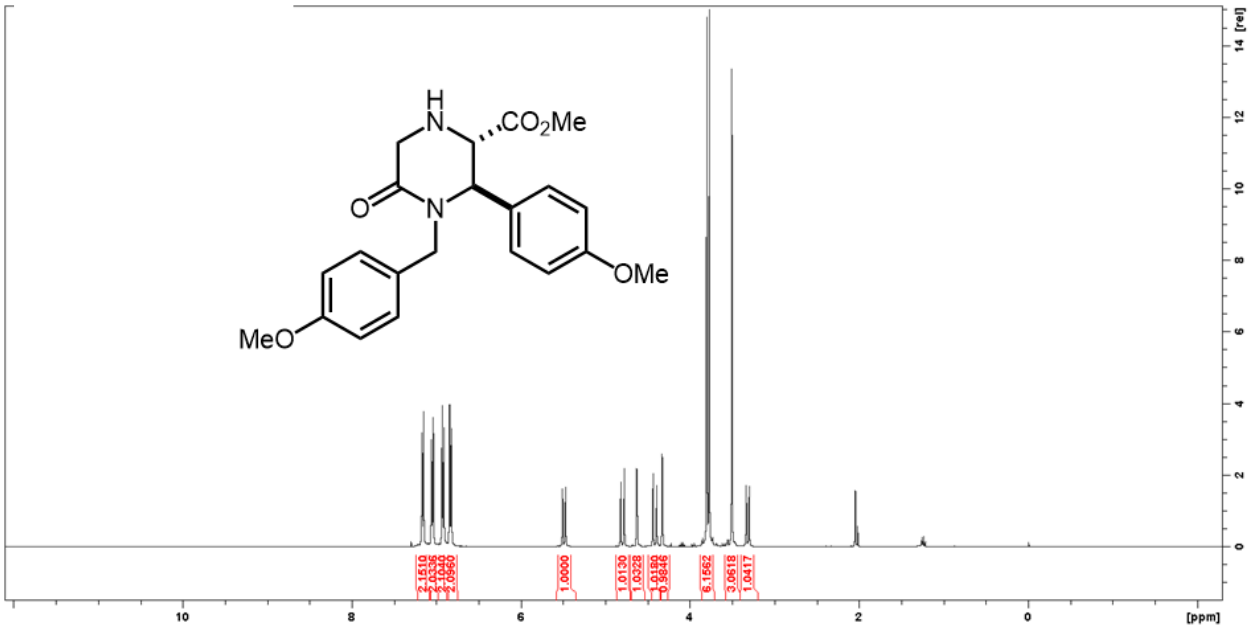

Spectra 1-120 Proton NMR spectrum of **15.**

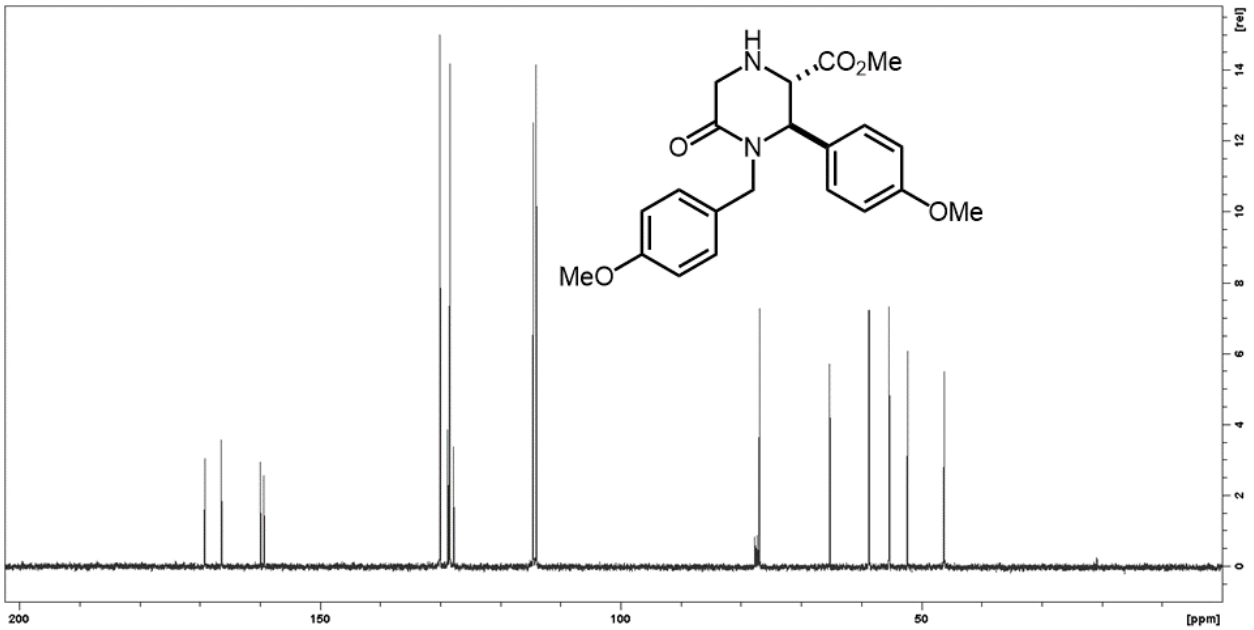

Spectra 1-121 Carbon NMR spectrum of **15.**

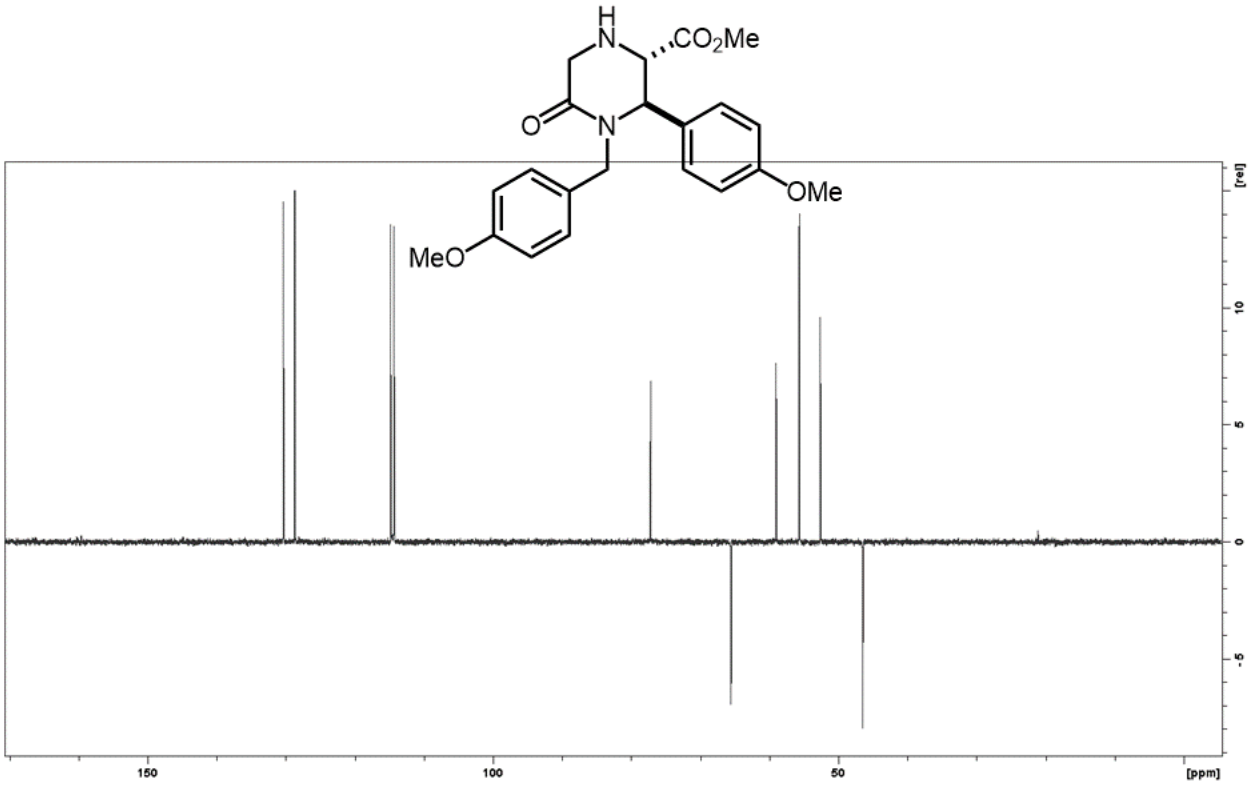

Spectra 1-123 DEPT-135 NMR spectrum of **15.**

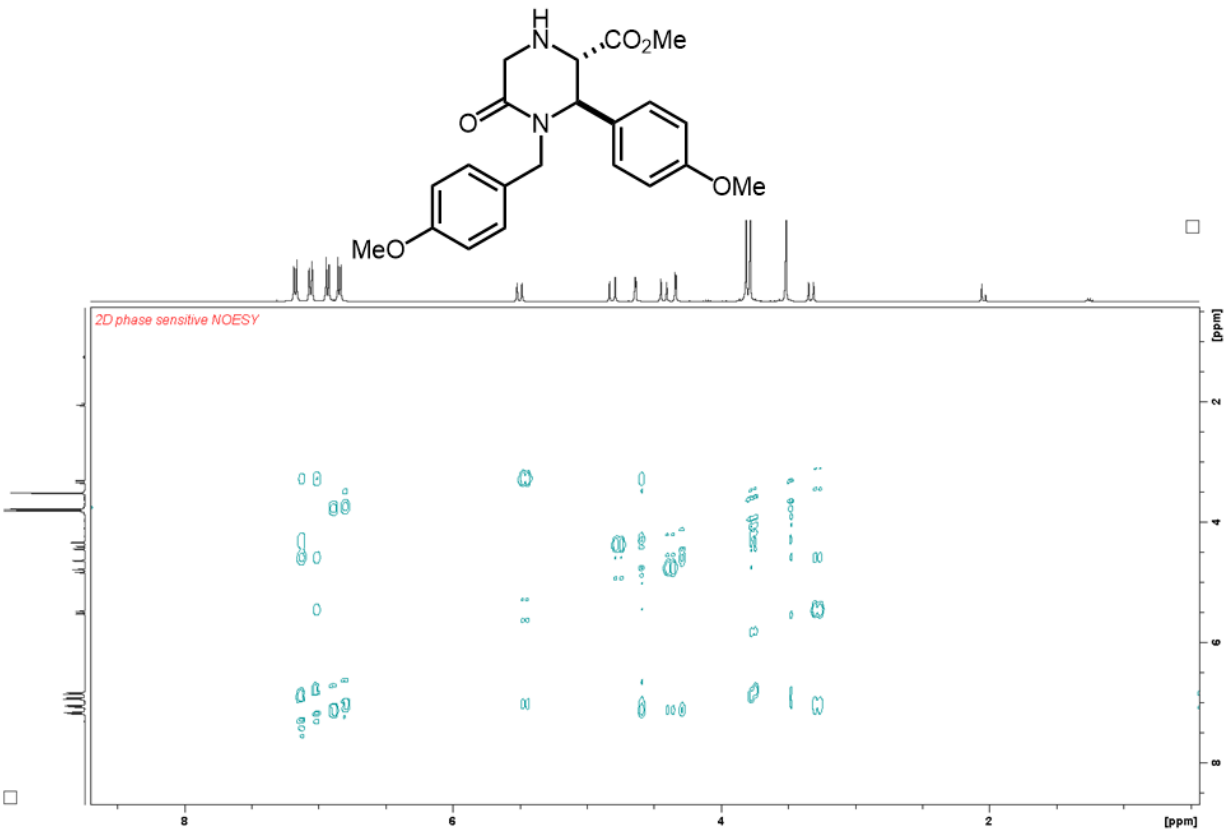

Spectra 1-124 NOESY NMR spectrum of **15.**

APPENDIX B: CHAPTER 3 SPECTROSCOPIC DATA

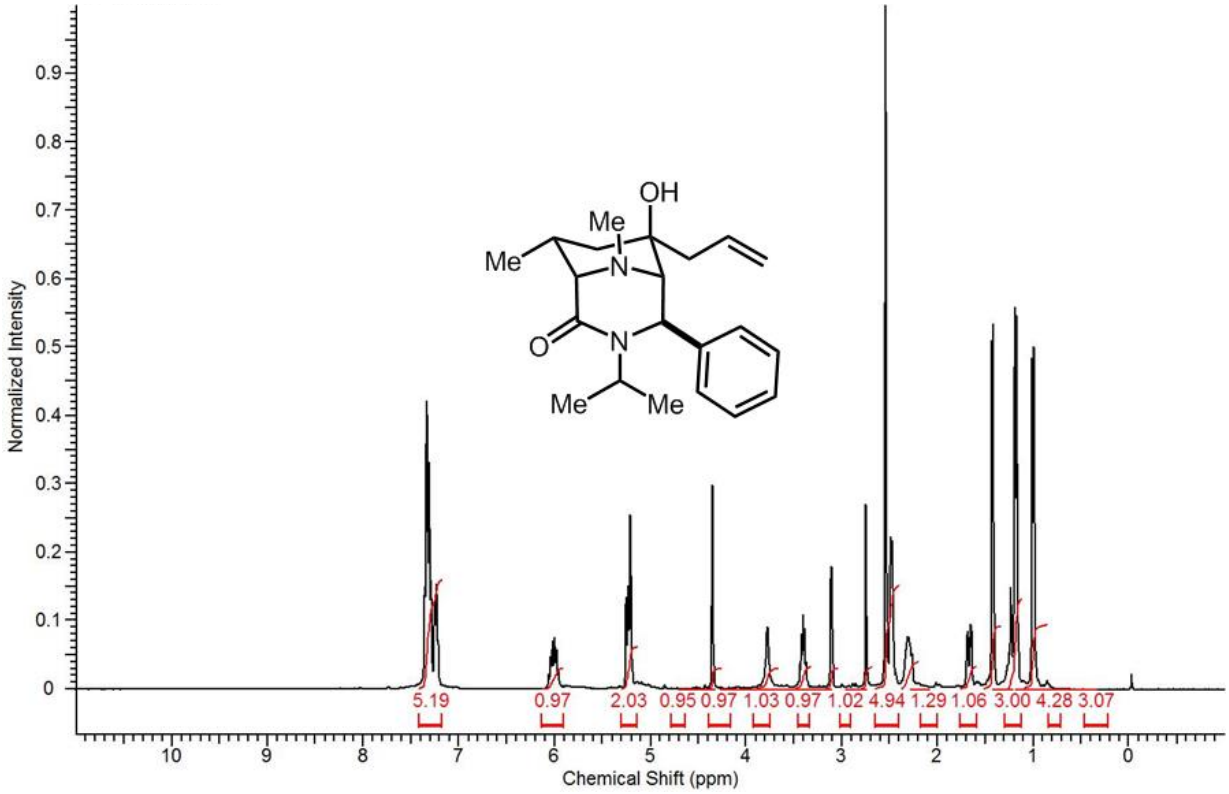

Spectra 2-1 Proton NMR spectrum of **2a.**

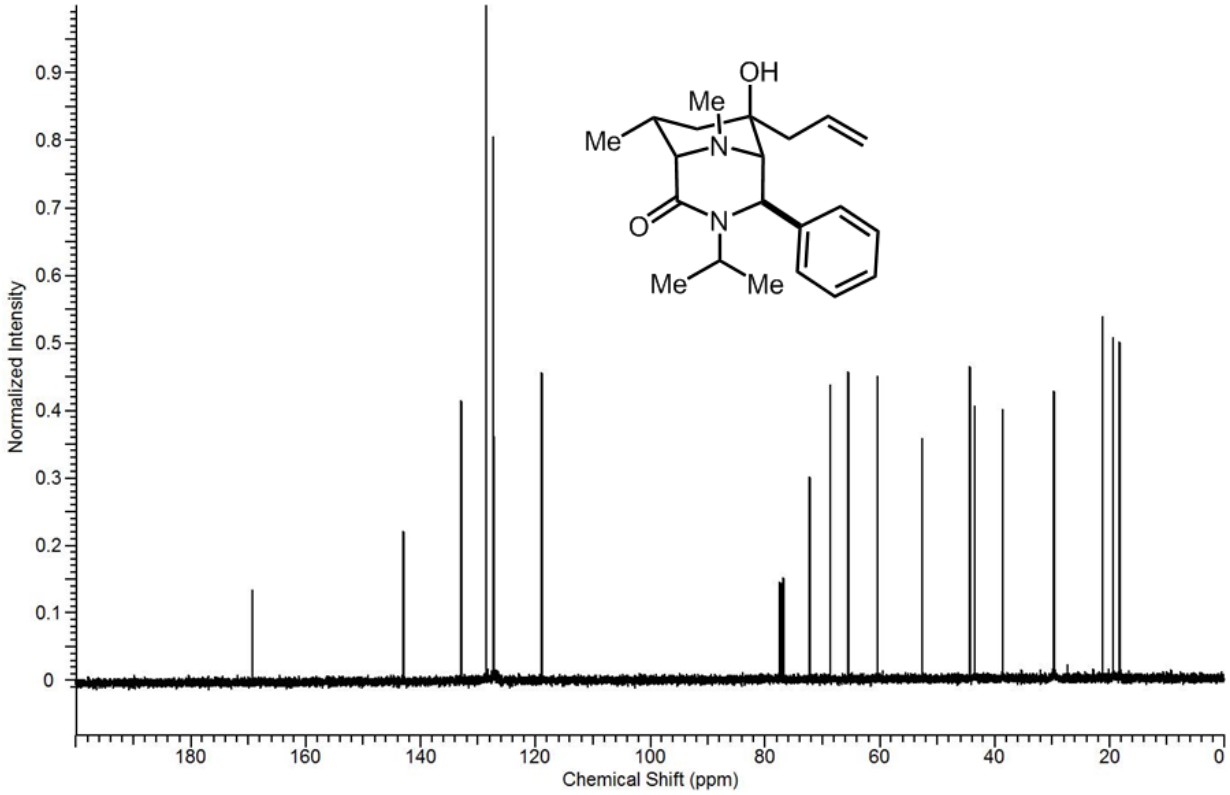

Spectra 2-2 Carbon NMR spectrum of **2a.**

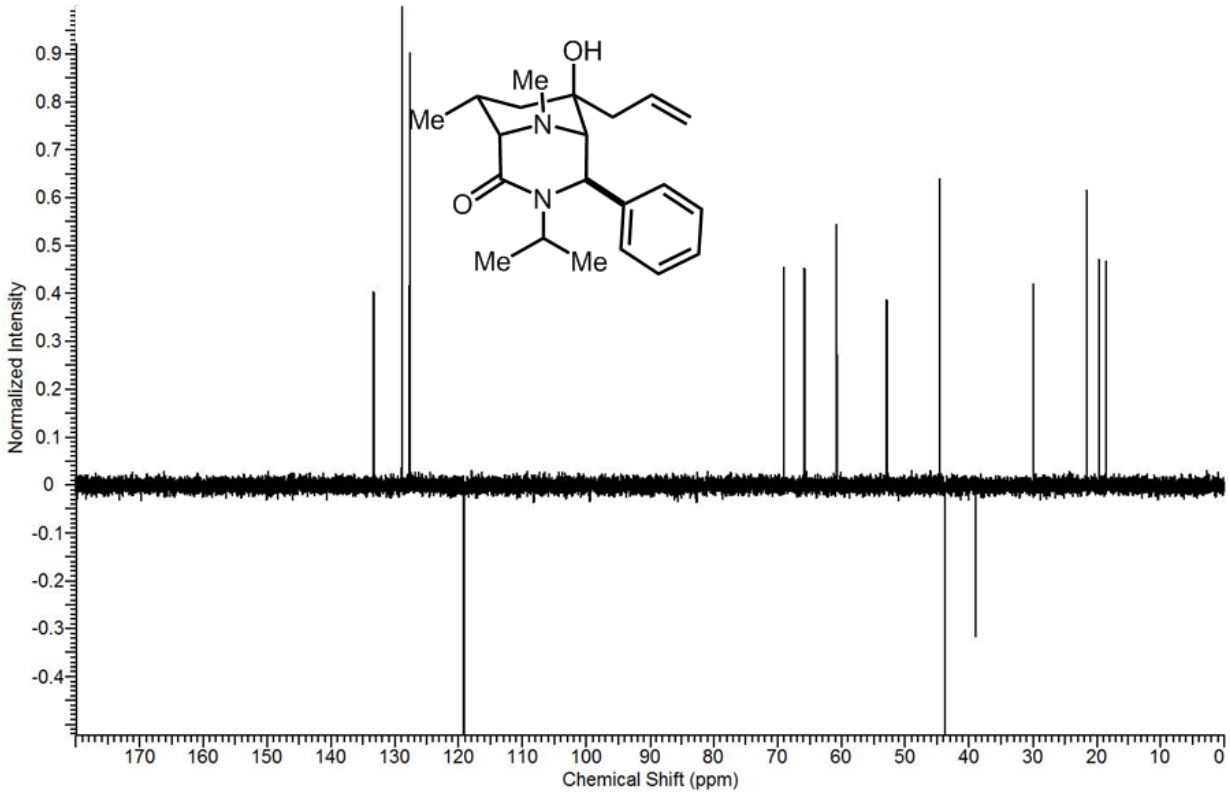

Spectra 2-3 DEPT-135 NMR spectrum of **2a.**

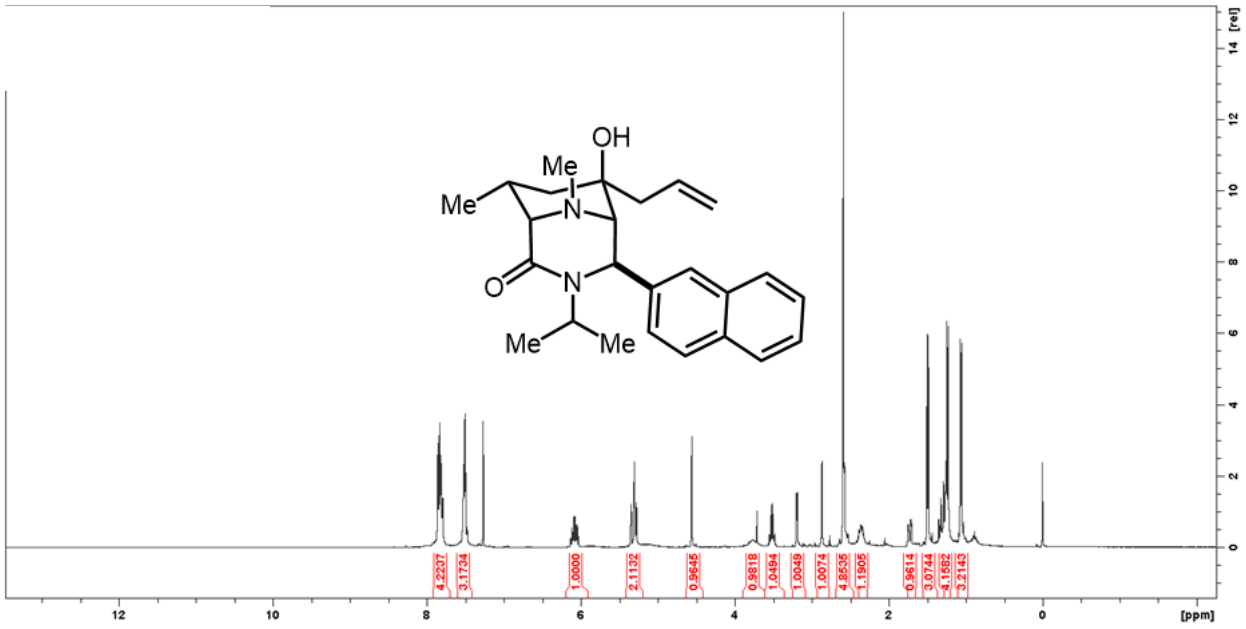

Spectra 2-4 Proton NMR spectrum of **2b.**

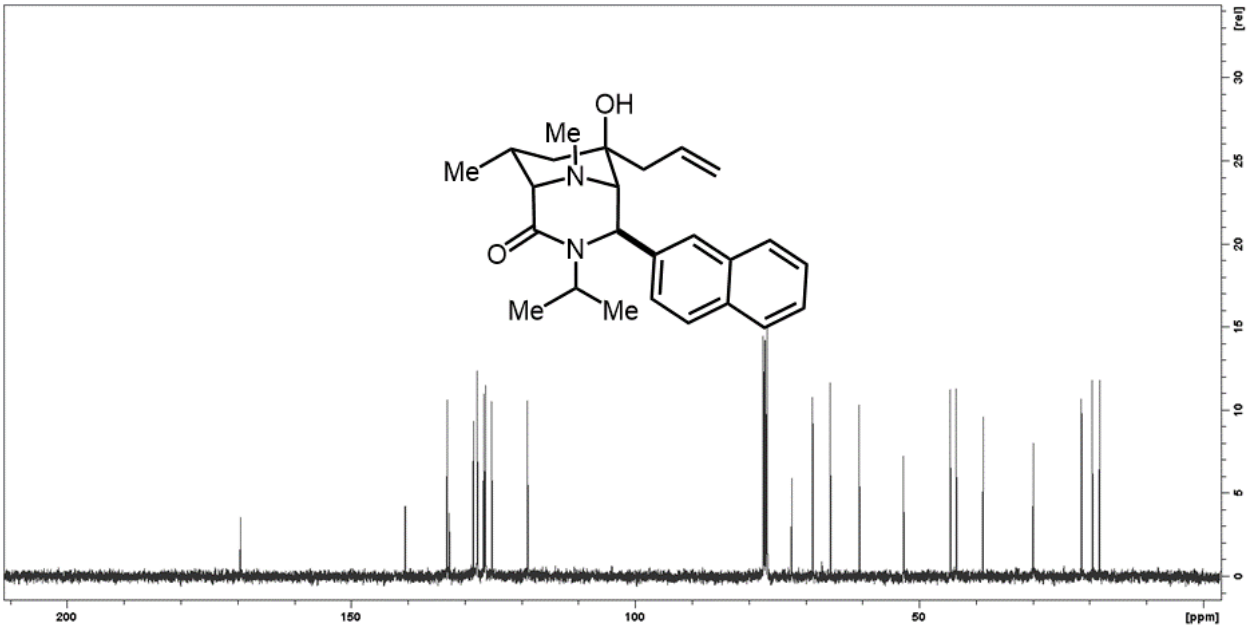

Spectra 2-5 Carbon NMR spectrum of **2b.**

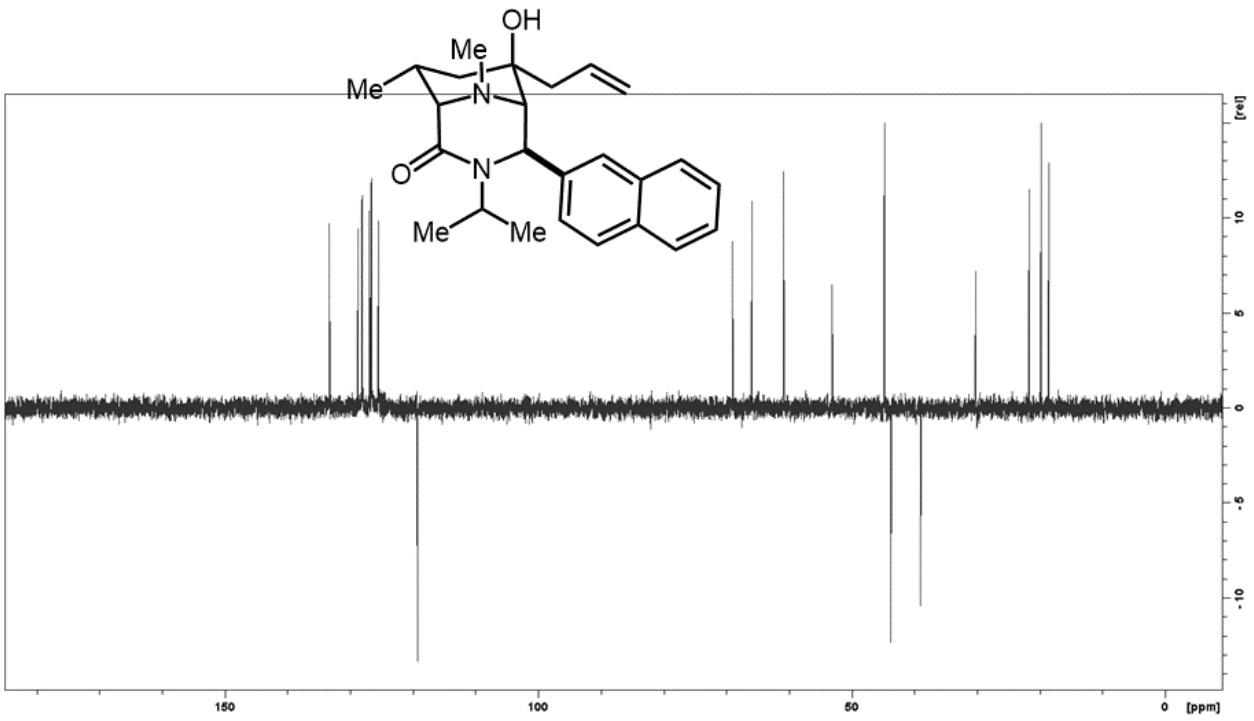

Spectra 2-6 DEPT-135 NMR spectrum of **2b.**

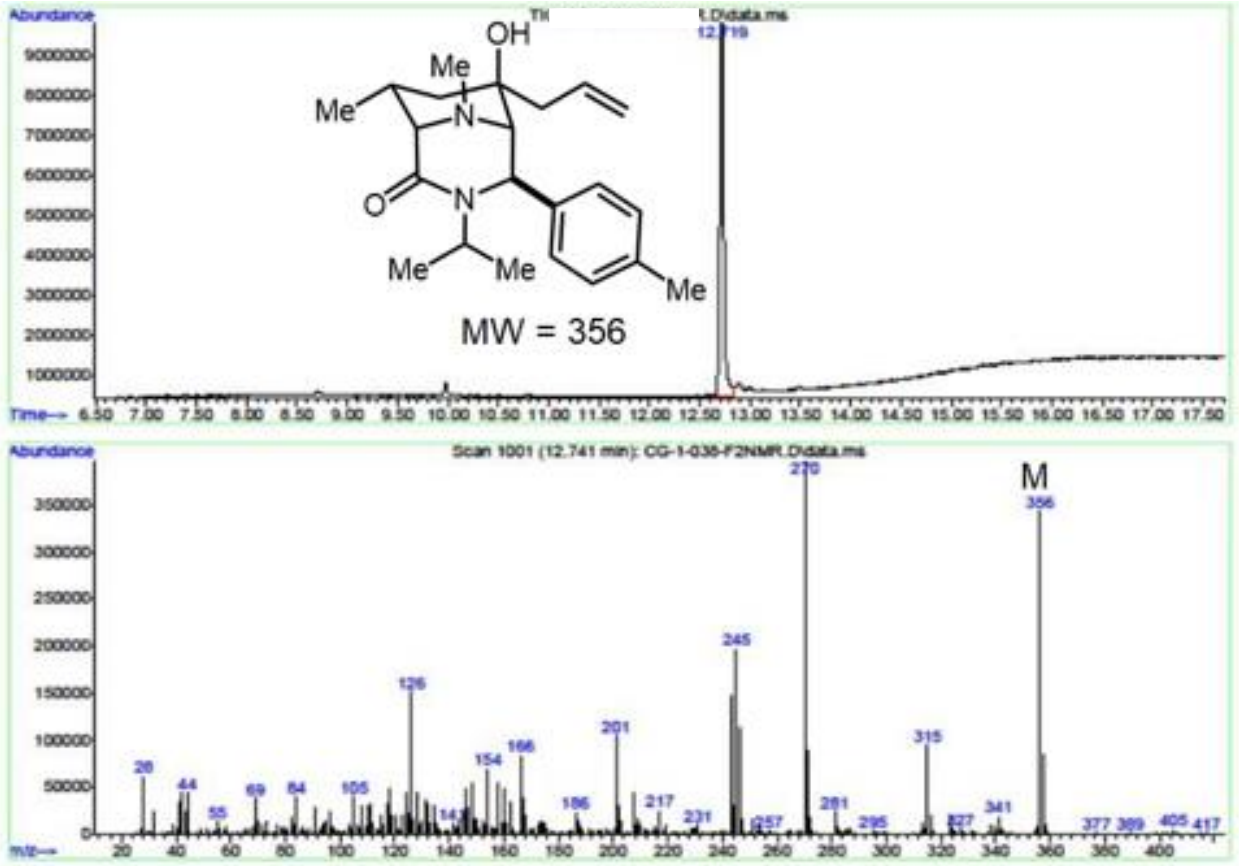

Spectra 2-7 DEPT-135 NMR spectrum of **2c.**

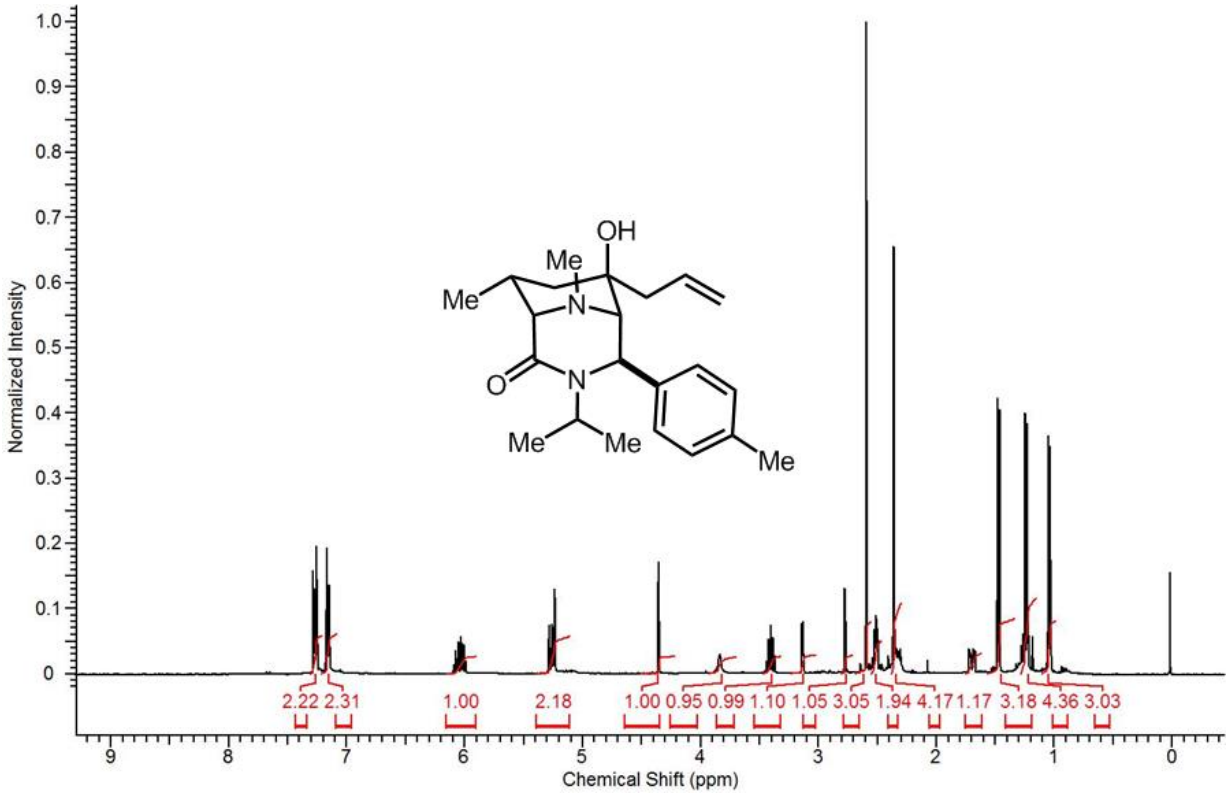

Spectra 2-8 Proton NMR spectrum of **2c.**

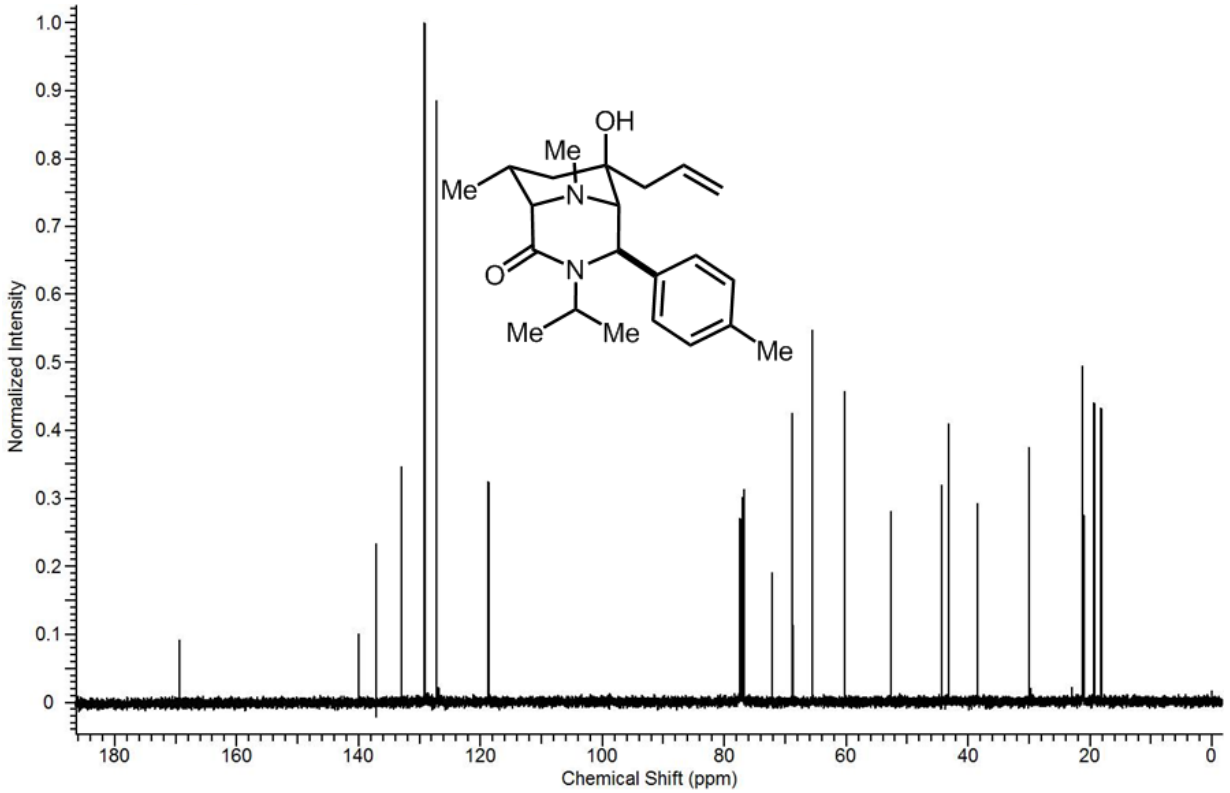

Spectra 2-9 Carbon NMR spectrum of **2c.**

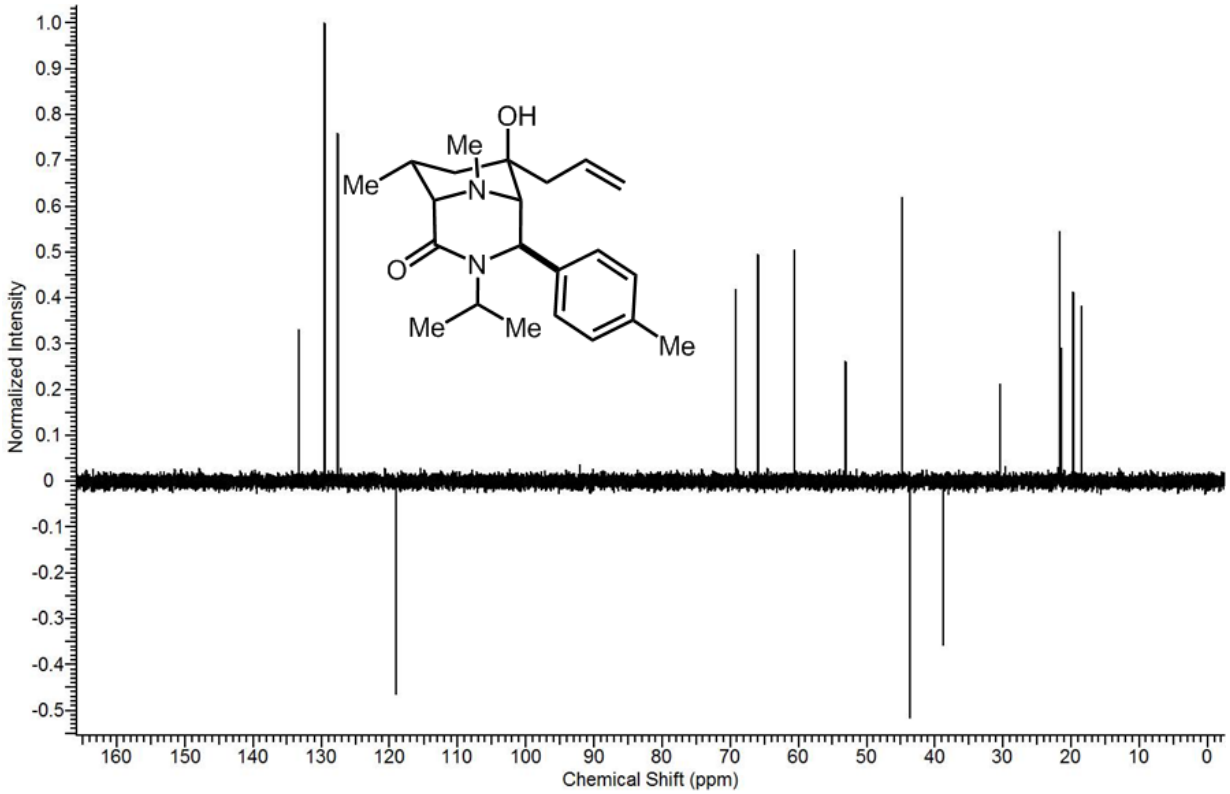

Spectra 2-10 DEPT-135 NMR spectrum of **2c.**

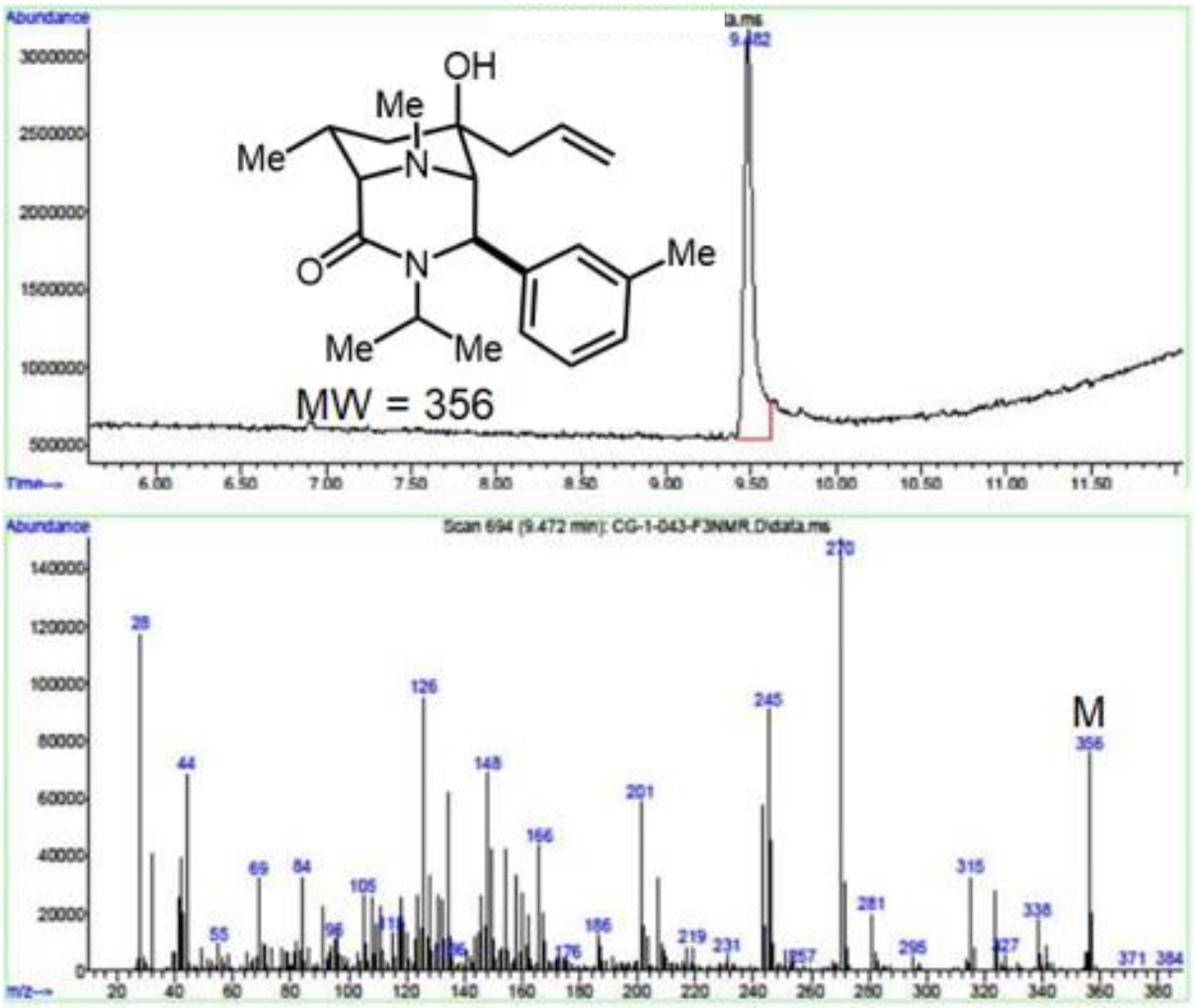

Spectra 2-11 DEPT-135 NMR spectrum of **2d.**

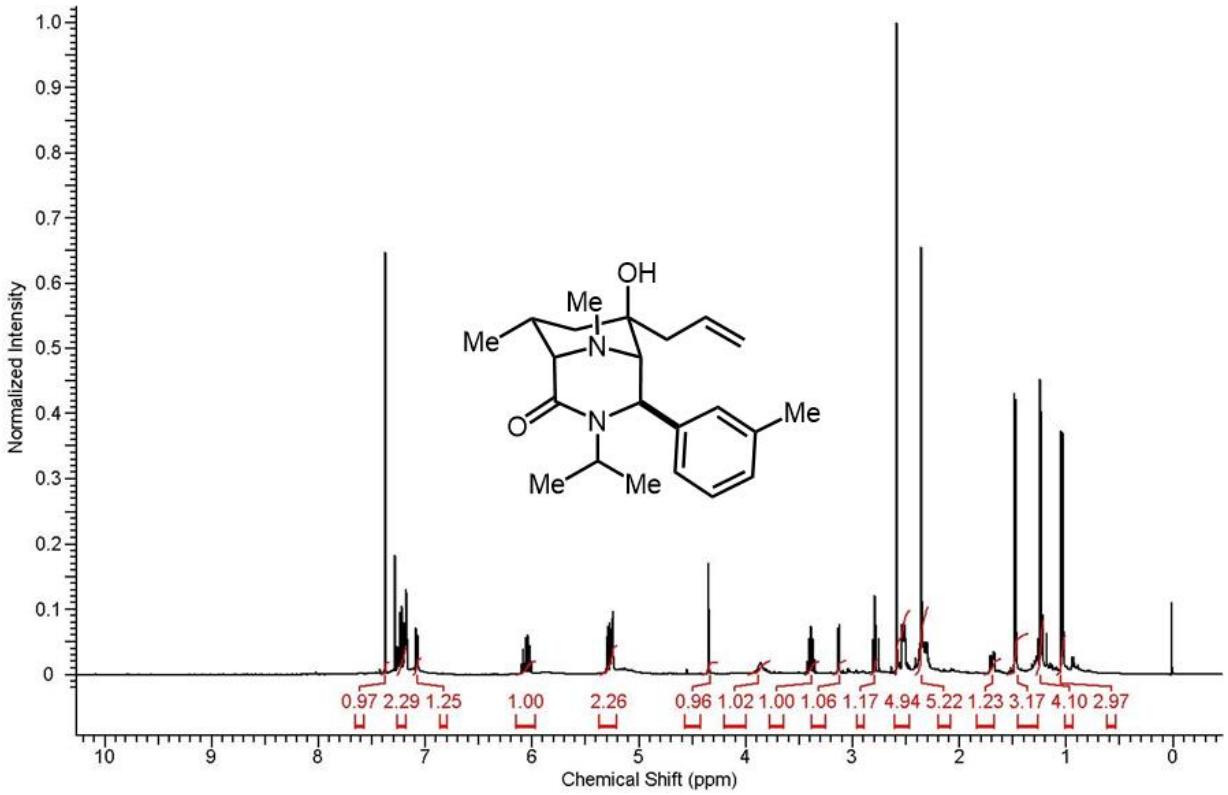

Spectra 2-12 Proton NMR spectrum of **2d.**

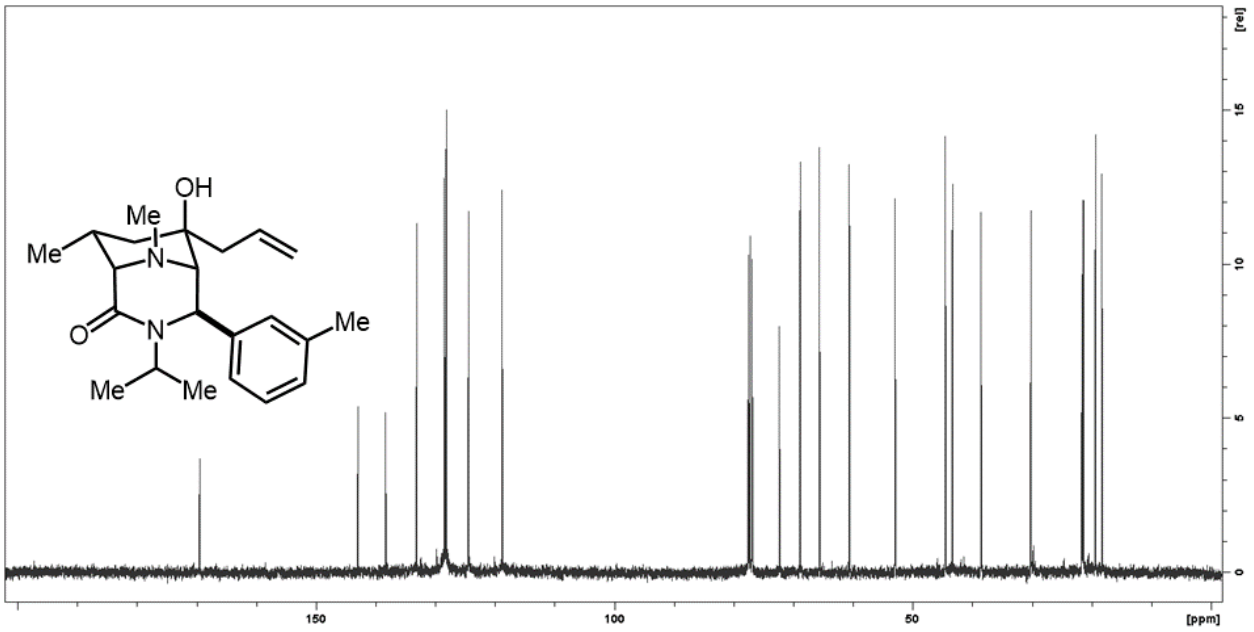

Spectra 2-13 Carbon NMR spectrum of **2d.**

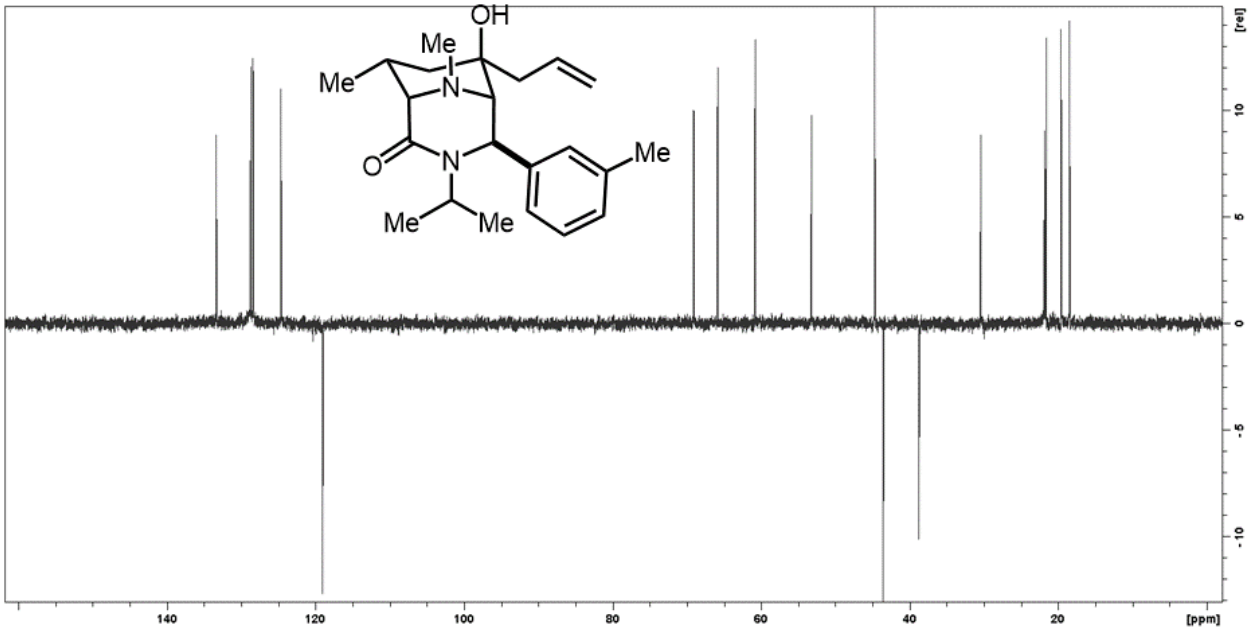

Spectra 2-14 DEPT-135 NMR spectrum of **2d.**

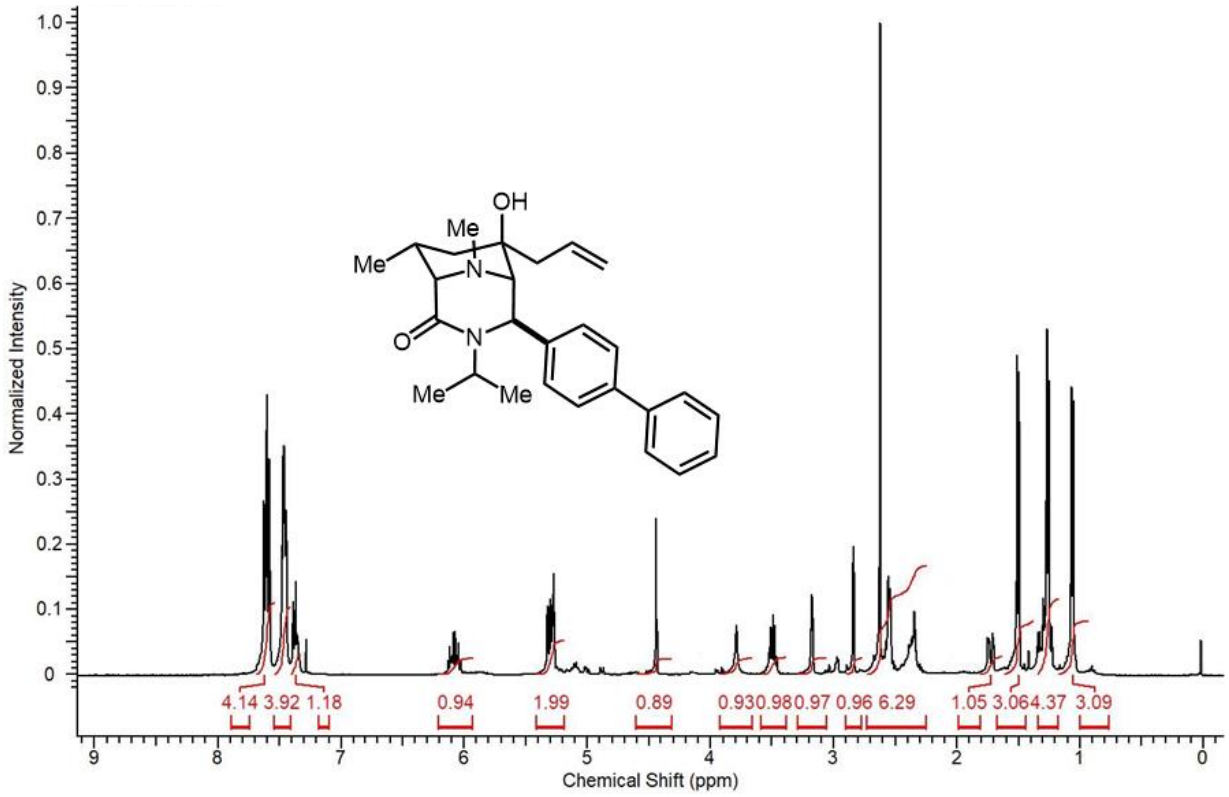

Spectra 2-15 Proton NMR spectrum of **2e**

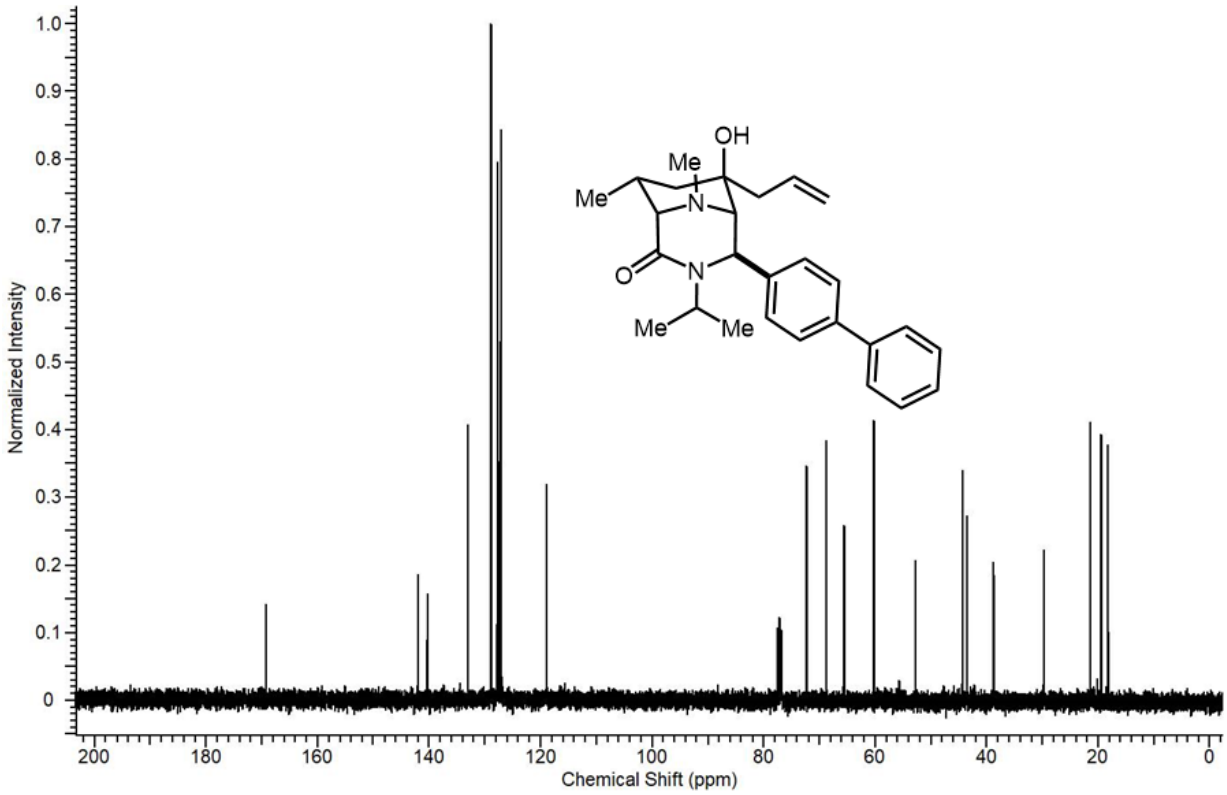

Spectra 2-16 Carbon NMR spectrum of **2e.**

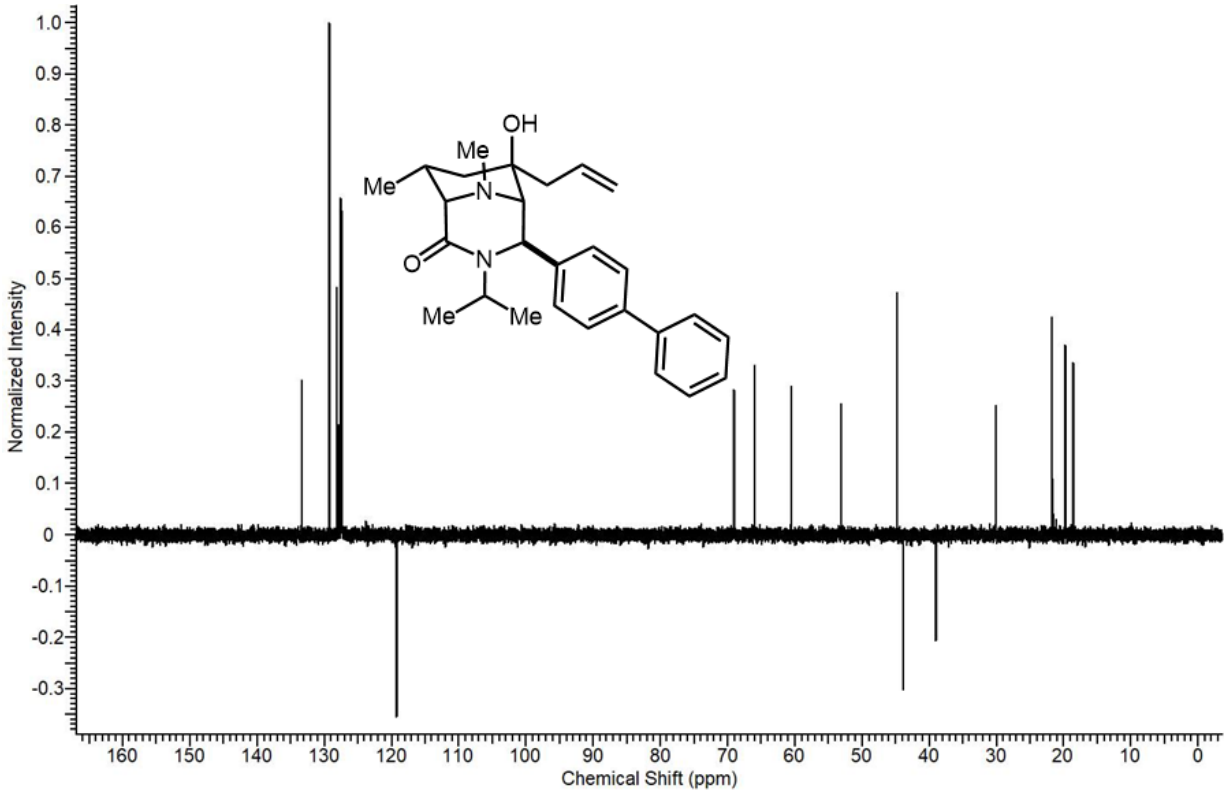

Spectra 2-17 DEPT-135 NMR spectrum of **2e.**

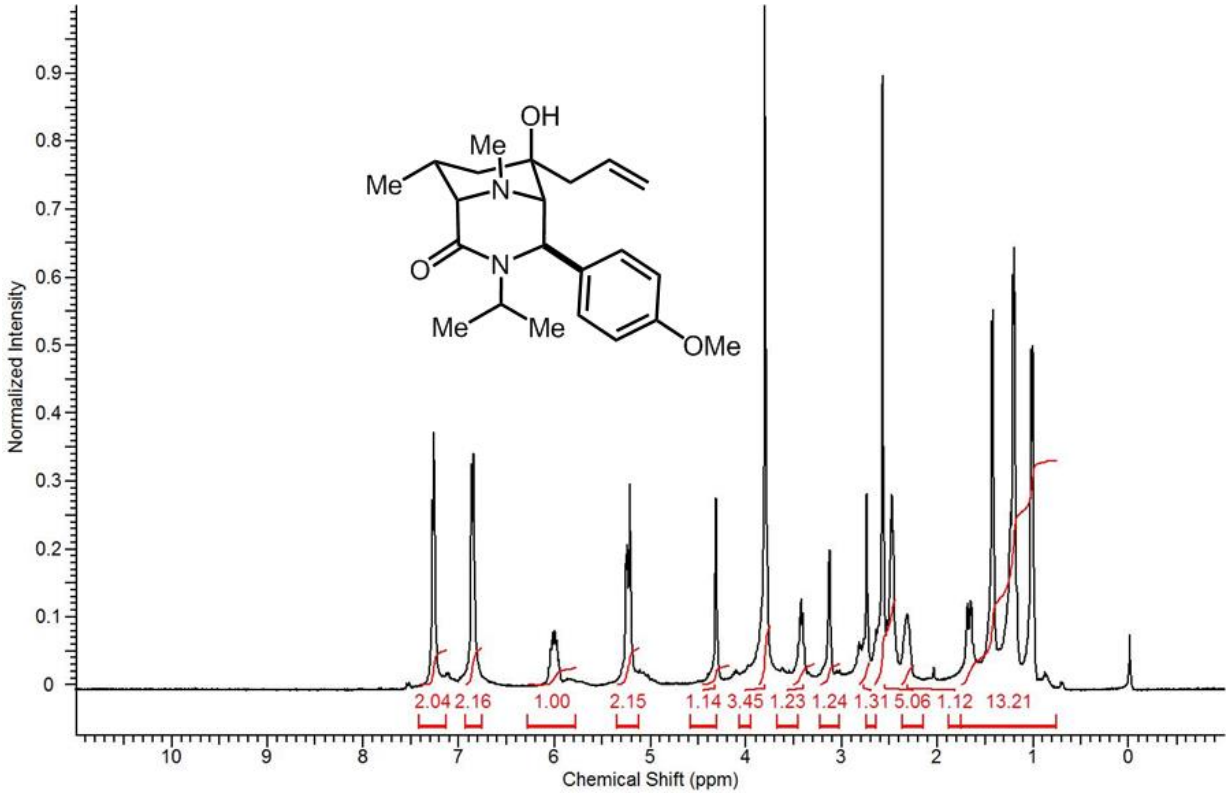

Spectra 2-18 Proton NMR spectrum of **2f.**

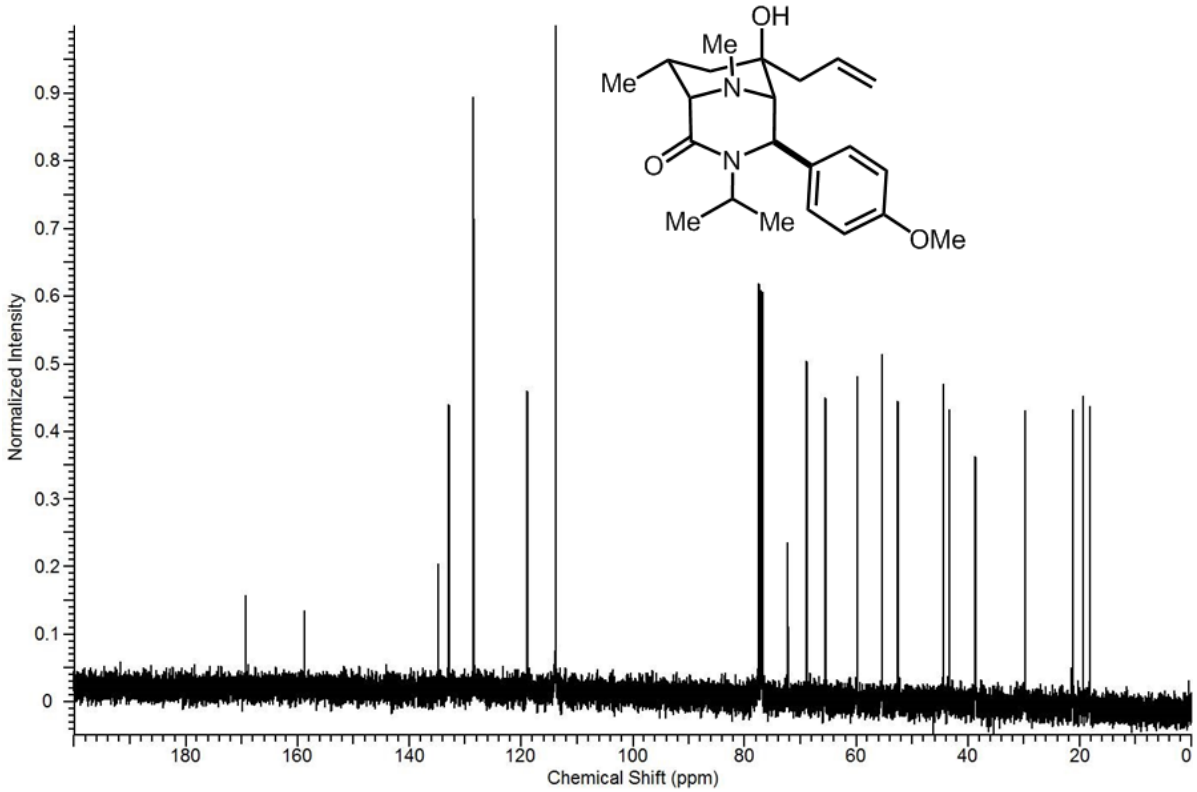

Spectra 2-19 Carbon NMR spectrum of **2f.**

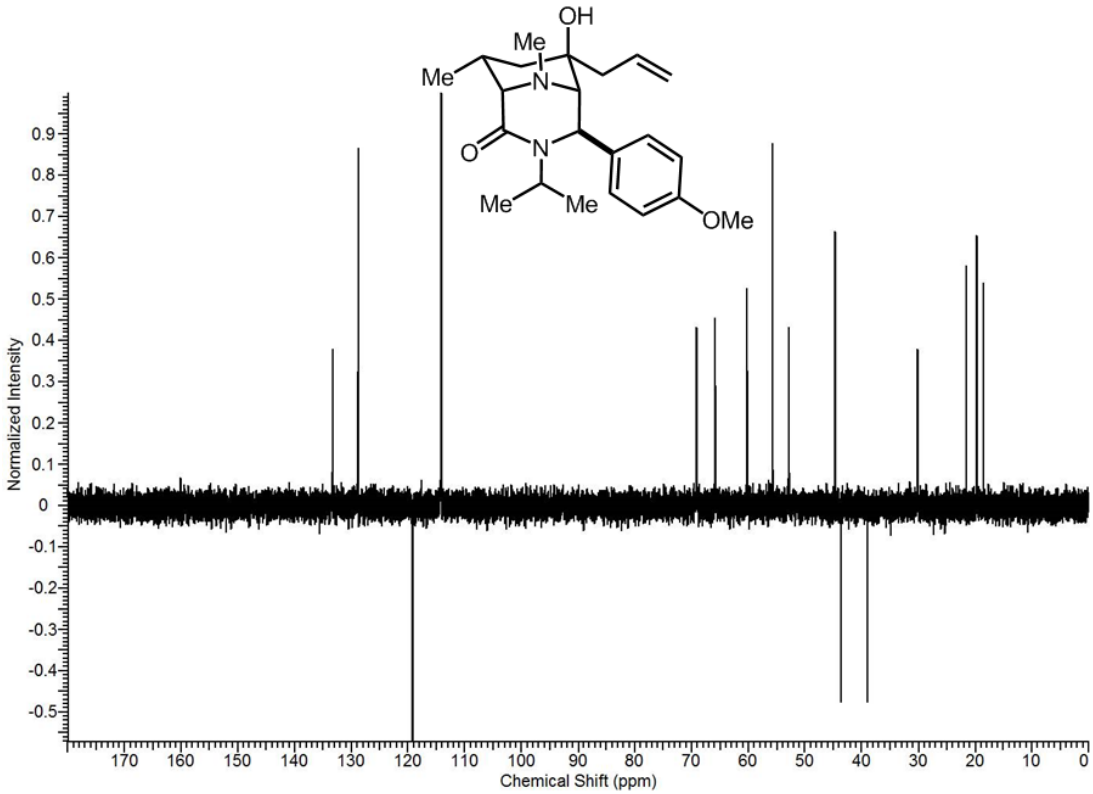

Spectra 2-20 DEPT-135 NMR spectrum of **2f.**

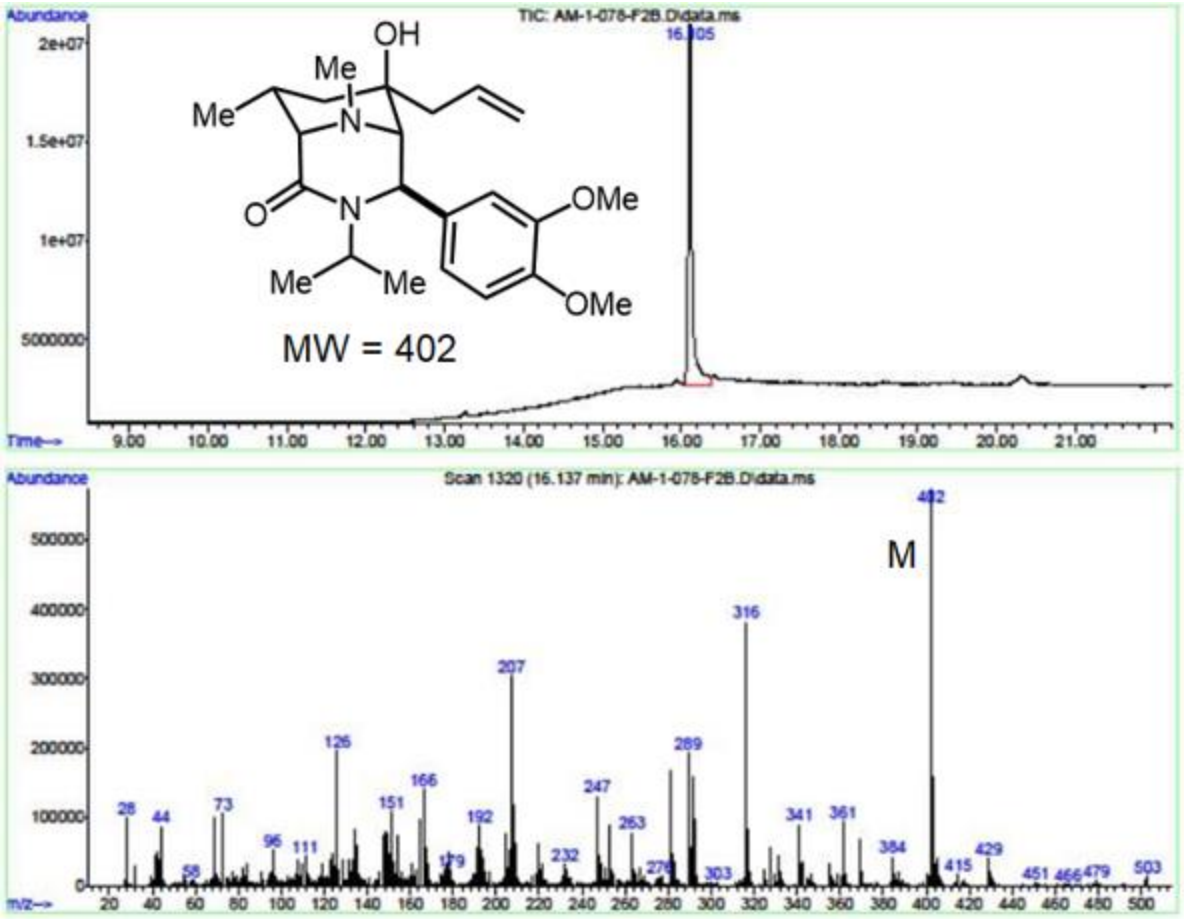

Spectra 2-21 GC-MS spectrum of **2g.**

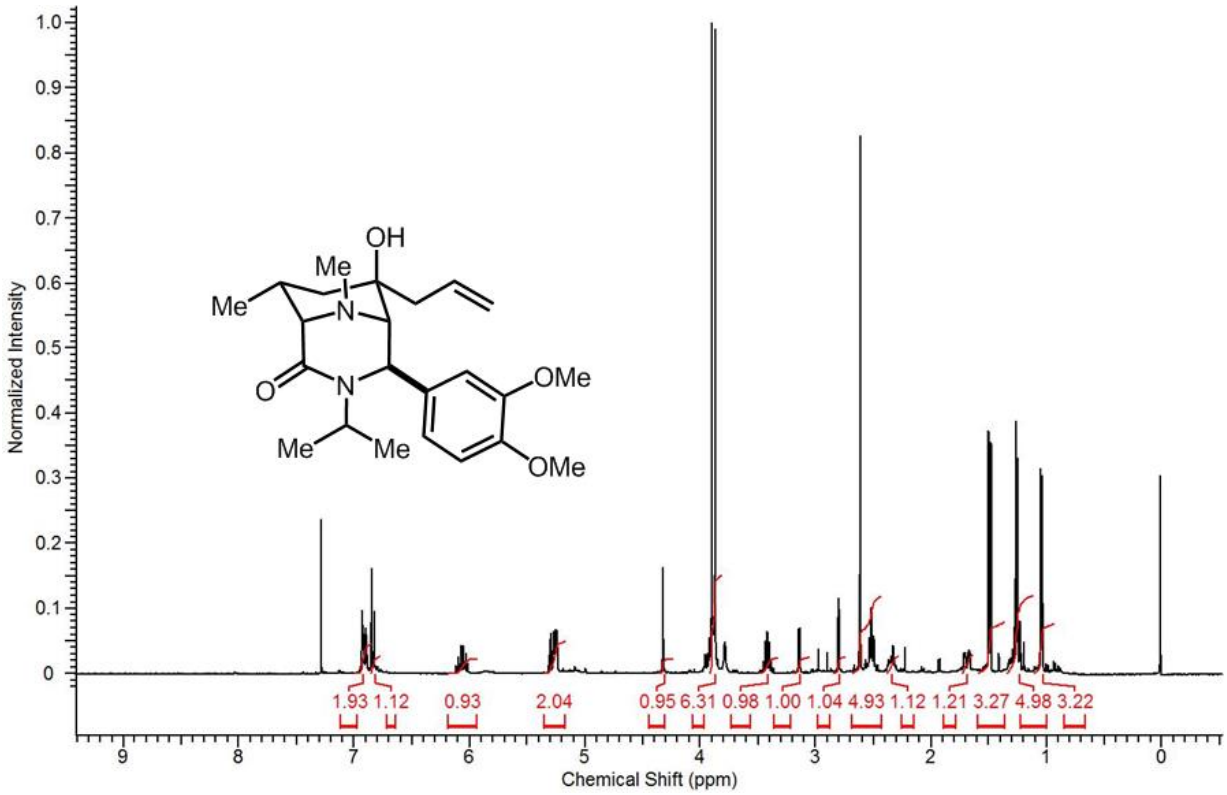

Spectra 2-22 Proton NMR spectrum of **2g.**

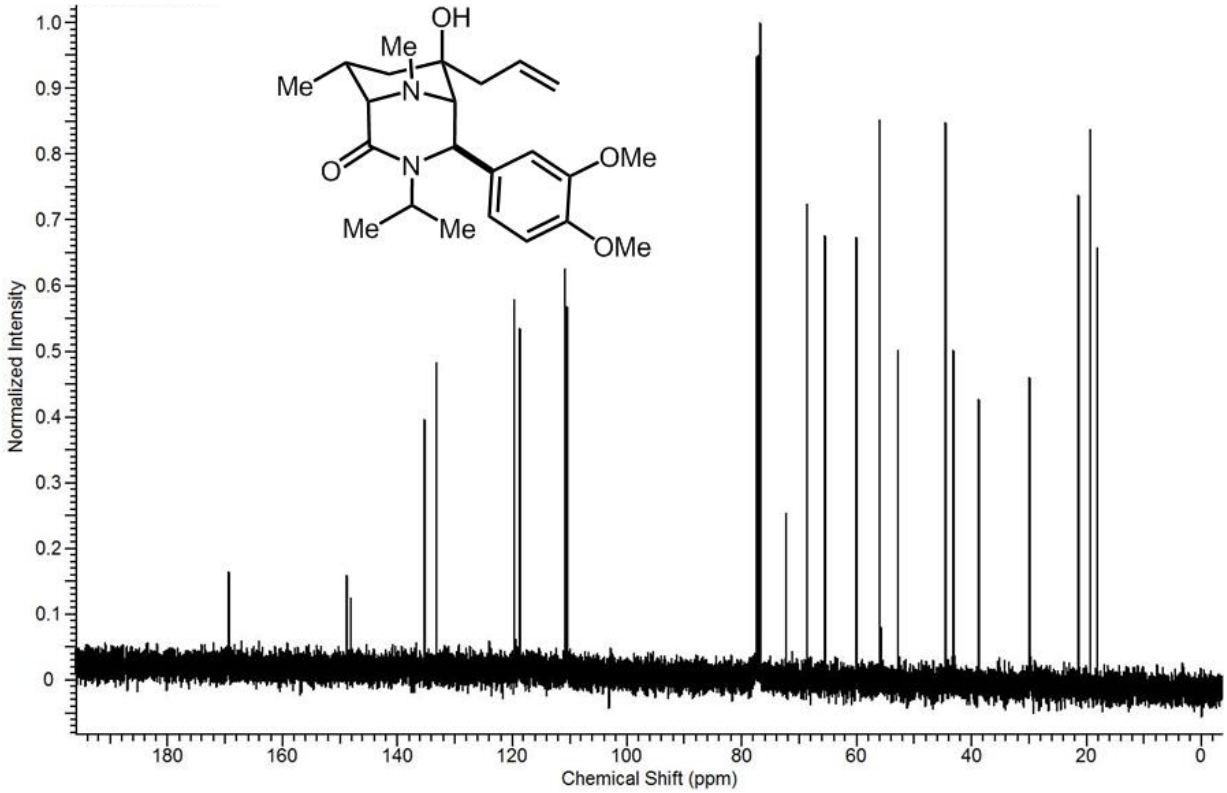

Spectra 2-23 Carbon NMR spectrum of **2g.**

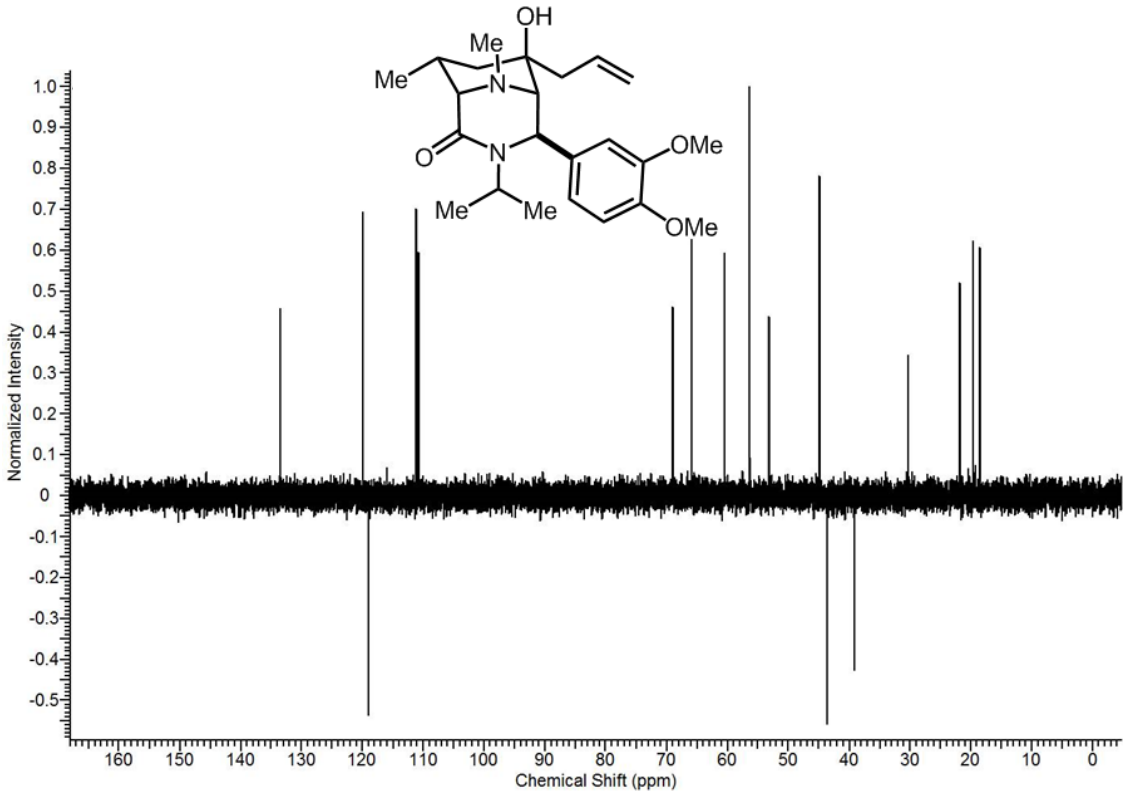

Spectra 2-24 DEPT-135 NMR spectrum of **2g.**

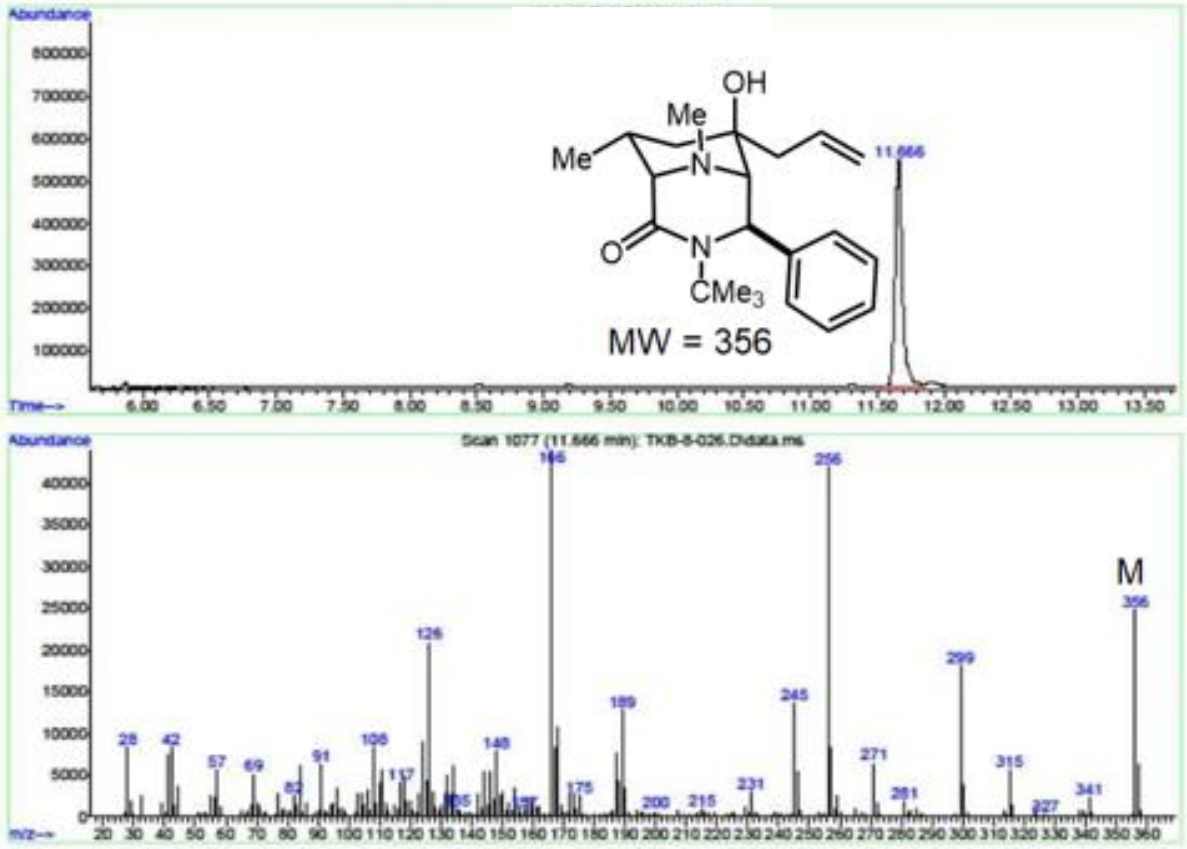

Spectra 2-25 GC-MS spectrum of **2h.**

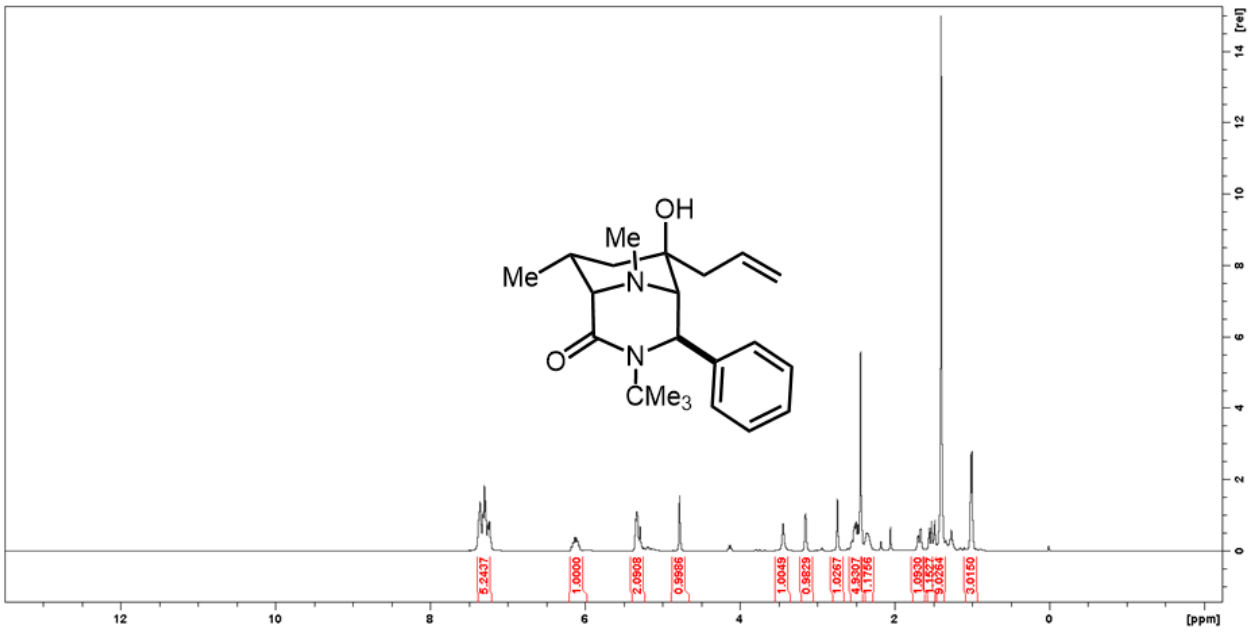

Spectra 2-26 Proton NMR spectrum of **2h.**

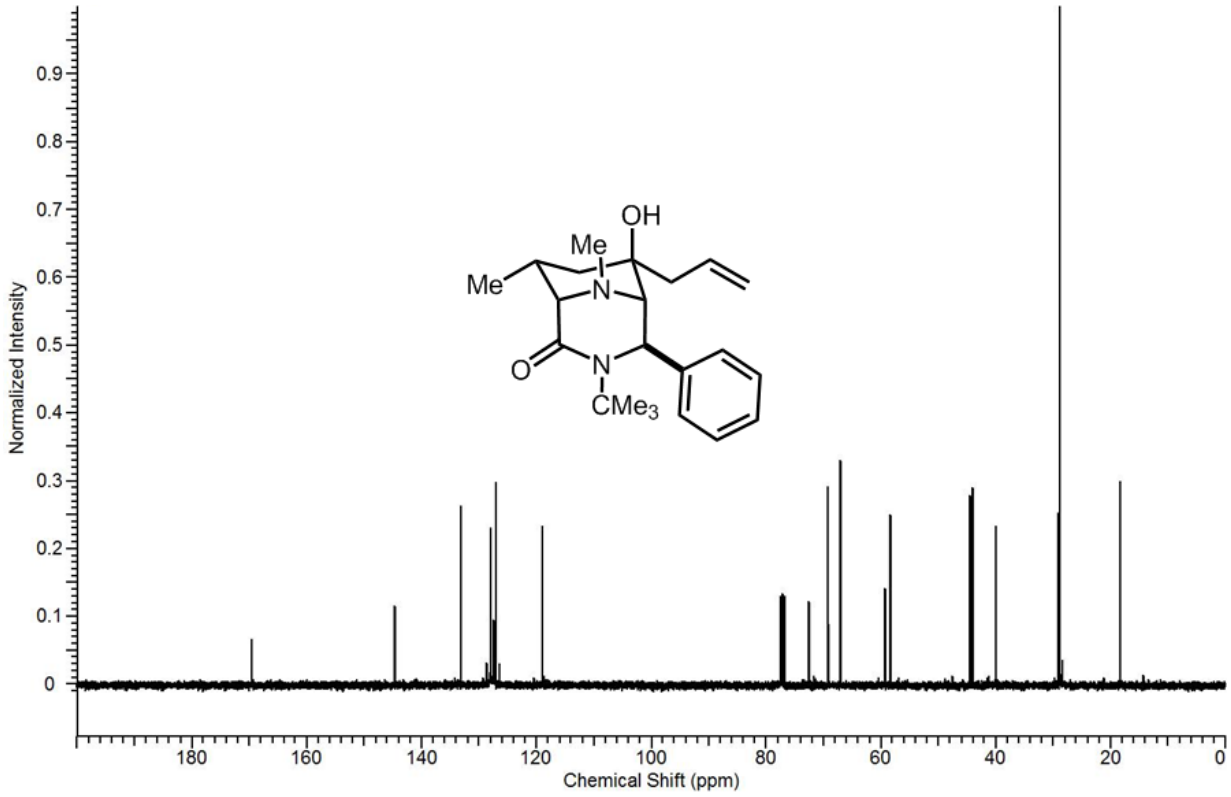

Spectra 2-27 Carbon NMR spectrum of **2h.**

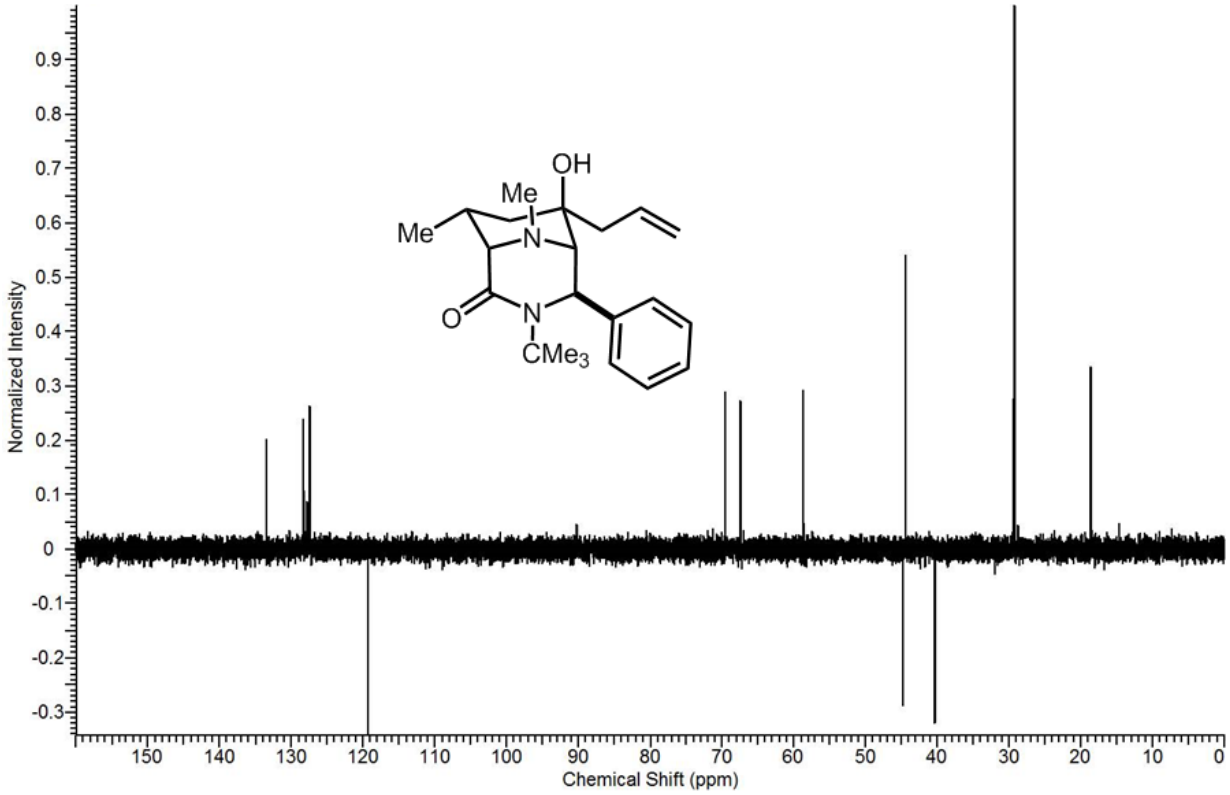

Spectra 2-28 DEPT-135 NMR spectrum of **2h.**

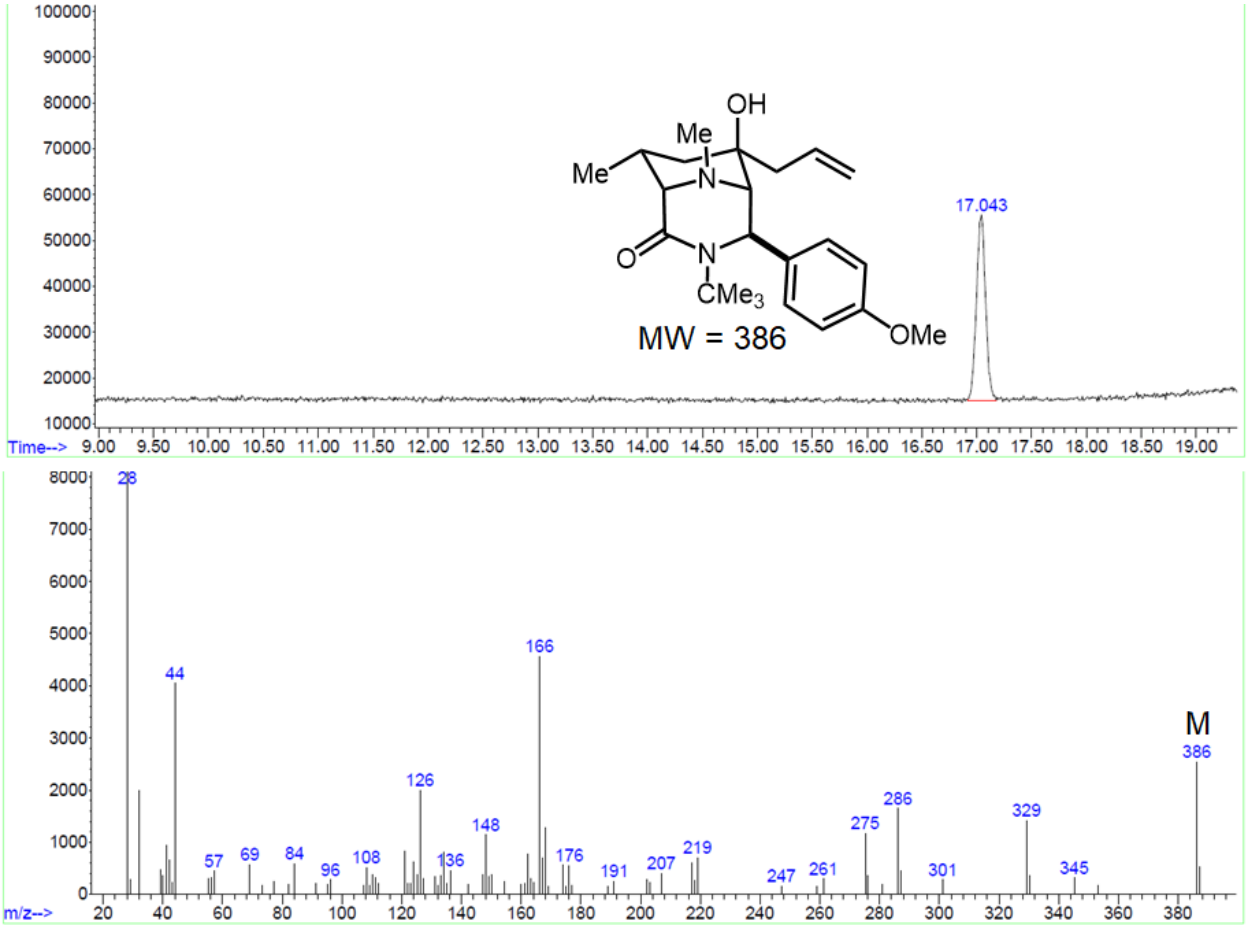

Spectra 1-29 DEPT-135 NMR spectrum of **2i.**

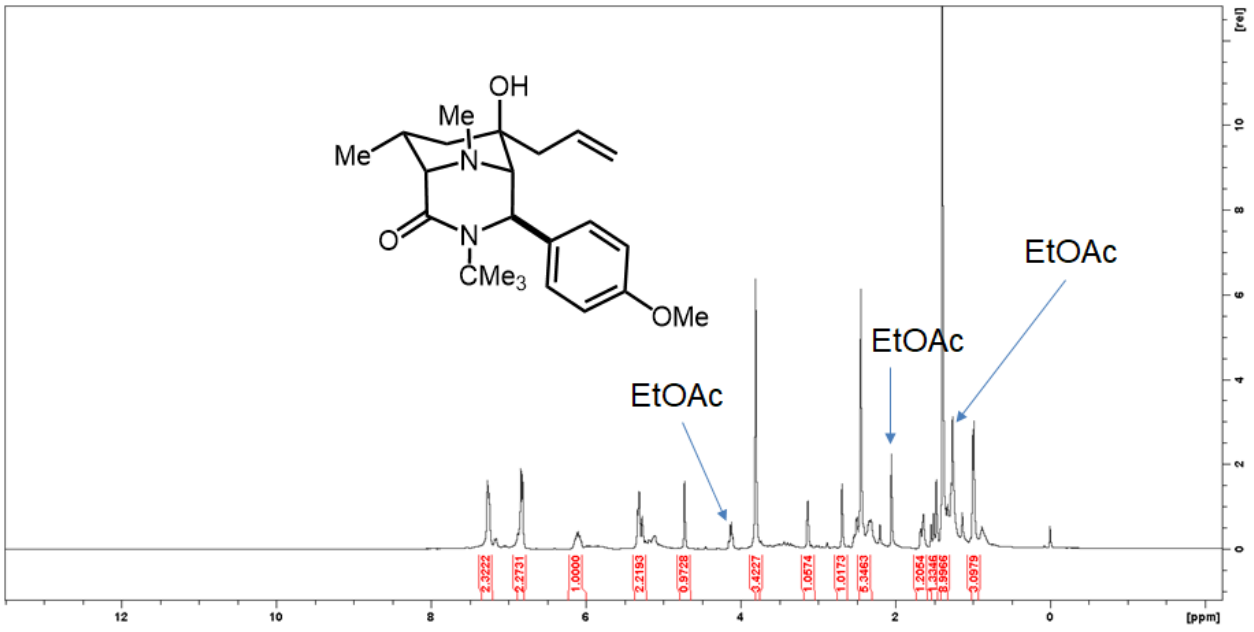

Spectra 2-30 Proton NMR spectrum of **2i.**

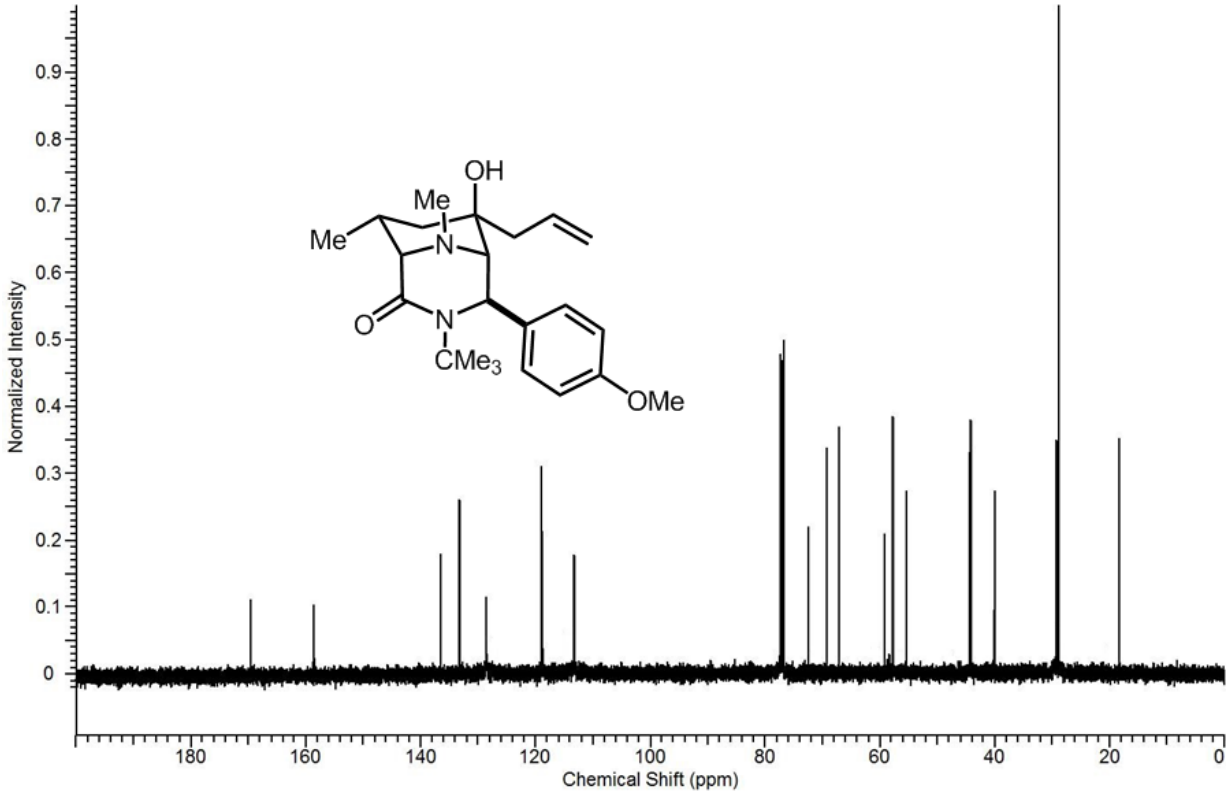

Spectra 2-31 Carbon NMR spectrum of **2i.**

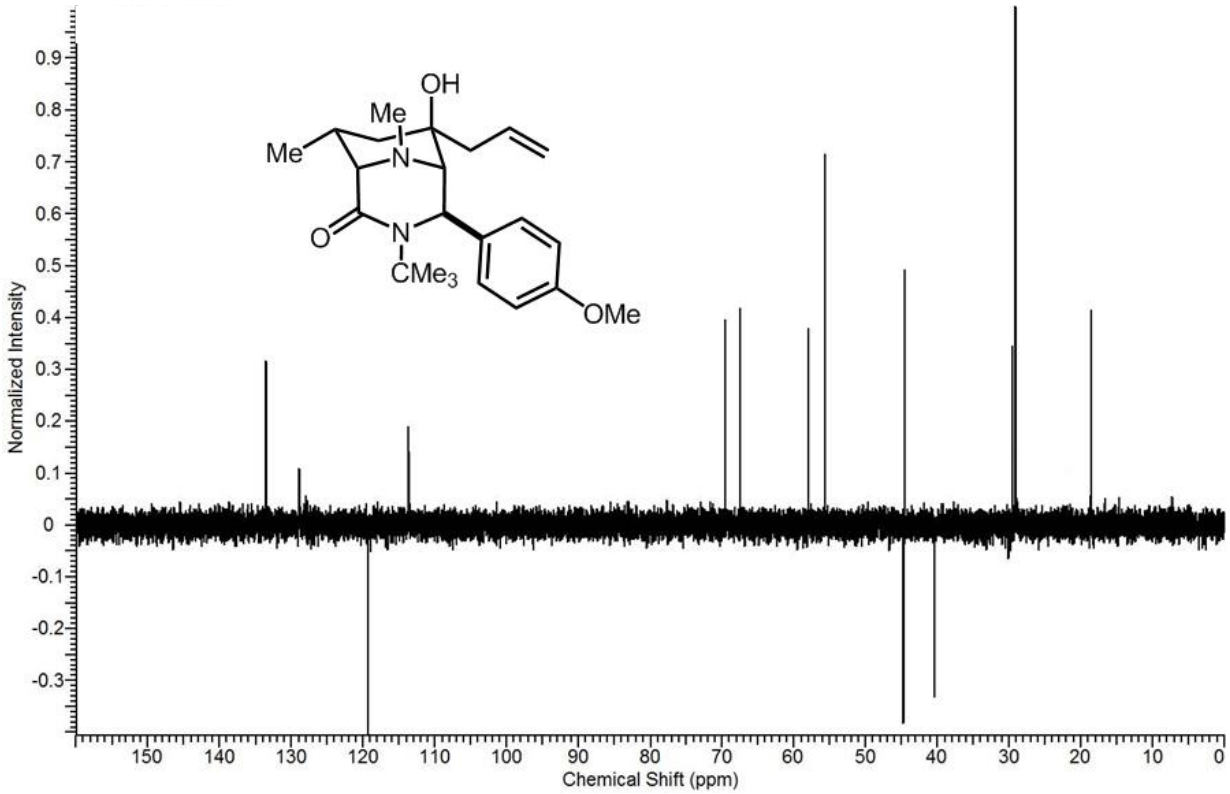

Spectra 2-32 DEPT-135 NMR spectrum of **2i.**

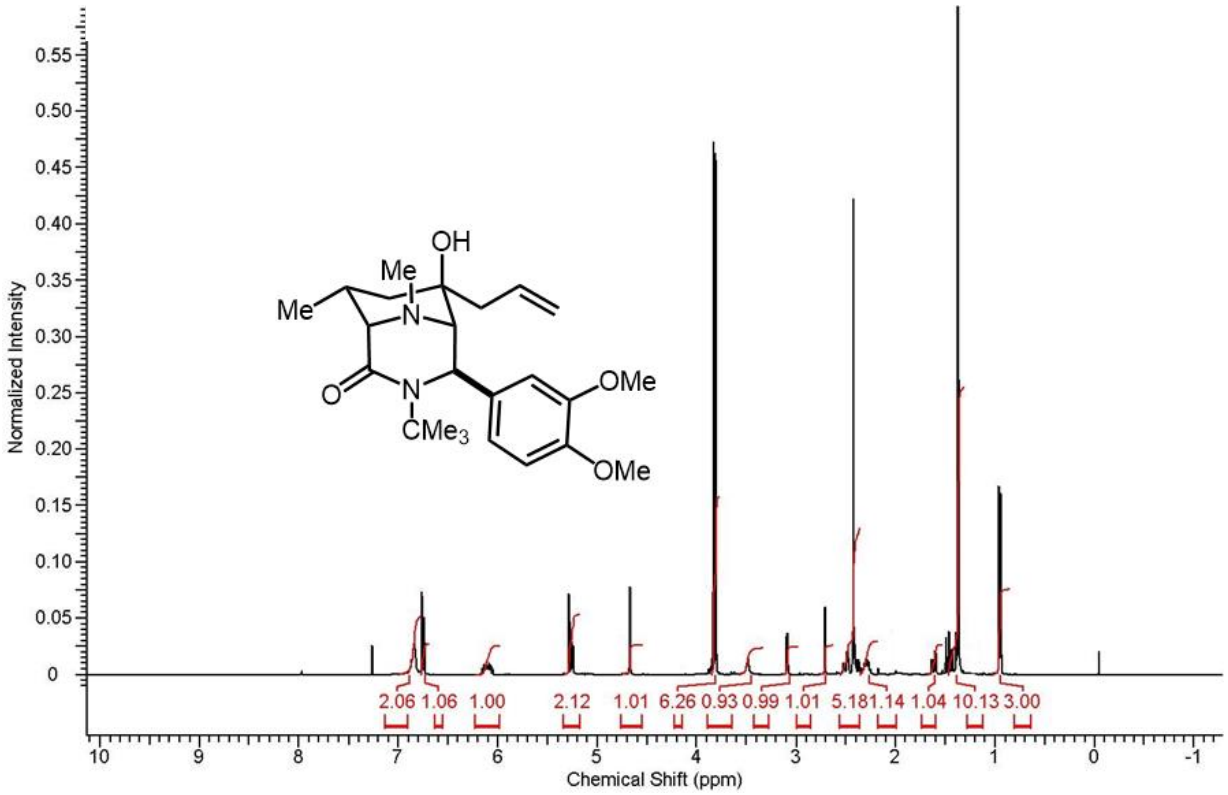

Spectra 2-33 Proton NMR spectrum of **2j.**

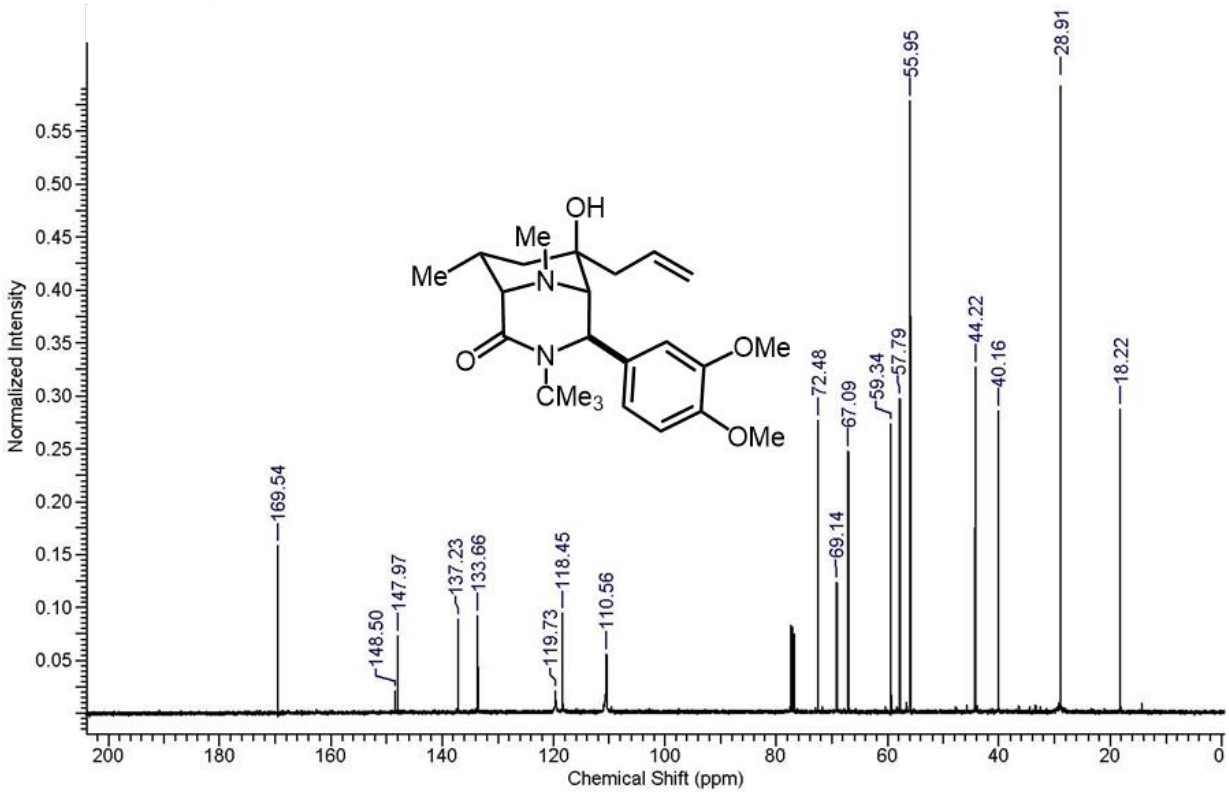

Spectra 2-34 Carbon NMR spectrum of **2j.**

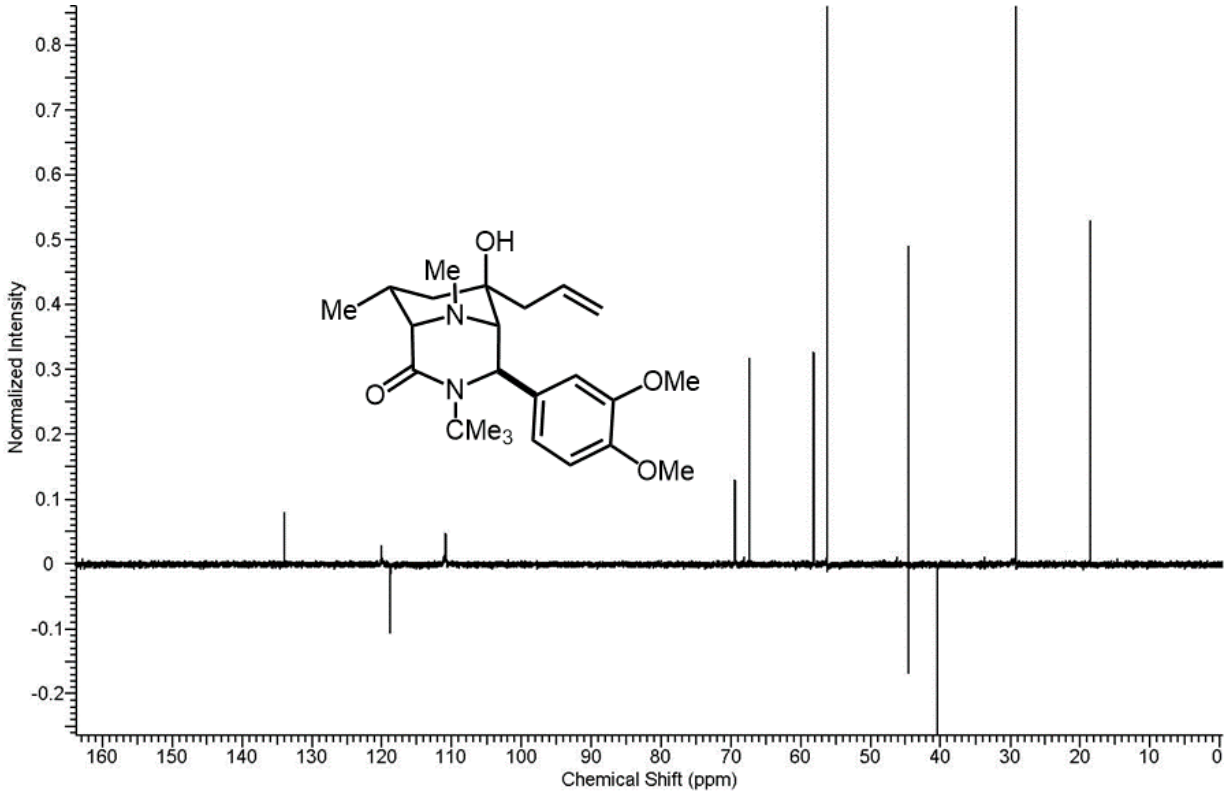

Spectra 2-35 DEPT-135 NMR spectrum of **2j.**

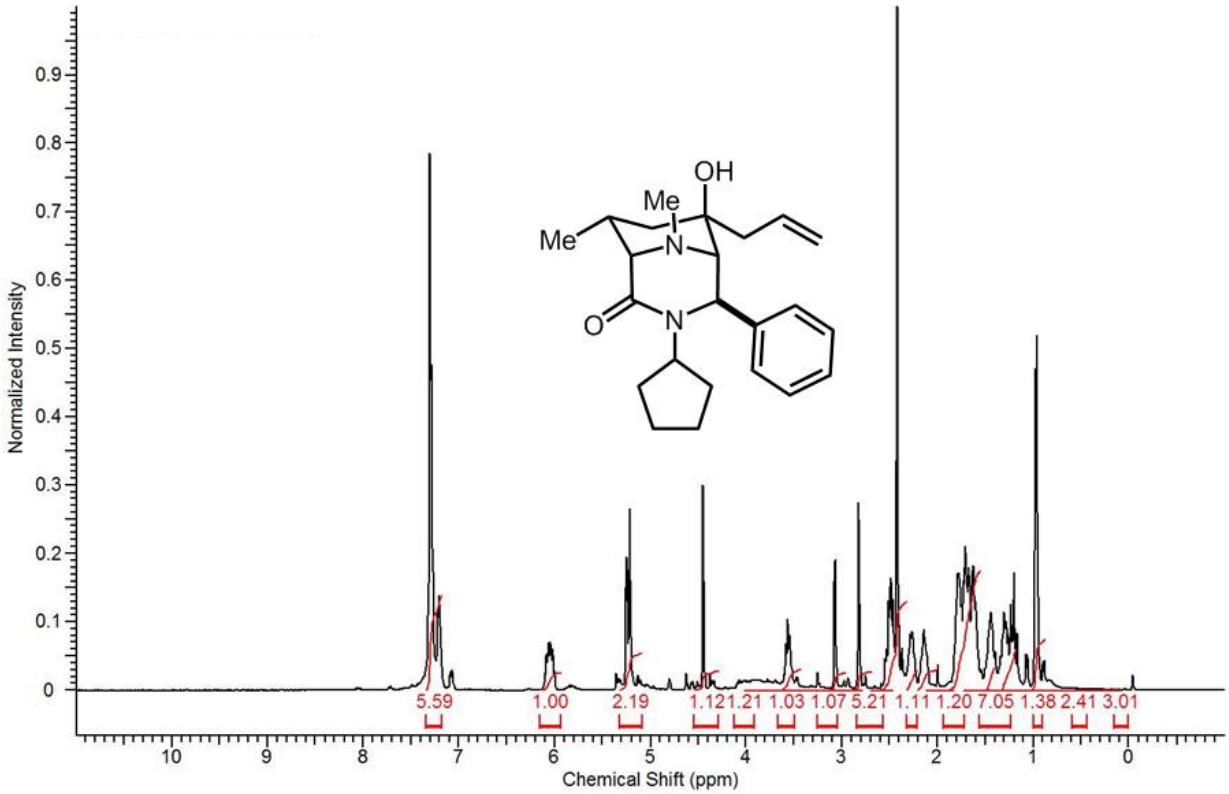

Spectra 2-36 Proton NMR spectrum of **2k**

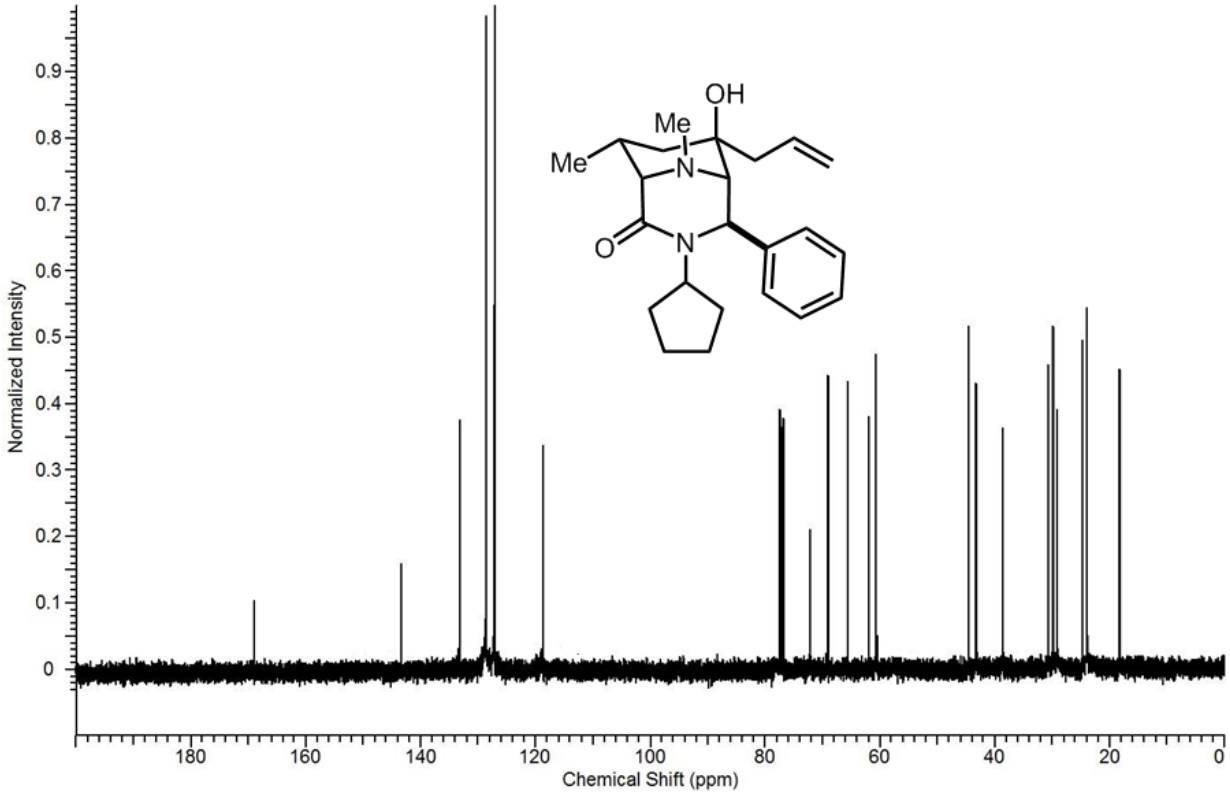

Spectra 2-37 Carbon NMR spectrum of **2k.**

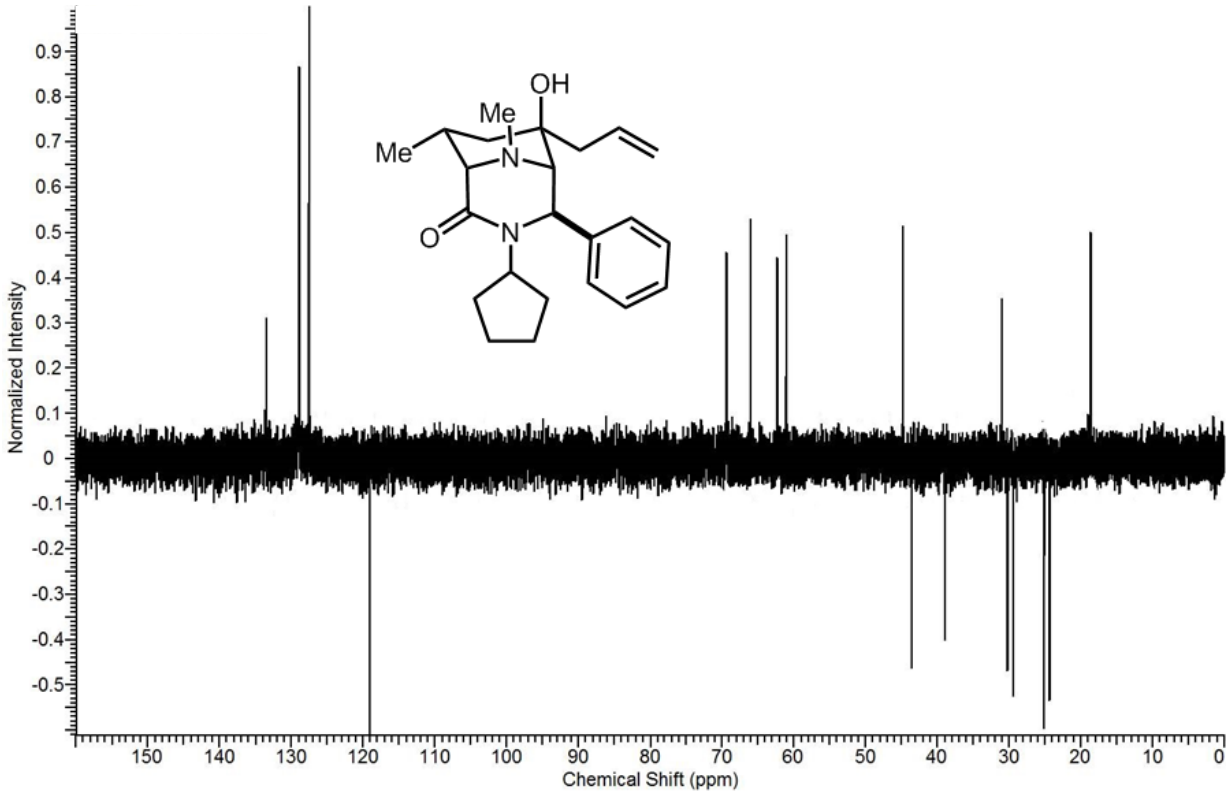

Spectra 2-38 DEPT-135 NMR spectrum of **2k.**

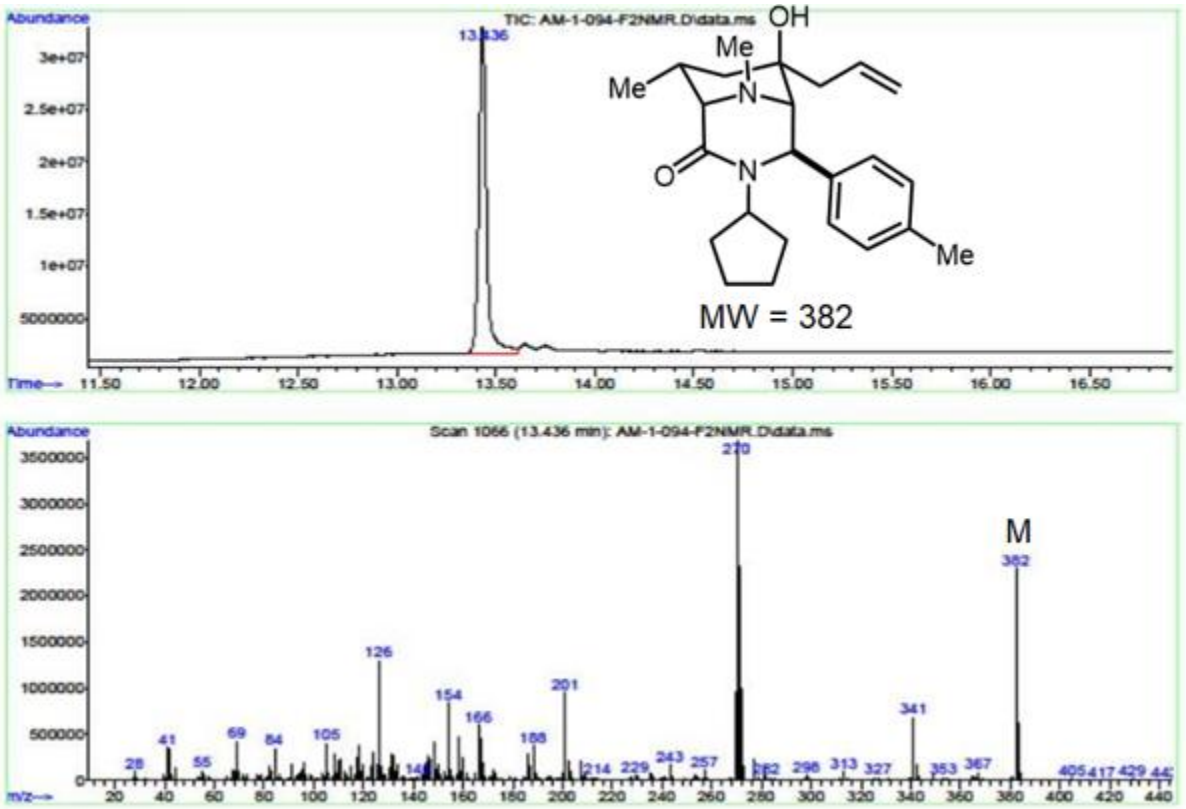

Spectra 2-39 GC-MS spectrum of **2l.**

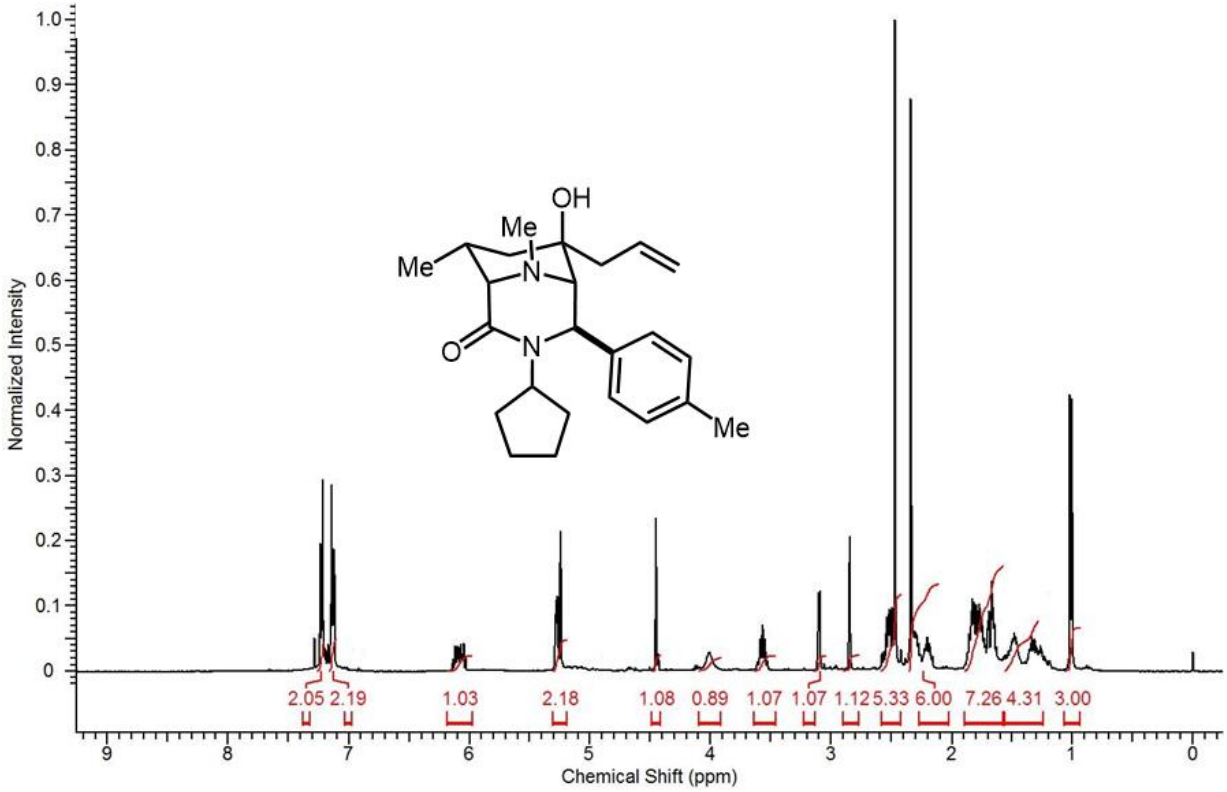

Spectra 2-40 Proton NMR spectrum of **2l.**

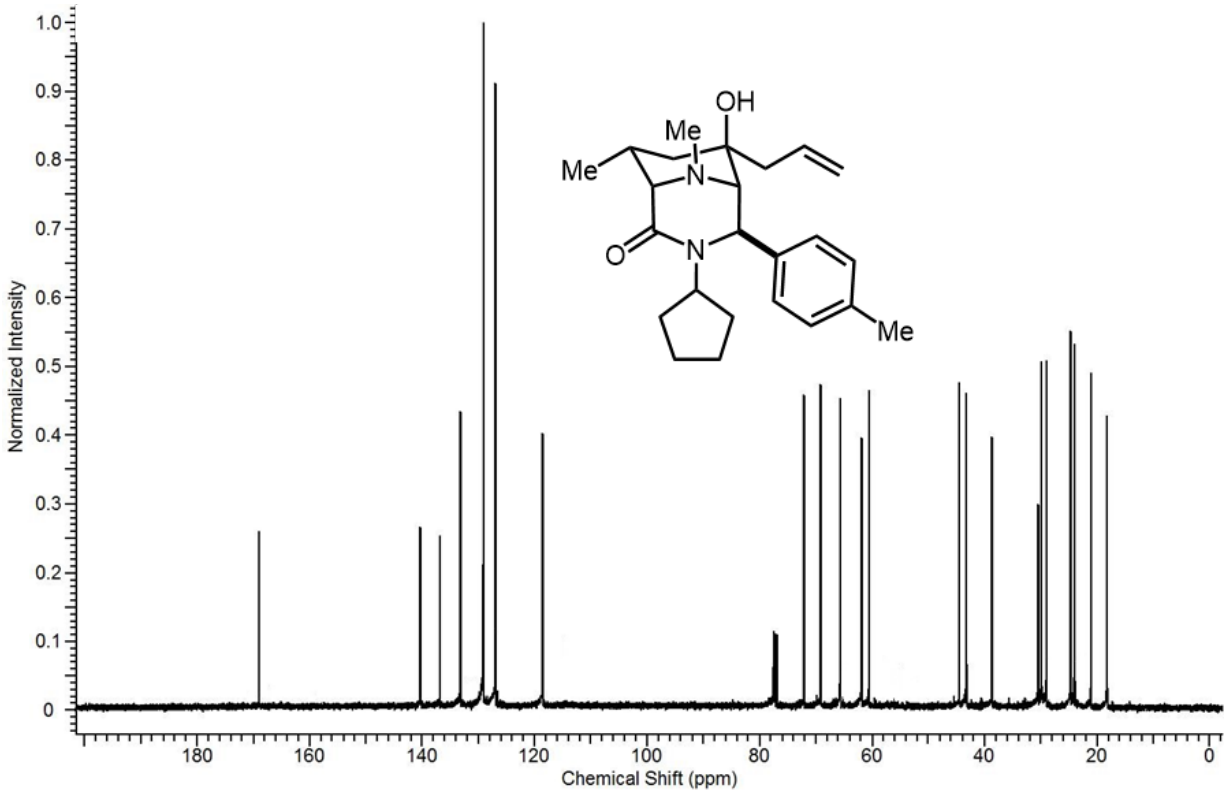

Spectra 2-41 Carbon NMR spectrum of **2l.**

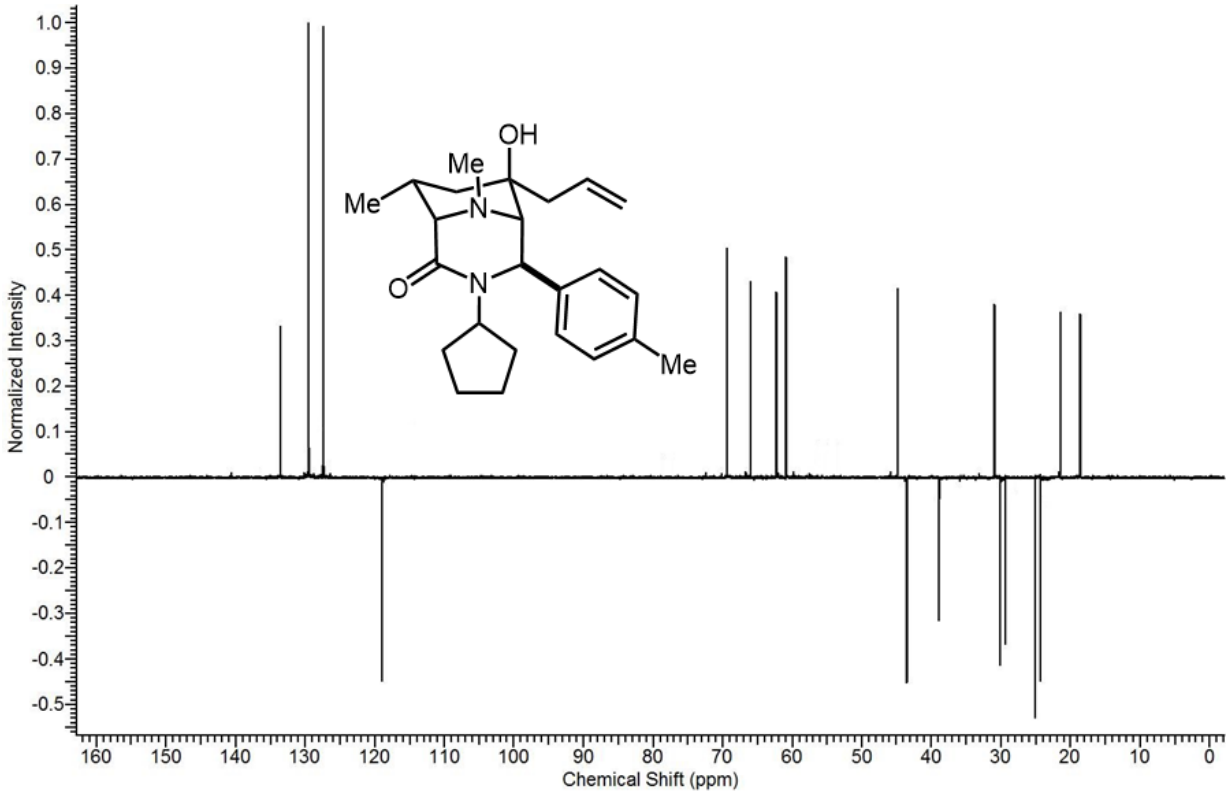

Spectra 2-42 DEPT-135 NMR spectrum of **2l.**

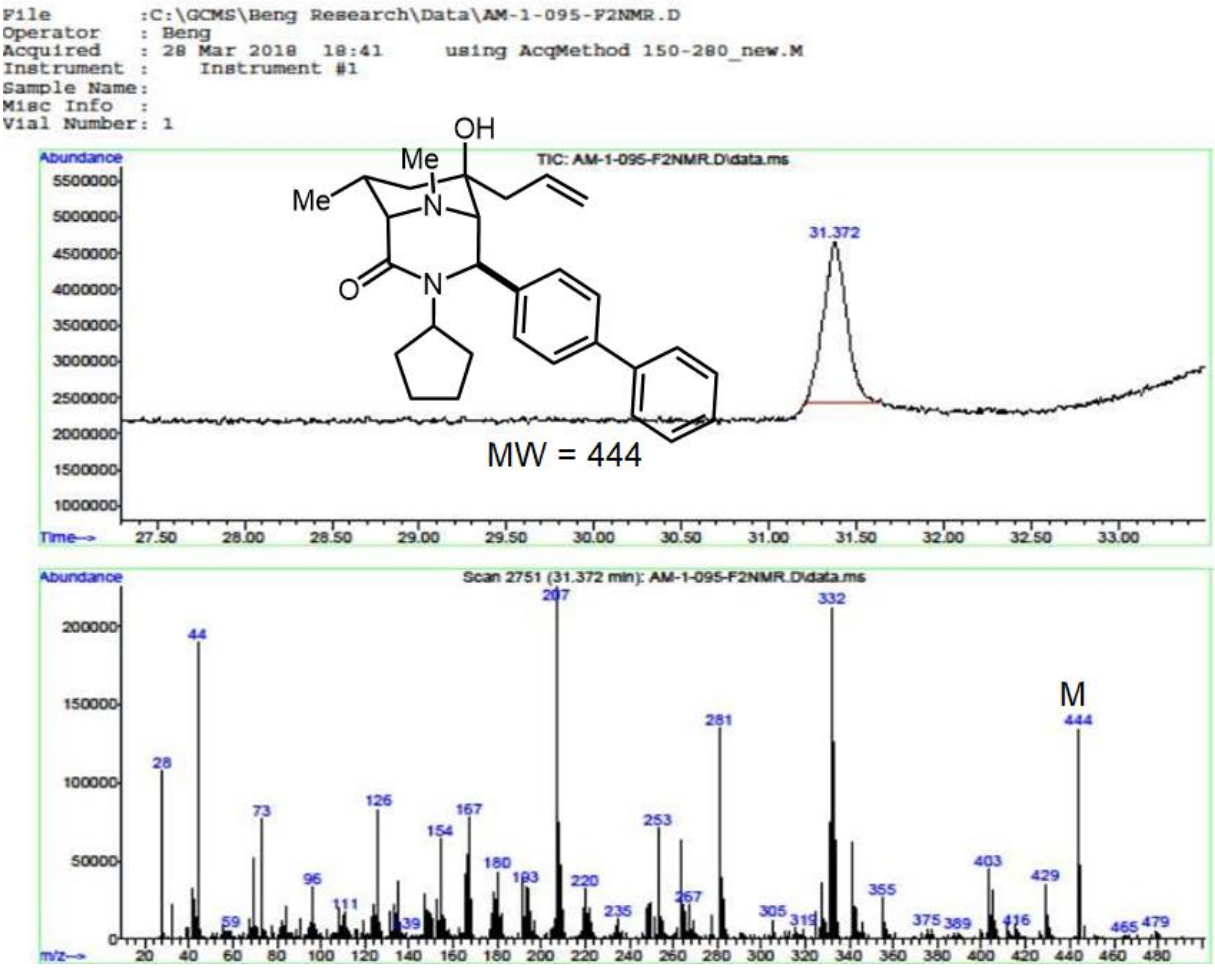

Spectra 2-43 GC-MS spectrum of **2m.**

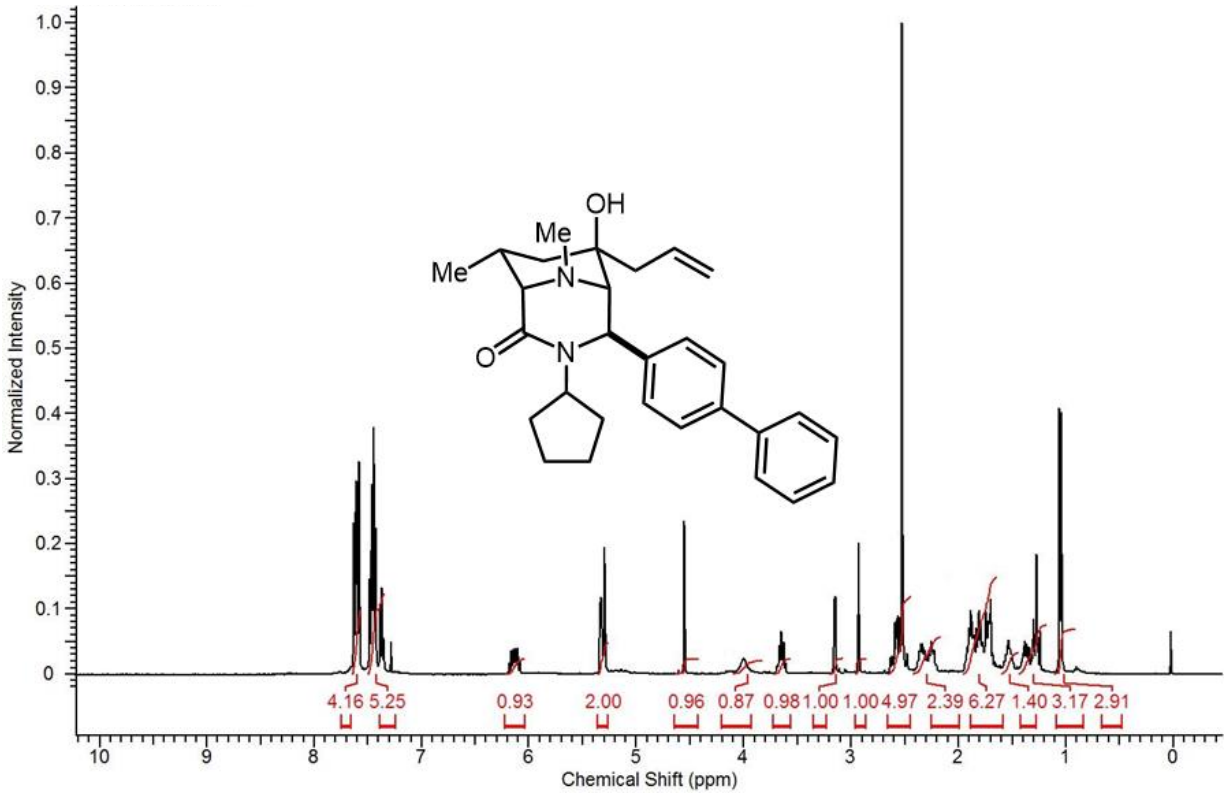

Spectra 2-44 Proton NMR spectrum of **2m.**

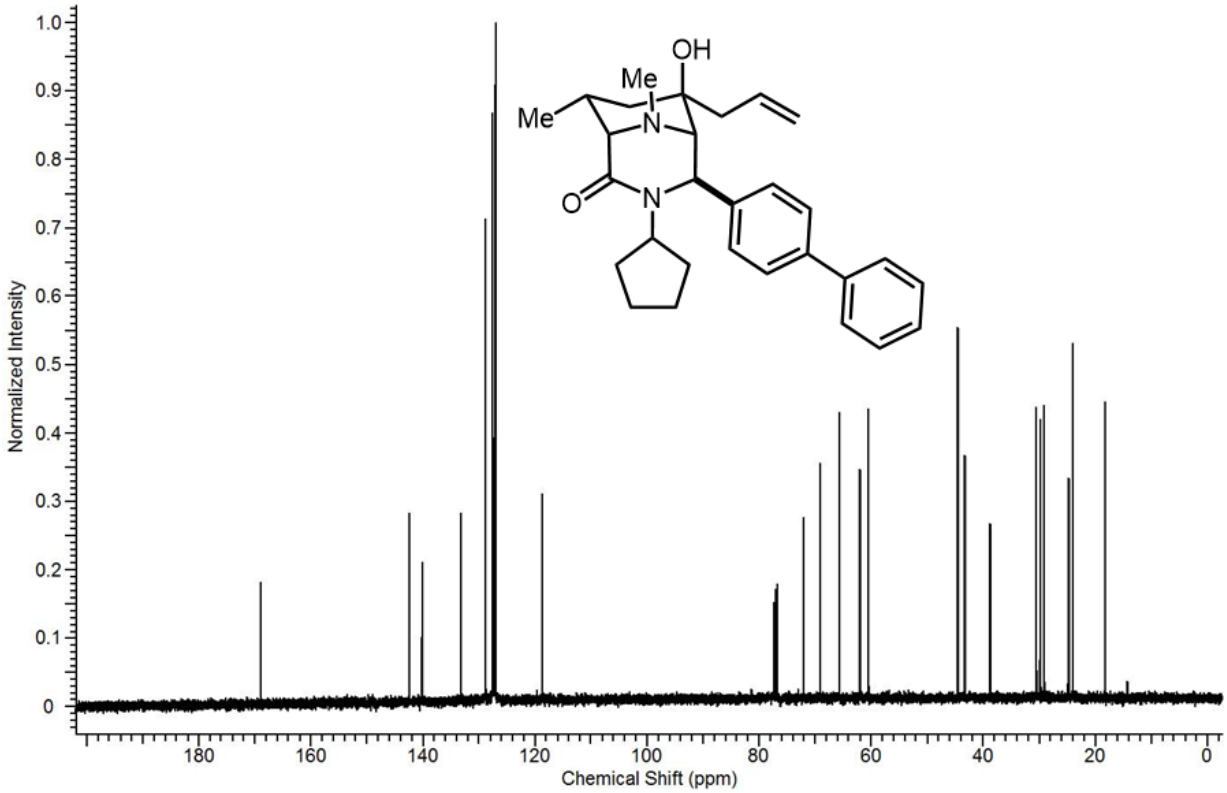

Spectra 2-45 Carbon NMR spectrum of **2m.**

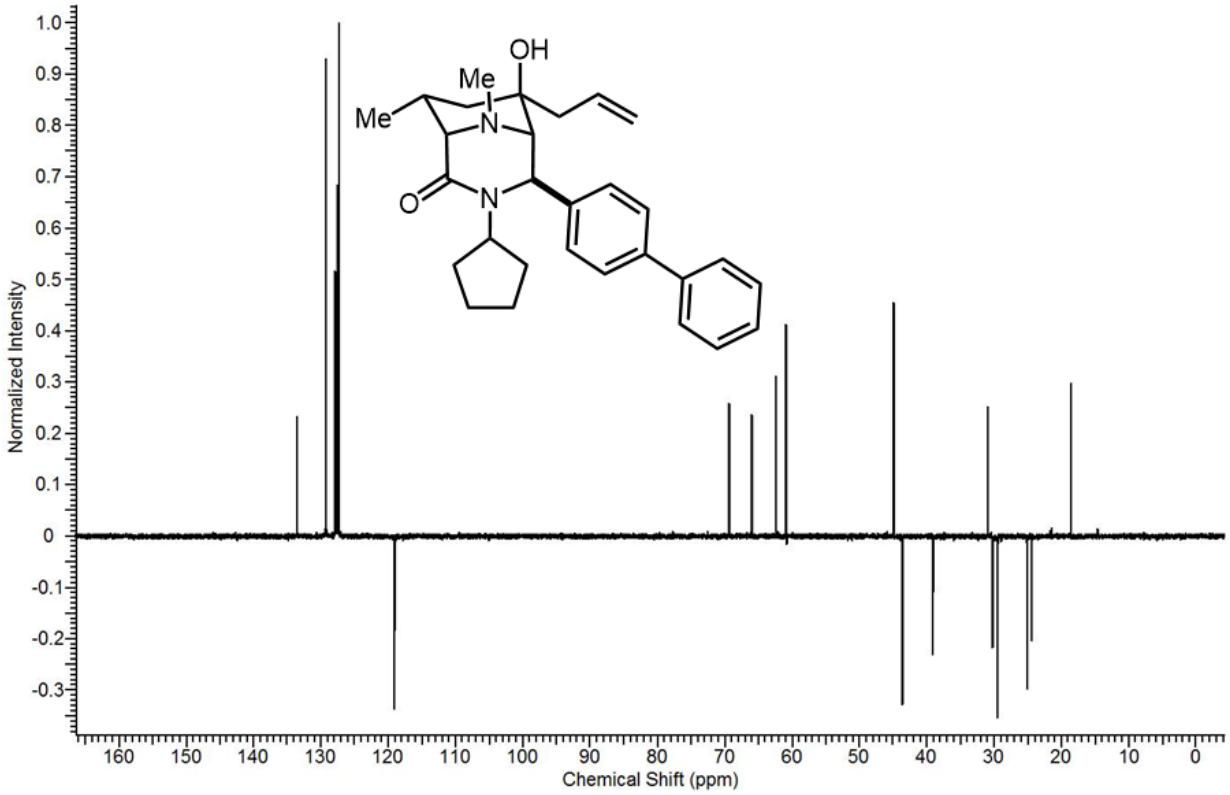

Spectra 2-46 DEPT-135 NMR spectrum of **2m.**

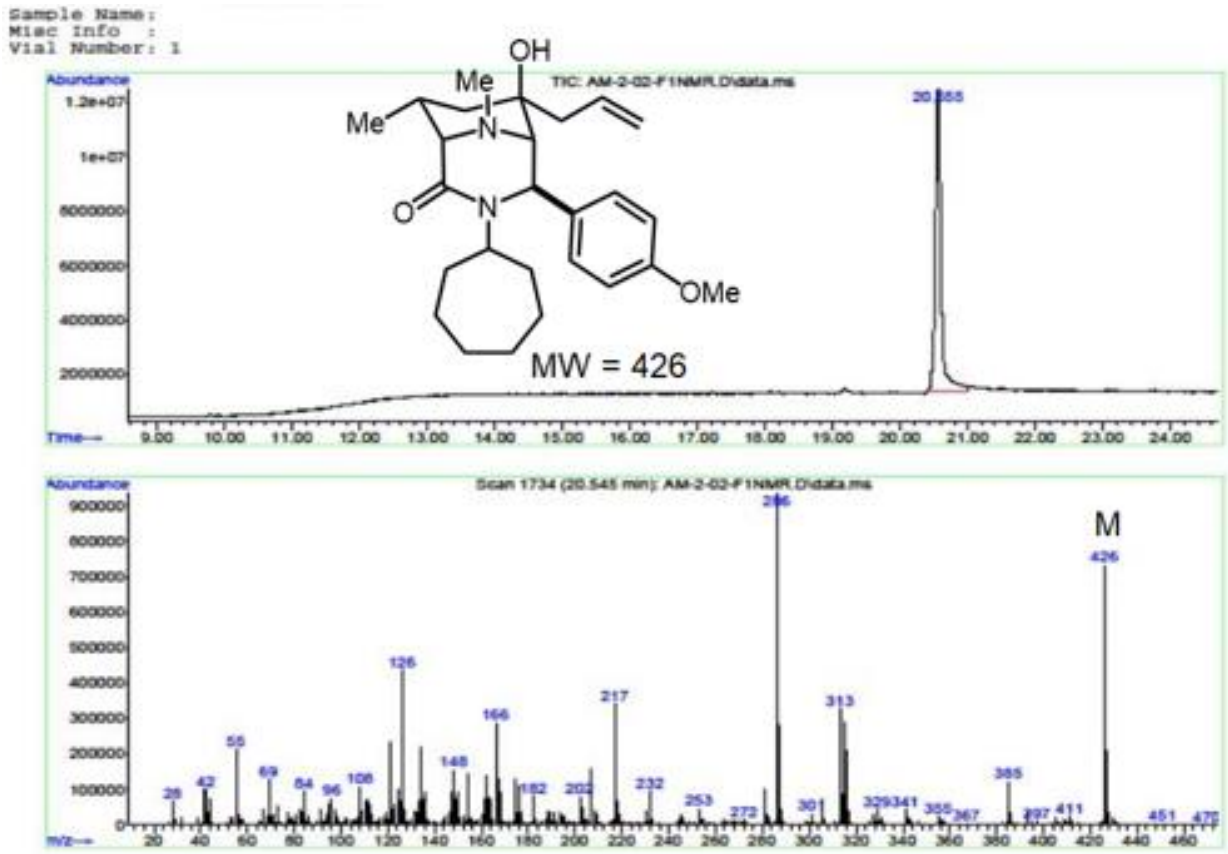

Spectra 2-47 GC-MS spectrum of **2n.**

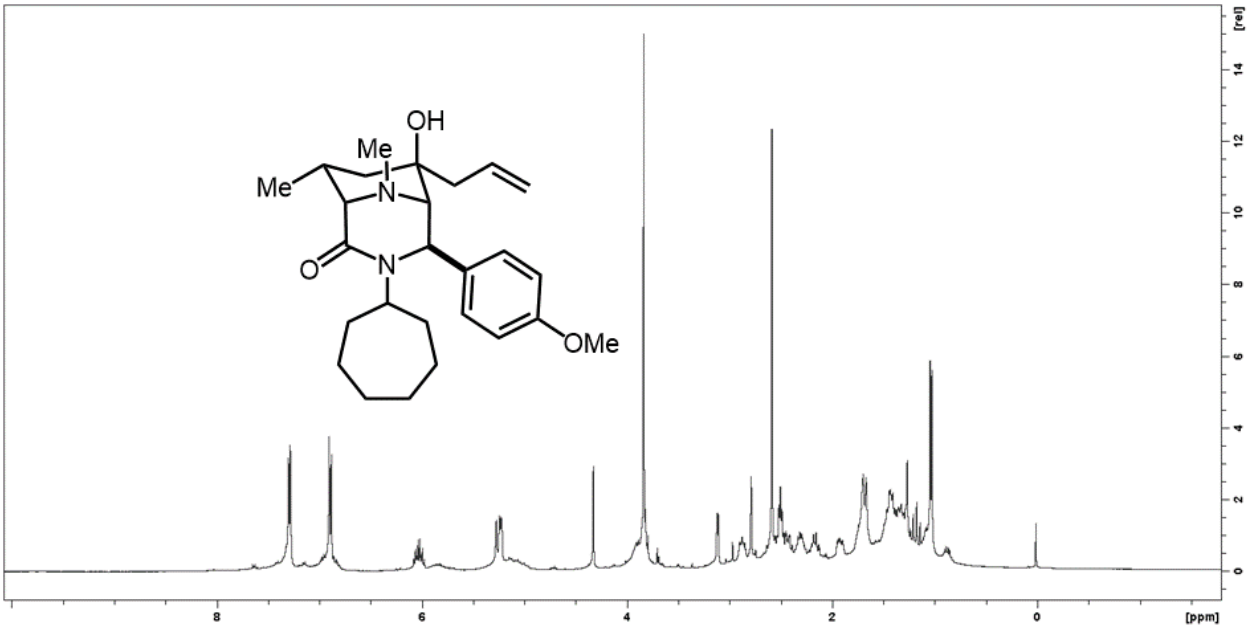

Spectra 2-48 Proton NMR spectrum of **2n.**

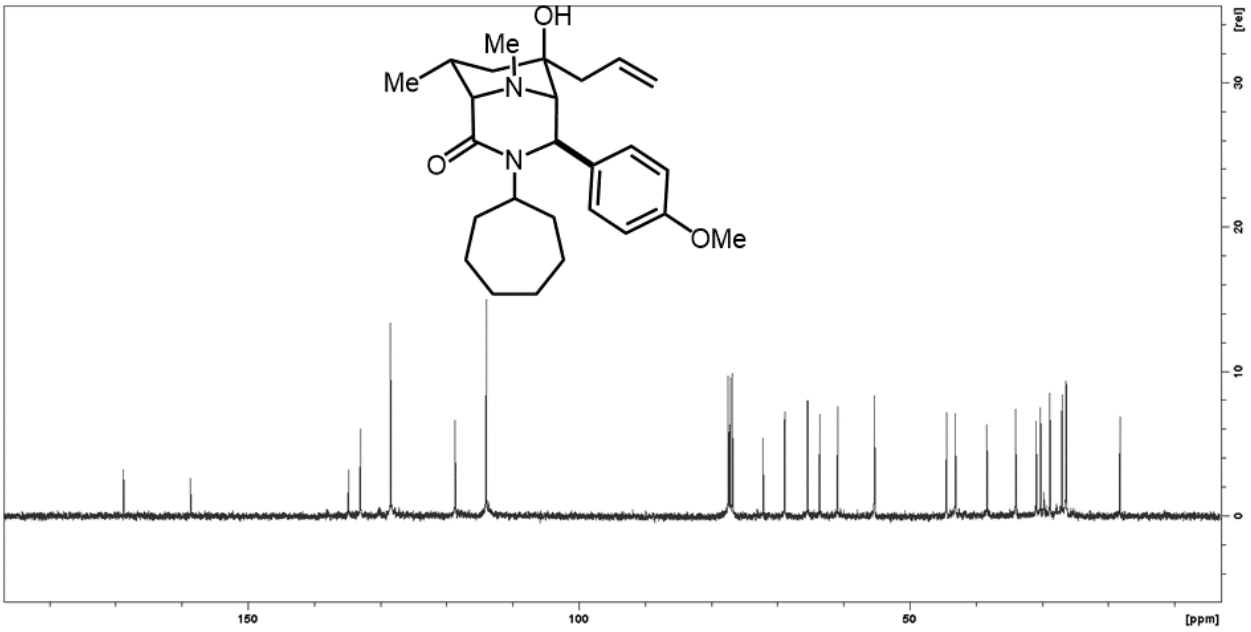

Spectra 2-49 Carbon NMR spectrum of **2n.**

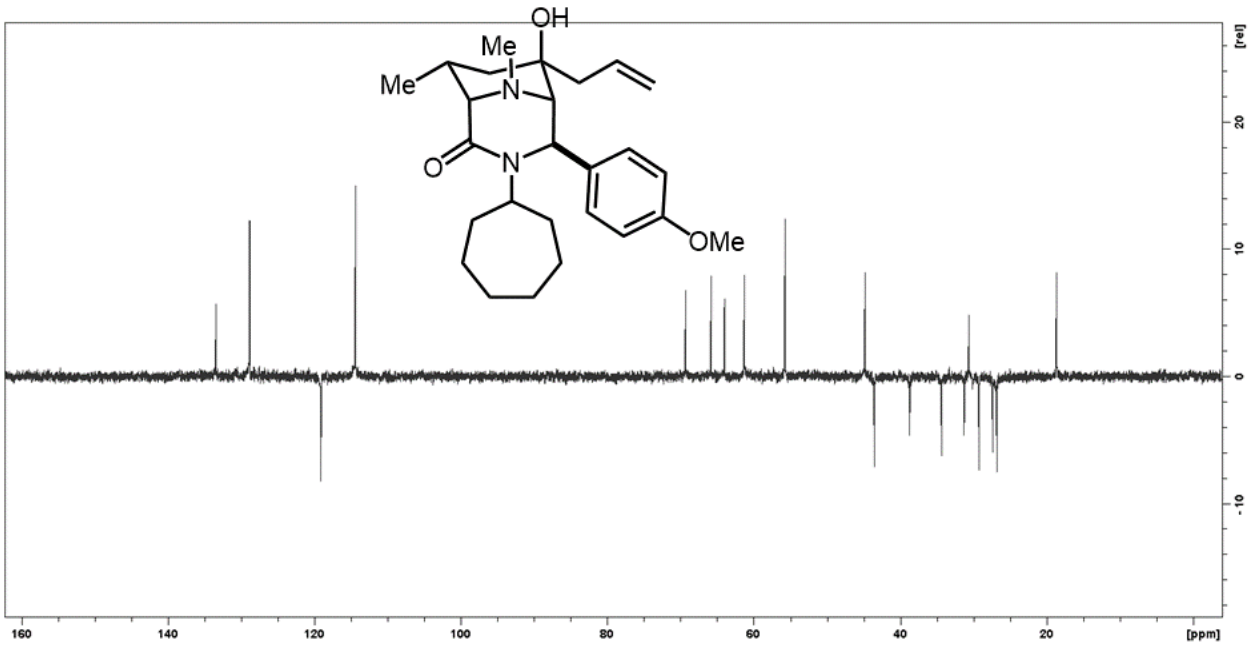

Spectra 2-50 DEPT-135 NMR spectrum of **2n.**

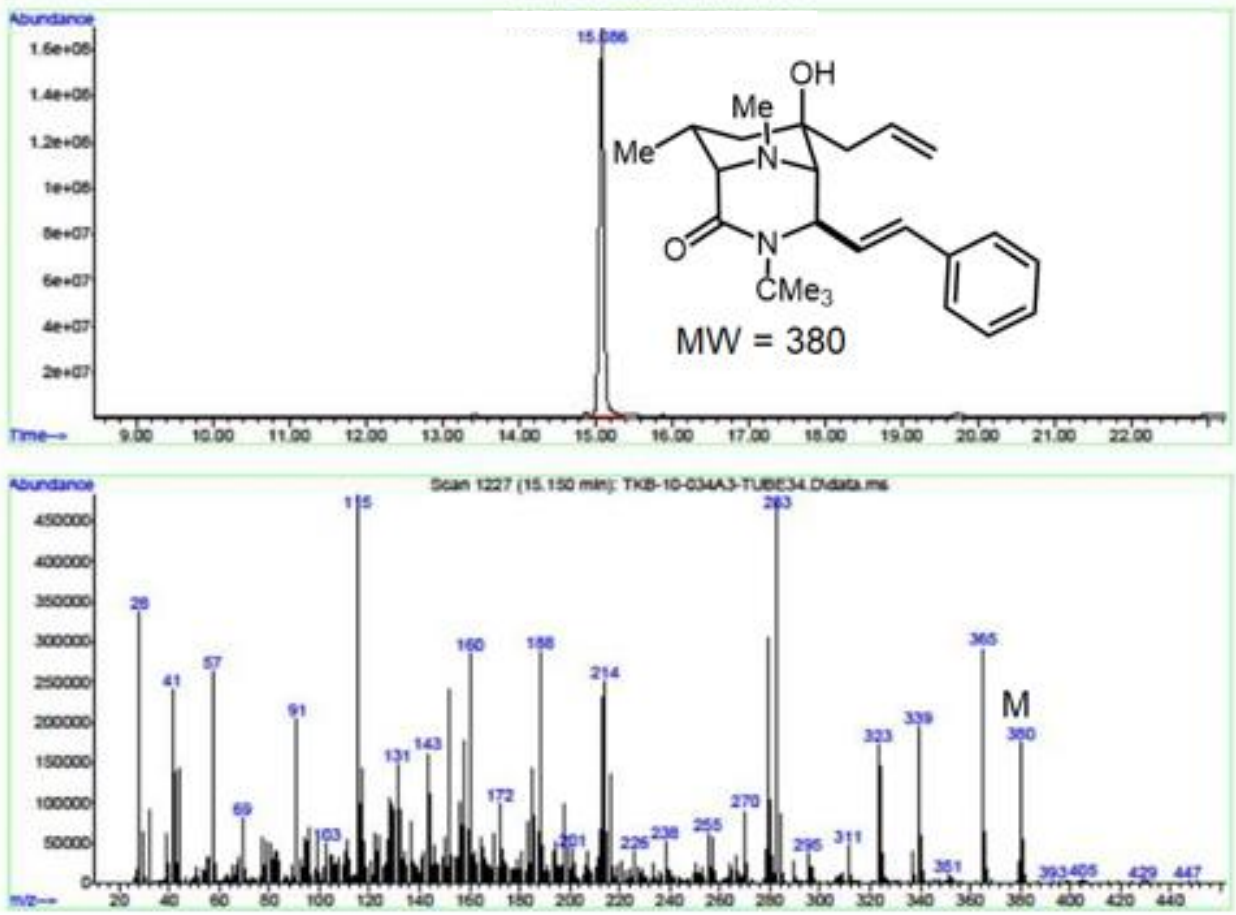

Spectra 2-51 GC-MS spectrum of **2o.**

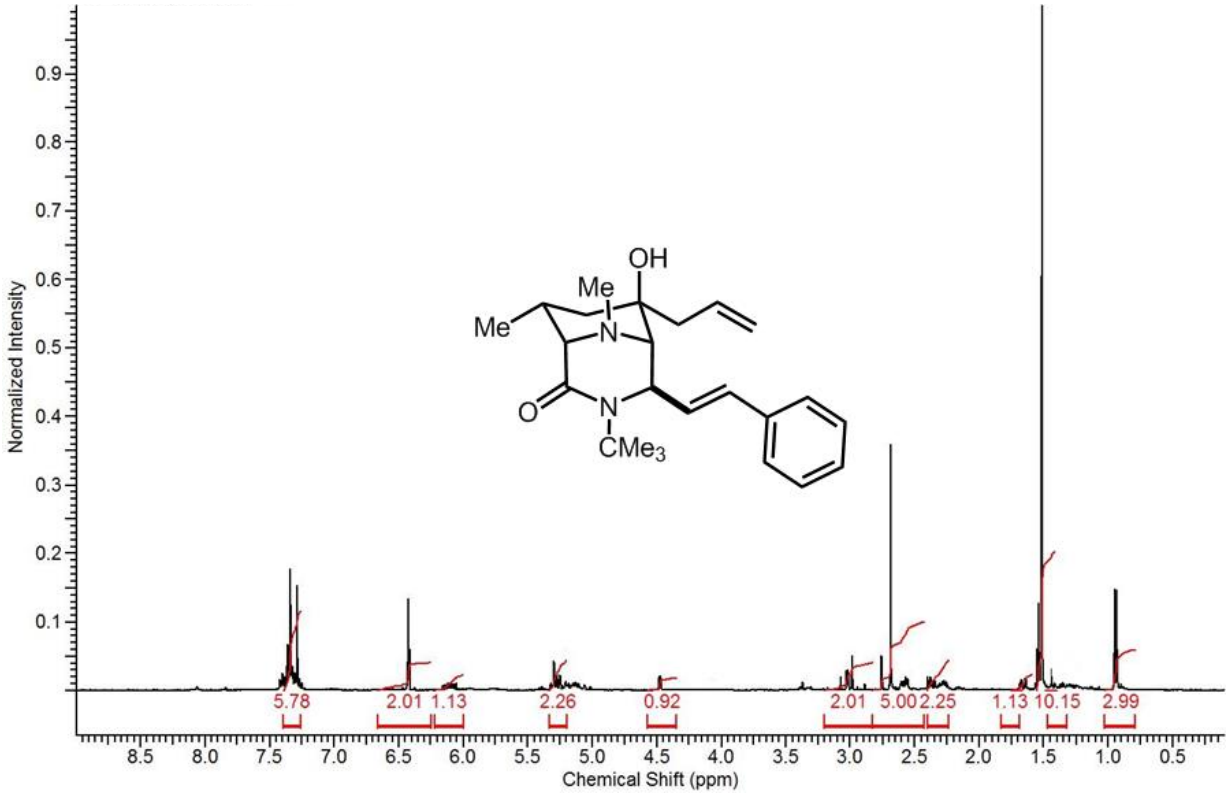

Spectra 2-52 Proton NMR spectrum of **2o.**

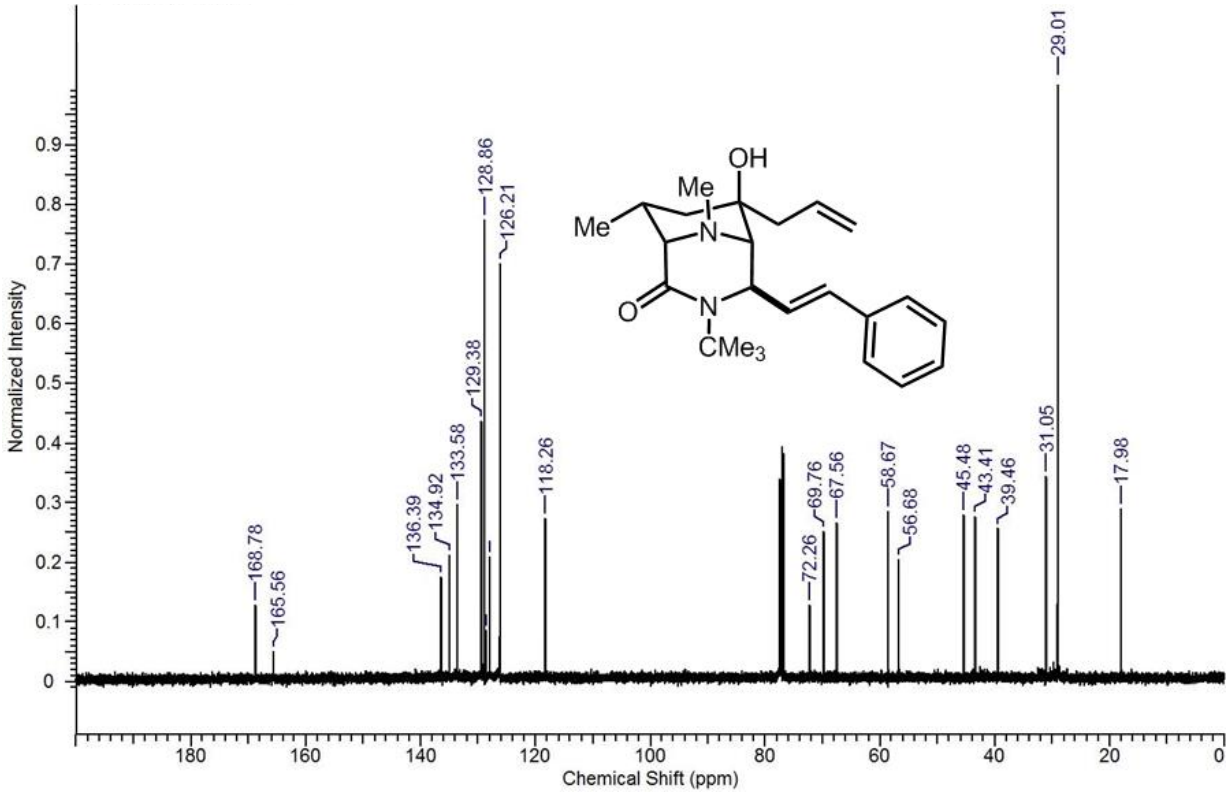

Spectra 2-53 Carbon NMR spectrum of **2o.**

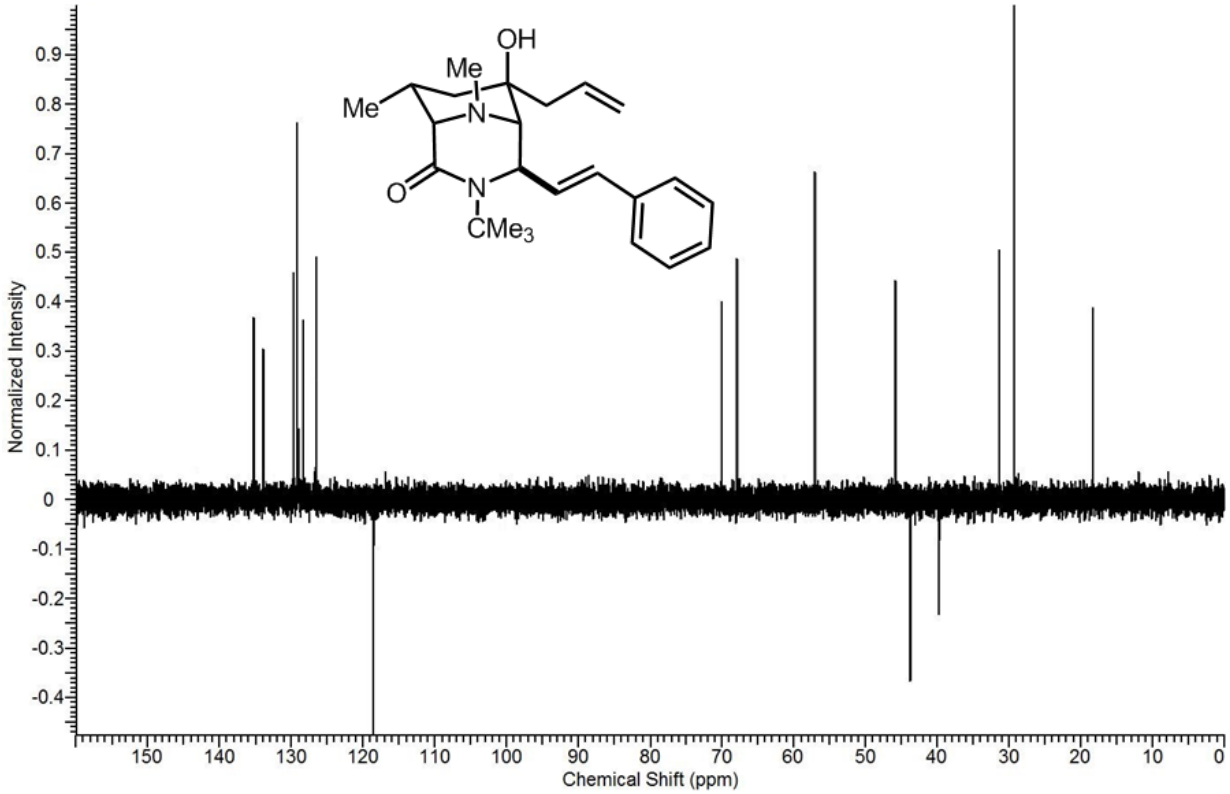

Spectra 2-54 DEPT-135 NMR spectrum of **2o.**

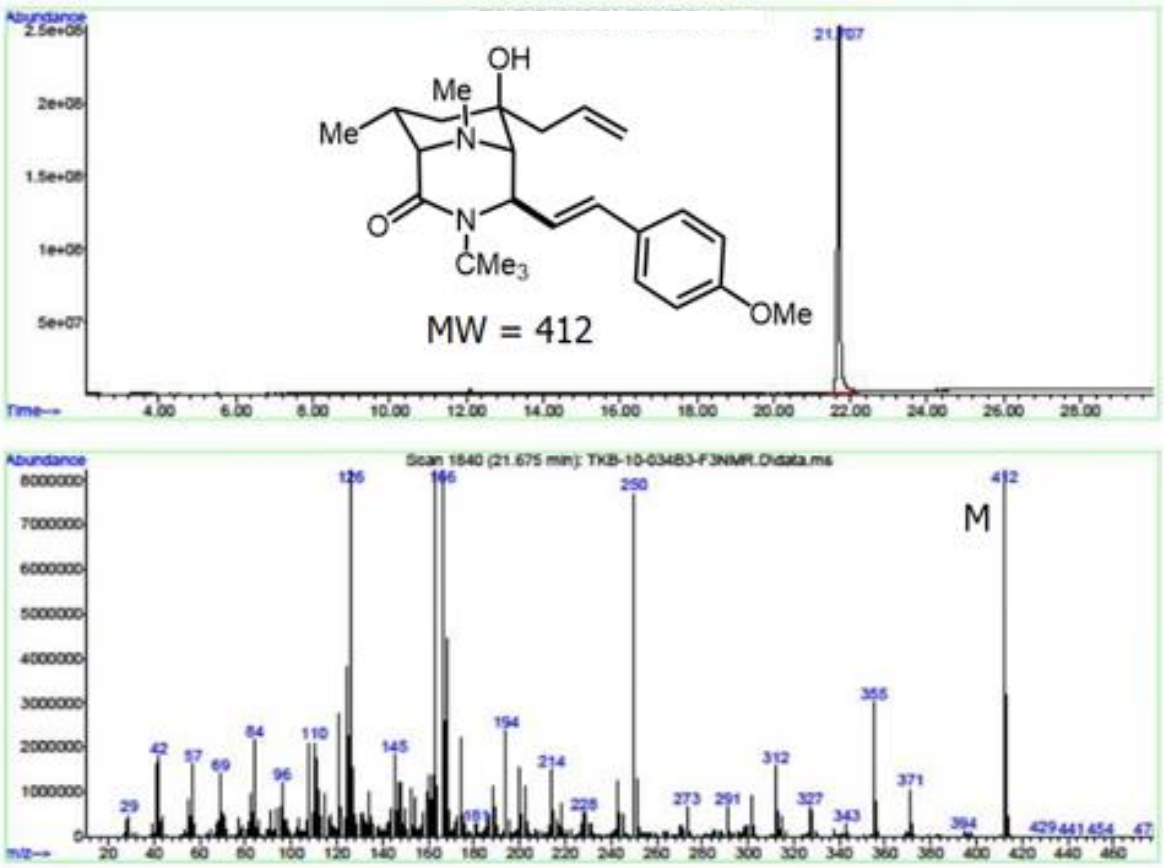

Spectra 2-55 GC-MS spectrum of **2p.**

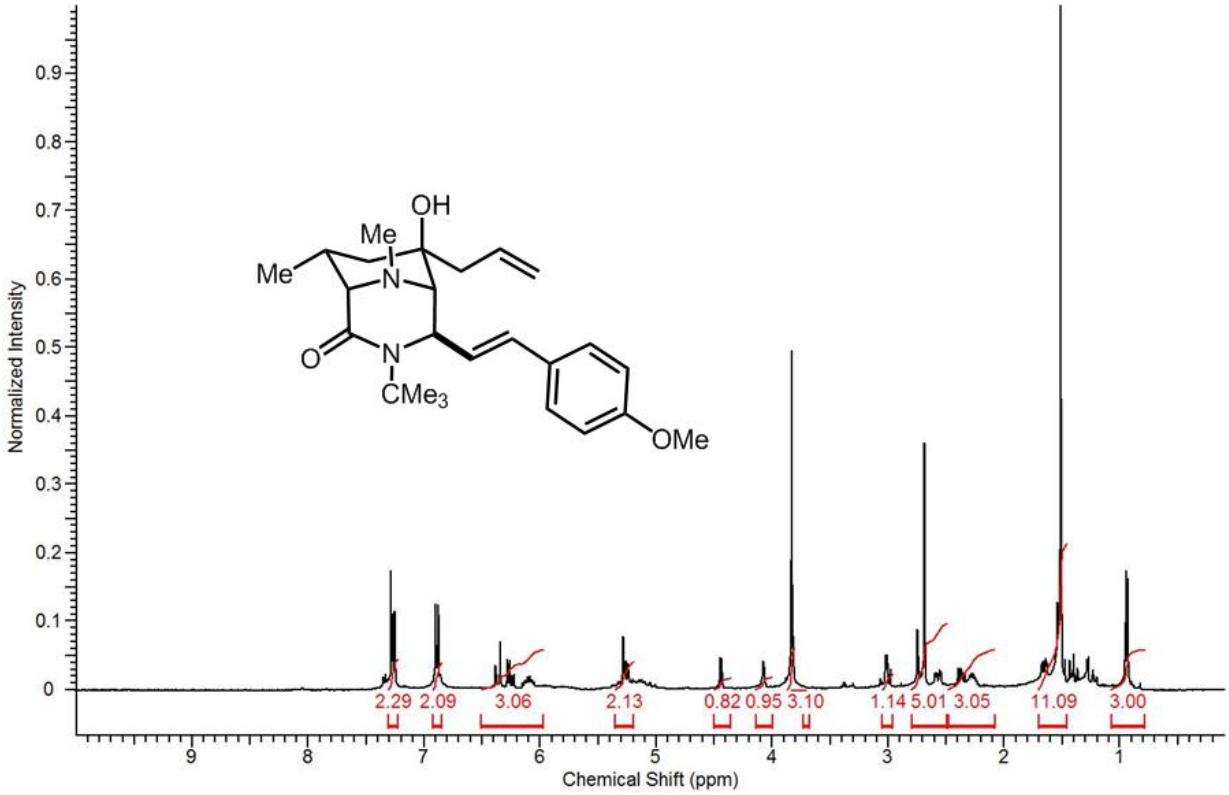

Spectra 2-56 Proton NMR spectrum of **2p.**

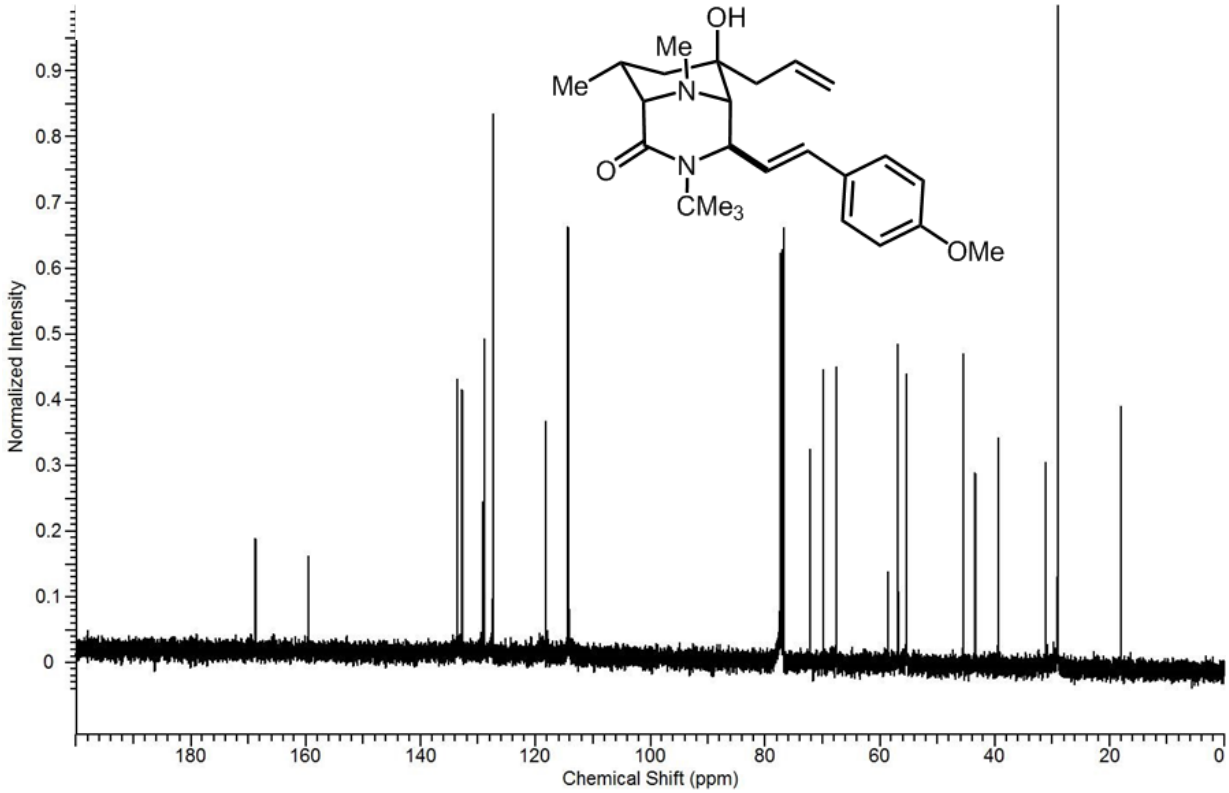

Spectra 2-57 Carbon NMR spectrum of **2p.**

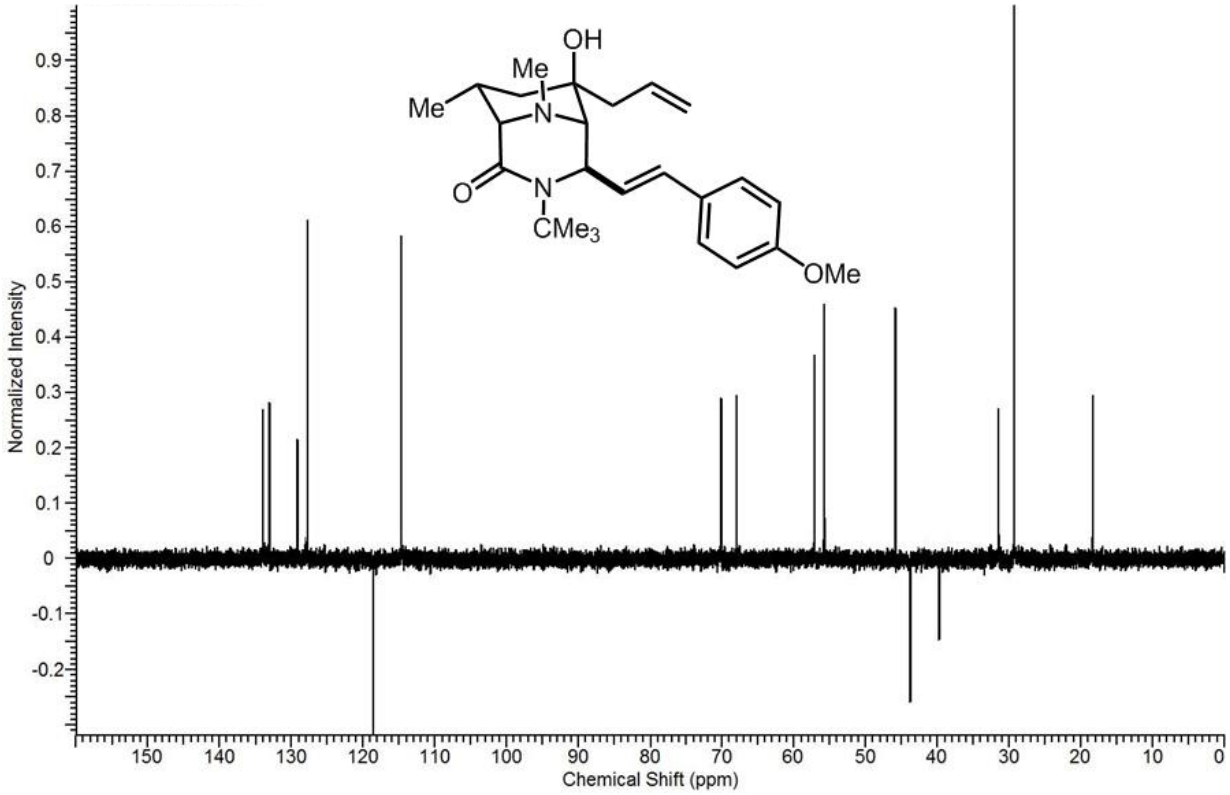

Spectra 2-58 DEPT-135 NMR spectrum of **2p.**

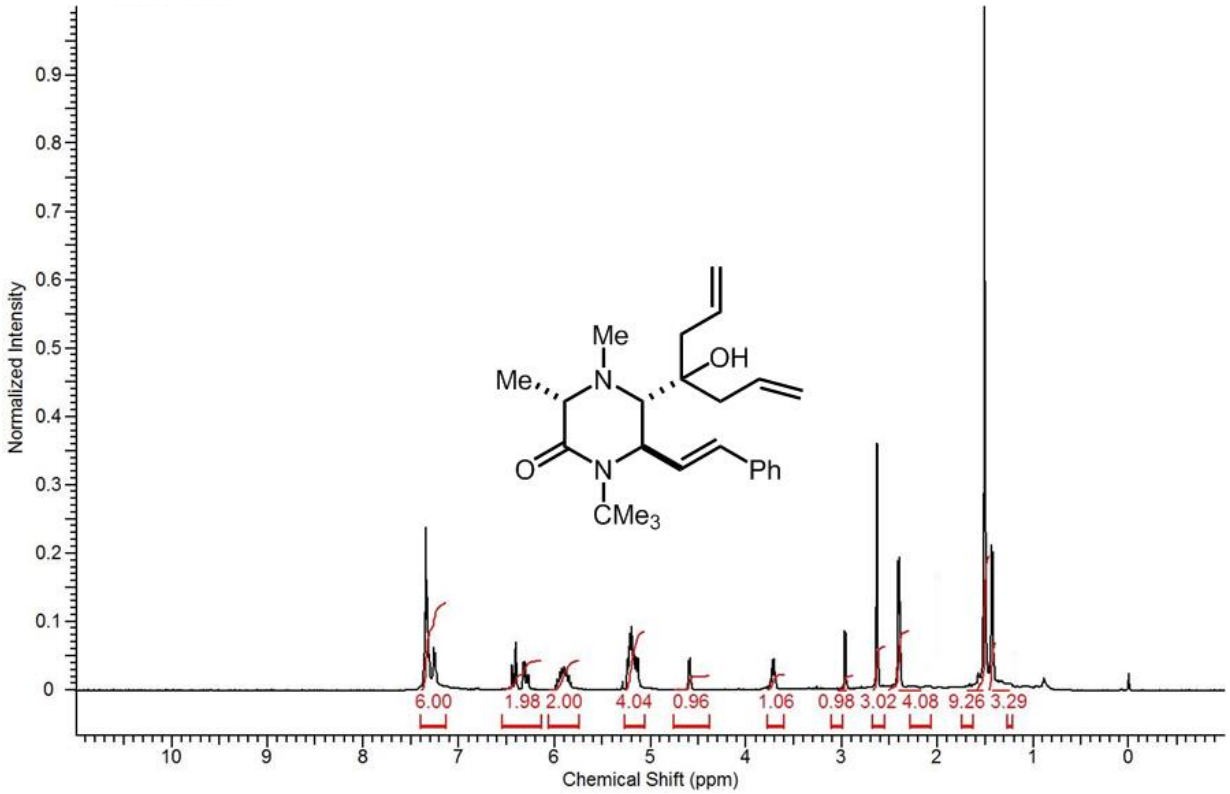

Spectra 2-59 Proton NMR spectrum of **9.**

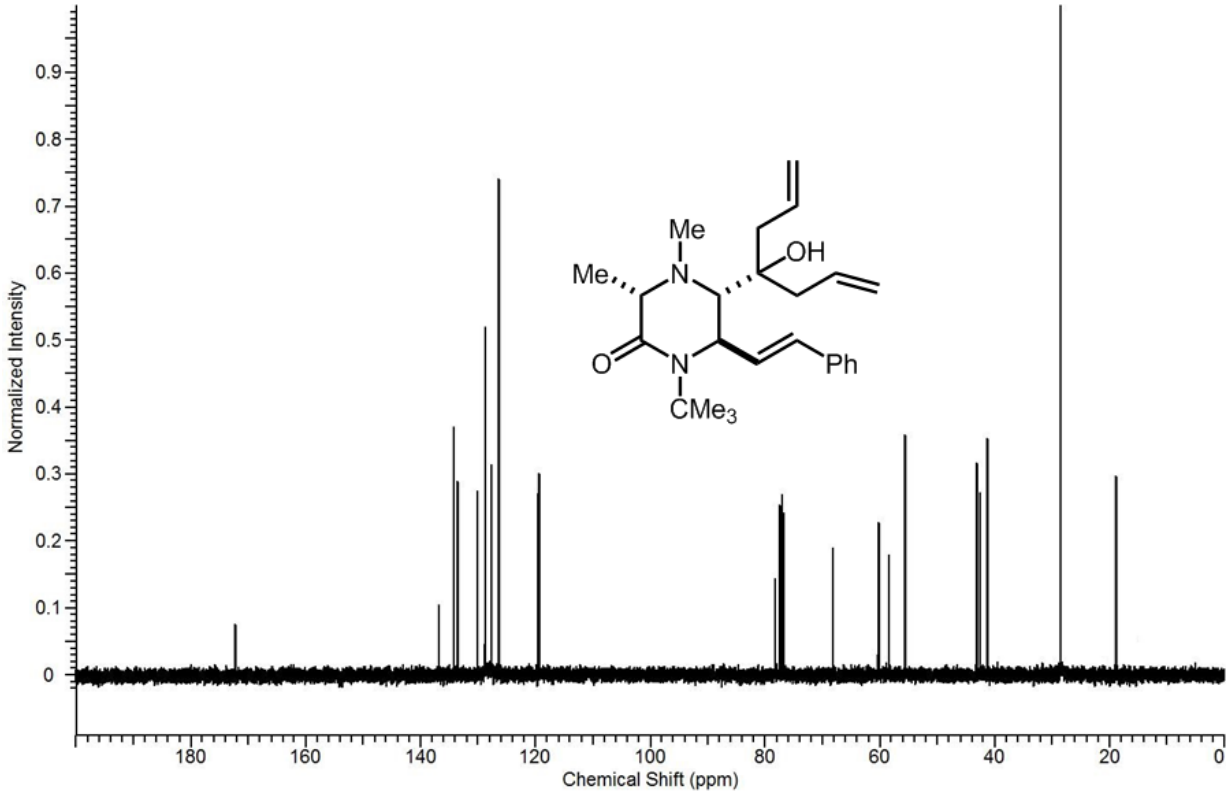

Spectra 2-60 Carbon NMR spectrum of **9.**

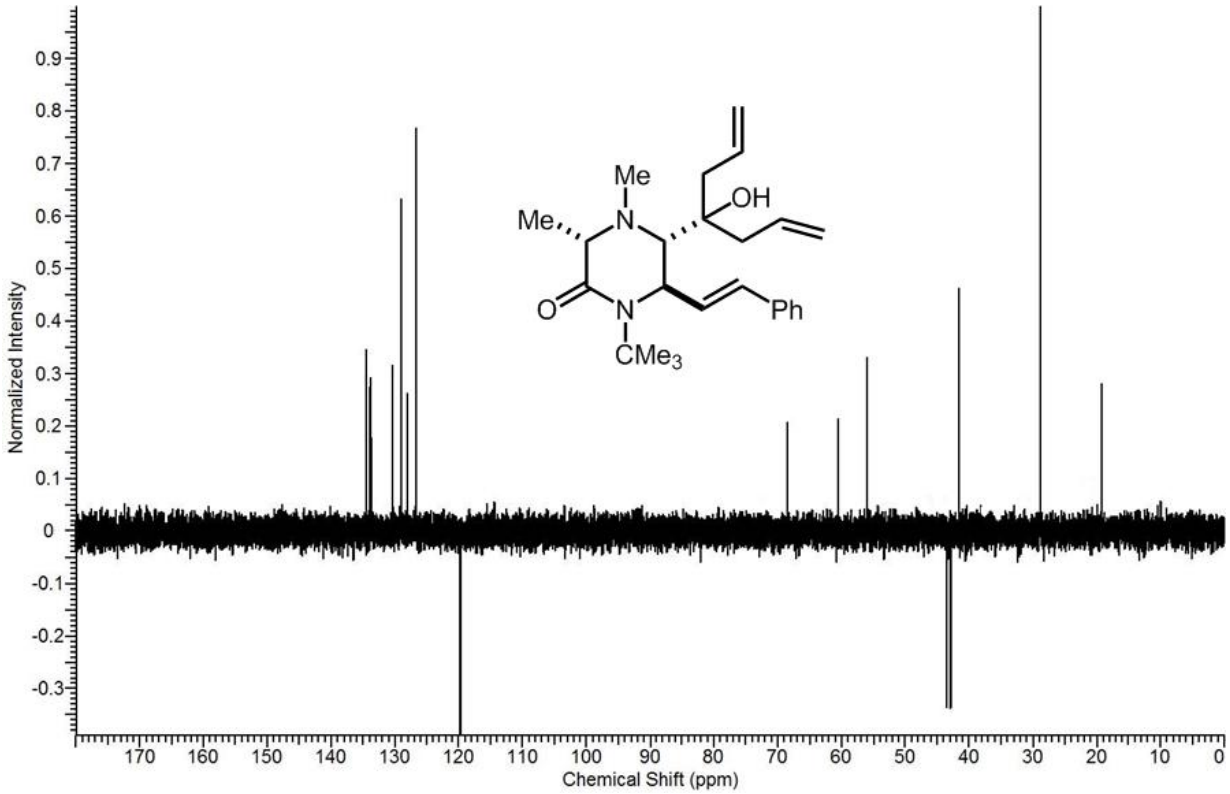

Spectra 2-61 DEPT-135 NMR spectrum of **9.**

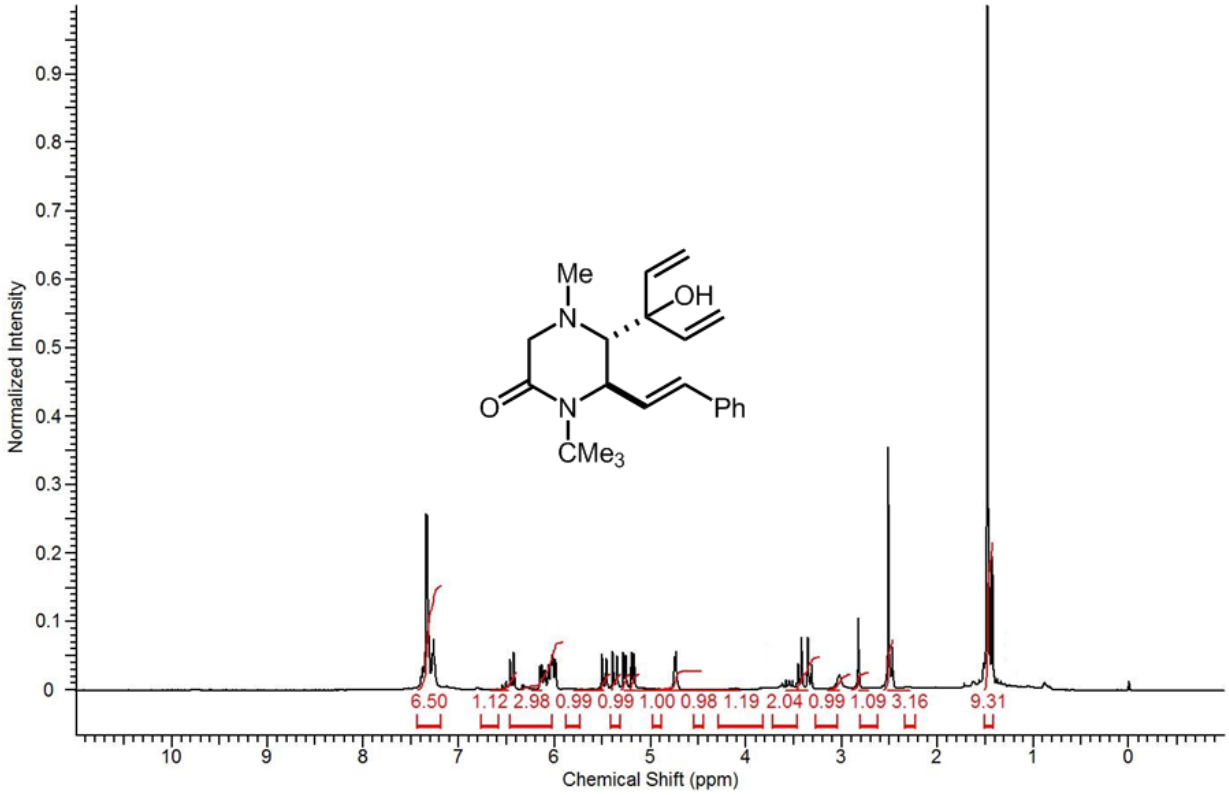

Spectra 2-62 Proton NMR spectrum of **6.**

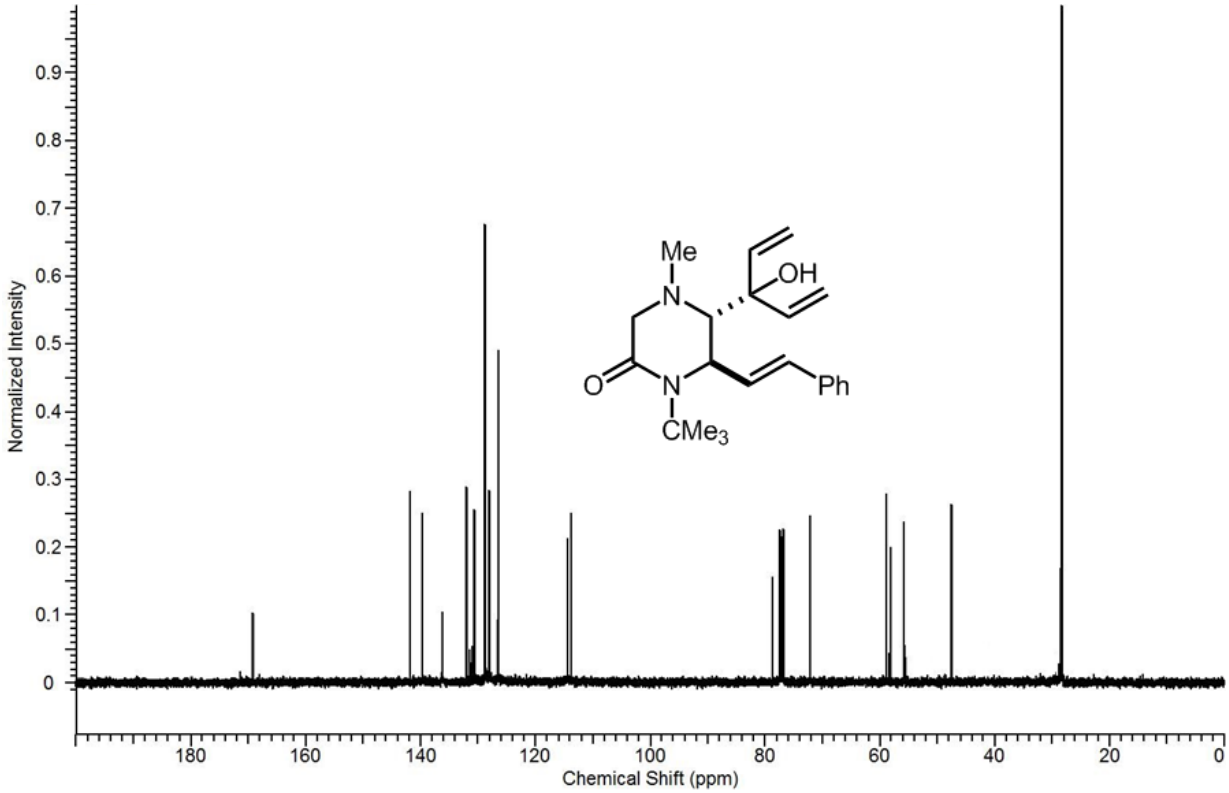

Spectra 2-63 Carbon NMR spectrum of **6.**

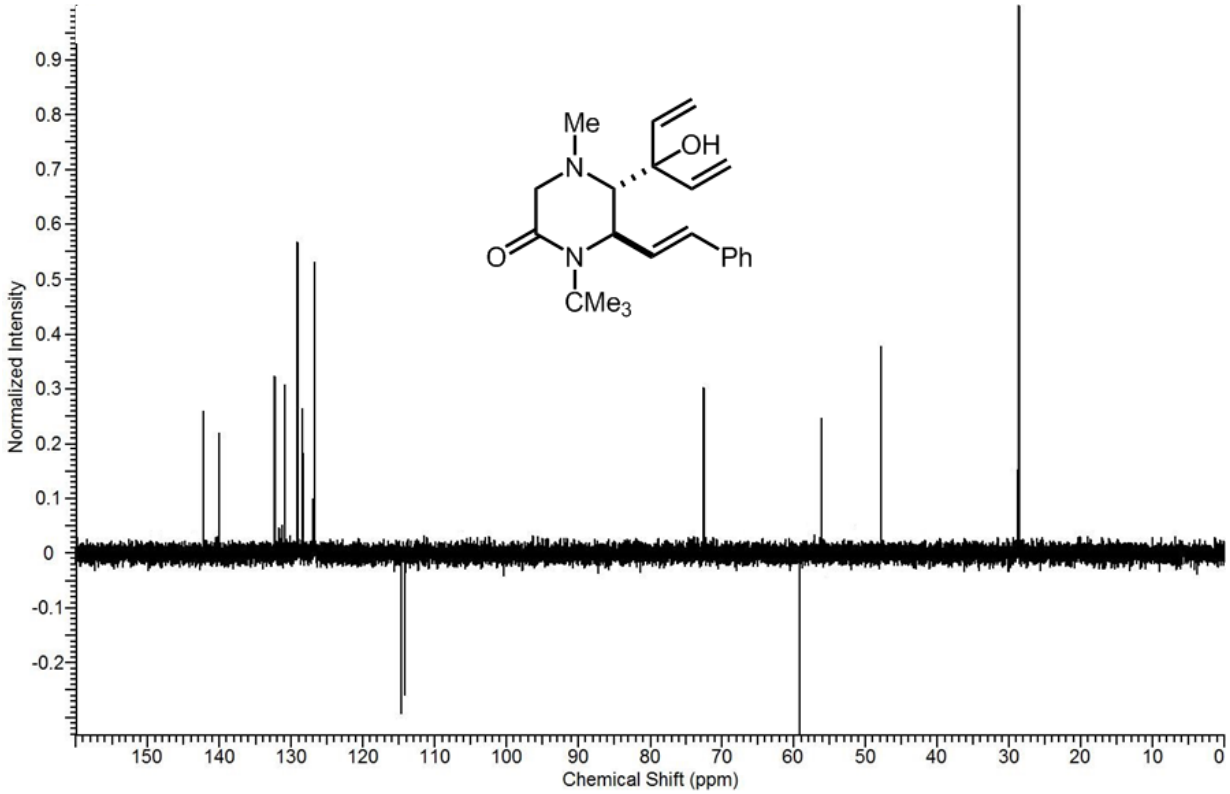

Spectra 2-64 DEPT-135 NMR spectrum of **6.**